

Ministry of Energy, Mines & Petroleum Resources
Mining & Minerals Division
BC Geological Survey

**ASSESSMENT REPORT
TITLE PAGE AND SUMMARY**

Third Mineralogical Report detailing the Finding of two 'new' gold-

TITLE OF REPORT [type of survey(s)] associated bismuth sulphotelluride minerals... on Nox Fort Project	TOTAL COST recorded \$3100-
--	---------------------------------------

AUTHOR(S) W.R. HOWARD and N.J. Cook of Oslo Norway **SIGNATURE(S)** Wm R Howard

NOTICE OF WORK PERMIT NUMBER(S)/DATE(S) N/A **YEAR OF WORK** 2007-2008

STATEMENT OF WORK - CASH PAYMENT EVENT NUMBER(S)/DATE(S) Event No 4241547

PROPERTY NAME Nox Fort Project about Bunker Hill mine (formerly CLY Group)

CLAIM NAME(S) (on which work was done) 516584 and work on the Crown Grants Bunker Hill Lot 2939 and Mormon Girl Lot 1949, not accredited and provided gratis

COMMODITIES SOUGHT gold bismuth tungsten

MINERAL INVENTORY MINFILE NUMBER(S), IF KNOWN Bunker Hill 082FSW002

MINING DIVISION Nelson **NTS** 082F03 W 1/2 Salmo

LATITUDE 49° 03' 36" **LONGITUDE** 117° 23' 15" (at centre of work)

OWNER(S)

1) Clarke Gold Inc. 2) _____
c/o Wm R Howard

MAILING ADDRESS

215 Silver Mead Cres. NW
Calgary AB T3B 3W4

OPERATOR(S) [who paid for the work]

1) Clarke Gold Inc. 2) _____

MAILING ADDRESS

as above

PROPERTY GEOLOGY KEYWORDS (lithology, age, stratigraphy, structure, alteration, mineralization, size and attitude):

Reduced Intrusion Related Gold System intrusion-hosted or proximal placed mid Cretaceous Wallack Ck stock Bunker Hill sill biotite granite Lefevre tungsten + gold skarn/hornfels quartz veins ikunolite ingodite native bismuth native gold electrum bismuthinite hedleyite BizTe pilsenite galena

REFERENCES TO PREVIOUS ASSESSMENT WORK AND ASSESSMENT REPORT NUMBERS Howard 2000 #26159 Ray 2004 #27513 Howard 2005 #27893, 2006a #28748, 2006b #28749, Koffeyburg and Howard 2008, Howard 2008

(OVER)

TYPE OF WORK IN THIS REPORT	EXTENT OF WORK (IN METRIC UNITS)	ON WHICH CLAIMS	PROJECT COSTS APPORTIONED (incl. support)
GEOLOGICAL (scale, area)	nil		
Ground, mapping			
Photo interpretation			
GEOFYSICAL (line-kilometres)	nil		
Ground			
Magnetic			
Electromagnetic			
Induced Polarization			
Radiometric			
Seismic			
Other			
Airborne			
GEOCHEMICAL (number of samples analysed for ...)			
Soil			
Silt			
Rock			
Other	minerals analyzed - 105 formulae by Energy Dispersive Spectrometry nil	516584 (in part)	
DRILLING (total metres; number of holes, size)			
Core			
Non-core			
RELATED TECHNICAL			
Sampling/assaying			
Petrographic			
Mineralographic	polished sections prepared 18	6 on 516584	Less than 20%
Metallurgic	Scanning Electron Microscope 142 images nil	of \$15,778.80, \$3,100-	project costs apportioned
PROSPECTING (scale, area)			
PREPARATORY/PHYSICAL	nil		
Line/grid (kilometres)			
Topographic/Photogrammetric (scale, area)			
Legal surveys (scale, area)			
Road, local access (kilometres)/trail			
Trench (metres)			
Underground dev. (metres)			
Other			
TOTAL COST			\$ 3100.00

Third Mineralogical Report detailing the finding of two ‘new’ gold-associated bismuth sulphotelluride minerals and identifying other opaque minerals, namely native silver electrum **pilsenite **tetradymite** hessite pavonite bismuthinite–aikinite and greenockite characterizing a RIRG system in claim # 516584 and the Bunker Hill & Mormon Girl Crown Grants on Nox Fort Project, south of Salmo in Nelson Mining Division southernmost British Columbia**

2008 Assessment Report – Mineralogical Research

Work on claim # 516584 (former name CLY 2)
Latitude 49° 03' 36" Longitude 117° 23' 15" or
NAD 83 Zone 11 UTM 471,652 mE / 5,434,400 mN
BGS 082F.004 (1:20,000 scale) NTS 082F03 W1/2 (1:50,000 scale)

Owner, operator and author
(Part I)

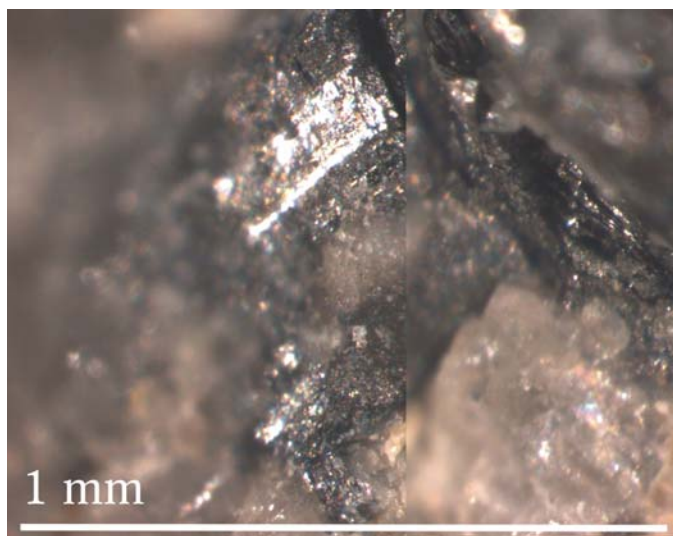
Wm. R. Howard, B.Sc. Geol.
President, Clarke Gold Inc.
215 Silver Mead Cres. NW
Calgary AB
Canada
T3B 3W4
wm.howard@shaw.ca

**BC Geological Survey
Assessment Report
30475**

Consultant and author
(Part II)

Nigel J. Cook (Prof.)
Natural History Museum
Geology section
University of Oslo
Boks 1172 Blindern
0388 Oslo Norway
nigelc@nhm.uio.no

Jan. 14 2009



see Fig. 6 p. 49

Table of Contents

List of Figures	6
List of Tables.....	6
List of Maps.....	7
List of Appendices.....	7
MTO Online Inserts follow this page.....	9
1 Summary.....	10
1.1 Gold mineralogy of the veins	11
1.2 Iron sulphide minerals in two polished sections carry no 'invisible' or dissolved gold	12
1.3 Gold Fineness in the Adit 2 Underhand Stope Vein and Eloise Vein	12
1.4 Two 'new' mineral phases $\text{Bi}_4\text{Te}_3\text{S}_2$ and $\text{Bi}_8\text{Te}_5\text{S}_4$ in Eloise Vein	13
1.5 Newly identified minerals; <i>gold tellurides</i> do not occur.....	13
1.6 Unnamed Bi_2Te and hedleyite occurrences appear spatially zoned	13
1.7 Minerals have very low selenium content; ikunolites are Te-rich.....	14
1.8 Lefevre skarn has Bi-Te-S mineral assemblages similar to the veins	14
1.9 Chemical conditions of mineral deposition well compare to Pogo and Fort Knox deposits.....	15
1.10 Tally of the same rare gold-associated Bi-Te-S minerals on Nox Fort as in the Pogo deposit.....	15
1.11 Considering the sub-type of RIRG mineralization represented, Nox Fort is a prime target for an economic gold + bismuth deposit	16
1.12 Low-cost gold extraction indicated	16
1.13 Geochemistry and mineralogy of the 'Bismuth Gold Zone' on the Jersey- Emerald property differs, as does the targeted commodities.....	16
1.14 Recommendations for further mineralogical work	16
1.15 Synopses of the first 2006 report.....	17
1.16 Synopses of the second 2008 report.....	19
1.17 Discussion of formation conditions of Au-Bi-Te mineralization in the second report.....	20
1.18 Overprinting deformation identified that nucleated gold minerals.....	21
1.19 Two analogous <i>intrusion-hosted</i> RIRG deposits in the Czech Republic	22
1.20 Two general types of economic deposits host Bi-Te-S-(Se) minerals	22
1.21 Research goals of this report.....	22
2 Introduction	24
2.1 Physiographic and Geographic Location •	24
2.2 Access •	24
2.3 Topography, Vegetation and Climate •	24
2.4 Claims •	25
3 Work Performed	26
3.1 Software used.....	30
4 Brief property history •.....	31
5 Brief economic assessment	33
6 Geology at regional to district scale •	35
7 Local Scale Geology.....	36
7.1 Layered rocks •	36
7.2 Intruding Bunker Hill Sill granitoids •	36
7.3 Description of Bunker Hill Sill granitoids •	36
8 Detailed Economic assessment	38
8.1 Regional Setting in an area with 9 Million ounce gold •	38

Third Mineralogical Report detailing the finding of two 'new' gold-associated bismuth sulphotelluride minerals and identifying other opaque minerals, namely native silver electrum **tetradymite** **pilsenite** **hessite** bismuthinite–aikinite pavonite and greenockite characterizing a RIRG system in claim # 516584 and the Bunker Hill & Mormon Girl Crown Grants, on Nox Fort Project south of Salmo in Nelson Mining Division, southernmost British Columbia p. 3

8.2 Discussion of the applicable exploration model – a Reduced Intrusion Related Gold [RIRG] System.....	40
8.3 Favourability for the 'Group 1' subtype of RIRG deposit	41
8.4 Process metallurgy that could be used to recover gold is deemed economical	41
9 Mineral Deposits in the District •.....	42
9.1 Geochemistry and mineralogy of the 'Bismuth Gold Zone' in the Jersey-Emerald property differs from Nox Fort.....	43
10 Gold minerals on Nox Fort.....	44
10.1 Silver-rich electrum in Bunker Hill mine veins.....	44
10.2 Native gold to gold-rich electrum in Eloise Vein	45
10.3 Gold-rich electrum in Blue Quartz Vein	46
11 The rare minerals	47
11.1 Two 'new' mineral phases $\text{Bi}_4\text{Te}_3\text{S}_2$ and $\text{Bi}_8\text{Te}_5\text{S}_4$	47
12 Ikunolite Bi_4S_3.....	50
12.1 Ikunolite – its stability, parageneses and compositional range.....	50
12.2 Ikunolite type locality – Ikuno mine in Japan	50
12.3 Ikunolite is characteristic of RIRG deposits and polymetallic Sn Mo W Bi Cu Ag Pb Zn bearing deposits in the Russian Far East.....	51
12.4 Ikunolite is prominent in international RIRG deposits.....	51
12.5 Ikunolite in some polymetallic Sn Mo W Bi Cu Ag Pb Zn deposits	54
12.6 Composition of Nox Fort ikunolites.....	58
12.7 Table of global ikunolite formulae and three Nox Fort.....	60
occurrences	60
12.8 Interpretation: Significance of ikunolite and other Bi-Te assemblages in the Blue Quartz Vein and the texturally-indicated alteration processes	61
12.9 Formation conditions of the Blue Quartz Vein inferred from mineral assemblages with ikunolite 63	
13 Ingodite Bi_2TeS.....	64
13.1 Ingodite: its rarity and compositional range	64
13.2 Ingodite type locality – Verkhne-Ingodinskoye tin deposit, Russia	64
13.3 Ingodite in some global RIRG deposits	64
13.4 Ingodite in some polymetallic Sn W Mo Bi Cu Pb Zn Ag As deposits	66
13.5 Composition of Eloise Vein ingodites	68
13.6 Table of global ingodite formulae and that in Eloise Vein.....	70
13.7 Interpretation: Compare conditions of formation of ingodite in the Fort Knox and Pogo deposit GBT mineral assemblages	70
13.8 Ingodite carries gold and silver in solid solution in the Nakdong South Korea As + Bi deposit	71
13.9 Conclusion: Eloise Vein ingodite grains carry gold and silver that may have nucleated with formation of unnamed Bi_2Te	72
14 Unnamed Bi_2Te.....	74
14.1 Unnamed Bi_2Te – a partly characterized mineral	74
14.2 Unnamed Bi_2Te first described in Ergelyakh Au-W-Bi deposit Far East Russia.....	74
14.3 Problem identifying unnamed Bi_2Te and hedleyite considering the minerals do not have uniform compositions.....	75
14.4 Unnamed Bi_2Te in some global RIRG deposits.....	75
14.5 Unnamed Bi_2Te in some global polymetallic deposits	76
14.6 Near-stoichiometric unnamed Bi_2Te in three Nox Fort occurrences.....	77

14.7 Table of global unnamed Bi_2Te formulae, in Eloise Vein and in Lefevre skarn and vein mineralization	78
14.8 In Eloise Vein early-formed ingodite may react to form unnamed Bi_2Te with native gold (or electrum) deposited	79
15 Hedleyite Bi_7Te_3 or $\text{Bi}_{2+x}\text{Te}_{1-x}$	80
15.1 Hedleyite type locality – former Good Hope mine in BC, properties and associated minerals	80
15.2 Hedleyite – its formula and compositional range	80
15.3 Three other hedleyite localities in the Hedley district	80
15.4 Hedleyite in two other RIRG deposits in Canada	81
15.5 Hedleyite in some global RIRG deposits	82
15.6 Composition of Nox Fort hedleyites	83
15.7 Recalculating Ortosa gold skarn hedleyite analyses finds some are unnamed Bi_2Te	84
15.8 'Hedleyite' composition varies between Bi_3Te and unnamed Bi_2Te in the Viceroy gold mine	85
16 Pilsenite Bi_4Te_3	86
16.1 Pilsenite – type locality Nagyörzsöny in Hungary and its compositional range	86
16.2 Pilsenite and other Ag-Pb-Bi-Te-Se bearing minerals in the 'Bismuth Gold Zone' on the Jersey-Emerald property near Salmo	86
16.3 Pilsenite in the Buckhorn Mountain [Crown Jewel] RIRG gold skarn in northern Washington State	87
16.4 Pilsenite occurrence in some global RIRG systems	88
16.5 Pilsenite occurrence in two polymetallic deposits	89
16.6 Occurrence of Pilsenite in Adit 1 Crush Vein	89
17 Pavonite	90
17.1 Pavonite – type locality Bolivar Mine in Bolivia, properties	90
17.2 Pavonite – sole other Canadian locality	90
17.3 Pavonite some international localities	90
17.4 Composition of Pavonite in Lefevre vein	91
18 Tetradymite $\text{Bi}_2\text{Te}_2\text{S}$	92
18.1 Tetradymite – type locality Župkov in Slovakia	92
18.2 Tetradymite properties and compositional range	92
18.3 Tetradymite is stable at more oxidizing formation conditions	92
18.4 Tetradymite some BC localities	93
18.5 Tetradymite in Dublin Gulch, an 'oxidized' IRG deposit	94
18.6 Tetradymite in some global RIRG deposits	94
18.7 Tetradymite in some global polymetallic Sn W Bi Au Fe Pb Zn Ag and Cu deposits	95
18.8 Occurrence of Tetradymite in Adit 1 Crush Vein	96
19 Hessite Ag_2Te	97
19.1 Hessite properties	97
19.2 Hessite – type locality in eastern Kazakhstan	97
19.3 Hessite some localities in BC	97
19.4 Hessite occurrence in some global RIRG deposits	98
19.5 Hessite occurrence in two global polymetallic deposits	99
19.6 Composition of hessite in Adit 2 Underhand Stope Vein	99
20 Bismuthinite–aikinite series mineral in a Lefevre quartz + arsenopyrite vein cross-cutting the Lefevre skarn / hornfels	100
21 Does Jonassonite $\text{Au}(\text{Bi,Pb})_5\text{S}_4$ a new gold + bismuth mineral occur on Nox Fort?	101

Third Mineralogical Report detailing the finding of two 'new' gold-associated bismuth sulphotelluride minerals and identifying other opaque minerals, namely native silver electrum **tetradymite** **pilsenite** **hessite** bismuthinite–aikinite pavonite and greenockite characterizing a RIRG system in claim # 516584 and the Bunker Hill & Mormon Girl Crown Grants, on Nox Fort Project south of Salmo in Nelson Mining Division, southernmost British Columbia p. 5

22 Blue Quartz Vein has similar 'fracture-trails' of bismuth minerals as in secondary 'Type III' two-phase liquid and vapour fluid inclusions in the Batman gold orebody, Australia	102
23 Conclusions	104
24 Appendices.....	107
24.1 Appendix 1 Bismuth.....	107
24.2 Appendix 2 Tellurium.....	107
24.3 Appendix 3 Claim list.....	108
24.4 Appendix 4 Itemized Cost Statement	109
24.5 Appendix 5 Statement of Qualifications for Prof. Nigel J. Cook.....	112
24.6 Appendix 6 Statement of Qualifications for William R. Howard	113
24.7 Appendix 7 Mineralogy of the Kontaktovyi Stock <i>intrusion-hosted</i> RIRG system deposit in Far Northeast Russia	114
Dedication.....	115
25 References in chronological order.....	116
Part II Mineralogical report on the CLY property	151

List of Figures

- Fig. 1 Location of Nox Fort Project in the Nelson Mining Division, West Kootenays, southernmost BC, with some mineral deposits in the region (fig. from Jackaman & Höy 2004)
- Fig. 2A Index Map: CLY Group Location in BC
- Fig. 2B CLY Group Claim Maps 1:50,000 & 1:80,000 scale with tenures outlined
- Fig. 3 Gold Production & Reserves in the Extended Boundary–West Kootenay District hosts > 9 Million oz gold
- Fig. 4 Microphotos under reflected light of gold assemblages within pyrite in polished section of Adit 2 Underhand Stope Vein. Fig. 6 of Cook & Ciobanu Aug. 2006 in Howard 2006a
- Fig. 5 Close-up photos of Eloise Vein bismuth (sulpho)tellurides through binocular microscope by N. Cook
- Fig. 6 Enlarged close-up photo of Eloise Vein EL-05 ... likely joséite–B ... with hundreds of micron-sized native gold grains
- Fig. 7 Close-up photo of **ikunolite** from Ikuno mine, Japan
- Fig. 8 Back-scattered electron images showing assemblages of GBT minerals in sample 0414 from the Blue Quartz Vein.
- Fig. 9a & 9b Two back-scattered electron images of Maiskoe gold deposit GBT mineral assemblages from Cook et al. (2002)
- Fig. 10 Typical hand specimen of Eloise Vein North with mm-sized seams of dark blue-grey Bi-Te-S-(Se) minerals, slightly weathered
- Fig. 11 Four reflected light microphotos showing assemblages of gold and Bi-minerals in Eloise Vein South sample 0441. Figs. 11A & 11B display a well developed 'gold corona' texture at **ingodite**–**unnamed Bi₂Te** grain boundaries.
- Fig. 12 Back-scattered electron image of Ortosa gold skarn Bi-Te-Ag-Au patch with native bismuth Bi + **hedleyite** hed (or is it correctly **unnamed Bi₂Te**, see below), possibly an equilibrium assemblage, and **hessite** hs surrounding native gold
- Fig. 13 SEM back-scattered image showing a smooth curvilinear triple-junction between three bismuth minerals in L-11 skarn suggesting they formed at equilibrium conditions. Both **hedleyite** and **unnamed Bi₂Te** are identified by SEM analyses in L-11 skarn.
- Fig. 14 False-coloured image of a polished section of the Buckhorn Mountain gold skarn, from the South West Ore Zone.
- Fig. 15 Back-scattered electron image showing array of oriented blebs of "various bismuth minerals (bismuthinite, joséite–A and native bismuth) plus galena within [matrix] quartz" in polished section BQ-02 of the Blue Quartz Vein.

List of Tables

- Table 1A Details on the new tenure mineral claim #516584 in Nelson Mining District British Columbia owned by Clarke Gold Inc.
- Table 1B Details on the Crown Grant Mineral Claims in the Pend d'Oreille River area, Kootenay Land district, British Columbia owned by Clarke Gold Inc.
- Table 2 Microanalytical work on polished microscopic mounts prepared from 18 mineralized occurrences. Sections prepared from 6 samples on claim #516584 marked '■'
- Table 3 **ikunolite** formulae compared
- Table 4 **ingodite** formulae compared
- Table 5 **Unnamed Bi₂Te** formulae compared

Third Mineralogical Report detailing the finding of two 'new' gold-associated bismuth sulphotelluride minerals and identifying other opaque minerals, namely native silver electrum **tetradymite** **pilsenite** **hessite** bismuthinite–aikinite pavonite and greenockite characterizing a RIRG system in claim # 516584 and the Bunker Hill & Mormon Girl Crown Grants, on Nox Fort Project south of Salmo in Nelson Mining Division, southernmost British Columbia

p. 7

List of Maps

Map 1 Sites of Oct. 2007 mineralogical specimens on BiTel Knoll 1:200 scale

Map 2 Mineralogical specimens collected Oct. 2007 from... [the other showings] 1:2,000 scale

List of Appendices

Appendix 1 Bismuth

Appendix 2 Tellurium

Appendix 3 Claim list

Appendix 4 Itemized Cost Statement

Appendix 5 Statement of Qualifications for Prof. Nigel J. Cook

Appendix 6 Statement of Qualifications for William R. Howard

Appendix 7 Mineralogy of the Kontaktovyi Stock *intrusion-hosted* RIRG gold deposit in Far Northeast Russia

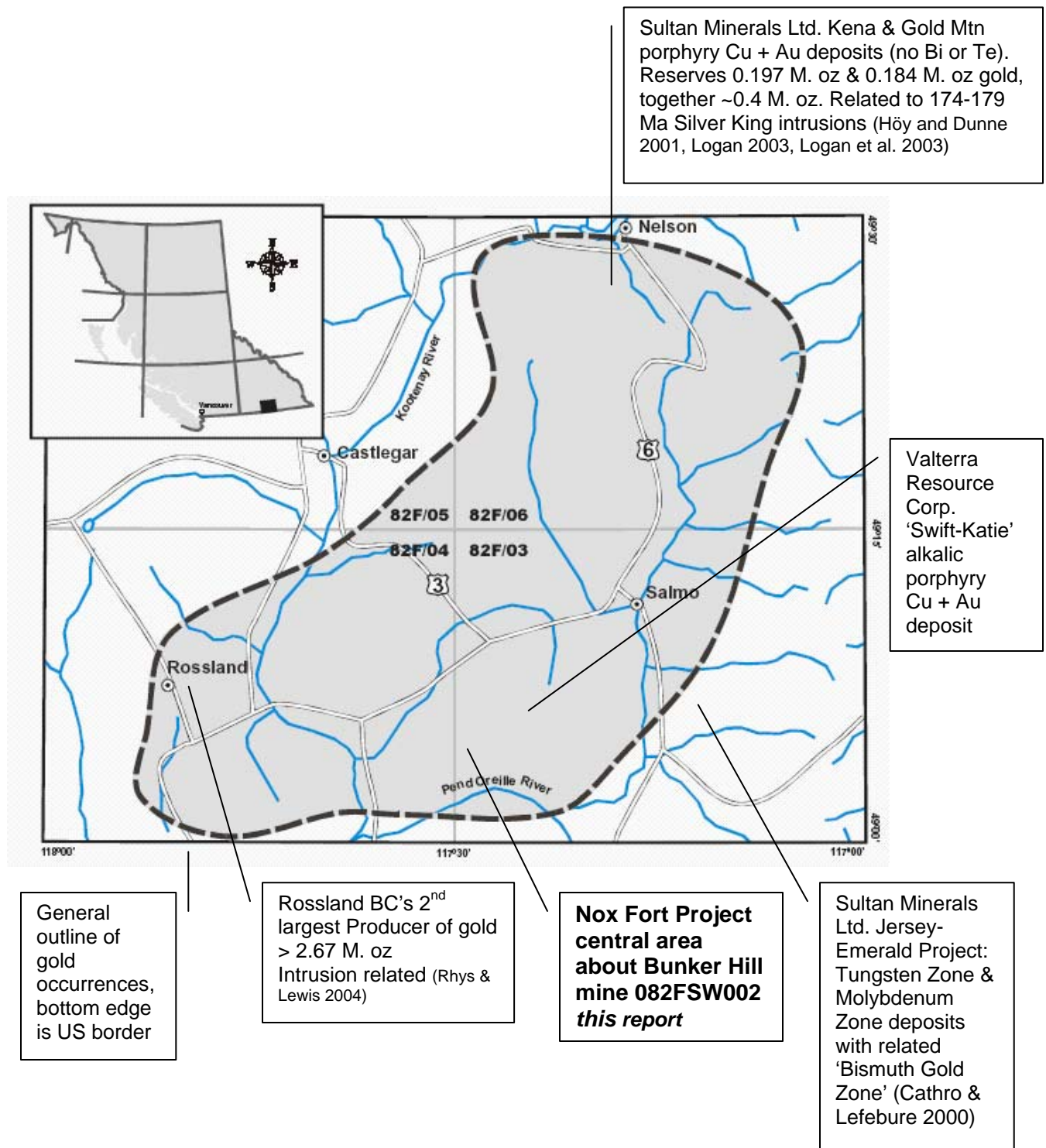


Fig. 1 Location of Nox Fort Project in the Nelson Mining Division, West Kootenays, southernmost BC, with some mineral deposits in the region (fig. from Jackaman & Höy 2004)

Third Mineralogical Report detailing the finding of two 'new' gold-associated bismuth sulphotelluride minerals and identifying other opaque minerals, namely native silver electrum **tetradymite** **pilsenite** **hessite** bismuthinite–aikinite pavonite and greenockite characterizing a RIRG system in claim # 516584 and the Bunker Hill & Mormon Girl Crown Grants, on Nox Fort Project south of Salmo in Nelson Mining Division, southernmost British Columbia

p. 9

MTO Online Inserts follow this page

Fig. 2A CLY Group Location Map in BC

Fig. 2B CLY Group Claim Map with two tenures outlined, creeks & roads at 1:50,000 scale

MTO Mineral Claim Exploration and Development Work/Expiry Date Change Confirmation
2008/Oct/15

See Appendix 3 for claim information

CLY Group Location Map

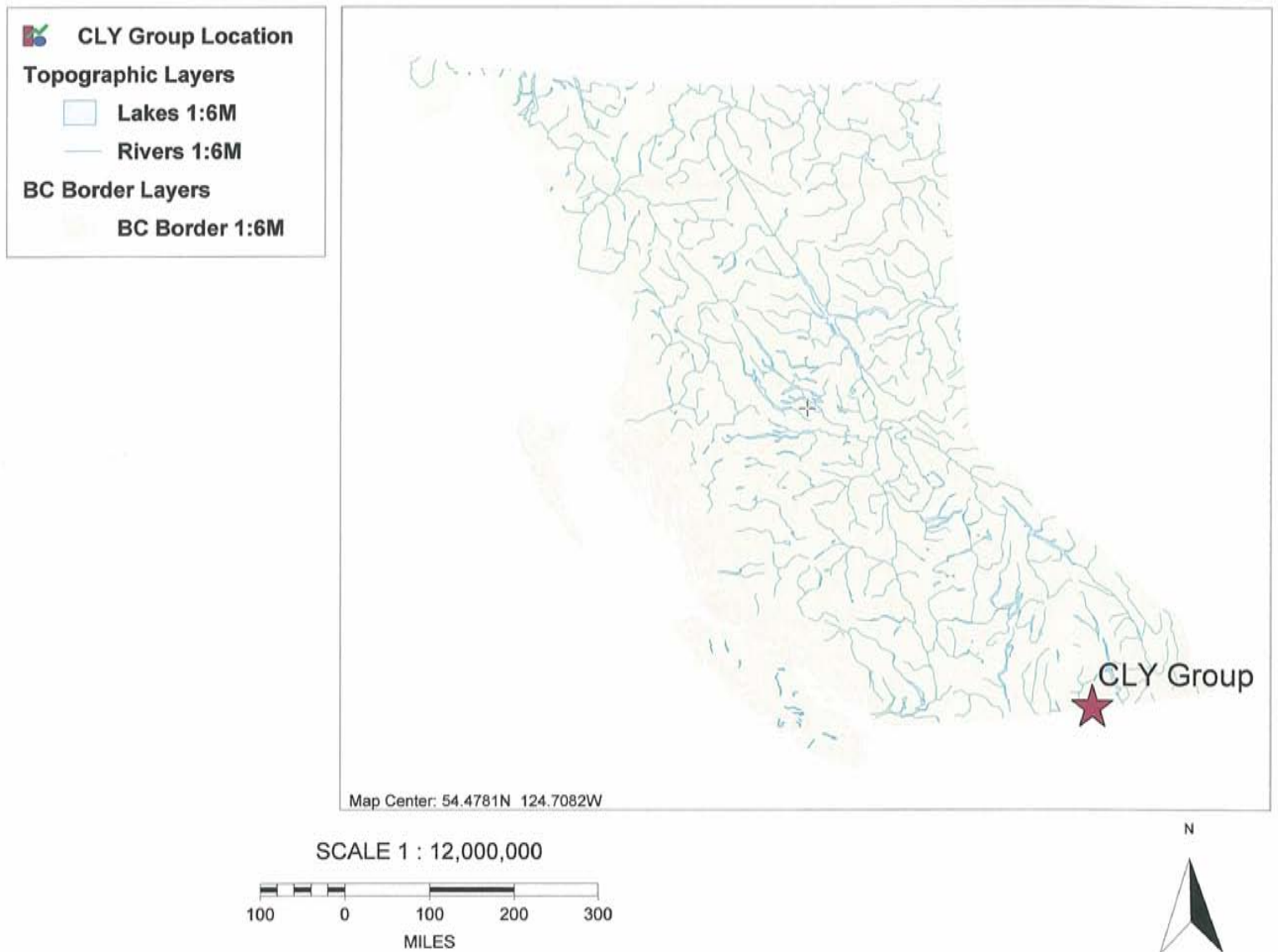


Fig. 2A

CLY Group Claim Map

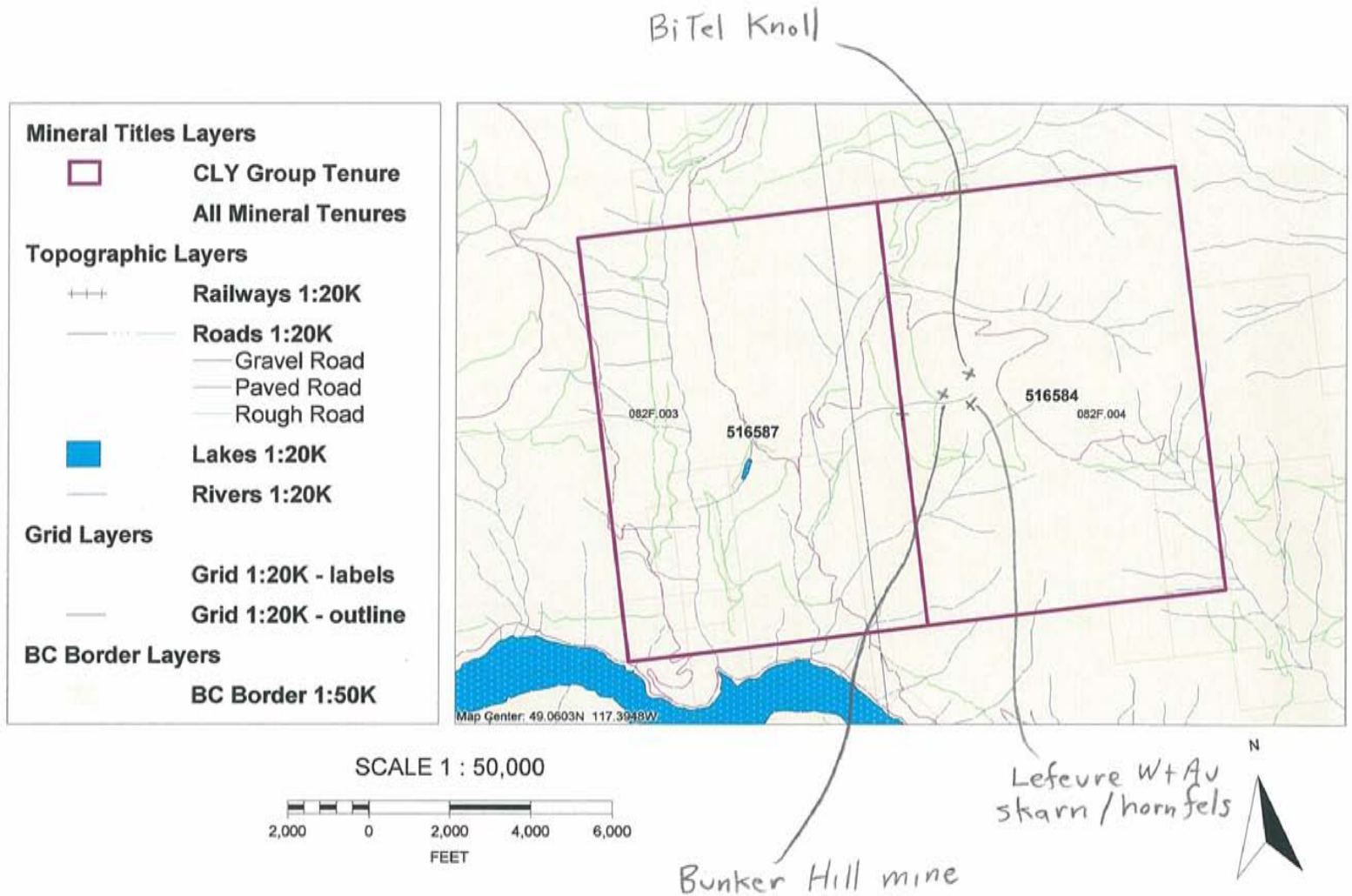


Fig. 2B


[Contact Us](#) [Help ?](#)

B.C. HOME

Mineral Titles

**Mineral Claim
Exploration and
Development
Work/Expiry Date
Change**

- ☒ Select Input Method
- ☒ Select/Input Tenures
- ☒ Input Lots
- ☒ Data Input Form
- ☒ Review Form Data
- ☒ Process Payment
- ☒ Confirmation

- [Main Menu](#)
- [Search for Mineral /
Placer / Coal Titles](#)
- [View Mineral Tenures](#)
- [View Placer Tenures](#)
- [View Coal Tenures](#)
- [MTO Help Tips](#)
- [Free Miner Land Owner
Notification](#)

[Exit this e-service](#)

Mineral Titles Online

**Mineral Claim Exploration and Development Work/Expiry Date
Change**

Confirmation

Recorder: CLARKE GOLD INC. (210814) Submitter: CLARKE GOLD INC. (210814)
 Recorded: 2008/OCT/15 Effective: 2008/OCT/15
 D/E Date: 2008/OCT/15

Your report is due in 90 days. Please attach a copy of this confirmation page to the front of your report.

Event Number: 4241547

Work Start Date: 2007/OCT/16
 Work Stop Date: 2008/OCT/15

Total Value of Work: \$ 3100.00
 Mine Permit No:

Work Type: Technical Work
 Technical Items: Geochemical

Summary of the work value:

Tenure #	Claim Name/Property	Issue Date	Good To Date	New Good To Date	# of Days Forward	Area in Ha	Work Value Due	Sub-mission Fee
516584		2005/jul/10	2012/mar/10	2012/Jun/13	95	740.85	\$ 1542.60	\$ 77.13
516587		2005/jul/10	2012/mar/10	2012/Jun/13	95	740.88	\$ 1542.65	\$ 77.13

Total required work value: \$ 3085.25

PAC name: Clarke Gold Inc.
 Debited PAC amount: \$ 0.00
 Credited PAC amount: \$ 14.75

Total Submission Fees: \$ 154.26

Total Paid: \$ 154.26

The event was successfully saved.

Please use **Back** button to go back to event confirmation index.
[Back](#)
[COPYRIGHT](#) | [DISCLAIMER](#) | [PRIVACY](#) | [ACCESSIBILITY](#)

1 Summary

This is the third and most comprehensive report detailing mineralogical research on mineralized samples from the CLY property, newly named the Nox Fort Project by Jaxon Minerals Ltd. [TSX-V JAX], the present operator. Previous reports Howard 2006a and 2008 identify some of the rarest minerals known in surface samples of auriferous quartz veins and skarn. The present research would be esoteric and academic if not for the fact that these are gold-associated minerals; some are often gold-bearing. From 32 mineralized specimens sent to Norway in Dec. 2007 18 polished thick sections including some polished thin sections were successfully prepared and examined with a reflected-light ore petrographic microscope (Table 2). The researcher Prof. Nigel J. Cook is a recognized authority and author of many research papers on bismuth (sulpho)telluride mineralogy (Appendix 5).

Large gold concentrations forming economic, mineable deposits are about as uncommon as the uncommon to exceptionally rare gold-associated Bi-Te-S-(Se) minerals in Nox Fort identified and described herein and in two previous reports. Gold showings on the central part of the property are greatly enriched in the uncommon element bismuth and moderately enriched in the very rare element tellurium (Appendices 1 & 2).

Formerly Howard (2006a & 2006b) proposed occurrences of native gold / electrum¹, native bismuth, bismuth telluride and bismuth sulphotelluride minerals, collectively 'GBT' Gold-Bismuth-Tellurides on the property characterized a newly discovered Reduced Intrusion Related gold 'RIRG' system (Hart 2007). This comprises *intrusion-hosted*, *proximal* and *intermediate* placed mineralization. In the central part of the property GBT are associated with sparse native gold in large quartz veins along an intrusive contact with the Bunker Hill sill (Map 1). This is a mid Cretaceous age felsic granitic body. One vein set, Clarissa Transverse veins, is visibly sheeted (i.e. repeated.) These features and the Bi-Au numerical systematics (Howard 2006b) well support applying C. Hart's RIRG system model (2005 & 2007).

The present research reinforces this interpretation with additional confirming evidence, e.g. "the comparable mineralogy in veins and skarn, identification of arsenopyrite and broad distribution of reduced Bi-mineral assemblages across the deposit. The study has proven that gold is associated, paragenetically, with bismuth minerals in all ore types on the property. CLY [Nox Fort] is demonstrated to be a single mineralised system, with mineralization consisting of both veins and skarns, all closely tied to the [Bunker Hill sill] granite which is the likely source of metals (Part II, conclusion by N. Cook)."

This report also thoroughly investigates other **worldwide occurrences of GBT minerals**, most easily attributed to parts of RIRG systems. There exists only a limited number of Bi-Te-S-(Se) mineral localities known worldwide; fewer are well researched. Incredibly a lot of these are small parts, though signposts, of large and valuable mineral deposits. The present study determines that these **comprise two types: RIRG systems² and polymetallic intrusion-related deposits of any combination of Sn Mo W Bi Cu Ag Pb Zn**. Silver bismuth tellurium and tungsten may be important in central parts of RIRG systems. Clearly Nox Fort is the central part of a RIRG system: "The property is interesting from a scientific as well as economic perspective, in that it represents an archetypal³ example of a RIRG deposit.

¹ Electrum is native gold with 20-80% silver by weight

² parts of these may have 'oxidized' Bi-Te-S-(Se) mineral assemblages, e.g. the Dublin Gulch Eagle Zone, see discussion under tetradymite

³ Representing or constituting an original type after which other similar things are patterned. Synonyms: archetypical, prototypal, prototypic, prototypical

This study, and any others that follow, can help increase understanding of how such mineralised systems form, and how gold may be distributed within them (in Conclusions and Recommendations, op cit.).”

1.1 Gold mineralogy of the veins

In the central area quartz veins native gold grains (correctly they are most often gold-rich electrum) associate with very minor to trace amounts of “a number of different bismuth tellurides (most commonly joséite–A $\text{Bi}_4\text{S}_2\text{Te}$, joséite–B $\text{Bi}_4\text{Te}_2\text{S}$, **hedleyite** Bi_7Te_3 and unnamed Bi_2Te), but also with bismuthinite (in Conclusions and recommendations, op cit.).” With the GBT minerals minor amounts of any of: galena molybdenite arsenopyrite pyrrhotite pyrite and marcasite occur. These form differing mineral assemblages.

Mineralogical study of polished section BH UHS-4 from the Bunker Hill mine Adit 2 Underhand Stope Vein (Map 2) determines that the gold mineral is actually silver-rich electrum. More than 20 grains were counted; these commonly are inclusions in pyrite grains, most “less than 10 μm in diameter. Many are elongate to 30 μm long (Bunker Hill mine section, op cit.).”

The Bunker Hill mine veins “carry significant amounts of gold, as fine-sized [silver-rich electrum] grains not necessarily tied to Bi-minerals ... [these are] closely associated with pyrite and not finely distributed throughout the quartz. This was known previously:

‘The operation of the old 10-stamp mill erected in 1900 is reported to have been of very short duration as the ore was not amenable to straight amalgamation, the gold values being chiefly associated with pyrite {AR 1934 p. E24}’ (op. cit.).”

Concluding, very practically pyrite content may reliably indicator gold and silver content in the Bunker Hill mine veins, as included 5-30 micron-sized, silver-rich electrum grains.

In a former study of polished section 0407 of Clarissa Main Vein (Map 1) “No Bi-minerals were observed in the section. We note relict magnetite and also rutile. Several grains of native gold, typically 5-20 μm in size were observed (photograph). A number of much finer gold grains were also noted in the matrix (Cook & Ciobanu 2006).

In three Eloise Vein polished sections plotted on Map 1:

EL-02 has 2 gold-rich electrum grains ca. 10 μm in diameter

EL-05 has 29 native gold grains most <10 μm ; minor grains associated with Bi-Te minerals are generally larger sized (to 20-25 μm)

EL-07 has 11 gold-rich electrum grains <20 μm sized, “roughly equally divided between being scattered throughout the quartz matrix and in paragenetic association with the Bi-minerals [bismuthinite and the ‘new’ phase $\text{Bi}_4\text{Te}_3\text{S}_2$] (Eloise Vein section, Part II)”.

Concluding, Eloise Vein has common, generally 5-20 micron-sized, native gold to gold-rich electrum grains, isolated in matrix quartz or spatially associated with patches of Bi-Te-S minerals. The latter may be larger.

1.2 Iron sulphide minerals in two polished sections carry no 'invisible' or dissolved gold

Laser ablation analysis of polished sections BHUS-01 from Adit 2 Underhand Stope Vein of the Bunker Hill mine and L-11 from the Lefevre skarn (both on Map 2) finds no 'invisible gold' (a term for both gold in the pyrite lattice itself and sub-microscopic gold inclusions) in the iron sulphides pyrite pyrrhotite and marcasite. "The contents of As are negligible. The only minor components at levels in the hundreds of ppm range are cobalt and nickel.

Concentrations of other elements commonly occurring in Fe-sulfides (Cu, Se) are very low, excepting Bi at 462 ppm and Pb at 687 ppm in BHUS-01 (spot 1). There Te is also enhanced at 0.77 ppm (Laser ablation analysis section in Part II)."

These results are important for economic recovery of the gold (ore beneficiation), discussed in section 8.4. Some Eloise Vein bismuth minerals host 'invisible' gold, notably three **unnamed** Bi_2Te grains 57 ± 8 , 6.8 ± 1 , 3.6 ± 0.7 ppm Au, **ingodite** 9 ± 1.8 and joséite–A or –B 26 ± 5 ppm (Cook et al. 2007c). Though as "bismuth is nonrefractory as pertains to cyanide, the associated gold is thus highly amenable to cyanide leach (McCoy et al. 2002)".

1.3 Gold Fineness in the Adit 2 Underhand Stope Vein and Eloise Vein

The mean 'atomic' gold fineness 0.521 for eight electrum grains analyzed in polished section BH UHS-4 of the Adit 2 Underhand Stope Vein well compares with the 588 'bulk' fineness⁴ of the 1934 91 ton lot mined from the Adit 2 Underhand Stope Vein. Ray (2004) observed "minor sericite and calcite" in the veins; the implied sericitic alteration concurs with the low fineness of the gold. McCoy (2000) describes lower temperature sericitic alteration, generally <400 °C, at Fort Knox with a different fineness range 801-890. Clearly, applying the RIRG model, the Bunker Hill mine veins are *intermediate* (to even *distal*) placed w.r.t. the Bunker Hill Sill.

Gold grains with compositions bordering native gold to gold-rich electrum in Eloise Vein have variable mean gold fineness. In three sites along the vein

[1] Eloise Vein South EL-02 fineness is 778 for 2 determinations

[2] Eloise Vein North EL-05 fineness is 843 for 2 of 29 observed gold grains

[3] Eloise Vein North EL-07 fineness is estimated ~600, no values on 11 observed electrum grains.

Using a fineness range 778-843 for Eloise Vein, this is less than the Fort Knox potassic alteration range 907-977 and albitic alteration range 913-1000 tabled by McCoy (2000, p. 78). More fineness determinations are necessary. Eloise Vein's approximate mean fineness is 811 for the 4 values.

⁴ 'Bulk' fineness considers total gold & silver present. In high fineness ore most of the gold is metallic [native] gold, with low silver content in any accompanying ore minerals (after Boyle 1979). For this case 'bulk' fineness approximates the 'true' fineness of the gold grains present. Fineness is $(\text{Au} / (\text{Au} + \text{Ag})) * 1000$, metals in weight percent, as parts per thousand. Fineness varies from nil (pure silver) to 1000 (pure gold).

1.4 Two 'new' mineral phases $\text{Bi}_4\text{Te}_3\text{S}_2$ and $\text{Bi}_8\text{Te}_5\text{S}_4$ in Eloise Vein

Repeated semi-qualitative EDS analyses on several grains in two polished sections of Eloise Vein suggests **two new previously unidentified mineral phases on the property** (Eloise section, Part II):

$\text{Bi}_4\text{Te}_3\text{S}_2$

mean of 2 analyses in EL-05 is close-to-stoichiometric

$(\text{Bi}_{3.775}\text{Pb}_{0.25}\text{Sb}_{0.10}\text{Ag}_{0.025}\text{As}_{0.01})\text{sum}_{3.985}\text{Te}_{2.60}\text{Se}_{0.04}\text{S}_{2.20}\text{sum}(\text{Se} + \text{S})_{2.24}$

mean of 8 analyses in EL-07 is near-ideal

$(\text{Bi}_{3.905}\text{Pb}_{0.086}\text{Sb}_{0.019})\text{sum}_{4.01}\text{Te}_{2.863}\text{Se}_{0.008}\text{S}_{2.118}\text{sum}(\text{Se} + \text{S})_{2.126}$

Considering analytical error the only real difference in the formulae from the two sites is minor Pb with trace Ag Sb & Se in EL-05 vs. trace Pb in EL-07 (ignoring element contents $<0.01 \text{ apfu}^5$).

$\text{Bi}_4\text{Te}_3\text{S}_2$ is pink-brown in reflected light, homogeneous and generally enclosed (mantled) by bismuthinite. In EL-05 grain size is ~0.5 mm.

$\text{Bi}_8\text{Te}_5\text{S}_4$

mean of 3 analyses in EL-05 is near-stoichiometric:

$(\text{Bi}_{7.517}\text{Pb}_{0.453}\text{Sb}_{0.137})\text{sum}_{8.107}\text{Te}_{4.973}\text{Se}_{0.013}\text{S}_{3.96}\text{sum}(\text{Se} + \text{S})_{3.973}$

$\text{Bi}_8\text{Te}_5\text{S}_4$ occurs as ~60 micron sized tabular crystals, variably replaced.

These new phases are gold-associated, and well deserve further analytical characterization to substantiate them as 'new' minerals. Metal:Chalcogen ratios are ideally $4:5 = 0.80$ and $8:9 = 0.89$, analyses giving 0.813 for $\text{Bi}_4\text{Te}_3\text{S}_2$ (mean ratio in EL-05 & EL-07) and 0.912 for $\text{Bi}_8\text{Te}_5\text{S}_4$ (in EL-05). **Both ratios are slightly less than one.** This contrasts with ratios ≥ 1 for most all other bismuth (sulpho)telluride minerals in Nox Fort, these considered 'reduced' mineral species.

1.5 Newly identified minerals; *gold tellurides* do not occur

In addition to minerals noted in previous reports native silver electrum **pilsenite** **tetradymite** **hessite** pavonite an undetermined bismuthinite–aikinite series mineral and the two unknown phases $\text{Bi}_4\text{Te}_3\text{S}_2$ $\text{Bi}_8\text{Te}_5\text{S}_4$ (above) are identified herein. In all examine polished sections gold tellurides are completely absent. This indicates the chemical concentration (fugacity) of tellurium, abbreviated $f\text{Te}_2$, was not sufficiently high to reach the stability field of calaverite AuTe_2 .

1.6 Unnamed Bi_2Te and **hedleyite** occurrences appear spatially zoned

Near-stoichiometric unnamed Bi_2Te occurs in two polished sections of Eloise Vein South EL-02 and 0441⁶ (both on Map 1) and in a Lefevre quartz-arsenopyrite vein, section L-04QVXtry (on Map 2). The latter is one of two veins crosscutting the Lefevre skarn in trench #5. **These occurrences of proximal-placed unnamed Bi_2Te contrast with intermediate-placed **hedleyite** occurrences in three Bunker Hill mine veins:**

⁵ atom per formula unit

⁶ for description see Cook et al. 2007c)

in BH UHS 1 from Adit 2 Underhand Stope Vein, two analyses have $x = 0.16$ and 0.17

in BHA-1-8 from Adit 1 Crush Vein, one analyses with $x = 0.18$

possibly in BH-0567 from near Adit 1 (analysis is suspect), all on Map 2

X refers to the hedleyite formula $\text{Bi}_{2+x}\text{Te}_{1-x}$ where $x = 0.13$ to 0.19 . Surprisingly, in Lefevre skarn / hornfels section L-11 skn both **hedleyite and **unnamed Bi_2Te** occur.** In that microscope mount they are both near–stoichiometric (that is near–ideal) phases.

In discussing bismuth (sulpho)tellurides the Metal:Chalcogen ratio = Sum (Bi + Pb + Sb + Cd) vs. Sum (Te + Se + S) is useful (Godovikov et al. 1971). The three **hedleyites** from the Bunker Hill mine veins have excess metal cations Bi Pb and/or Sb, the Metal:Chalcogen ratios respectively 2.57 2.61 2.56 and 2.37. The ideal ratio is $7/3 = 2.33$.

“**Ingodite**, joséite–A, **unnamed Bi_2Te** and the two uncharacterized ‘new’ phases found in Eloise Vein do not occur in the Bunker Hill veins (Part II)”. The reason is unknown.

1.7 Minerals have very low selenium content; **ikunolites** are Te-rich

Selenium is near absent in all the SEM-EDS analyses presented herein and in the former microprobe analyses (2008). Thus on Nox Fort ‘ideal’ **ikunolite** is properly Bi_4S_3 , not $\text{Bi}_4(\text{S},\text{Se})_3$, the formula in the second report ‘Continuing Mineralogical Research...’.

Ikunolite grains in BHA-1-8 section of Adit 1 Crush Vein and in L-04QVXtry, a polished section of a quartz-arsenopyrite vein cutting the Lefevre skarn / hornfels, (Map 2) both have significant Te-for-(Se,S) substitution. Te substitutes for S; Se is near absent. **Adit 1 Crush Vein ikunolite is the most tellurium-rich known, comparing 11 other worldwide localities, and L-04QVXtry ikunolite from a Lefevre vein is the second-richest (Table 3).**

Researchers in the USSR note in granitoid-related gold deposits of the Russian Far East “Native gold of later paragenetic stages [though still early-stage assemblages] occurs with bismuthinite, **ikunolite**, **hedleyite**, joséite [-A] and native bismuth (Gamyagin 1995). It is surprising that occurrence of **ikunolite** in the western hemisphere has not been previously documented.

Ingodite solely found in Eloise Vein is near-stoichiometric. Pb at ~ 0.1 apfu is typical; Sb & Se are trace. Metal:Chalcogen ratios are slightly lower than the expected 0.98-1.08 range (Cook et. al. 2007b). Metal ion content is slightly lower than chalcogen content in the formula.

Unnamed Bi_2Te is near near-stoichiometric in three Nox Fort occurrences.

1.8 Lefevre skarn has Bi-Te-S mineral assemblages similar to the veins

Fig. 13, an electron image of polished section L-11 skn of the Lefevre skarn / hornfels, illustrates smooth curvilinear boundaries forming a triple-junction between a patch of three bismuth minerals native bismuth joséite-B and **hedleyite** (or **unnamed Bi_2Te**). This suggests the patch formed at equilibrium conditions from a Bi-Te-S bearing melt. This well illustrates the ‘liquid bismuth gold-collector model of Douglas et al. 2000. Almost certainly some of the minerals in L-11 skarn are gold-bearing (like fig. 6).

L-11 skarn (on Map 2) has diopside and a carbonate mineral, dominant pyrite and small amounts of both **hedleyite** and **unnamed Bi₂Te**, native bismuth, pyrite, marcasite, pyrrhotite, sphalerite, galena, chalcopyrite and scheelite. **Hedleyite** and **unnamed Bi₂Te** are identified by SEM analyses. That the same Bi-Te-S minerals occur in skarn as in quartz veins shows the same mineralizing processes operated throughout the central area of the property. The Nox Fort occurrences are parts of the same RIRG system. As the Lefevre skarn is a large body, it is a prime drill target.

1.9 Chemical conditions of mineral deposition well compare to Pogo and Fort Knox deposits

“The environment of formation of the gold-associated Bi-Te mineral assemblages at CLY [Nox Fort] is like that proposed for the Pogo [3.51 M. oz.] and Fort Knox deposits (Rombach et al., 2004) with the same late stage sulphidation. Chemical environments were highly localised as the bismuth telluride mineral species vary from one polished section to the next (Part II)”. Fort Knox is a ‘type’ deposit defining the RIRG model {Bakke et al. (1998) abstract in refs., McCoy et al. (1997), McCoy (2000)}. Pogo is more controversial but McCoy (2000) and Ebert et al. (2003) consider it intrusion-related. Both are in Alaska. Pyrite overgrowths on pyrite cores in the Moly Quartz vein polished section M-01 is firm evidence of late stage sulphidation.

1.10 Tally of the same rare gold-associated Bi-Te-S minerals on Nox Fort as in the Pogo deposit

Presently **9 of 13 GBT minerals that characterize the Pogo deposit (Rombach et al. 2002) occur** on central Nox Fort. These are identified microscopically in polished sections of specimens of veins at the surface and in mine dumps, with identification of **tetradymite** and **pilsenite** in the present study. Listed in order of their abundance in Pogo these are:

joséite–B Bi₄Te₂S
gold with fineness 850-1000
tetradymite Bi₂Te₂S
pilsenite Bi₄Te₃
native bismuth Bi
bismuthinite Bi₂S₃
ingodite Bi₂(Te,S)
hedleyite Bi₇Te₃
joséite–A Bi₄TeS₂

Thus far sulphotsumoite Bi₃Te₂S maldonite Au₂Bi tsumoite BiTe and baksanite Bi₆Te₂S₃ are not identified. Upon re-reading D. McCoy’s (2000) thesis, in his Fig. 43 **two mineral analyses plotted from Pogo deposit white/gray quartz veins have the composition of unnamed Bi₂Te**. With three occurrences of **unnamed Bi₂Te** on Nox Fort, the analogous mineralogy is even more striking: consider **Nox Fort hosts 10 of 14 GBT minerals in Pogo**.

1.11 Considering the sub-type of RIRG mineralization represented, Nox Fort is a prime target for an economic gold + bismuth deposit

Practically, considering the deeper-formed central-placed sub-type of RIRG deposits that Nox Fort represents, “Due to the large resource and non-refractory nature of the ore, [these] deposits are certainly attractive exploration targets (McCoy 2000).” There is numerical evidence from geochemistry that Nox Fort may hold a large gold resource (e.g., Howard 2006d letter to G. Schellenberg).

The property is in the extended Boundary–West Kootenay District in south BC, a region that hosts 9 Million oz gold (after Caron 2003, fig. 3). Importantly GBT minerals “control the distribution and impact on the overall gold balance in ... ores” (Ciobanu et al. 2006b); as they are direct associates of gold the research presented herein is quite relevant to property exploration.

1.12 Low-cost gold extraction indicated

Several mineralogical and geochemical features of Nox Fort mineralization favour low-cost gold recovery, if an ore body is drill-indicated (section 8.4).

1.13 Geochemistry and mineralogy of the ‘Bismuth Gold Zone’ on the Jersey- Emerald property differs, as does the targeted commodities

The geochemistry and mineralogy of the ‘Bismuth Gold Zone’ on Sultan Mineral's Jersey-Emerald property 13 km east (fig. 3) differs from Nox Fort's. Bismuth minerals there are Ag, Pb, Sb and often Se-bearing; some are selenides, not tellurides (section 16.2). Contrast these with the Pb and Sb poor bismuth (sulpho)telluride minerals directly associated with native gold or electrum on Nox Fort described herein. Sb and Se are near absent. **The geochemistry and mineralogy reflects which elements are possibly concentrated in economic deposits at the property scale:** Mo W Pb Zn in the Jersey-Emerald property of Sultan Minerals Inc. vs. Au (Ag) Bi Te W in the Nox Fort property of Jaxon Minerals Inc., at least about the central part investigated herein.

1.14 Recommendations for further mineralogical work

The goal of exploration is to find concentrations of auriferous GBT minerals on the property. Mineralogical research has been found to be a practical and cost-effective tool to understand formation conditions of the diverse gold-associated minerals. Further mineralogical research is suggested.

[1] Additional reflected light ore microscopy, Scanning Electron Microscopy – Energy Dispersive Spectrometry ‘SEM-EDS’ and electron microprobe study of new specimens from:

- {a} outcropping Adit 1 Gallery Quartz Vein [4 sections along its ~ 80 m exposed length]
- {b} Lefevre quartz vein in **N wall** of pit in trench #5, well exposed [2]
- {c} Cleave granite-hosted shear veins [4]. These Bi + Te auriferous semi-brittle shears have sericitic alteration + pyrite overprinting feldspathic alteration. C.f. Eloise Vein Ag and As are more abundant, and bulk gold fineness values lower, with a larger range.
- {d} Eloise Vein to clarify the unusual mineralogy [at least 6]

{e} Clarissa Main Vein [2]. (Clarissa Vein)

Two sections were prepared from sample 0407 by N. Cook in 2006 (Howard 2006a, Part II). "One section contained no opaque phases. The other section revealed gold within the vein matrix (his Fig. 5). No Bi-minerals were observed ... [but] relict magnetite and also rutile. Several grains of native gold, typically 5-20 µm in size were observed (photograph). A number of much finer gold grains were also noted in the matrix." New sections should be prepared in an effort to identify the associated Bi-minerals indicated by assays (0404 ran 217 ppm Bi / 13.8 Te / 13 Mo / 30.19 Ag / 186 Pb with 3.24 g/t Au).

{f} Cm-sized blue grey quartz veins in feldspathic altered granitoid below - very early-stage [4 over a length of over ten meters]

{g} Moly Quartz Vein hosts since-unfound gold values (Minister of Mines 1936). Uncover this for further samples [2]

{h} additional sample of Blue Quartz Vein from present scarce material [1]

{i} Blue grey quartz along Bunker Hill mine road in aplite dyke [2]

and any other Au-bearing occurrences unknown to the writer [~10 sections]

Total about 37 polished sections. More gold fineness determinations are necessary on the three existing Eloise Vein polished sections.

[2] A thorough fluid inclusion study of quartz veins and skarn to quantify the P-T-X conditions of formation of this diverse and potentially economic Au-Bi-Te-(S) mineralization.

[3] Mineralogical characterization of the **two 'new' gold-associated minerals $\text{Bi}_4\text{Te}_3\text{S}_2$ and $\text{Bi}_8\text{Te}_5\text{S}_4$** in Eloise Vein in further specimens, contracting microprobe and XRD research to confirm their existence as new substances.

1.15 Synopses of the first 2006 report

The first report "Rare to exceptionally rare Gold-associated Bi–Te–S–(Se) ore minerals new to Canada: **ingodite** **ikunolite** and **unnamed Bi_2Te** ..." (Howard 2006a) details preliminary mineralogical research by N. Cook & C. Ciobanu on opaque ore minerals from surface samples of BiTel Knoll quartz veins on claim # 516584 (former name CLY 2) and a dump piece of the Bunker Hill mine Adit 2 Underhand Stope Vein. Eight polished sections [microscopic mounts for ore petrography] were prepared from 5 occurrences. The rare minerals occur in three sections: two of the Blue Quartz Vein sample 0414, and one of Eloise Vein South 0441. Both veins partly outcrop on BiTel Knoll. Associates are joséite-A $\text{Bi}_4\text{S}_2\text{Te}$, joséite-B $\text{Bi}_4\text{Te}_2\text{S}$, **hedleyite** **Bi_7Te_3** , native gold, native bismuth and scheelite CaWO_4 . Molybdenite and bismuthinite Bi_2S_3 are the only sulphides present. These form varied mineral assemblages (parageneses). "Native gold (electrum) is identified in all samples investigated. It is generally fine-grained (> 50 µm) and occurs in intergrowths with various Bi-minerals, as well as isolated grains within the matrices of the veins" (Cook & Ciobanu 2006).

It is surprising that these especially rare minerals occur in 3 polished sections of the only 8 prepared from surface samples of only two quartz veins. The area is generally well covered. **Ingodite** in Eloise Vein is only its third documented occurrence in North America. It occurs in all three mineral assemblages defined by C. Rombach et al. 2004 in the Liese Zone **Pogo AK deposit** [3.51 M. oz]. Auriferous Au-Bi bearing hydrothermal fluids that formed Pogo are proposed to be magmatic-sourced (Moore 2000); field relationships of Eloise Vein also suggest the same. Preliminary mineralogical research in 2006 infers formation conditions are markedly similar.

A section of a dump sample of the mined *intermediate placed* Bunker Hill mine Adit 2 Underhand Stope Vein shows pyrrhotite altering to pyrite and marcasite with nucleation of native gold grains. The same change of formative chemical conditions is suggested for Fort Knox (McCoy 2000) and Pogo: “data indicate a change from very low fS_2 and/or high T (loellingite-pyrrhotite stable) to higher fS_2 and/or lower T (pyrite stable) over time (Rombach et al. 2002).”

R. Ramik of the Royal Ontario Museum provided stereomicroscope descriptions of Eloise Vein Eloise Vein South 0441 and Eloise Vein North 0412 samples.

The preliminary mineralogical work was commissioned as in 2005 R. Goldfarb of the USGS in Denver reported an X-Ray Diffraction pattern of a mineral in a hand specimen of Eloise Vein South gave “a very distinct Bi-Te-S signature with no trace of other species. The XRD analysis indicated **ingodite**, bismuthinite and ...native bismuth. Also, although not 100% certain, there is likely a trace of **tetradymite**⁷ (p.c. Nov. 2005)”. Goldfarb first reported **ingodite** in Canada.

The Bi–Te–S–(Se) ore minerals occur in apparently barren quartz veins as mm or sub-mm sized silvery-white patches with brilliantly glistening metallic lustre. Hand lens examination does not distinguish them. Thus laboratory analytical work is necessary to identify these gold-associated minerals.

The first report qualitatively identifies the GBT minerals by reflected light ore microscopy and Scanning Electron Microscope – Energy Dispersive Spectroscopy (SEM-EDS). Microphotographs show native gold grains with blebs of GBT minerals in various assemblages. Several show textures inferring sub-microscopic ‘dissolved’ gold in **ingodite** Bi_2TeS grains that later nucleated to form native gold grains in surrounding **unnamed** Bi_2Te grains close to the boundaries of these mineral. Figs. 11A & 11B well display this corona texture.

Generally these rare GBT ore minerals are identified after much more thorough mineralogical examination of developed or presently-mined worldwide RIRG deposits, specifically Pogo in Alaska [3.51 M. oz.] has **ingodite** in all three mineral assemblages (Rombach et al. 2002 & 2004) and Petráčková hora [1.03 M. oz.] in Czech Republic has **ingodite** and **unnamed** Bi_2Te (Zachariáš et al. 2001). The report interprets the genesis of the Bi–Te–S–(Se) mineral assemblages with reference to more thoroughly researched deposits.

That report proposes that the consistent group of bismuth tellurides and sulphotellurides present in the polished thick sections distinguish and characterize an *intrusion-hosted / proximal* placed sub-type of Reduced Intrusion-Related gold deposit. It includes a thorough review of the scarce occurrences of similar mineralization worldwide. Appendix 1 lists occurrences of rare Bi–Te–S minerals identified in BC deposits with original references. **ingodite** and **ikunolite** are unknown; **unnamed** Bi_2Te is also identified by N. Cook & C. Ciobanu in a sample of the Hedley district Good Hope skarn. Part II of the first report is the preliminary Aug. 2006 report by N.J. Cook & C.L. Ciobanu.

The first report notes the property’s Au–Bi–Te mineralization with abundant bismuth and tellurium appears to be unique in British Columbia. The mineralogical study confirms mineral and element zoning of the RIRG system which is at least half a km in extent. A recent genetic model for gold concentration was discussed as applicable (section 7.4) and formation conditions were surmised (7.5). As in both the Fort Knox and Pogo deposits (Rombach et al. 2004) latter stage sulphidation may be a key mechanism of gold deposition in Nox Fort. The first report is preliminary work with so few samples examined. Further mineralogical investigation was deemed useful as an intrusion (granite)-centered, bulk tonnage, low grade, non-refractory economic gold deposit might occur.

⁷ This report first confirms tetradymite does occur

1.16 Synopses of the second 2008 report

The second report "Continuing Mineralogical Research on rare to exceptionally rare gold-associated Bi-Te-S-(Se) ore minerals new to Canada..." (Howard 2008) quantifies the elemental chemistry of the Bi-Te minerals by electron microprobe analysis. This allows calculation of precise empirical mineral formulae⁸. Bismuth telluride and sulphotelluride minerals are only ideally stoichiometric, meaning the constituent atoms Bi Te and S have integer values in the individual mineral formulae. Microprobe analyses show the Nox Fort Bi-Te-S-(Se) minerals are near stoichiometric. Lead is near absent except in Blue Quartz Vein **ikunolite**. Details are in the research paper 'Bi-tellurides in gold veins, BiTel Knoll (CLY prospect), southeastern British Columbia, Canada' by N.J. Cook, C.L. Ciobanu & W. Howard. This was published Aug. 2007 by the Geological Survey of Finland [GTK], Part II of the second 2008 report.

Five polished sections of three occurrences were investigated. Sixteen mineral formulae were obtained, 11 of minerals in samples from Eloise Vein South and North in claim #516584 and 5 of Blue Quartz Vein minerals. Compositional formulae of the Bi-Te-S-(Se) minerals in the BiTel Knoll quartz veins have Bi + trace Pb + trace Cd more abundant than Te + Se + S (fig. 8 therein). In other words the Metal:Chalcogen ratio is greater than 1. Consequently the minerals are considered 'reduced' phases stable with pyrrhotite, arsenopyrite and löllingite (Cook et al. 2002).

The rationale for this is that in chemical space concentrations of oxygen⁹ fO_2 and sulphur fS_2 form stability fields for the four common iron sulphide and iron oxide minerals pyrite pyrrhotite hematite and magnetite. At BiTel Knoll the Bi-Te-S-(Se) minerals occur in varied mineral assemblages in quartz veins, generally with native gold, native bismuth and molybdenite. That the minerals and their assemblages are considered 'reduced' is compatible with the siting of the quartz veins near reduced graphitic metasediments. These are close to a contact with an ilmenite-bearing felsic biotite granitoid, the Bunker Hill sill, itself considered to be reduced as the magnetic susceptibility is near nil. N. Cook (in Cook & Ciobanu 2006) observed "relict magnetite and rutile" in polished section 0407 from Clarissa Main vein with "several grains of native gold, typically 5-20 μ m in size". The second report suggests the Nox Fort mineral assemblages formed in the pyrrhotite / magnetite¹⁰ stability fields.

Compositions of these rare minerals are compared to other localities, mostly past or presently producing deposits. Research work on other occurrences is noted, advancing the understanding of the ore genesis, meaning estimating the formation conditions of gold deposition. **The second report notes 7 of 13 GBT minerals identified in a thorough research study of the Liese Zone in the Pogo AK deposit [3.51 M. oz] (Rombach et al. 2002) occur in only five polished sections of Eloise Vein and the Blue Quartz Vein:**

native gold native bismuth bismuthinite joséite-B joséite-A **ingodite** and **ikunolite**.

From the literature it is observed that trace **ingodite**, **ikunolite** and unnamed Bi_2Te also occur sparsely in some researched intrusion-linked 'contact metasomatic' mined polymetallic deposits of any of Sn Mo W Bi Pb Zn Ag worldwide. Kingsgate NSW Australia Mo + Bi deposits have **ikunolite**. Intriguingly, three polymetallic deposits are very large and productive ore bodies in Far East Russia (Siberia)¹¹:

⁸ the minerals often include other elements in their formulae, notably Pb Cd & Sb

⁹ f is fugacity or standard chemical activity

¹⁰ this report first identifies magnetite in sample BH UHS 1 from the Adit 2 Underhand Stope Vein of the Bunker Hill mine. Some mineral assemblages on the property formed in the pyrrhotite / pyrite stability fields.

¹¹ a pessimist would note Russian researchers are very adept at investigating ore mineralogy; this does not negate the practical utility of the present research.

ikunolite in Vysokogorsk tin deposit

ikunolite in Vostok-2 skarn scheelite–sulphide tungsten deposit

ingodite in Tyrnyauz tungsten + molybdenum deposit

Why do these peculiar minerals denote high prospectivity for very large polymetallic mineral deposits, as well as well-endowed RIRG gold deposits?

The second report also includes results of a state-of-the-art microanalytical technique, micro-ablation by Laser Ablation - Induction Coupled Plasma - Mass Spectrometry [LA-ICP-MS]. Minerals in three sections of Eloise Vein North and Eloise Vein South were ablated. Results show “Au contents [of four Bi-Te minerals from Eloise Vein North] are higher [than five minerals from Eloise Vein South] by at least one order of magnitude¹². Gold content in bismuthinite is comparable to that in coexisting tellurides. The highest Au concentrations do not appear to be restricted to one bismuth telluride species in particular. For example, **ingodite** can be the most and least Au-enriched within individual patches (Cook et al. 2007c in Part II).” The reader might think this similar to the ‘gold nugget effect’ at macroscopic (hand specimen) scales. On the microscopic scale varying gold is due to a ‘blebby bismuth’ effect: individual blebs of Bi-Te melt scavenged varying amounts of gold from diverse hydrothermal fluids. The blebs crystallized as patches of native gold, native bismuth, bismuthinite and Bi-Te minerals, notably including variably auriferous **ingodite**, subject to their individual bulk composition.

LA-ICP-MS finds Eloise Vein South **ingodite** carries submicroscopic ‘dissolved’ gold to 57 g/t. In some grains this has nucleated forming coronas of native gold at grain boundaries of **unnamed Bi₂Te**. The ‘gold corona’ texture displaying this is quite pronounced (fig. 8 therein). Thus **ingodite** must be early formed.

It is proposed in the second report that other rare Bi-Te-S-(Se) minerals may be expected as Nox Fort’s bismuth content is high, e.g. a newly defined gold mineral jonassonite Au(Bi,Pb)₅S₄ (Paar et al. 2006) may occur. Zachariáš et al. (2001) identifies jonassonite in the **Petráčkova hora** RIRG deposit. The present work identifies two unknown mineral species.

1.17 Discussion of formation conditions of Au-Bi-Te mineralization in the second report

Mineralogical research suggests GBT patches in the BiTel Knoll quartz veins exsolved (crystallized) from gold-bearing Bi + Te (+ S) melts. These formed from cooling felsic granitic magma of the Bunker Hill sill and solidified at temperatures ~ 277°C (after Ciobanu et al. 2003).

The mineralogy infers BiTel Knoll Au-Bi-Te mineralization formed early at high temperatures in ‘reduced’ conditions with very low fS_2 . Similar conditions formed the Alaskan **Fort Knox** [5.4 M. oz] & **Pogo** [3.51] deposits (Rombach et al. 2004) and the **Petráčkova hora** [1.01] & **Mokrsko** [3.08] (Zachariáš et al. 2001, 2006) RIRG deposits SW of Prague in Czech Republic, discussed in 1.18 below.

¹² this also roughly concurs with Acme Analytical Laboratory metallic screen fire assay analyses on ~500 g vein samples, 8.6 g/t Au vs. 26 g/t, see table 1 in Howard 2006a

¹⁶ 11 selected grab samples from J. Zachariáš p.c. 2005 & 2006

In C. Hart's deposit model (2007) the above are classed as *intrusion-hosted* and *proximal-placed* RIRG gold deposits. More categorically D. McCoy (2000) proposes a subclass of RIRG deposits: '**Group 1' higher temperature + pressure deposits**. Early stage pyrrhotite ± loellingite ± arsenopyrite formed at ~620-300 °C with $fS_2 - fO_2$ in the magnetite-pyrrhotite stability field at depths > 5 km. Later sulfidation with sericitic alteration at moderate temperatures 250-400 °C formed pyrite with $fS_2 - fO_2$ in the pyrrhotite-pyrite stability field (McCoy 2000 and Rombach et al. 2004). **Low Sb content of all analyzed bismuthinite grains** (~0.4 wt % in Eloise and 0.15% in the Blue Quartz Vein) is additional evidence that Nox Fort hosts early stage mineralization: in Fort Knox later stage bismuthinite grains are Sb-bearing (McCoy 2000).

On Nox Fort it is hypothesized that after bismuth + tellurium -bearing melts accumulated gold and solidified. Thereafter reaction with cooling hydrothermal solutions with increased sulphur chemical activity fS_2 was one mechanism of gold deposition. **In Nox Fort, as in both the Fort Knox and Pogo deposits the**

"Bi-Te mineralogy changes in kind with the gold composition and the sulphide-alteration assemblages. In general paragenetically early, high temperature, and very low fS_2 (löllingite–pyrrhotite stable) native bismuth, bismuth telluride and S-poor sulphotelluride assemblages [with joséite-B $Bi_4Te_2S \pm$ **hedleyite** Bi_7Te_3] yield to late, lower temperature, higher relative fS_2 (pyrite stable) S-rich sulphotelluride [joséite-A Bi_4S_2Te], Sb-bearing bismuthinite and sulphosalt assemblages (Rombach et al. 2004)."

Early formed are joséite–B Bi_4Te_2S and **ingodite** in Eloise Vein, and native bismuth / **unnamed** Bi_2Te + joséite–B ± native gold / joséite–B + native bismuth ± native gold in the Blue Quartz Vein.

In the Blue Quartz Vein any of the assemblages **ikunolite** / **ikunolite** + joséite–A / bismuthinite / joséite–A + native bismuth are later. These replace, by sulphidation, early formed native bismuth.

1.18 Overprinting deformation identified that nucleated gold minerals

Telluride mineralogy is a practical tool in understanding gold deposits (Cook & Ciobanu 2003). Confirming its usefulness, ore microscopy suggested an overprinting deformation before it was seen in the field by the researchers: "Preserved textures in the ores are interpreted as a primary Au-Bi-Te assemblage that may have been deposited in the molten state and *overprinted* during a later orogenic episode that led to significant recrystallization and redistribution of gold (Kojonen et al. 2007)." Outcrops and hand specimens of the BiTel Knoll and other auriferous quartz veins in Nox Fort generally have pervasive cm-spaced healed fractures like pages-of-a-book texture (photos figs. 4 & 5 in Howard 2008). This is entirely consistent with latter, overprinting Eocene? extensional normal faulting described in the region. Advantageously this may re-concentrate gold and assist formation of an economic gold deposit. "The highly variable gold contents in the Bi-tellurides from one location to another along Eloise Vein, as well as between patches in the same sample, indicates the impact of the overprinting event that assisted Au redistribution and is beneficial for nucleation of native gold [electrum] (Cook et al. 2007c)."

1.19 Two analogous *intrusion-hosted* RIRG deposits in the Czech Republic

The 1.03 M. oz **Petráčkova hora RIRG deposit** in Czech Republic (Zachariáš et al. 2001, 2006, p.c. 2006) **has Bi-Te mineralogy similar to Nox Fort** with minor **ingodite** and trace **unnamed Bi₂Te**. It is an *intrusion-hosted* RIRG gold deposit. There quartz veins are “characterized by low sulfide content, native gold with auriferous Bi-Te minerals and no visible alteration” (Zachariáš et al. 2006). The Bi:Au ratio of 74.8 to 1, a very high Bi-Au correlation of +0.892 with a max. rock value of 5,625 ppm Bi¹⁶ is much like Nox Fort at ~ 76 to 1, +0.969 and > 2,000 ppm Bi (Howard 2006b).

BiTel Knoll veins have Bi-Te mineral assemblages similar to the 3.08 M. oz **Mokrsko RIRG deposit**¹⁷, also in Czech Republic. In this **unnamed Bi₂Te** is “younger than maldonite or native gold and older than **tetradymite**, joséite–A, joséite–B or bismuthinite (Zachariáš et al. 2006).” Textures in microphotos of Eloise Vein South sample 0441 (fig. 11A & 11B) infer **unnamed Bi₂Te** is older than the mantling **ingodite** and the native gold – electrum deposited at the grain boundaries. Like in the Mokrsko deposit, fig. 2E in Cook et al. 2007c shows **unnamed Bi₂Te** is older than joséite–A, joséite–B or bismuthinite.

1.20 Two general types of economic deposits host Bi-Te-S-(Se) minerals

Only a limited number of Bi-Te-S-(Se) mineral localities are known worldwide; fewer are well researched. These are often small parts, though signposts, of large and valuable mineral deposits. The present study determines that **two general types host the rare Bi-Te-S-(Se) minerals present on Nox Fort, based on the commodity present: Reduced Intrusion Related Gold systems and polymetallic Intrusion-related deposits of any combination of Sn Mo W Bi Cu Ag Pb Zn**. Ore grade for bismuth is ~0.2% and above. Clearly Nox Fort is the former type. Silver bismuth tellurium and tungsten may be important in central parts of Nox Fort and other RIRG systems.

1.21 Research goals of this report

With the above significant results from investigation of only a few selected occurrences, additional state-of-the-art mineralogical research was contracted to further objectively characterize gold occurrences in the central part of the property. It was thought that additional rare gold-associated Bi-Te minerals might occur. Thus during a property field trip Oct. 22 - 25 2007 the writer with N. Cook & C. Ciobanu collected¹⁸ numerous mineralogical specimens using hand tools.

Polished thick sections and some polished thin sections (microscope mounts) with opaque ore minerals were successfully prepared from 18 mineralized specimens (Table 2). Four sections are from specimens collected in claim # 516584. For mineralogical research N. Cook, Professor in the Geology section, Natural History Museum at the University of Oslo in Norway used a binocular microscope and a reflected light ore petrographic microscope with 5, 10, 20, 40 times magnification air-immersion objectives. The microscopes are fitted with digital cameras. A scanning electron microscope captured back-scattered images and semi-quantitative Energy Dispersive Spectroscopic (EDS) analyses [Part II].

¹⁷ Bi-Au numerical systematics not available

¹⁸ Mineral collecting without the written permission of Clarke Gold Inc. is strictly prohibited. Specimen collectors who steal private property are subject to all legal recourse.

As a previous laser ablation study (Ciobanu et al. 2006b) finds evidence for the role of Bi-minerals in controlling the distribution of gold in economic ores, three polished sections were laser-ablated by an Agilent HP4500 Quadripole ICP-MS instrument at CODES, University of Tasmania in Hobart Australia by N. Cook & C. Ciobanu [also Part II].

One focus was to determine formation conditions: "...telluride speciation can be readily predicted from the local redox environment at the time of crystallisation, as reflected by the observed host minerals. Modelling of trace mineralogy can therefore assist in identifying formation conditions and deposition during processes characterised by abrupt changes in physical-chemical fluid parameters (Ciobanu & Cook 2003)". Local, property-scale geographic and temporal trends may be indicated; active changes are expected in the varied hydrothermal fluids and magmatic melts that deposited gold and associated minerals on Nox Fort.

With extremely low base metal content and almost nil arsenic and antimony content Eloise Vein is an ideal 'natural laboratory' for determining bismuth (sulpho)telluride speciation to discern the formation conditions. Otherwise with abundance of some other base metals "Phase relations among [Pb-Sb-Zn] sulphosalts themselves and also with gold, bismuthinite, maldonite, native bismuth and galena in such cases are extremely complex... (Nekrasov 1996, p. 186)." Cook et al. 2007a discuss lead-bearing bismuth (sulpho)tellurides; the Pb-Bi-Te-S-(Se) system with an additional component is complicated.

The Bunker Hill mine veins were a research priority as formerly bismuth (sulpho)tellurides were not identified associated with gold. Cook & Ciobanu (2006) previously identified trace sub-10 micron sized inclusions of cosalite $\text{Bi}_2\text{Pb}_2\text{S}_5$ in galena (see fig. 4).

Few polished sections of Lefevre skarn / hornfels specimens have GBT mineral assemblages. The exception is L-11 skn from Lefevre trench #3. Nevertheless due to its size (Map 2) and considering the poor outcrop and the geophysical response (Bowman 2008) the Lefevre skarn / hornfels body may hold a significant gold resource.

Sections labelled • are similar in the 2008 report "Combined Magnetometer & VLF-EM Ground Geophysical Survey about the old Bunker Hill mine...."

2 Introduction

2.1 Physiographic and Geographic Location •

The project is in the rounded southern Bonnington Range of the Columbia Mountains, north of the Pend d'Oreille River valley, approximately 16 km southwest of the town of Salmo and 6 km north of the Canada-US border (fig. 1). The Pend d'Oreille River (fig. 2B) is a reservoir for hydroelectric power generation with two major power stations south of Trail. The National Topographic System map is NTS 082F03 W ½, Salmo sheet. The 1:20,000 BGS map sheets are 082F.004 and 082F.003 (thin black line on fig. 2B). At BiTel Knoll the UTM Zone 11 (NAD83) coordinates are 471,652 mE / 5,434,400 mN for sample site 0441 of Eloise Vein South. BiTel Knoll is part of the well mineralized vicinity referred to as the Bunker Hill mine - central area.

2.2 Access •

Road access is by driving S of Salmo on Hiway #6 to the Nelway customs station, then W (right turn) on the paved, then gravel, Pend d'Oreille Road. Continue north and north-westerly (right) for approx. 4 km uphill on the 4x4 Limpid Creek Forest Service Road [LCFS Rd] to just before a logging landing. The LCFS Rd is maintained by the Ministry of Forests (road is in purple on fig. 2B).

After parking at a side park at UTM 471,910 mE / 5,434,450 mN (on Map 2) access to the BiTel Knoll veins is by a short hike about 200 m due W downhill then slightly uphill to the height of land. Here the land rises to the W intrusive contact of the granitic Bunker Hill sill. About the Knoll hiking is easy as under brush is comparatively light and elevation changes only moderate. The Lefevre workings in skarn and quartz veins are accessed by a new skid trail off the LCFS Rd (Map 2). The re-built Bunker Hill mine road provides access to the old caved and closed adits at the mine site. Elsewhere under brush can be heavy and difficult to traverse. The present survey benefited from recent logging with considerably enhanced foot and road access.

2.3 Topography, Vegetation and Climate •

The topography is moderate and plateau-like in the central area. The land slopes moderately to the W and SW with no extreme cliffs. There are some steep land-slips. Ground elevation ranges from approximately 1100 m above sea level at the Bunker Hill mine site to the west to 1280 m at BiTel Knoll. Forest cover is thick, second growth merchantable Douglas fir and lodge pole pine with some stands of mature cedar. Some slopes have dense alder brush growing downhill, bushy and almost impassable. Recently small areas have been clear cut and re-planted including parts of the two Crown Grants. The east edge of BiTel Knoll on claim # 516584 is a cut block boundary. Undergrowth is variably heavy to light brush cover. Alders grow thickly on old clear cuts and road beds. Some slopes have dense alder brush growing downhill, bushy and difficult to pass through. Recent logging benefits mineral exploration as foot and road access is considerably easier. Thick forest cover did not hinder GPS geo-positioning.

Tens of cm to about 2 meters of glacial drift, mostly ablation till, covers most all bedrock. Thin soil is well development on this. Creek valleys have thick, bedded glaciofluvial deposits. Rock exposure is better than usual about BiTel Knoll (about 20%) as it is a height of land and well drained due to its resistant hornfels bedrock. Tens of meters away drift covers all. Rock is only occasionally exposed with ground cover generally more than 99.5%.

The climate is moderately dry with hot summers and only minor rainfall. The project area is generally snow free from mid April to early November.

2.4 Claims •

New Tenure claim # 516584 (former name CLY 2) is located in Nelson Mining Division, southeastern British Columbia in the southern Bonnington Mtns (Index map fig. 2A). It and claim #516587 surround two 'freehold', fee-simple Crown Granted claims Bunker Hill Lot 2939 and Mormon Girl Lot 1949 (Tables A & B in Appendix 2, fig. 2B Claim map, Map 1). The claims are presently owned by Clarke Gold Inc. Jaxon Minerals Inc. (TSX-V 'JAX') may acquire the property subject to an April 2008 option agreement.

3 Work Performed

During a property field trip Oct. 22 to 25 2007 the writer with N. Cook & C. Ciobanu collected numerous mineralogical specimens using hand tools. A. Koffeyburg assisted on Oct. 22. 32 specimens were air shipped to Norway Dec. 6 2007. From these 18 polished thick sections, including some polished thin sections, were successfully prepared and microscopically examined (Table 2). Sites are on Maps 1 & 2 and UTM co-ordinates in the descriptions. Initially polished blocks of 6 samples EL-02, -05, -06, -07, C-01, CLS-0448 consisted only of gangue quartz with no ore minerals visible (always a risk). Subsequently specimens EL-02, -05, -07 were re-prepared, and CLS-0448 examined regardless. Table 2 lists the 18 examined sections. Six sections (microscope mounts) are specimens collected on claim # 516584 (former name CLY 2).

For mineralogical research N. Cook, Professor in the Geology section, Natural History Museum at the University of Oslo in Norway used a binocular microscope and a reflected light ore petrographic microscope fitted with 5, 10, 20, 40 times magnification air-immersion objectives. Both microscopes are fitted with digital cameras.

Sections were carbon-coating under vacuum for the Hitachi E-SEM Scanning Electron Microscope. This is "equipped with an Oxford Instruments wavelength-dispersive spectrometer allowing minerals to be identified and analysed. While the data quality is slightly less than using an electron microprobe (due to the routine being standardless), past experience by the author has shown the data to be reliable for the type of minerals under investigation here. Analytical conditions were typically an acceleration voltage of 15 kV and 30 second count times [Part II]." This Energy Dispersive Spectroscopy 'EDS' gives semi-quantitative analyses.

Most of the investigation was conducted using back-scattered electron imaging. In the BSE images shades of grey correspond to the average atomic mass of each mineral, allowing the experienced researcher to readily identify the minerals.

Table 2 Microanalytical work on polished microscopic mounts prepared from 18 mineralized occurrences. Sections prepared from 6 samples on claim #516584 marked '■'

Occurrence & label of polished thick section	No. reflected light microphotos	No. back-scattered SEM images	SEM-EDS microanalyses, mineral [no.], minerals identified microscopically	Former sample, analysis at right	Au g/t all by Fire Assay	Ag	Bi	Te	Pb
Bunker Hill mined quartz veins from dumps: BH UHS-1 Adit 2 Underhand Stope Vein	1	6	hessite [2] bismuthinite [2] native bismuth [2] hedleyite [2] pyrite pyrrhotite magnetite galena unidentified bismuth oxides / hydroxides	BH-306 (Howard 2000)	29.76	2.9	1,150	92	60
BH UHS-4 Adit 2 Underhand Stope Vein	-	13	> 20 electrum grains [8*] pyrite bismuthinite native bismuth scheelite	-	-	-	-	-	-

Occurrence & label of polished thick section	No. reflected light microphotos	No. back-scattered SEM images	SEM-EDS microanalyses, mineral [no.], minerals identified microscopically	Former sample, analysis at right	Au g/t all by Fire Assay	Ag	Bi	Te	Pb
BHA-1-8 Adit 1 'Crush Vein' a.k.a. Adit 1 'B' vein	-	16	electrum [1] tetradymite [2] hedleyite [1] bismuthinite–aikinite [2] joséite–B [6] pilsenite [1] ikunolite [2] pyrite native bismuth bismuthinite galena chalcopyrite	BH-059 (Caron 2006)	0.122 (Caron 2006)	-	-	-	-
BH-0567 from dump near Adit 1, uncertain vein	2	16	electrum [7] native silver [1] joséite–B [5] hedleyite [1] $\text{Bi}_4\text{Te}_3\text{S}_2$ (?) [1] native bismuth bismuthinite pyrite arsenopyrite galena bismite	-	-	-	-	-	-
Eloise Vein: ■ EL-02 Eloise Vein South	1 & 1 binocular microscope photo	5	2 electrum grains [2] unnamed Bi_2Te [3] joséite–B [1] bismuthinite native bismuth scheelite	0441	8.17	1.43	564	33	4.8
■ EL-05 Eloise Vein North	2 & 1 binocular microscope photo	12	29 gold grains [2] unnamed $\text{Bi}_4\text{Te}_3\text{S}_2$ [3] ingodite [4] joséite–A [1] unnamed $\text{Bi}_8\text{Te}_5\text{S}_4$ [3] joséite–B [2] bismuthinite native bismuth scheelite	0424	9.94	1.52	476	55.8	15.4
■ EL-07 Eloise Vein North	2 & 2 binocular microscope photos	8	11 electrum grains [1] unnamed $\text{Bi}_4\text{Te}_3\text{S}_2$ [11] bismuthinite [1]	0412	27.03	4.15	1,601	95.4	84.1
Blue Quartz Vein: ■ BQ-01	-	2	galena native bismuth trace bismuthinite	-	-	-	-	-	-

Occurrence & label of polished thick section	No. reflected light microphotos	No. back-scattered SEM images	SEM-EDS microanalyses, mineral [no.], minerals identified microscopically	Former sample, analysis at right	Au g/t all by Fire Assay	Ag	Bi	Te	Pb
■ BQ-02	-	12	joséite–A [2] galena bismuthinite native bismuth	0414	8.65	1.18	478	23	13
Moly Qtz Vein: §M-01	2 reflected light & 5 transmitted light	-	pyrite molybdenite	0540	0.28	80.39	23	1.8	†
Lefevre tungsten + gold skarn / hornfels & crosscutting vein: L-04QVXtry trench #5 E wall of pit	-	9	unnamed Bi ₂ Te [5] bismuthinite–aikinite [1] ikunolite [2] joséite–A [3] pavonite [2] arsenopyrite pyrite molybdenite monazite	■LS-12	14.17	2.97	1299	40.2	6.83
§L-07 skn trench #4	1 reflected light & 1 transmitted light	6	pyrite pyrrhotite scheelite	LS-04	0.190 by ICP-MS	0.126	21.1	0.4	4.07
§L-09 skn trench #7	1 reflected light & 1 transmitted light	4	pyrrhotite chalcopyrite native bismuth	LS-02	8.84	1.110	637.5	20.0	9.6
L-10a skn trench #10	2	4	pyrrhotite marcasite scheelite	BH-314 (2000)	1.23	0.60	100.0	31	17
L-11 skn trench #3, S end	-	9	joséite–B [1] hedleyite [1] unnamed Bi ₂ Te [1] native bismuth pyrite marcasite pyrrhotite sphalerite galena chalcopyrite scheelite	LS-13	1.86	0.933	96.1	2.2	3.2
^L-12 Sp skarn trench #1	-	6	sphalerite pyrite chalcopyrite galena greenockite (CdS) identified & a Na-Zn bearing sulphate phase	0421	nil	0.22	1299	40.2	6.8
L-15 skn trench #13	4	6	pyrite marcasite chalcopyrite sphalerite pyrrhotite bismuthinite native Bi scheelite	0483	0.627	0.23	54.4	0.82	2.5

Occurrence & label of polished thick section	No. reflected light microphotos	No. back-scattered SEM images	SEM-EDS microanalyses, mineral [no.], minerals identified microscopically	Former sample, analysis at right	Au g/t all by Fire Assay	Ag	Bi	Te	Pb
■ Cleese occurrence "0446 shear" or 'Cleese 0446-BHCK-13 Shear'	-	8	phengitic white mica, zircon rutile ilmenite hematite apatite monazite	0446	6.411	1.921	462	16.7	18.5

*average atomic proportion is 0.521 Au

† >10,000 ppm Pb or >1.0% Pb

■ from Kennedy (2003), almost certainly a *diff't vein*, quoted analysis is a vein in *N wall* of trench #5 pit

■ work on claim # 516584

§ polished thin section

^ Sphalerite skarn

Analyses of mineralized rock samples by Acme Analytical Labs Vancouver in Howard (2005 or 2006a) unless otherwise referenced.

Totals:

- ❖ 18 polished sections, 3 of these are polished thin sections. Symbol ■ marks 6 sections prepared and examined from claim # 516584
- ❖ 18 reflected light, 7 transmitted light, and 4 binocular microscope photos.
- ❖ 142 back-scattered SEM images
- ❖ 105 mineral formulae determined, most bismuth (sulpho)telluride or bismuth minerals or native gold-electrum-native silver grains.

Two Blue Quartz Vein samples are very close to the Crown Grant boundaries. Thus the work is apportioned 4 out of 18 samples [sections] = 0.22 on claim # 516584, or conservatively 0.20 = 20% or 1/5th of the value was accredited to claim # 516584. Only travel in BC is accounted for, and no airfare (Appendix 4).

Three samples collected from the Crown Grants L-11 skn, L-12 Sp skarn & BH UHS-1 were subject to Laser Ablation - Induction Coupled Plasma - Mass Spectrometry 'LA-ICP-MS' microanalysis, similar to a study by Ciobanu et al. (2006b). Cost of this additional work reported herein was not applied as accredited assessment work on tenure claims. An Agilent HP4500 Quadripole ICP-MS instrument at CODES, University of Tasmania in Hobart Australia was used for the laser ablation research. Operating conditions were a constant 5 or 10 Hz pulse rate with laser energy typically 5-6 Jcm⁻² as Cook notes in for L-12 Sp skarn in the Lefevre section, Part II. This also details the calibration. 20 element isotopes were monitored in 22 ablated (analyzed) spots:

8 spots on sphalerites in sample L-12 Sp skarn of Lefevre tungsten + gold skarn / hornfels
 7 spots of Fe-sulphides in sample L-11 skn of Lefevre tungsten + gold skarn / hornfels
 7 spots of Fe-sulphides in BHUS-01 from Bunker Hill mine Adit 2 Underhand Stope Vein

The physical address of CODES is University of Tasmania, Hobart Campus, Geography-Geology Building, room 356 and postal address is CODES, Private Bag 79, Hobart Tasmania 7001 Australia.

3.1 Software used

This report is written using Microsoft® Word 2002 SP3 software. Maps 1 & 2 were drafted with MapInfo Professional Software V9.5 2008 using the software add-on Discover V9.1 ©Encom Technology Pty. Limited Australia (2008). Inserted maps figs. 2A & 2B were from ARIS MapBuilder at 'The MapPlace' online. For the LA-ICP-MS analyses the Agilent HP4500 Quadripole ICP-MS instrument used MeoLaser 213 software. Microsoft® Excel 2002 SP3 software calculated the mineral formulae. Adobe Acrobat made the pdf documents.

4 Brief property history •

Assessment reports investigating the gold potential of the Bunker Hill mine - central CLY area, now part of the Nox Fort Project of Jaxon Minerals Ltd., are by Kaufman 1984 #12,758, Howard 2000 #26,159; Kennedy 2003 #27,231; Ray 2004 #27,513; Howard 2005 #27,893; Howard 2006a #28,748; Howard 2006b #28,749; Howard 2008 and Koffeyburg & Howard 2008. A NI 43-101 report was filed with the TSX venture exchange in 2008 (Koffyberg & Gilmour 2008).

MINFILE 082FSW002 collectively names all mineralization in the Bunker Hill mine - central area 'Bunker Hill'. For thorough detail of the development and exploration history of the Bunker Hill mine and Nox Fort Project [formerly CLY Group] see Howard (2005). Recent geological and mineralogical oriented studies indicate many of the few outcropping quartz veins have native gold grains, generally sub-mm in size, associated with bismuth and bismuth (sulpho)telluride minerals. These are uncommon to especially rare.

In 2007 an integrated exploration program of magnetic and VLF-EM ground geophysics and soil, till, rock & drainage geochemistry was conducted. This was modified after L. Caron's 2007 recommendations. Two private companies Clarke Gold Inc. and Bis-Gold Resources Inc. managed surveys performed by Discovery Consultants of Kelowna of various geochemical media: stream sediments [silts], bulk stream sands for heavy mineral [HM] concentrates, basal lodgement tills and B horizon soils. A. Koffeyburg, P. Geo. of Discovery Consultants also collected mineralized rocks from known showings to confirm gold and silver concentrations. Irrespective of surface surveys L. Caron recommends 1,700 m of large-diameter core drilling in about 6 targets. The property has not been drilled aside from three short holes drilled underground in 1936 (Waneta Gold Mines Ltd. 1936a & 1936b, Annual Report of Minister of Mines 1936. These were misdirected.

In 2008 Aurifer Capital Corp., now Jaxon Minerals Ltd. (TSX-V JAX), agreed to an option with Clarke and Bis-Gold to earn 100% of the claims subject to payments, work commitments and certain Net Smelter Return royalties. Jaxon did significant field work and contemplates exploratory drilling on several identified targets (Howard 2006c, Caron 2006, B. Ballantyne , p.c.).

Minor production of silver and gold is recorded from the three Bunker Hill mine adits and two trenches in the Moly Quartz Vein and the Blue Quartz Vein (tabled in Howard 2005). Opaque minerals in the mined Bunker Hill quartz veins comprise pyrite + marcasite + pyrrhotite and minor galena arsenopyrite + galena + electrum, plus traces of any of magnetite scheelite chalcopyrite bornite cosalite native bismuth bismuthinite **hedleyite** joséite–B joséite–A **unnamed** Bi_2Te **ingodite** **ikunolite** **pilsenite** **tetradymite** and **hessite** (Cook & Ciobanu 2006 in Howard 2006a and Conclusions, Bunker Hill mine in Part II).

Veins were mined from Adits 1 to 3 on the Mormon Girl Crown Grant (Map 2, Map 1 in Howard 2006b). Early production in 1900 is unrecorded (1901 Annual Report p. 846). Bunker Hill Gold Mines, Limited (N.P.L) a private company operated to 1935; Waneta Gold Mines, Limited of Nelson to 1937. In 1938 5 oz. gold and 76 oz. of silver was recovered from a 74 ton lot mined underground from a silver-rich structure, presently unknown; R.G. Hall of Aberdeen Washington USA was owner (1938 Annual Report p. A35, E40).

Third Mineralogical Report detailing the finding of two 'new' gold-associated bismuth sulphotelluride minerals and identifying other opaque minerals, namely native silver electrum **tetradymite** **pilsenite** **hessite** bismuthinite–aikinite pavonite and greenockite characterizing a RIRG system in claim # 516584 and the Bunker Hill & Mormon Girl Crown Grants, on Nox Fort Project south of Salmo in Nelson Mining Division, southernmost British Columbia p. 32

Recovery in 6 years from 1933 to 1942 was 3,332 grams gold = 3.33 kg and 9,639 g silver from 309 tonnes at 8.479 g/t Au, 24.526 g/t Ag. In imperial units this is 107.1 oz gold and 309.8 oz silver from 356.5 tons = 0.30 oz/ton Au and 0.87 oz/ton Ag. Howard (2005) tables this referring to the original Annual Reports, correcting errors in the MINFILE database entry for Bunker Hill 082FSW002 production totals.

5 Brief economic assessment

Briefly, Nox Fort Project hosts various types (or styles) of variably placed Au(Ag)-Bi-Te-Mo-W ± As mineralization comprising a Reduced Intrusion Related Gold [RIRG] system (Lefebure et. al. 1999, Ray 2004, Caron 2006, Howard 2005, 2006b, 2007 & Field Trip Guide 2007b). C. Hart discusses the confusing nomenclature (2005) and details the defining criteria of RIRG systems (2007):

★“The reduced IRGS model is among the best classified of intrusion-related models and is easily differentiated from other gold deposit classifications by a set of distinguishing characteristics...” (Hart 2005)

The phrase “gold-telluride mineralization” poorly describes the Nox Fort occurrences. The occurrences are better termed gold-bearing bismuth telluride mineralization or more briefly gold + bismuth deposits (Ren et al. 2005). Nox Fort RIRG mineralization formed at paleodepths of 5 - 8 km, an estimate of the present level now exposed (section 3.11.7 in Howard 2006a). In contrast gold-telluride deposits generally formed in a shallow epithermal environment (<5 km) for example Cripple Ck in Colorado (Cook et al. 2007d).

Gold deposits were known to be associated with Bi-Te minerals and reduced granitoids previous to development of the RIRG model (Boyle 1979 for one). Gold-skarn and gold-greisen deposits in northeast Russia have native gold associated with native bismuth, bismuthinite, **ikunolite**, tellurides and sulphotellurides (Gamyanin 1995, Gamyanin et al. 1998). These deposits are genetically related to late Mesozoic granitoids; like in the Nox Fort occurrences the native gold grains are tiny, “90% less than 0.1 mm. Gold fineness varies (400-950 fine). The distribution of gold in ores is irregular, **often a bonanza** in the lode type. Geological, mineralogical-geochemical, and P, T geochemical data show the genetic relation ... [is] with I-type granitoids of the ilmenite and magnetite series in collisional and marginal-continental magmatic arc environments (Gamyanin et al. 1998).”

More than nineteen gold showings are known. These are spatially and likely genetically related to the Bunker Hill Sill, a particular outlying satellitic-body of the Wallack Ck stock. The latter is considered a mid Cretaceous age Bayonne magmatic suite felsic granitoid (Logan 2000, 2001, 2002a, 2002b). Cathro & Lefebure (2000) review some RIRG occurrences genetically related to this granitic suite in the West Kootenay region.

There is strong evidence that the central Nox Fort [CLY] area hosts the exemplar – the prime or best example – of a Au-Bi-Te -bearing, deeply formed RIRG system (see graph Howard 2006b p. 82 or Howard 2007). Construction of a log Au vs. log Bi graph of rock geochemical analyses of 19 showings confirms this. Comparing the regression line with other known, mostly productive, worldwide deposits the line has high slope and a high position on the graph – the latter as the Bi:Au ratio is very high. The advantage of this approach is its objectivity: it rationally and arithmetically judges a RIRG system's economic potential (Flanigan et al. 2000). Thus subjective personal opinion is not involved in estimating gold prospectivity.

Au-Bi-Te in Nox Fort mineralization has an excellent triple correlation (co-association); these elements strongly co-vary (Howard 2006c). In support of this mathematical relationship micron-sized gold (or electrum) grains occur along laminae in fine grained Bi-Te minerals, notably **joséite-B** in GBT patches in the auriferous Elsie Vein (figs. 5 & 6). Hart (2007) finds in RIRG systems “*Intrusion-hosted* ores are dominated by a Au-W-Bi-Te signature with Au correlating well with Bi and Te, but not at all with W (his fig. 11)”.

Third Mineralogical Report detailing the finding of two 'new' gold-associated bismuth sulphotelluride minerals and identifying other opaque minerals, namely native silver electrum **tetradymite** **pilsenite** **hessite** bismuthinite–aikinite pavonite and greenockite characterizing a RIRG system in claim # 516584 and the Bunker Hill & Mormon Girl Crown Grants, on Nox Fort Project south of Salmo in Nelson Mining Division, southernmost British Columbia p. 34

Bi and Te have pronounced correlations with Au on Nox Fort; the W-Au association has not been investigated. N. Cook calls Nox Fort an “an archetypal example of a RIRG deposit (Part II, Summary)”.

Targets considered most prospective are clusters of intrusion hosted to proximal placed sheeted quartz veins derived from magmatic-sourced Bunker Hill Sill granitoids. This sub-type of RIRG system may form a high value but low grade deposit ~1 g/t gold with large tonnage on the property.

6 Geology at regional to district scale •

The property is in a compressional fold and thrust belt, thereafter faulted and intruded by at least two plutonic suites. It is within the Omineca Belt, the region of overlap between volcanic and sedimentary strata of the Intermontane Belt to the west and sedimentary rocks of ancestral North America to the east. The tectonic divisions Quesnellia (also 'Quesnel'), Slide Mountain and Kootenay Terranes are arranged NW to SE on the property. Corresponding litho units are the well-mineralized Rossland Group Elise & Hall Formations (Höy & Andrew 1990a, 1990b, Höy & Dunne 2001), the Cs Unit of H. Little (1965, 1985) divided into the Charbonneau Ck Assemblage & Harcourt Ck Assemblage [HCA] by Einarsen (1995) and the unconformably underlying Cambrian age Lardeau Group Index Formation. This contact is not known on the property.

Einarsen (1995) describes regional stratigraphy, district scale structural assemblages and provides a structural-tectonic synthesis. In summary rocks on Nox Fort become older to the SE, in order of the above named terranes. This is also the proposed direction of aging of the three HCA Units (Howard 2000, 2005).

The colour map of Höy & Dunne 1999 requires updating over the prospect area. H. Little's 1960 map outlines larger areas of drift; this is the best map of the project area.

Howard (2005) details the nature of the layered rocks and this is not repeated herein. North of Nox Fort Höy & Andrew (1990a, 1990b) detail polyphase structures in the Mount Kelly - Hellroaring Creek Map Area. They mapped only to Swift Ck headwaters several km north of the central area.

7 Local Scale Geology

7.1 Layered rocks •

Uncertainly correlated metasediments and metavolcanics host the mineralized showings in the Bunker Hill mine - central area. H. Little (1965, 1985) names these layered rocks Carboniferous sediments the 'Cs Unit'. Ages are now ascribed to a longer range.

J. Einarsen from district-scale structural-geologic mapping divides the Cs Unit into two structural divisions, the Harcourt Ck Assemblage [HCA] & Charbonneau Ck Assemblage [CCA] (1995). These structural divisions are fault-bounded lithologic assemblages, not stratigraphic formations. The *Tillicum Ck Fault* 340 m NW of BiTel Knoll separates the structurally higher CCA from the underlying HCA to the east and southeast. CCA exposures are unknown in the Bunker Hill mine - central area.

Howard (2000) subdivides the HCA into three recognizable lithologic assemblages or Units. These are only defined W of the Bunker Hill Sill. The HCA Units are thought to be internally fault-bounded and thus likely discontinuous along trend. Country rock underlying BiTel Knoll is argillaceous metaquartzite of the HCA Quartzite + Tuff Unit, the structurally lowest tripartite division. It is considered the oldest. "In the Bunker Hill mine [central] area rocks strike mainly N to NNE and dip mostly E to ESE (Ray 2004)". See Howard (2000) for description of the HCA Units; this is not repeated herein.

In the region Eocene age, extensional, high angle NNE – NNW striking normal faults offset and transect older folds and thrusts but these are not firmly identified on the property. Nucleation of gold grains in the Bi-Te-S mineral assemblages may be due to this Eocene orogenic event, at least in part (see section on ingodite).

7.2 Intruding Bunker Hill Sill granitoids •

H. Little (1965) and M. Kaufman (1984) map a sill or dyke-like body of granite in the central part of Nox Fort. This felsic granitoid is named the 'Bunker Hill Sill.' It intrudes the HCA country rocks close to the investigated showings. It is considered an outlier of the Wallack Ck stock²³. The Bunker Hill Sill is at least 2.5 km long N-S and 0.5 - 1.5 km wide; it is named a sill after its elongate shape (though this pluton may be dyke-form). Two 'granite dykes' mapped underground in the Bunker Hill Mine (Minister of Mines 1934 p. E24, 1936 p. E18) are probably related.

7.3 Description of Bunker Hill Sill granitoids •

Bunker Hill Sill outcrops are mafic-poor, off white to speckled grey, medium to very coarse crystalline biotite ± hornblende felsic (leucocratic) granitoids. They are variably feldspar porphyritic and generally always hydrothermally altered. Ray (2004) notes "sporadic sericite and hornblende" and trace disseminated pyrite and lesser pyrrhotite (?). Uncommonly muscovite may be primary; detailed petrographic descriptions are lacking.

Bunker Hill Sill granitoids have variable grain sizes, textures and mafic mineral contents, evidence for fractionation (igneous differentiation). More felsic phases may be younger.

²³ Howard (2000) mistakenly refers to the Bunker Hill Sill as the Wallack Ck granitic pluton or granitoid.

Magnetic susceptibility measurements with a hand held Kappa meter (manufactured by ZH Instruments Brno, Czech Republic) are very low (R.G. Anderson, p.c. Sept. 19 2006). This indicates the Bunker Hill Sill is a gold-favourable, 'reduced' ilmenite- or titanite-bearing granitoid.

Importantly in some 'reduced' ilmenite-bearing granitic melts

“gold and other metals become enriched during fractional crystallization ... no gold-enriched precursor melt is required [to] enrich gold concentration to economic levels (Mustard et al. 2006).”

Examples are the Vogl stock of the Fort Knox Alaska deposit (McCoy et al. 1997) and the Stanthorpe leucocratic monzogranite of the Timbarra NSW Australia deposit (Mustard 2001). This model of gold concentration is much like the 'liquid bismuth gold collector' model of Douglas et al. (2000), Cook et al. (2002), Ciobanu et al. (2003), Ciobanu et al. (2006a & 2006b) and Tooth et al. (2007).

It is easy to visual this process. Blobs of metallic bismuth ± incorporated tellurium would stay liquid to low temperatures in a granitic magma body. This fluid dissolves any gold present – sequestering or scavenging it from dilute hydrothermal solutions – on moving about any irregularities in the networks of silicate crystals, that is the meshes of nearly-solidified rock. Bismuth is about 70 times as abundant as gold in mineralization in the central area (Howard 2006b), in ample amounts for this perceived process “the liquid bismuth gold collector model” of Douglas et al. (2000). Ciobanu et al. (2005) and Tooth et al. (2007) also well explain this. Figs. 5 & 6 spectacularly demonstrate the result.

8 Detailed Economic assessment

8.1 Regional Setting in an area with 9 Million ounce gold •

Nox Fort Project (formerly CLY) is at the exploration stage, with no known mineral reserves. It is located within the east extension of the highly mineralized Boundary District. "The Boundary District includes the Republic, Belcher, Rossland and Greenwood Mining Camps in southern British Columbia and northern Washington State, and has total past production exceeding 7.5 Million ounces of gold (Caron 2003)". Fig. 3 extends this gold mineralized area slightly N and E to include production and reserves in the West Kootenays: Sheep Ck camp produced 0.76 M. oz gold, Ymir 0.27. Near Nelson the Kena and Gold Mtn deposits (Logan 2003, Logan et al. 2003) together have known reserves 0.38 M. oz (Giroux & Dandy 2004). Conservatively the extended Boundary–West Kootenay District hosts 9 Million oz gold and has produced 7.5 M. oz. "Important gold deposits within the Boundary District can be broadly classified into six deposit types, including skarns, epithermal and mesothermal veins, mineralization associated with Jurassic alkalic intrusives, mineralization associated with serpentinite, and gold-bearing volcanogenic magnetite-sulfide deposits (Caron 2003)." Nox Fort is an example of a mineral deposit type presently unknown in the extended Boundary–West Kootenay District though in the most recent review of RIRG systems by **C. Hart (2007)**. He writes under "**Areas of High Potential in Canada**"

...In southeastern British Columbia, most effort has been directed towards large solitary veins, but potential also exists in targeting bulk tonnage deposits in pluton cupolas. The greatest potential in BC exists with the Bayonne plutonic suites... [in] smaller stocks or apophyses...

Third Mineralogical Report detailing the finding of two 'new' gold-associated bismuth sulphotelluride minerals and identifying other opaque minerals, namely native silver electrum **tetradymite** **pilsenite** **hessite** bismuthinite-aikinite pavonite and greenockite characterizing a RIRG system in claim # 516584 and the Bunker Hill & Mormon Girl Crown Grants, on Nox Fort Project south of Salmo in Nelson Mining Division, southernmost British Columbia

p. 39

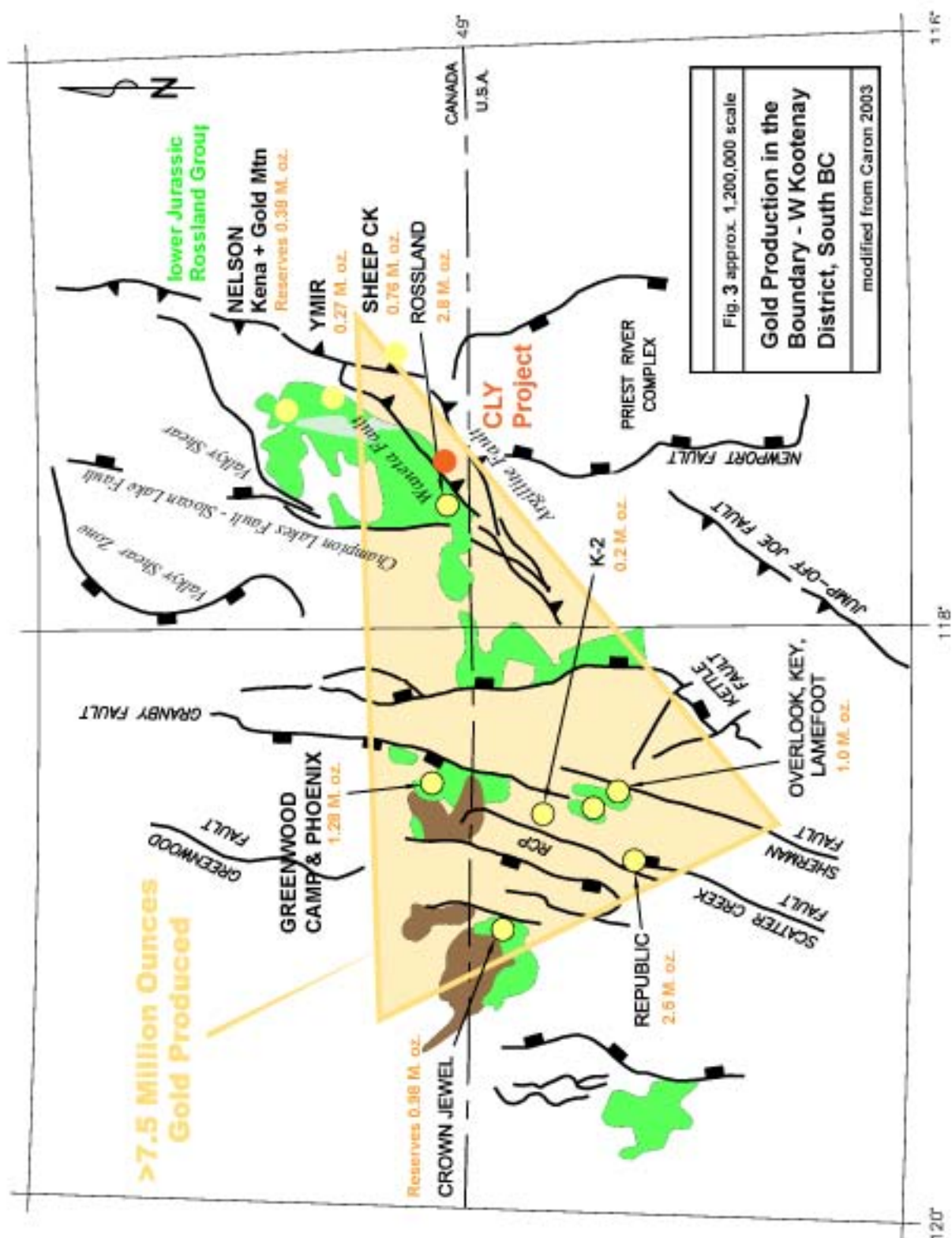


Fig. 3, previous page Gold Production in the Boundary–West Kootenay District, South BC has produced > 7.5 Million oz and is endowed with a gold resource > 9 M. oz. (modified from Caron 2003)

8.2 Discussion of the applicable exploration model – a Reduced Intrusion Related Gold [RIRG] System

“The RIRG system model is among the best classified of intrusion-related models and is easily differentiated from other gold deposit classifications by a set of distinguishing characteristics ... (Hart 2005)”. These criteria are met by the gold-bearing occurrences in the present survey area (Howard 2006b). Howard (2007) is a brief review. N. Cook finds Nox Fort an archetype RIRG system (Part II).

The target considered most prospective for an economic gold + bismuth deposit by the present writer would be a dense cluster of *intrusion-hosted* to (*very*) *proximal-placed* sheeted quartz veins (Caron 2006) derived from the magmatic-sourced Bunker Hill Sill granitoids. This sub-type of RIRG system can form high value deposits, generally of low grade ~1-4 g/t gold but with large tonnages.

In some occurrences in the survey area the density of auriferous quartz veining is sufficient for its presence, e.g. the Clarissa veins on BiTel Knoll. Vein density is measured as cumulative vein width or ‘vein aperture’ in cm per linear m of outcrop (Lang et al. 2001). Outcrops of the *very proximal-placed* Clarissa Transverse Veins on BiTel Knoll have sheeted veins, as do the *intrusion-hosted* Clease showings (Howard 2006b) south of the present survey. In the subsurface volume of quartz veining as cm³ per m³ of rock would be a critical factor in outlining an ore deposit. It is quite apparent from the abundance of VLF-EM conductors that there are many previously unidentified faults present in the survey area of unknown age.

Confusingly centrally-placed Reduced Intrusion Related Gold [RIRG] system deposits have also been called ‘gold porphyry’ (Bakke 1995, Hitchens & Orssich 1995) or ‘Plutonic-Related Gold’ (McCoy et al. 1997) or ‘Plutonic-Related Au Quartz Veins & Veinlets’ (Lefebure & Hart 2005 type L-02). Hart (2005) reviews the nomenclature. RIRG deposits are quite distinct from porphyry copper ± gold deposits derived from oxidized intrusions like the Katie alkalic porphyry copper ± gold deposit a few km north (Makepeace & Price 2007, Hart 2007 see schematic plot fig. 14 therein). These porphyry Cu ± Au deposits are also intrusion related.

RIRG systems may be systematically zoned about a causative pluton (figs. in Hart & Burke 2003, Hart 2006 and 2007) with different mineral assemblages concentrating various elements. Various styles²⁴ (spatial forms) of mineralization are expected about a causative intrusion.

²⁴ Style is used in a spatial or geometric sense, type as used by this writer refers to geochemistry with some *genetic* connotation

8.3 Favourability for the 'Group 1' subtype of RIRG deposit

Tungsten as scheelite CaWO_4 in a RIRG occurrence may indicate a more economically favourable 'Group 1' system. "Tungsten is more elevated in the low-salinity, carbon dioxide-bearing fluid inclusions in deposits at deeper levels [formed at paleodepths >5 km], consistent with high tungsten in the deposits and likely due to formation of tungstate rather than chloride complexes. Shallow-level deposits are characterized by gold associated with arsenic and antimony and locally elevated base metals, whereas **deeper systems commonly contain abundant bismuth, tungsten, and arsenic** (Baker et al. 2006)."

"Deeper systems (~ >5 km) have characteristics of mesothermal environments, and are hosted by plutons containing sheeted veins, greisen, and disseminated gold. ...Early feldspathization, with albite more abundant than K feldspar, is common in the deeper deposits (Lang et al. 2000). Metals such as antimony, arsenic, silver, and mercury are more common in the shallow environments, whereas tungsten, molybdenum, bismuth, and tellurium are dominant in the deeper systems (Baker 2002)."

"Sheeted vein-style deposits are common in the deeper intrusion-related gold systems. The largest deposit of this type is Fort Knox AK, which is characterized by mineralized pegmatites and sheeted veins hosted by Middle Cretaceous granodiorite and granite (Baker 2002)."

8.4 Process metallurgy that could be used to recover gold is deemed economical

If an economic ore body is outlined by drilling on Nox Fort, the nature of the mineral assemblages (parageneses) would determine the metallurgical methods used to recover gold. McCoy et al. (2002) suggest **"a high Bi-Au correlation, together with a low arsenic content, may be predictive of ore that is more easily beneficiated."** **Nox Fort has these features** (see Howard 2006b). The presence of specific mineral phases affects the processing and extraction procedures used and ultimately the economic viability of mining a deposit. Physical properties of particular ore minerals including grain size and inter-granular relationships are important. These factors influence the ease of liberation of ore minerals from gangue and / or other ore minerals present. 'Process metallurgy' or 'ore beneficiation' considers these features. Thus before mining the economics of extracting gold can be appraised.

The following favour economical gold recovery on Nox Fort. 'Free-milling' gold ore occurs. Finely grinding mineralized quartz or skarn would recover some native gold (electrum) grains by simple gravity separation. These are generally 5-20 microns in size in the polished sections reported on herein (see section on native gold minerals); visible gold grains to half a mm across (500 microns) have been observed (Howard 2005). Arsenic content is low (excepting the Lefevre skarn and Lefevre veins). The bismuthian (bismuth-rich) mineralogy and high Bi-Au correlation (Howard 2006b) all indicate the gold ore on Nox Fort is **non-refractory** (McCoy et al. 2002), thus amenable to low-cost recovery. Infrastructure is excellent considering the two power transmission lines crossing the property, the Pend d'Oreille water reservoir to the south and the inter-provincial natural gas pipeline to the north.

9 Mineral Deposits in the District •

The region is exceptionally well mineralized. BC GSB Bulletin 109 outlines features of the many past producing polymetallic mineral deposits (Hoy & Dunne 2001).

Noranda Exploration Company Ltd. & Yellowjack Resources Ltd. extensively drilled Katie MINFILE 082FSW290 an alkalic copper-gold porphyry 10 km northeast of Nox Fort in the 1990's (Naciuk & Hawkins 1995), location on fig. 3. Katie has a 'geological potential' of 200 M tonnes at estimated 0.17% Cu & 0.17 g/t Au (Schroeter et al. 2004). On July 21, 2006 Valterra Resource Corp. of Vancouver acquired the option to earn up to a 100% interest in Katie MINFILE 082FSW290 and Swift 082FSW215. In 2007 "a total of 1,126 metres of drilling was completed in three holes that tested two different mineralized zones on the property. Drill holes VKT07-059 and VKT07-060, were successful in extending copper and gold mineralization to the northeast in the Katie Main Zone. The third drill hole VKT07-061, demonstrated continuity of a well mineralized horizon that was previously intercepted between two historical "higher grade" holes on the 17 Zone (May 27 2008 news release). Also in 2007 an Airborne DIGHEM EM / Resistivity/ Magnetic geophysical survey was flown over the property.

Just 5 km S of Knox Fort project the former Reeves MacDonald zinc-lead-silver-cadmium mine is a "Kootenay Arc-type sedimentary exhalative deposit hosted by a dolomitized envelope of Reeves Member limestone of the Lower Cambrian Laib Formation. Production from the various ore bodies for the period 1949 to 1971 inclusive totalled 5,848,021 tonnes. From this 19,842 kg of silver, 203,616,006 kg of zinc, 57,692,784 kg of lead, 1,215,665 kg of cadmium and 27,584 kg of copper were recovered (MINFILE 082FSW026)." In 2008 ReMac Zinc Corp. (TSX-V 'RMZ') announced the discovery of a new occurrence of zinc-lead mineralization (referred to as "No. 4 Zone West") in drill holes up to 800 metres to the west of previously known zinc-lead zones at the past producing Reeves MacDonald.

Near Nelson the Sultan Minerals Inc. **Kena and Gold Mountain Zones are two significant porphyry Au-Cu deposits**, locales on fig. 3 (Höy & Dunne 2001, Logan 2003, Logan et al. 2003) with gold reserves (Giroux & Dandy 2004):

Kena Gold Zone

Measured plus Indicated 6,330,000 tonnes at 0.969 g/t (197,000 ounces gold)

Inferred 1,440,000 tonnes at 1.216 g/t (56,000 ounces gold)

Gold Mountain Zone

Measured plus Indicated 5,490,000 tonnes at 1.040 g/t (184,000 ounces gold)

Inferred 10,710,000 tonnes at 0.967 g/t (333,000 ounces gold)

Together the resource is 0.381 or ~0.4 M. ounces. Sultan plans to drill at depth the extension of the Gold Mountain Zone (Nov. 7 2007 news release).

On the **Jersey-Emerald property** of Sultan Minerals Inc., located on fig. 3, 13 km E of Nox Fort centre, the Tungsten and Molybdenum Zones have reserves:

"Within the tungsten zones, using a cut-off grade of 0.15% WO₃, the results show 2.51 M. tons averaging 0.37% WO₃ classed as measured plus indicated, with and an additional inferred resource of 1.21 million tons averaging 0.40% WO₃, both at a cut off grade of 0.15% WO₃. In the molybdenum zone the results at a 0.05% Mo cut-off show 28,000 tons averaging 0.098% Mo classed as indicated, with a further 481,000 tons averaging 0.103% Mo classed as inferred" (Giroux & Grunenberg 2006). There is "excellent exploration potential in both the historically mined areas and the surrounding terrain".

A preliminary scoping study by Wardrop Engineering Inc. of the Invincible and Dodger Tungsten Zones “has identified a potentially commercial operation at current prices” (May 23 2007 Sultan Minerals Inc. news release). “The tungsten skarn mineralization at Jersey Emerald occurs as disseminated scheelite with small amounts of powellite, rare wolframite and scattered flakes of molybdenite {refs. Rennie and Smith, 1957; Fyles and Hewlett, 1959} (Cathro & Lefebure 2000).”

9.1 Geochemistry and mineralogy of the ‘Bismuth Gold Zone’ in the Jersey-Emerald property differs from Nox Fort

Underground in Sultan Minerals’ Jersey-Emerald property “The ‘Bismuth Gold Zone’ contains pyrrhotite, arsenopyrite, quartz, native bismuth and stibnite {Troup, 1994}. It is exposed in the Jersey mine workings near the east end of the Dodger cross cut. ...Pyrrhotite is typically the most abundant sulphide ... however there are areas where arsenopyrite and bismuth minerals are more common, including several underground exposures in the Jersey mine (Cathro & Lefebure 2000).”

G. Ray sampled the ‘Bismuth Gold Zone’ at Site ‘A’ in the 4200 Dodger cross cut. This was visited by N. Cook, C. Ciobanu and the writer on Oct. 25 2007 courtesy Ed Lawrence of Sultan Minerals Inc. Very coarse grained pyrrhotite + arsenopyrite masses resemble melted, re-mobilized sulphidic skarn deposits in Sweden (N. Cook, p.c.). That granite occurs within 10’s of m substantiates his interpretation.

Table 3 in Cathro & Lefebure (2000) has rock geochemistry of three Site ‘A’ samples. Howard (section 14.7 in 2006b) calculates Bi/Au ratios and bulk gold fineness values and notes the geochemistry is that of a Sb and Bi rich sulphidic replacement skarn. **In conclusion the geochemistry of the ‘Bismuth Gold Zone’ is very unlike Nox Fort’s gold-associated bismuth (sulfo)telluride mineralization.**

Exotic Pb-Ag-Bi-Se bearing minerals found by electron microprobe analyses of Site ‘A’ ‘Bismuth Gold Zone’ specimens (p. 60 Ray & Webster 1997) confirms this interpretation. Section 16.2 discusses the mineralogy. **Concluding, the geochemistry and the mineralogy of the ‘Bismuth Gold Zone’ differ from Nox Fort mineralization. This reflects which elements are possibly concentrated in economic deposits at the property scale: Mo W Pb Zn vs. Au (Ag) Bi Te W.**

²⁷ ‘Bulk’ fineness considers total gold & silver present. In high fineness ore most of the gold is metallic [native] gold, with low silver content in any accompanying ore minerals (after Boyle 1979). For this case ‘bulk’ fineness approximates the ‘true’ fineness of the gold grains present. Fineness is $(\text{Au} / (\text{Au} + \text{Ag})) * 1000$, metals in weight percent, as parts per thousand. Fineness varies from nil (pure silver) to 1000 (pure gold).

10 Gold minerals on Nox Fort

10.1 Silver-rich electrum in Bunker Hill mine veins

In the 2006 sample BH Adit 2 of the Underhand Stope Vein “Gold is abundant as fine- to very-finely dispersed inclusions within pyrite (never marcasite). Many of these are sub-microscopic. Larger grains (though still only 10-20 μm in size) are noted along pyrite grain boundaries or at triple points between pyrite grains. The gold (electrum) is relatively Ag-rich ($\sim\text{Au}_{55}\text{Ag}_{45}$). Some gold is also seen outside of the pyrite domains or at the boundaries of pyrite with gangue.”

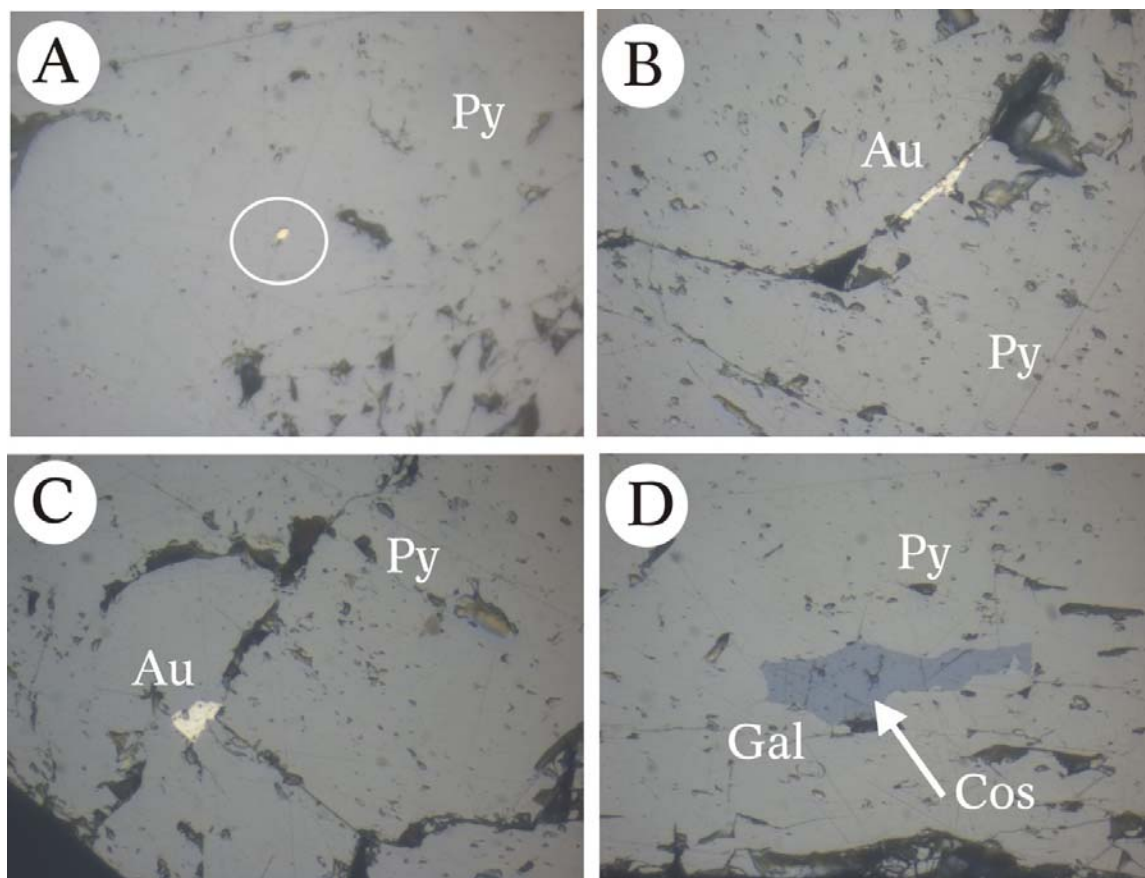


Fig. 4 Microphotos under reflected light of gold assemblages within pyrite in polished section of Adit 2 Underhand Stope Vein. Symbols: Au electrum ($\sim\text{Au}_{55}\text{Ag}_{45}$) circled on A, Py pyrite, Gal galena, Cos cosalite. Fig. 6 of Cook & Ciobanu 2006 in Howard 2006a.

In BH UHS-4 also from the Adit 2 Underhand Stope Vein “more than 20 individual grains of electrum were counted (see Figs. 1 and 2 Part II). The majority of these are less than 10 μm in diameter. Many are elongate to 30 μm long. Some (10%) are in paragenetic association with bismuthinite; ...otherwise electrum occurs as monophase inclusions in the pyrite grains. Some are clustered within, seemingly aligned along pyrite grain cleavage planes (Fig. 1). ...EDS analyses show most are silver-rich, occupying a central position in the Au-Ag solid solution series. Individual ‘atomic’ fineness values $\text{Au} / (\text{Au} + \text{Ag})$ of eight grains are 0.517, 0.498, 0.561, 0.566, 0.558, 0.528, 0.522 and 0.416. The average is 0.521. (Part II).” This average well compares to $\text{Au}_{55}\text{Ag}_{45}$ (atomic ratios) from 2006.

Electrum occurs as “fine-sized grains not necessarily tied to Bi-minerals ... closely associated with pyrite and not finely distributed throughout the quartz. This was known previously: “The operation of the old 10-stamp mill erected in 1900 is reported to have been of very short duration as the ore was not amenable to straight amalgamation, the gold values being chiefly associated with pyrite (AR 1934 p. E24)”.

In sample BHA-1-8 Adit 1 Crush Vein “electrum was observed together with **tetradymite** (Fig. 2B) and in a smaller inclusion together with **joséite–B**. The electrum grains in Fig. 2B have approx. atomic compositions $\text{Au}_{70}\text{Ag}_{30}$ (Part II)”.

In sample BH-0567 from a dump close to Adit 1 “eleven grains of gold (actually electrum, and in one case, native silver) were noted – six are intimately associated with Bi-Te minerals and in grain contact, five occur as discrete grains enclosed within the quartz, but always close to (i.e., within 500 μm) Bi-Te minerals. No gold grains were observed in parts of the section away from clusters of Bi-Te minerals.” Electrum has variable composition: “Spot analyses of seven electrum grains gave contents of 22.8, 26.3, 39.4, 47.4, 50.0, 50.8 and 62.8 wt % Ag. One grain (82.8 wt % Ag) [is] **native silver** (Part II)”. The mean of these 8 is 47.79 wt % Ag or 52.21 % Au, the mean fineness of electrum grains 522.

The ‘bulk’ fineness²⁷ of the 1934 production lot mined from the Adit 2 Underhand Stope Vein is low at a moderate 588. In no other year did Bunker Hill mine production exceed this. The value well compares with the mean atomic gold fineness 0.521 for eight electrum grains analyzed in the BH UHS-4 polished section and the mean electrum grain fineness 522 in BH-0567.

Adit 2 Underhand Stope Vein has high sulphide (mostly pyrite) content, $\text{Ag} > \text{Au}$ and minimum *in-place* grade 10.73 g/t Au and 7.54 g/t Ag. The mineral paragenesis is latter-stage with dominant pyrite, minor marcasite, pyrrhotite, galena and trace chalcopyrite bornite and cosalite. Ray (2004) also finds “arsenopyrite and black sphalerite.” Textures record at least five vein opening and infilling events in one large boulder-sized piece on the upper landing (Howard 2006b p. 56). Mineralization is spatially and genetically *intermediate* placed w.r.t the Bunker Hill Sill.

10.2 Native gold to gold-rich electrum in Eloise Vein

In Eloise Vein South 0441 coarser electrum grains also occur towards the margins of the Bi-Te minerals (2006). Atomic ratio is stated $\text{Au}_{76}\text{Ag}_{24}$.

EL-02 of Eloise Vein South has two electrum grains, one in a fractured scheelite grain (BSE images Fig. 1 & Fig. 3, upper right) and another ~10 μm in diameter, composition 23.2 wt % Ag, within one of the Bi-mineral patches. At 21.2 and 23.2 wt % Ag the grains are correctly named electrum (paraphrasing Part II). **The mean is 22.2 wt % Ag or 77.8 wt % Au corresponding to 778 mean gold fineness.**

In sample 0412 of Eloise Vein North atomic ratios are $\text{Au}_{75}\text{Ag}_{25}$. “Scarce native gold is present as <10 μm -sized inclusions in bismuthinite, sometimes combined with tellurides (**joséite–B** in Fig. 2f) (Cook et al. 2007c).” In EL-05 collected from Eloise Vein North near 0424 “A total of 29 gold grains are observed; most < 10 μm in size. ... Two analyses 15.2 and 16.1 wt % Au show the grains are **native gold** and not electrum as in EL-02 [from Eloise Vein South]. Grains in paragenetic association with Bi-Te minerals are the exception rather than the rule; these are however generally larger in size (up to 20–25 μm) (Part II)”. **The mean is 15.65 wt % Ag, 84.35 wt % Au or mean gold fineness 843.**

In EL-07 of Eloise Vein North a total of 11 electrum grains were observed. “These occur as tiny (<20 µm) grains, roughly equally divided between being scattered throughout the quartz matrix and in paragenetic association with the Bi-minerals. Electrum grains associate with both the undetermined Bi-telluride phase and bismuthinite, though mostly the latter (Fig. 5). ... [they] have surprisingly high Ag content, ca. 40 wt %; they are thus correctly named electrum rather than native gold (Part II)”. **Gold fineness is 600 (only approximately).**

10.3 Gold-rich electrum in Blue Quartz Vein

In the Blue Quartz Vein “both bismuth minerals and gold (~Au₇₅Ag₂₅) occur as µm-sized blebs along fractures in quartz (Cook et al. 2007c).” In sample ‘0414b’ gold ranges from Au₇₆Ag₂₄ to Au₈₀Ag₂₀ (Short report on electron probe microanalysis Nov. 12 2006 in Part II of Howard 2008).

11 The rare minerals

The following provides extensive background material on the Bi-Te-S-(Se) minerals and pavonite & hessite identified by N. Cook in the polished sections. Many occurrences are in either productive intrusion-related gold or polymetallic deposits. The minerals are described in approximate order of their rarity in nature. Joséite–A and joséite–B are not described as they appear to be more common worldwide and appear not to be characteristic of RIRG (c.f. **ikunolite**, Gamyranin (1995) & Gamyranin et al. (1998)) or polymetallic deposits. **Tetradymite** and the silver telluride **hessite**, being most common, are last. This background information allows the reader to compare worldwide occurrences and demonstrates the economic significance of identification of these exceptionally rare, rare, or at least uncommon minerals.

Color-coding some mineral names allows the reader to readily note patterns in the mineral assemblages.

11.1 Two 'new' mineral phases $\text{Bi}_4\text{Te}_3\text{S}_2$ and $\text{Bi}_8\text{Te}_5\text{S}_4$

Repeated semi-qualitative EDS analyses on several grains in two polished sections of Eloise Vein suggests **two new, previously unidentified, mineral phases** (Eloise section, Part II):

$\text{Bi}_4\text{Te}_3\text{S}_2$

mean of 2 analyses in EL-05 is close-to-stoichiometric:

$$(\text{Bi}_{3.775}\text{Pb}_{0.25}\text{Sb}_{0.10}\text{Ag}_{0.025}\text{As}_{0.01})\text{sum}_{3.985}\text{Te}_{2.60}\text{Se}_{0.04}\text{S}_{2.20}\text{sum}(\text{Se} + \text{S})_{2.24}$$

$$\text{sum Chalcogens Te} + \text{Se} + \text{S} = 4.84$$

$$\text{sum Metal:Chalcogens} = 3.985/4.84 = 0.823$$

mean of 8 analyses in EL-07 is near-ideal:

$$(\text{Bi}_{3.905}\text{Pb}_{0.086}\text{Sb}_{0.019})\text{sum}_{4.01}\text{Te}_{2.863}\text{Se}_{0.008}\text{S}_{2.118}\text{sum}(\text{Se} + \text{S})_{2.126}$$

$$\text{sum Chalcogens Te} + \text{Se} + \text{S} = 4.989$$

$$\text{sum Metal:Chalcogens} = 4.01/4.989 = 0.803$$

Considering analytical error the only real difference in the formulae from the two sites is minor Pb with trace Ag Sb & Se in EL-05 vs. trace Pb in EL-07 (ignoring element contents <0.01 *apfu*). In reflected light $\text{Bi}_4\text{Te}_3\text{S}_2$ is pink-brown. It is homogeneous and generally enclosed (mantled) by bismuthinite; these are the only identified bismuth minerals in EL-07 (two binocular microscope photographs, top of fig. 5). $\text{Bi}_4\text{Te}_3\text{S}_2$ + bismuthinite may be an equilibrium assemblage. In EL-07 polished section the $\text{Bi}_4\text{Te}_3\text{S}_2$ **grain size is ~0.5 mm; if it is the mineral in fig. 5 larger sized grains are fully expected in additional material.**

$\text{Bi}_8\text{Te}_5\text{S}_4$

mean of 3 analyses in EL-05 is near-stoichiometric:

$$(\text{Bi}_{7.517}\text{Pb}_{0.453}\text{Sb}_{0.137})\text{sum}_{8.107}\text{Te}_{4.973}\text{Se}_{0.013}\text{S}_{3.96}\text{sum}(\text{Se} + \text{S})_{3.973}$$

$$\text{sum Chalcogens Te} + \text{Se} + \text{S} = 8.89$$

$$\text{sum Metal:Chalcogens} = 8.107/8.89 = 0.912$$

$\text{Bi}_8\text{Te}_5\text{S}_4$ occurs as ~60 micron sized tabular crystals, variably replaced.

These new phases are gold-associated, and well deserve further analytical characterization to substantiate them as new minerals. They are tetradymite group minerals. Metal:Chalcogen ratios are ideally $4:5 = 0.80$ and $8:9 = 0.89$, analyses giving 0.813 (mean ratio in EL-05 & EL-07) and 0.912 (EL-05). Both are slightly less than one. This contrasts with ratios >1 for most all other bismuth (sulpho)telluride minerals in Nox Fort, considered 'reduced' species.

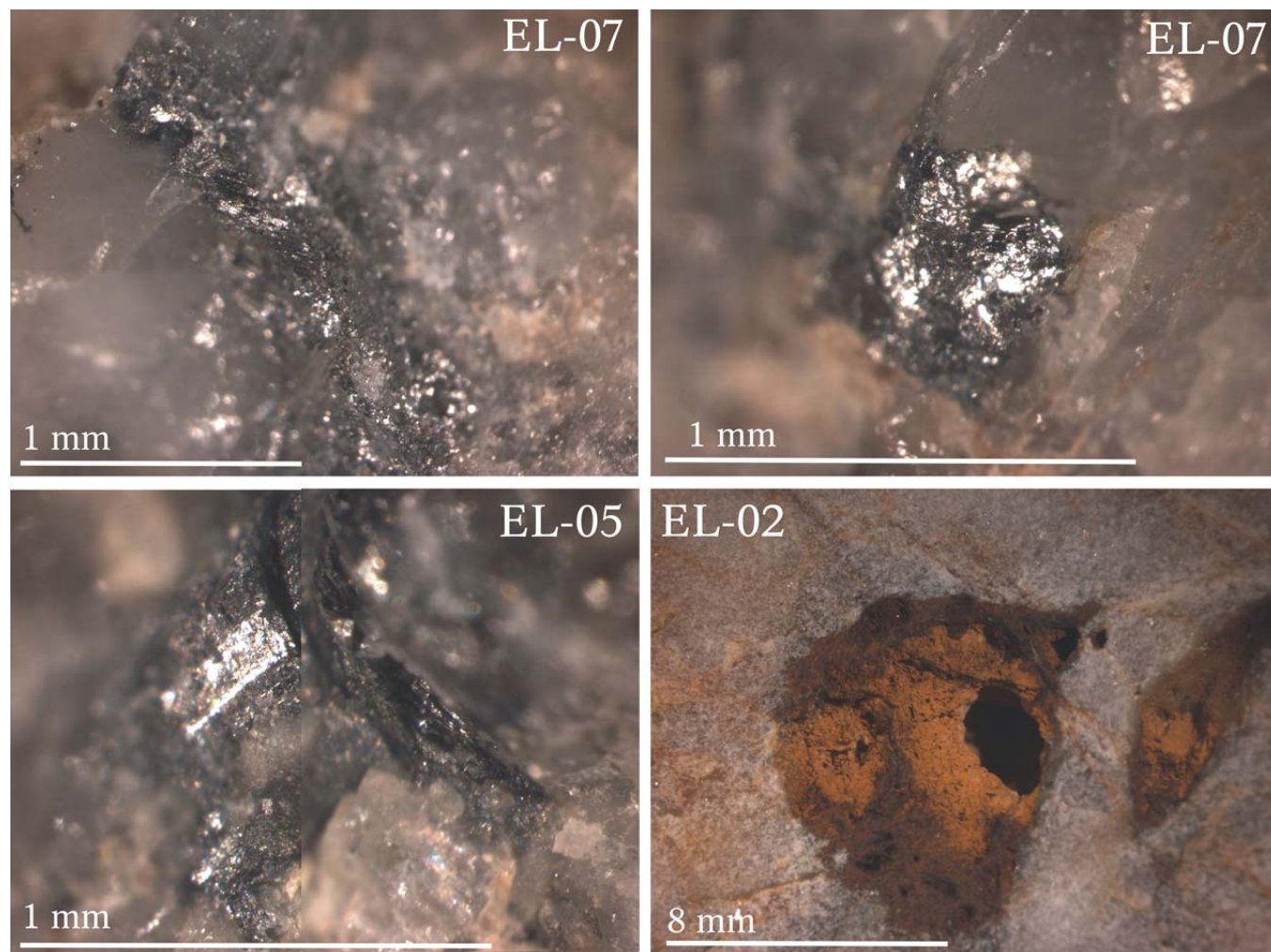


Fig. 5 Close-up photos of Eloise Vein bismuth (sulpho)tellurides through binocular microscope by N. Cook. Two top photos of EL-07 are bismuthinite or possibly unnamed $\text{Bi}_4\text{Te}_3\text{S}_2$ mantled by bismuthinite on quartz matrix; these are the only bismuth minerals identified in the polished section. Left photo is viewed end-on displaying striations, in right photo Bi-Te-S mineral appears molded to the matrix quartz. Bottom left is two vertically joined photos, uncertainly of joséite–B as in EL-05 “Joséite–B appears to be the most common” Bi mineral. The exterior crystal form is well displayed – perceive the angled ‘white line’ on the front crystal face as the c-axis, perpendicular to the near-perfect cleavage. Face angles indicate a hexagonal crystal system mineral like joséite–B. Likely not bismuthinite, also identified in EL-05, as the habit of bismuthinite is stout prismatic to acicular crystals and crystal form is orthorhombic. Bottom right photo is a weathered spot of limonite or goethite in EL-02 – any GBT minerals have weathered away.

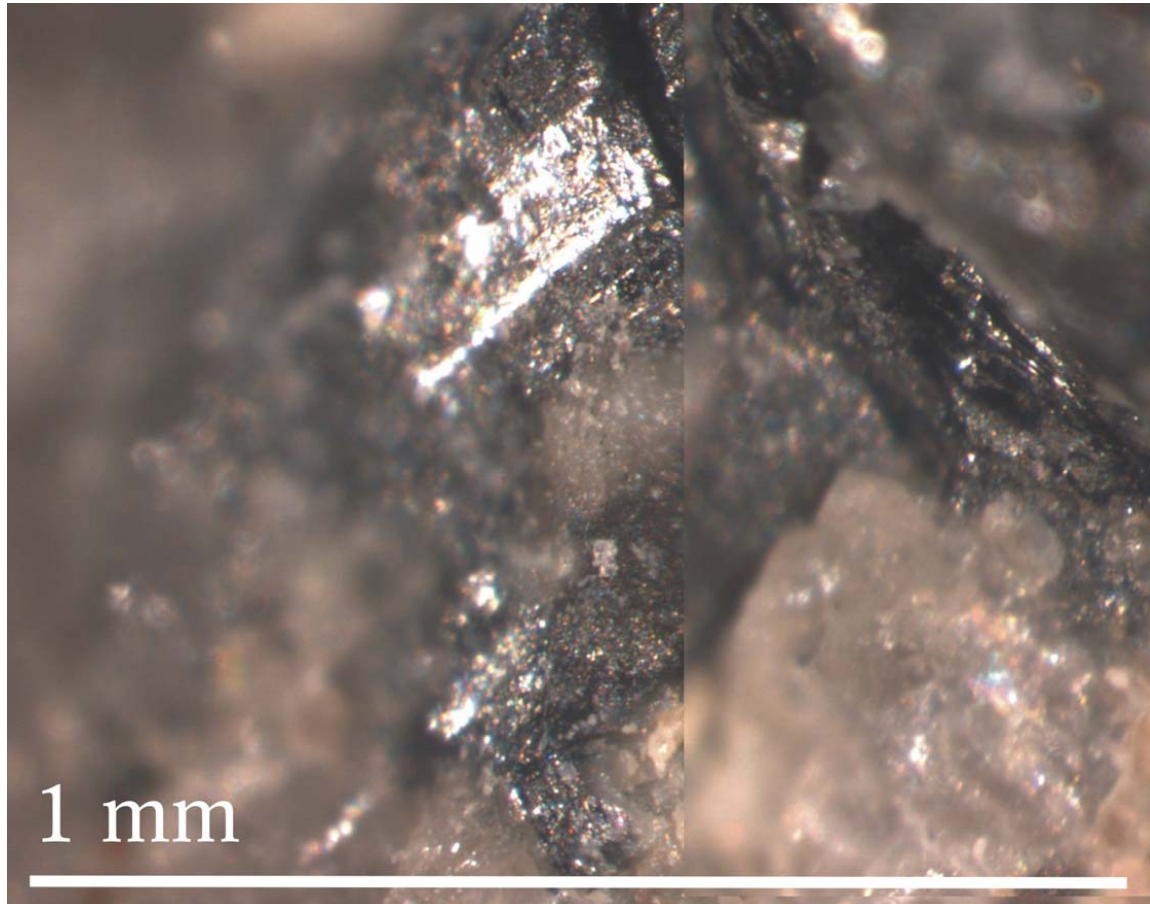


Fig. 6 Enlarged close-up photo of Eloise Vein EL-05 through binocular microscope by N. Cook, two images aligned vertically. Undetermined bismuth mineral, likely joséite–B as it has hexagonal crystal form and is the most common mineral in the polished section. The nearest face has a thin cover of white quartz. Hundreds of micron-sized native gold grains can be discerned. On close look they precisely align along cleavage planes as inter-lamellar 'gold trails'. Individual gold grains are 20-25 μm sized in the polished section. This is demonstrative of the bismuth-gold collector model of Douglas et al. (2000). Enlargement of the two EL-07 photos above show it is also peppered with inter-lamellar native gold. Analysis shows this is actually gold-rich electrum.

12 Ikunolite Bi_4S_3

12.1 Ikunolite – its stability, parageneses and compositional range

“**Ikunolite** has only been recognized from a relatively small number of localities (e.g., Kato 1959, Markham 1962, Nechelyustov et al. 1978, Finashin et al. 1979, Bortnikov et al. 1982, Imai & Chung 1986 [also Lawrence & Markham 1962, Dobosi & Nagy 1989, Gamyranin et al. 1998]). Although **appreciably less common than bismuthinite**, the mineral is nevertheless stable in several telluride- and selenide bearing deposits. In our experience, it is most stable where pyrrhotite is the stable Fe-sulfide. **Ikunolite** may occur together with laitakarite, joséite–A or joséite–B, **hedleyite**, native bismuth and bismuthinite... Compositional data show a range of compositions from end-member Bi_4S_3 to $\text{Bi}_4(\text{S}_{2.5}\text{Se}_{0.5})_3$ [there is] very limited Te-for-(Se,S) substitution in most natural specimens (Cook et al. 2007b and Fig. 9 therein)”. **Ikunolite** Bi_4S_3 is less sulphurated than bismuthinite Bi_2S_3 , so it is logical its formation would require a lower $f\text{S}_2$ or a higher activity of Bi.

Solid solution between laitakarite Bi_4Se_3 and **ikunolite** Bi_4S_3 is limited; **most ikunolite compositions are near ideal Bi_4S_3** . Commonly laitakarite and **ikunolite** have significant lead content 2.92–5.80 wt % (Wagner & Jonsson 2001). In polished section **ikunolite** is white with a faint creamy tint. <http://www.mindat.org/min-2008.html> lists 21 localities. Regarding the sequence of mineralization (the paragenetic sequence) in typical Au-Bi-Te-S deposits, Nekrasov (1996) finds “In the early stage, high grade gold is deposited ... mainly with bismuthinite and native bismuth ... and maldonite, **tetradymite**, **ikunolite**, tsumoite, **hedleyite** and joséite–A, joséite–B, joséite–E and joséite–K ...”

12.2 Ikunolite type locality – Ikuno mine in Japan

Kato (1959) first described **ikunolite** from the Ikuno mine as

“lead-grey platy crystals, ranging from microscopic to about 1 mm diameter (although multi-cm plates are also alleged), very flexible, showing only (0001) faces and cleavages, usually coated with bismuthinite (or the reverse, **ikunolite** coating Bi minerals) and intimately associated with bismuth, ferberite, chalcopyrite, pyrite, secondary Bi minerals and sporadic cassiterite in a high-temperature vein of fine-grained massive grey quartz in the Kanagase orebody ... The host rock for these polymetallic veins is Cretaceous pyroclastic rhyolite. Contains 1.98% Se, corresponding to the formula $\text{Bi}_{3.90}(\text{S}_{2.84}\text{Se}_{0.26})\text{sum}_{3.10}$. Streak is dark grey; Hardness 2; Density 7.8; stains grey in conc. HNO_3 acid, bluish grey in 1:1 HNO_3 .” Cleavages to 2.5 cm across (!) have come from the nearby Akenobe mine (Petrov 2006-2007).”

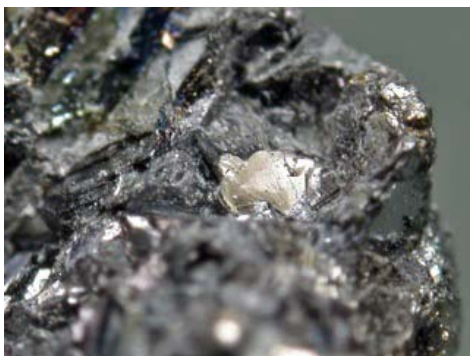


Fig. 7 Close-up photo of ikunolite from Ikuno mine in Japan. Intergrown crystals with perfect (0001) cleavage visible at top left. Horizontal width is 3.2 mm

The ideal **ikunolite** formula is $\text{Bi}_4(\text{S},\text{Se})_3$. The Ikuno mine is a tin-bearing cassiterite sulphide deposit with a few tens of g/t Au (Kato 1959, Nekrasov 1996) in Hyōgo Prefecture, Japan. It is a Sn-W-Cu-Zn-Pb-Ag vein deposit, “belonging to the xenothermal class ... in close proximity to regions of rhyolitic (and andesitic) rocks intruded by granitic rocks. The rhyolitic (and andesitic) rocks are products of the same igneous activities as the [late Cretaceous or early Tertiary] granitic intrusives. The Akenobe, Ikuno, and Tada mines in western Japan and the Ashio mine in eastern Japan” are similar (Imai et al. 1975).

12.3 **Ikunolite** is characteristic of RIRG deposits and polymetallic Sn Mo W Bi Cu Ag Pb Zn bearing deposits in the Russian Far East

Ikunolite typifies some mineral assemblages of granitoid-related gold deposits. In some RIRG deposits “Native gold in early paragenetic stages is frequently associated with arsenopyrite, loellingite, nickeline NiAs and cobaltite CoAsS. Native gold of later paragenetic stages (but still early-stage) occurs with bismuthinite, **ikunolite**, **hedleyite**, joséite and native bismuth characterizing granitoid-related gold deposits in the Russian Far East (Gamyanin 1995).” Examples are

- ❖ **Darasun gold deposit** in the Chita Region of Transbaikalia
- ❖ **Tuguchak-2** in northeast Yakutia, both discussed below, and
- ❖ **Kontaktovyi Stock** see Appendix 7.

Ikunolite characterizes large polymetallic deposits in Primor'ye Russian Federation, Sikhote Alin in the Russian Far East producing any of **Sn Mo W Bi Cu Ag Pb Zn**:

- ❖ **Vysokogorsk (alternate sp. Vysokogora) tin deposit**
- ❖ **Vostok-2 skarn scheelite–sulphide deposit**, W Cu Bi Pb Ag Au Te Se produced
- ❖ **Zabytoye tin + tungsten deposit**
- ❖ **some tin deposits of the Khingan-Olono district** in Khabarovskiy Kray, Russian Far East with Au Ag and Bi

12.4 **Ikunolite** is prominent in international RIRG deposits

The **Darasun gold deposit** is in the Chita Region of Eastern Transbaikalia, Russian Far East. Highland Gold Mining Ltd. reports Class 1 reserves of 1.1 M. oz. gold at average grade 10.3 g/t with resources 3.1 M. oz. at the same average grade (2006 website). Vein parageneses are: “(1) pre-ore boron (tourmaline) and molybdenite, (2) gold–bismuth, (3) antimony, and (4) post-ore quartz–calcite stages. Mineral aggregates of the [second] gold–bismuth stage are mainly composed of pyrite, arsenopyrite, galena, and sphalerite in the central, eastern, and northern sectors of the deposit with ores confined to granitoids and similar rocks. In contrast, chalcopyrite and pyrrhotite prevail in the western sector with ores confined to basic rocks.

...In the western sector of the **Darasun deposit**, jonassonite is developed in chalcopyrite–pyrrhotite aggregates at horizon 260 m of the **Novo-Elektricheskaya Vein**. Pyrrhotite is the monoclinic variety ... composition Fe_7S_8 . Chalcopyrite contains abundant inclusions of sphalerite exsolution. The subordinate minerals are represented by pyrite, arsenopyrite, sphalerite, **ikunolite**, cosalite, kobellite $\text{Pb}_{22}\text{Cu}_4(\text{Bi},\text{Sb})_{30}\text{S}_{69}$, native bismuth, **hedleyite**, tsumoite, **pilsenite**, **tetradymite**, native gold (fineness 871–902, average 883), and Te-joséite–B $\text{Bi}_4\text{Te}_2\text{S}$ (their Table 1). Jonassonite AuBi_5S_4 occurs as a replacement mineral associated with As-bismuthinite and Bi-plagionite $[\text{Pb}_5\text{Sb}_8\text{S}_{17}]$ in small patches of native bismuth [their Fig. 1]. Jonassonite encloses tiny (probably, relict) galena inclusions. The boundaries of [young pyrite crystals] crosscut intergrowths of jonassonite, bismuthinite, and plagionite (Krivitskaya et al. 2008).” No formula is given.

Ikunolite occurs in the **Tuguchak-2 gold deposit** in northeast Yakutia, Russian Far East. This is a granitoid-related Au deposit with W, Bi & Te. Grade is up to 10 g/t Au, to 0.25% Bi and to 0.08% Te. Steeply-dipping, cross-cutting quartz veins have tourmaline, muscovite, arsenopyrite, wolframite, bismuth, **ikunolite**, bismuthinite, **hedleyite**, joséite–A, joséite–B and 400-1000 fine gold. The gold-quartz veins range up to 1 m thick, to 100 m long and strike N-S. These cut earlier molybdenite-quartz veins of the Tuguchak-1 deposit. Tuguchak-2 is hosted in the Early Cretaceous Ulakhan-Tass granodiorite pluton. Beresite alteration is associated (Bakharev et al. 1988, Nokleberg et al. 1997). In C. Hart's (2007) current categorization the Tuguchak deposits are *intrusion-hosted* and / or *very proximal* RIRG deposits. Gamyranin (1995) & Gamyranin et al. (1998) note **ikunolite** occurs with native bismuth, bismuthinite and Bi-Te minerals in gold skarn and gold greisen deposits in NE Russia. No formula is given.

Ikunolite occurs in the **Ortosa 'reduced' gold skarn** in the Río Narcea Gold Belt near Asturias Spain (Cepedal et al. 2006). This is a *proximal* RIRG skarn developed in impure limestones at the top of Silurian siliciclastics. In one polished section **ikunolite** is adjacent to native gold on one side and native bismuth on the other in an interstitial patch in fluorapatite (op. cit., Fig. 6e). **A typical gold content is 0.28 wt % or 2,800 ppm Au** (op. cit., their Table 5). The mean formula of three **ikunolite** analyses is $\text{Bi}_{3.95}(\text{S}_{3.04}\text{Se}_{0.02})\text{sum}_{3.06}$. Analytical total is 100.18 wt % with **very significant 0.28 wt % gold and 0.18 wt % Ag unaccounted for in the structure.**

Ikunolite occurs in gold-bismuth-telluride-sulphide assemblages at the **Viceroy gold mine**, Harare-Bindura-Shamva greenstone belt in Zimbabwe (Oberthür & Weiser 2008). Extensional quartz veins in steep shear zones transect metabasalts of the Archaean Arcturus Formation. ...The ore paragenesis is dominated by arsenopyrite (>95 % of the ore minerals) followed by pyrrhotite (~4 %); all other constituents are accessories comprising chalcopyrite, mackinawite, galena, clausthalite, sphalerite, graphite, scheelite [and GBT minerals]. ...The gold mineralization is generally made up of banded or massive quartz carrying abundant coarse arsenopyrite. However, most striking is a distinct suite of Au-Bi-Te-S minerals, namely joséite–A Bi_4TeS_2 , joséite–B $\text{Bi}_4\text{Te}_2\text{S}$, **hedleyite** Bi_7Te_3 , **ikunolite** Bi_4S_3 , 'protojoseite' Bi_3TeS , an unnamed mineral $\text{Bi}_6\text{Te}_2\text{S}$, bismuthinite Bi_2S_3 , native Bi, native gold, maldonite Au_2Bi , and jonassonite AuBi_5S_4 . The majority of the Bi-Te-S phases is characterized by Bi / (Se + Te) ratios of <1. Accordingly, this assemblage formed at reduced conditions at relatively low $f\text{S}_2$ and $f\text{Te}_2$the close association of native gold, native bismuth and other Bi-Te-S phases suggests that gold was scavenged from the hydrothermal fluids by Bi-Te-S liquids or melts (op. cit.)." The abstract mentions no source intrusion. **Ikunolite 1 analysis has 0.25 wt % Au = 0.012 apfu**; clearly a gold-bearing mineral.

Old mining dumps of the abandoned **Nagybörzsöny precious and base metal deposit** in the Börzsöny Mountains, northern Hungary have **ikunolite** with many other minerals, including lillianite, possibly cannizzarite and newly named jonassonite $\text{Au}(\text{Bi,Pb})_5\text{S}_4$ (Paar et al. 2006). "Mineralization is hosted by Miocene calc-alkaline volcanic rocks and occurs as a stockwork in a propylitized dacite breccia pipe (op. cit.). "High temperature stockwork ore (Rózsza stockwork) mineralization consists of a high-temperature assemblage containing pyrrhotite, pyrite, melnikovite²⁸, marcasite, arsenopyrite, sphalerite, galena, chalcopyrite, valleriite, glaucodot, bismuthinite, tetrahedrite, cosalite, emplectite CuBiS_2 , native bismuth, galenobismutite, jamesonite $\text{Pb}_4\text{FeSb}_6\text{S}_{14}$, sartorite, proustite, stephanite, sternbergite and native gold (Panto and Panto 1972)." Jonassonite occurs as anhedral grains of up to 500 x 150 µm and contains inclusions of native bismuth, **ikunolite** and bismuthinite (Paar et al. 2006). Table 3 lists three individual Nagybörzsöny **ikunolite** formulae.

²⁸ A finely layered amorphous alternating pyrite and marcasite, presumably deposited from a sulfide gel.

In the **Maiskoe gold deposit**, Savran-Sinistovska ore zone, Dnister-Bug domain of the Ukrainian Shield in Ukraine “Associations of native gold, native bismuth and tellurides, tellurosulphides and sulphides of Bi (hereafter GBT) are abundant within assemblages of pyrrhotite (Po) + chalcopyrite (Cp) + pentlandite (Pn) + molybdenite. Molybdenite occurs as coarse laths, enclosed within Po, and commonly 'framing' the GBT assemblages.... Typical assemblages (their Figs. 1a-f) include native gold, native bismuth, **hedleyite** Bi_7Te_3 , joséite–B $\text{Bi}_4\text{Te}_2\text{S}$, bismuthinite Bi_2S_3 and **ikunolite** $\text{Bi}_4(\text{S},\text{Se})_3$. The latter has an extremely low Se/S ratio. These minerals tend to coexist, commonly as 100-300 μm sized segregations, with carbonate \pm silicate selvages. Coexisting **hedleyite** + joséite–B appears as a stable assemblage, and contains small inclusions of native bismuth and **ikunolite**. Cores of native bismuth, surrounded by bismuthinite, with rims of **ikunolite**, and eutectic intergrowths of gold and native bismuth, co-crystallised with calcite, are also observed. Bi-tellurides are also present as small droplets at the margins of gold grains. A close association of gold, native bismuth and GBT with pyrrhotite and chalcopyrite is evident... Au, Bi and GBT are most abundant as segregations and inclusions within fine-grained aggregates of marcasite / pyrite [Py] in which relictic lamellar pyrrhotite [Po] is preserved. **These relationships point to the fact that peak deposition of native gold, native bismuth and GBT was attained at the $f\text{S}_2$ buffer between Po and Py...**

However, the **coexistence of native bismuth and tetradymite within blades of hematite** indicates that this assemblage was formed at similar Bi concentrations [activity] as the above, yet at much lower $f\text{S}_2$ than either Po or Py stability. This different assemblage, including a distinct range of trace Bi-minerals, appears to be the result of a later overprinting (?) event characterised by highly oxidizing fluids. The presence, in association with **tetradymite** and **hessite**, of Bi-sulphosalts other than the otherwise ubiquitous bismuthinite, appears restricted to hematite-dominant environments (Cook et al. 2002). “Depositional temperatures $\sim 266^\circ\text{C}$ are indicated by paired Bi–telluride associations with Bi / (Te + S) > 1 [e.g. **hedleyite** + joséite–B; native bismuth + **ikunolite**], representing binary eutectics in the Bi–Te–(S) system. This can be correlated with pyrrhotite inversion and late pyrite formation. **An increase in $f\text{S}_2$ triggered Bi-Au-Te droplet precipitation** (Mudrovskaya et al. 2004).” No formula are given.

Sergeevske gold deposit also in Ukraine has **ikunolite**. This Archean age 3.5-3.1 Ga deposit is hosted in Middle Dnieprian block tonalite-greenstones (Stein et al. 1998). “It is associated with an astonishingly well preserved volcanoplutonic complex with a Au-Cu-Mo core and a Au-Ag-Bi-Te peripheral zone of mineralization”.

Ikunolite occurs in bismuthian gold ore in the **Baocun and/or Chaoshan skarns** in Tongling area, south China (Ren et al. 2004, 2005). No formulae are given. Native bismuth and bismuthinite are dominant, montanite pavonite **hedleyite** wehrliite²⁹ emplectite galenobismutite gustavite and maldonite are minor to trace ore minerals. At Baocun 1-25 mm wide quartz veins with native bismuth, bismuthinite, native gold and chalcopyrite crosscut copper + gold skarn. Gold correlates with Ag Cu and Bi: a “correlation coefficient matrix of 8 trace elements in 41 pieces of gold ore [has Pearson] correlation coefficients Au-Bi 0.6916, Cu-Bi 0.5030 and Ag-Bi 0.5836. There is a prominent positive correlation of gold, copper and silver with bismuth. ...gold and bismuth minerals synchronously developed ... [with] copper and silver (op. cit)”.

The grade of the Baocun copper-gold skarn is 0.63% Cu & 7 g/t Au with production 5 tons gold (Chen et al. 2007). Opaque minerals include magnetite, pyrrhotite, pyrite, chalcopyrite, native bismuth, bismuthinite, molybdenite, gold, electrum, sphalerite, bornite, arsenopyrite and galena (Zhao et al. 1999).

²⁹ A discredited mineral

The arsenical **Osikonmäki (Osikko) gold prospect** in Finland has minor **ikunolite**. This shear-zone hosted orogenic or 'mesothermal- style' deposit has reserves of 2.2 Mt @ 3.1 ppm Au = 7,330 kg = 7.33 t Au with 0.77% arsenic at a 1 ppm Au cut-off grade. "Native gold and electrum, with a set of Bi-Se-Te minerals, occur as inclusions and at grain boundaries within and between arsenopyrite, quartz and plagioclase. Native gold is more abundant towards the centres of early crystallised loellingite-arsenopyrite grains. Major opaque minerals are pyrrhotite, arsenopyrite, loellingite, chalcopyrite; marcasite, sphalerite, galena, ilmenite, rutile, cubanite, covellite, molybdenite, native gold, electrum, native bismuth, native antimony, maldonite, **ikunolite**, **hedleyite**, kawazulite, **pilsenite**, dyscrasite, tetrahedrite and stannite are minor.

Gold was precipitated by the sulphidation of the host rock in structurally favourable locations [with] ... arsenopyrite, löllingite and pyrrhotite ... the formation of certain Te- and Bi-bearing minor ore minerals took place during the fall of temperature, between 300-100 °C. Gold is geochemically associated with Bi and Te..." (<http://www.gsf.fi/explor/gold/osikonmaki.htm>). A beneficiation study obtained gold recoveries to 93% (Leppinen & Kontoniemi 1998). No formula is given.

Ililjarvi also in Finland has abundant Bi-Te-Se-S phases within galena: "**hedleyite**, joséite–B, joséite–A, and **ikunolite** with intergrowths between these phases (Ciobanu et al. 2002)." No formula is given.

Ikunolite also occurs with gold mineralization in **central Vietnam** with "tellurides, bismuthinite, native bismuth, rossvietite (AuBiS), scheelite and molybdenite (Borisenko et al. 2006)." No formula is given.

Gold and **ikunolite** occur in high-temperature fumarole gases of the **Kudryavy volcano on the Kurile Islands [Russia]**. "The lower-temperature zone is encrusted with elongated platy crystals of Pb–Bi–In–Sn sulfosalt minerals together with framboidal galena (their Fig. 9g), lamellar Se-bearing acanthite Ag₂S (their Fig. 9h), acicular **ikunolite** Bi₄(S,Se)₃, anglesite PbSO₄, anhydrite CaSO₄, and Na–K chlorides. ...The identified textures and mineral assemblages at Kudryavy volcano can be used to interpret geochemical origins of both ancient and modern ore deposits, particularly gold-rich porphyry and related epithermal systems (Yudovskaya 2006)." No formulae are given.

12.5 **Ikunolite** in some polymetallic Sn Mo W Bi Cu Ag Pb Zn deposits

Vysokogorsk (alternate sp. Vysokogora) **cassiterite-silicate-sulfide tin deposit** is in Primor'ye Russian Federation, Sikhote Alin, Russian Far East. In Vysokogorsk **ikunolite** is associated with cosalite and cannizzarite. This vein and stockwork deposit has been mined since the 1960's, tonnage is 'medium' sized and grade 1.0% Sn (Ariunbileg et al. 2003). Imai & Chung (1986) give the formula for Vysokogorsk **ikunolite** (Bi_{3.47}Pb_{0.30})sum_{3.77}(S_{2.77}Se_{0.15}Te_{0.08})sum_{3.00}; earlier Finashin et al. (1979) and Roberts et al. (1990) report (Bi_{3.59}Pb_{0.31})sum_{3.90}(S_{2.86}Se_{0.16}Te_{0.08})sum_{3.10}.

The **Vostok-2 skarn scheelite–sulphide deposit** is in northern Primor'ye Russian Federation, Sikhote Alin, Russian Far East. Mined by Primorsky GOK it was recently Russia's leading tungsten producer (Shedd 2004). **Average grade is 0.65% Cu and 1.64% WO₃ with production since the 1980's** (Ariunbileg et al. 2003). Vostok-2 is hosted by Permian to Triassic metasediments intruded by granitoids. **Bismuth, lead, silver, gold, tellurium, and selenium are extracted from ore** with galena, native bismuth, native gold, kobellite Pb₂₂Cu₄(Bi,Sb)₃₀S₆₉, Bi-containing jamesonite, **tetradymite** and other minerals (Gvozdev & Tsepina 2005). Electron microprobe analysis finds **ikunolite**, jaskolskiite Pb_{2+x}Cu_x(Sb,Bi)_{2-x}S₅ (x = 0.15–0.2), and cosalite with high Sb content. No formulae are given.

Some deposits of the **Khing-an-Olono tin district** in Russian Far East have “molybdenite, native gold, siliceous indium, ... bismuth- and silver-bearing galena, native bismuth, aikinite, **hedleyite**, joséite–B, **hessite**, wittichenite Cu_3BiS_3 , miharaitite $\text{Cu}_4\text{FePbBiS}_6$, native silver, **ikunolite**, benjaminite $(\text{Ag,Cu})_3(\text{Bi,Pb})_7\text{S}_{12}$ and bismuthinite...” (Korostelev et al., no date). No formulae are given. This may refer to the **Khing-an [or Khinganskoe] tin deposit** in Khabarovskiy Kray, Russian Far East. The deposit has been mined since the 1960's and has **medium tonnage with 0.6-0.7% tin**. This tin greisen deposit has “over 15 ore zones that range from 10-50 m across and 100 to 400-500 m depth that occur in a symmetrical breccia zone about 250-300 m across. The breccia zone is traced to depths of over 1200 m. At the upper levels ... breccia is replaced by chlorite, and at depths of 700-800 m the breccia is replaced by quartz-muscovite (sericite)-topaz greisen. The ore assemblage is quartz-fluorite-cassiterite. Arsenopyrite, marcasite, loellingite, chalcopyrite, and bismuth minerals are subordinate. The deposit occurs in pipe-shaped ore bodies of hydrothermal explosion breccia cutting felsic volcanic rocks. The deposit is ... related to a 80-90 Ma subalkaline potassium granite (Ognyanov 1986, Nokleberg et al. 1997)”.

Zabytoye greisen tin deposit in Amgu valley, Primo'rye Russian Federation, Sikhote Alin, Russian Far East has with pyrite pyrrhotite cassiterite arsenopyrite galena molybdenite sphalerite bertrandite cosalite hubnerite wolframite **ikunolite** **ingodite** and topaz (de Graff 2007, <http://www.mindat.org/loc-25400.html>). No formulae are given. Small stocks of specialized lithium-flourine granite occur.

Ikunolite is identified in the **Kara-Obo Mo + W deposit**, Bet-Pak-Dal Desert, central Kazakhstan (Nechelyustov et al. 1978). This is a large greisen W + Mo (+ Sn, Bi) porphyry deposit with 0.07% Mo and 0.20% W, age 292 Ma (Kotlyar et al. 1995, Mutschler et al. 1999).

At **Rędziny** in Lower Silesia, Poland dolomitic marble lenses occur in schist close to the Variscan-age [Hercynian] Karkonosze pluton. **Non-economic tin mineralization** in the active dolomitic marble quarry at Rędziny is “An abundant cassiterite–sulfide assemblage, consisting of several tens of mineral species... (see refs.). Arsenopyrite is the most common ore mineral, and is accompanied by cassiterite, pyrrhotite, chalcopyrite, sphalerite, galena, stannite, and $\text{Cu}(\text{Ag})\text{–Pb–Bi}(\text{Sb})$ sulfosalts, among which are aikinite, cosalite, gustavite, giessenite, berryite, tetrahedrite–tennantite, bournonite, wittichenite, and many others. ...The distance between the lens and the granite is only about 0.2–0.3 km. Ore minerals, most of which form small veins and nests, are disseminated in the schists and amphibolites at their contacts with the dolomitic marble (Parafiniuk et al. 2008)”.

Mineralization is skarn-related; a latter-stage bismuth (sulpho)telluride assemblage formed at “about 270-260 °C [with] native bismuth, Ag-poor galena, **ikunolite**, joséite–A, joséite–B, bismuthinite, chalcopyrite and traces of sphalerite and tennantite. In this assemblage, the aikinite-group minerals are commonly represented by members with compositions varying from friedrichite to gladite.... At **Rędziny**, **ikunolite**, ideally $\text{Bi}_4(\text{S,Se})_3$, has been found in fragments of quartz–chlorite–arsenopyrite veins containing a rich polymetallic mineralization, encountered in flexural cracks into a marginal zone of the dolomite lens. A typical association (their Fig. 2) includes chalcopyrite (most abundant), native bismuth and members of the aikinite group (commonly aikinite and friedrichite) in the form of large individual grains reaching about 1 mm in size. They are accompanied by subordinate **ikunolite**, bismuthinite, sphalerite, tennantite and successive members of the aikinite group up to gladite, commonly forming complex intergrowths or fine inclusions. Very small grains of unrecognized phases with compositions close to [unnamed] Bi_2S and PbBiS were sporadically found with them. Bismuth typically forms numerous inclusions in chalcopyrite and aikinite–friedrichite. The size of the **ikunolite** grains reaches 50 microns...

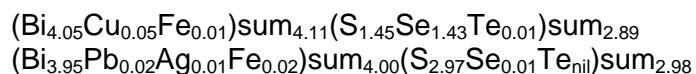
Ikunolite reveals a wide variation in S/Se. Its composition (their Table 1) ranges from the almost pure S end-member (2.97 *apfu* S and 0.01 *apfu* Se) to a variety in which the amounts of S and Se are almost equal (1.45 *apfu* S and 1.43 *apfu* Se). In none of the spots does Se exceed S, a case that would correspond to laitakarite, $\text{Se} > \text{S}$The conditions of crystallization [are] 280-240 °C and $\log f_{\text{S}_2}$ varying in the very narrow range -10.5 to -11.5 {Pieczka et al. 2009}.

...No significant substitution of Te has been found in the **Rędziny ikunolite**, and this mineral is also free of Sb and As. As the content of Te never exceeds 0.02 *apfu*, there are no compositional trends toward Te-rich members of the joséite group: pilsenite or joséite–A and joséite–B. **Pilsenite is not known** at Rędziny, but joséite–A and joséite–B are abundant, although not closely associated with **ikunolite**, as they probably formed at lower temperatures. However, small inclusions of other Te-bearing Bi chalcogenides, **tetradymite**, **ingodite** and kawazulite, crystallized earlier than **ikunolite** [are] sporadically found.

At Rędziny, selenium becomes concentrated at the lower-temperature stages of mineralization. Its main carrier is **ikunolite**, $\text{Bi}_4(\text{S,Se})_3$, with **Se contents** up to ca. 11 wt %. Some grains of Ag-bearing galena and aikinite also may be enriched in Se (above 1 wt %). The chemical composition of **ikunolite** shows a wide variability, never reported from any other locality. Results of our analyses document a full range of Se-for-S substitution in **ikunolite** and the existence of a complete solid-solution series from the sulfur end-member to a composition with a S:Se ratio ca. 1:1. According to data available in the literature, **ikunolite** also forms a continuous solid-solution series with laitakarite, $\text{Bi}_4(\text{Se,S})_3$.

Some **ikunolite** compositions reveal substantial amounts of Pb substituting for Bi, in the range 0 - 0.46 *apfu*. One sample has the composition $\text{PbBi}_3(\text{S,Se})_3$, indicating a compositional trend towards babkinite, $\text{Pb}_2\text{Bi}_2(\text{S,Se})_3$ (op. cit.). Lead is distributed erratically in the **Rędziny ikunolite** ... in some grains, Pb is one of the main components of **ikunolite**. Lead substitutes for Bi ... up to 0.64 *apfu* (Parafiniuk et al. 2008)".

Of 20 selected formulae in their Table 1 the most and least Se-rich **ikunolites** are:



Tellurian **ikunolite** occurs in the **Pangushan W + Bi vein-form deposit** in Jiangxi Province Ganzhou Prefecture, China. The formula given is $(\text{Bi}_{3.5}\text{Te}_{0.5})\text{sum}_{4.0}(\text{S}_{2.0}\text{Te}_{1.0})\text{sum}_{3.0}$ (Ren 1986a); here tellurium comprises 1.5 out of a total 7 *apfu*. No minor base metals, e.g. Pb & Sb, are recorded. At Pangushan "Metamorphosed Devonian sandstones and slates are underlain by a biotite granite stock. Alterations are silicification, sericitization and tourmalinization. Wolframite occurs in quartz veins; this and cassiterite zinnwaldite and tourmaline are characteristic of upper zone ones, wolframite scheelite molybdenite pyrrhotite and arsenopyrite lower zone quartz veins. Bi-Te minerals include joséite–A joséite–B **tetradymite** and **ingodite** (op cit.)."

From the **Yeonhwa 1 mine in the Wolam Zn Pb Ag skarn deposit**, then the largest producer of lead and zinc in South Korea, the mean composition of **ikunolite** from 10 microprobe analyses on 9 grains is $(\text{Bi}_{3.76}\text{Pb}_{0.22}\text{Ag}_{0.01})\text{sum}_{3.99}(\text{S}_{2.99}\text{Se}_{\text{nil}}\text{Te}_{0.01})\text{sum}_{3.00}$ (Imai & Chung 1986). Pb variably substitutes for Bi from grain to grain. Galena, galenobismutite, bismuthinite, native bismuth, gustavite $\text{Ag}_3\text{Pb}_5\text{Bi}_{11}\text{S}_{24}$ and pyrrhotite are associates in sphalerite and pyrrhotite-bearing clinopyroxene skarn. "From the paragenetic relations ... Yeonhwa 1 mine **ikunolite** is considered to represent later minerals in the sulphide – sulphosalt assemblages of the Ag_2S – PbS – Bi_2S_3 system ... pyrrhotite and sphalerite being earlier (op. cit.)." Se and Te may be non-essential components.

Ikunolite occurs in the **Ashio copper mine**, Ashio, Kamitsuga, Tochigi Prefecture in Japan with composition $(\text{Bi}_{4.33})(\text{S}_{2.38}\text{Se}_{0.62})\text{sum}_{3.00}$. 0.7 Mt copper were produced to 1973. "Permian sediments ... are intruded by felsic magmatic rocks. The Ashio rhyolite and the Permian sediments host the vein-type deposit (Schwarz-Schampera & Herzig 2002). Massive sulphides ("Kajika") formed in high to mid temperatures. Deposits are zoned:

Central upper zone: Sn W Bi Cu

Middle zone: Cu As Zn

Marginal zone: Zn Pb Cu As

Reported are native gold, copper, and bismuth; chalcopyrite marcasite arsenopyrite pyrrhotite sphalerite galena bismuthinite stannite stannoidite mawsonite cosalite ludlamite chalcocite cassiterite and wolframite.

At the **Kingsgate bismuth + molybdenite deposits** New South Wales Australia, irregular pipe-like high grade deposits are localized along a granite intrusive contact (Markham 1962):

"Molybdenite, bismuth and bismuthinite are the three principal metallic minerals with galenobismutite, cosalite, **ikunolite**, joséite–A, joséite–B, pyrrhotite, pyrite, arsenopyrite, galena, chalcopyrite, sphalerite, wolframite and cassiterite present in minor to trace amounts (Lawrence & Markham, 1962). **Ikunolite** ... occurs as well developed plates and foliated masses up to 3 cm in dimension associated particularly with native bismuth and molybdenite. It shows the perfect {0001} cleavage and splendid lead-gray color characteristic of all minerals of the tetradymite-joséite group. Polished section study reveals that **ikunolite** is associated with bismuth, bismuthinite, joséite A, molybdenite and gold. The most common assemblages recorded are:

1. **Ikunolite**-bismuth
2. **Ikunolite**-bismuth-bismuthinite
3. **Ikunolite**-bismuthinite
4. **Ikunolite**-bismuth-bismuthinite-joséite–A

though any combination of the above four minerals may be present... The assemblages noted above give no clear-cut textural evidence of disequilibrium. **Ikunolite** and bismuthinite are commonly intergrown."

Kingsgate **ikunolite** has 5.49% Pb and 0.78% Te in the analysis. Imai & Chung 1986 recalculate the formula as $(\text{Bi}_{3.58}\text{Pb}_{0.24}\text{Fe}_{0.01})\text{sum}_{3.83}(\text{S}_{2.92}\text{Se}_{0.03}\text{Te}_{0.05})\text{sum}_{3.00}$. "The rarity of **ikunolite** and the commonly reported association of bismuth with bismuthinite suggest that very special conditions are necessary for its formation. **Ikunolite** may, perhaps, be stable over a limited P-T range or form only in the presence of significant amounts of selenium and tellurium (Markham 1962)."

In the **Cobar Au Cu Pb Zn and/or Ag deposits** New South Wales Australia "Detailed studies of the different styles of mineralization ... suggest a consistent paragenetic sequence for the mineralization and alteration. Not all stages are developed in each deposit and the different stages can be developed to varying degrees". The second paragenetic stage is "A sulfur-poor assemblage of extremely fine-grained and high fineness (>950 fineness) gold, maldonite (Au_2Bi), native bismuth, **ikunolite** (Bi_4Se_3 - Bi_4S_3 solid solution series), clausthalite-galena (PbSe - PbS solid solution series) and other rare bismuth minerals in early-stage colloform quartz veins and quartz vein breccias associated with Fe-rich chlorite alteration (Stegman 2001)".

A complex 7-stage paragenetic sequence has been developed for the **Cobar field New Occidental mineralization**. "This sequence is more detailed than that available for the other deposits in the Cobar area.

Summarised in their Figure 9.9, stage 2 is

“a gold-bismuth assemblage comprising two parts. Stage 2A is a sulphur-poor assemblage of extremely fine-grained and-high fineness (>950 fineness) gold, maldonite (Au_2Bi), native bismuth, selenium-rich **ikunolite** (Bi_4Se_3 - Bi_4S_3 solid solution series), clausthalite (PbSe - PbS solid solution series) and other rare bismuth selenides associated with the earliest fine grained phases of Type 2B veining. It seems likely that this assemblage is also associated with Fe-rich chlorite alteration. Other minor gold-bearing phases like aurostibite AuSb_2 also appear to be associated with this assemblage (in Kaye et al. 2008).”

Stage 2A evolved to a “sulphur-deficient assemblage to a more sulphur-rich assemblage of **sulphur-rich ikunolite**, galena and minor pyrrhotite, generally associated with the latter coarse grained quartz within Type 2B veins (op. cit.).”

Paar et al. 2006 has colour microphoto fig. 1d of **ikunolite** from the **Cobar field New Occidental (Peak) mine**. “**Ikunolite** with traces of native bismuth is assumed to be cogenetic with jonassonite. Jonassonite is intergrown with native bismuth, bismuthinite and native gold. Pyrrhotite, sphalerite and chalcopyrite represent an earlier stage of mineralization (op. cit.).”

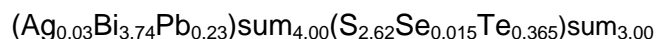
From the **Şoimuş III vein copper prospect** in the **Highiş Massif**, Western Apuseni Mtns of Romania, a representative analysis of **ikunolite** [n=8] is $(\text{Bi}_{3.19}\text{Pb}_{0.78})\text{sum}_{3.96}(\text{S}_{2.83}\text{Se}_{0.17}\text{Te}_{0.04})\text{sum}_{3.04}$ (Ciobanu et al. 2006a).

Ikunolite is also found in the dumps of the former **North Devon United Mine at Devon U.K.** with a complex assemblage of minerals including arsenopyrite, cobaltite, chalcopyrite, scheelite, bismuth, erythrite, quartz, fluorite, stannite, bismuth, bismuthinite, aikinite, cosalite, gersdorffite and various bismuth-bearing supergene minerals (Rumsey & Savage 2005).

Undersea in the Escanaba Trough, Southern Gorda Ridge, NE Pacific Ocean, a Bi-Au association occurs in pyrrhotite-rich massive sulfide deposits (Törmänen & Koski 2005). A SEM-EDS analysis, total 99.15 wt %, of an **ikunolite** (?) grain gives a formula $(\text{Bi}_{4.13}\text{Sb}_{0.02})\text{sum}_{4.15}\text{S}_{2.82}$. Significant is 0.13 wt % Au and 0.21 wt % Ag. Te was below the detection limit. “However the extremely fine grain sizes of the Bi-minerals in this occurrence may have caused some analytical difficulties and the data should be treated with care (Oberthür & Weiser 2008).

12.6 Composition of Nox Fort **ikunolites**

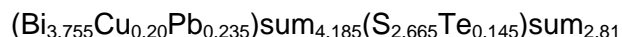
Ikunolite in sample BHA-1-8 of the Bunker Hill mine Adit 1 Crush Vein has average formula



This is the average of two grains imaged in Fig. 3D. The formula is near-stoichiometric. Te-for-(Se,S) substitution is pronounced; Te mostly substitutes for S as Se is present only in trace quantities. This is exceptional as “Compositional data for ikunolite indicate very limited Te-for-(Se,S) substitution in most natural specimens (Cook et al. 2007)”. **Adit 1 Crush Vein BHA-1-8 ikunolite is considerably more tellurian than all other 11 worldwide localities** table 3 lists. Substantiating the EDS analytical results sulfur is concomitantly low. “Bayliss (1991) observed the absence of Te and S ordering ... for the series Bi_4Se_3 – Bi_4S_3 (**ikunolite** – **pilsenite**), and he suggested the existence of a complete solid-solution series from **tellurian ikunolite** $\text{Bi}_4(\text{S},\text{Te})_3$ to **sulphurian pilsenite** $\text{Bi}_4(\text{Te},\text{S})_3$ (Dobbe 1993)”.

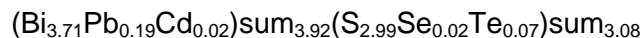
In Fig. 3D the small analyzed **ikunolite** grain “is positioned between JoB and Bi. This looks like a stable assemblage. Indented ‘dental caries’ texture infers **pilsenite** replaces JoB; possibly the released sulphur formed **ikunolite**. The association is unusual and atypical as **ikunolite** and **pilsenite** are unlikely to be stable together; this cannot be a ‘primary’ assemblage (Part II).”

Ikunolite in sample L-04QVXtry of a quartz vein cutting the Lefevre skarn / hornfels (Map 2) has an average formula, from two grains, of



This is not a stoichiometric formula. The minor copper content is unusual (table 3). **Te-for-(Se,S) substitution is significant, more than all other 11 worldwide localities except Viceroy** (0.202 apfu). The Bi-Te-S assemblages examined in sample L-04QVXtry are microscopic inclusions in fine grained arsenopyrite. In Fig. 2B “**ikunolite** (without Se) has formed, not bismuthinite, adjacent to earlier? co-existing native bismuth and unnamed Bi_2Te [mislabelled Hed]. **Ikunolite** may have crystallized after the other minerals, in a very local chemical environment with just the right amount of Bi and S to form this rarer bismuth sulphide. Figs. 2D and H are more difficult to interpret. After early (?) native bismuth both **ikunolite** and bismuthinite may have formed in a very localised closed system with approximately equal amounts of Bi and S. These two minerals are stable with one another as bismuthinite is not a member of the tetradymite group (Part II)”.

Ikunolite in sample 0414 of the Blue Quartz Vein, recalculated from data in Cook et al. 2007c, has average microprobe analyses of 2



The formula is very close to stoichiometric with significant Pb and trace Te Cd & Se. Native bismuth grains occur near **ikunolite** grains (Fig. 1D). Sb is near absent at 0.02 wt %. **Blue Quartz Vein ikunolite concentrates minor lead 4.15 wt %**; there is very little Pb in coexisting joséite–A and joséite–B (op. cit.). This Pb substitution is in the linear range for other occurrences (fig. 9, Cook et al. 2007b). Cadmium is trace at ~0.26 wt % or 0.02 apfu in this and the other three GBT minerals analyzed in the Blue Quartz Vein: joséite–A, joséite–B and bismuthinite. Metal:chalcogen ratio is 1.27.

Se is also trace at 0.15 wt % (op. cit.). **Te-for-(Se,S) substitution in Blue Quartz Vein ikunolite is very limited**, 0.97 wt % Te or 0.07 apfu, half that in L-04QVXtry **ikunolite** and inexplicably high in BHA-1-8 **ikunolite** at 0.365 apfu.

12.7 Table of global **ikunolite** formulae and three Nox Fort occurrences

Table 3 **ikunolite** formulae compared

	No. analyses	Method	Cu	Pb	Bi	Sum	Te	Se	S	Sum
RRIG deposits:										
*Ortosa	3	Mprobe	0.02	-	3.91	3.96	-	0.02	3.01	3.03
^o Viceroy	3	Mprobe	-	-	3.844	3.964	0.202	-	2.834	3.036
Nagybörzsöny 1	1	Mprobe	-	0.30	3.62	3.92	0.13	0.24	2.71	3.08
Nagybörzsöny 2	1	Mprobe	-	0.29	3.67	3.96	0.11	0.22	2.71	3.04
Nagybörzsöny 3	1	Mprobe	-	0.31	3.60	3.91	0.11	0.05	2.93	3.09
polymetallic deposits:										
Ikuno	?	Wet chem.?	-	-	3.90	3.90	-	0.26	2.84	3.10
Vysokogorsk Finashin 1979	6	Mprobe	-	0.31	3.59	3.90	0.08	0.16	2.86	3.10
Vysokogorsk Imai & Chung 1986	6	Mprobe	-	0.30	3.47	3.77	0.08	0.15	2.77	3.00
↳ Rędziny Se-rich	1	Mprobe	0.02	-	4.05	4.11	0.01	1.43	1.45	2.89
↯ Rędziny Se-poor	1	Mprobe	-	0.02	3.95	4.00	-	0.01	2.97	2.98
^a Wolam	10	Mprobe	-	0.22	3.76	3.99	0.01	0.00	2.99	3.00
Ashio	1	Mprobe	-	-	4.33	4.33	-	0.62	2.38	3.00
Kingsgate	?	Wet chem.	-	0.24	3.58	3.83	0.05	0.03	2.92	3.00
Şoimuş Ilii	8	Mprobe	-	0.78	3.19	3.96	0.04	0.17	2.83	3.04
§Escanaba Trough	1	Mprobe	-	-	4.13	4.15	-	-	2.82	2.82
Nox Fort:										
^ BHA-1-8 Adit 1 Crush Vein	2	SEM	-	0.23	3.74	^4.00	0.365	0.015	2.62	3.00
¤L-04QVXtry Lefevre Quartz Vein	2	SEM	0.20	0.235	3.775	4.185	0.145	-	2.665	2.81
+0414 Blue Quartz Vein (2006)	2	Mprobe	-	0.19	3.71	3.92	0.07	0.02	2.99	3.08

*average of three, with Au 0.28 and Ag 0.18 wt %↳ Fe 0.01 formula units

^o also Fe 0.120 *apfu*

↯ Ag 0.01 Fe 0.02 formula units

^a also with Ag 0.01 formula units

§ suspect non-stoichiometric analysis; Sb 0.02 included in Sum

^also with Ag 0.03 formula units

≠ not stoichiometric, with trace Cu. **ikunolite** 1 has metal sum 4.25 too high, still used in the mean.

+re-calculated, also has 0.26 wt % Cd, 0.02 wt % Sb giving formula

$(\text{Bi}_{3.71}\text{Pb}_{0.19}\text{Cd}_{0.02})\text{sum}_{3.92}(\text{S}_{2.99}\text{Se}_{0.02}\text{Te}_{0.07})\text{sum}_{3.08}$, near-stoichiometric with significant Pb and trace Cd Se & Te

12.8 Interpretation: Significance of **ikunolite** and other Bi-Te assemblages in the Blue Quartz Vein and the texturally-indicated alteration processes

In the Blue Quartz Vein both bismuth minerals and gold occur as micron-sized blebs along fractures in the quartz. In sample 0414 (Map 1) "...the Bi-mineral assemblage is dominated by jositite–A ($\text{Bi}_4\text{S}_2\text{Te}$), together with bismuthinite and native bismuth as major components ... and lesser amounts of jositite–B ($\text{Bi}_4\text{Te}_2\text{S}$), **hedleyite** (Bi_7Te_3) and close-to-end-member **ikunolite** (Bi_4S_3) (Cook & Ciobanu 2006)". Trace molybdenite is not spatially associated with native gold or the Bi-Te minerals.

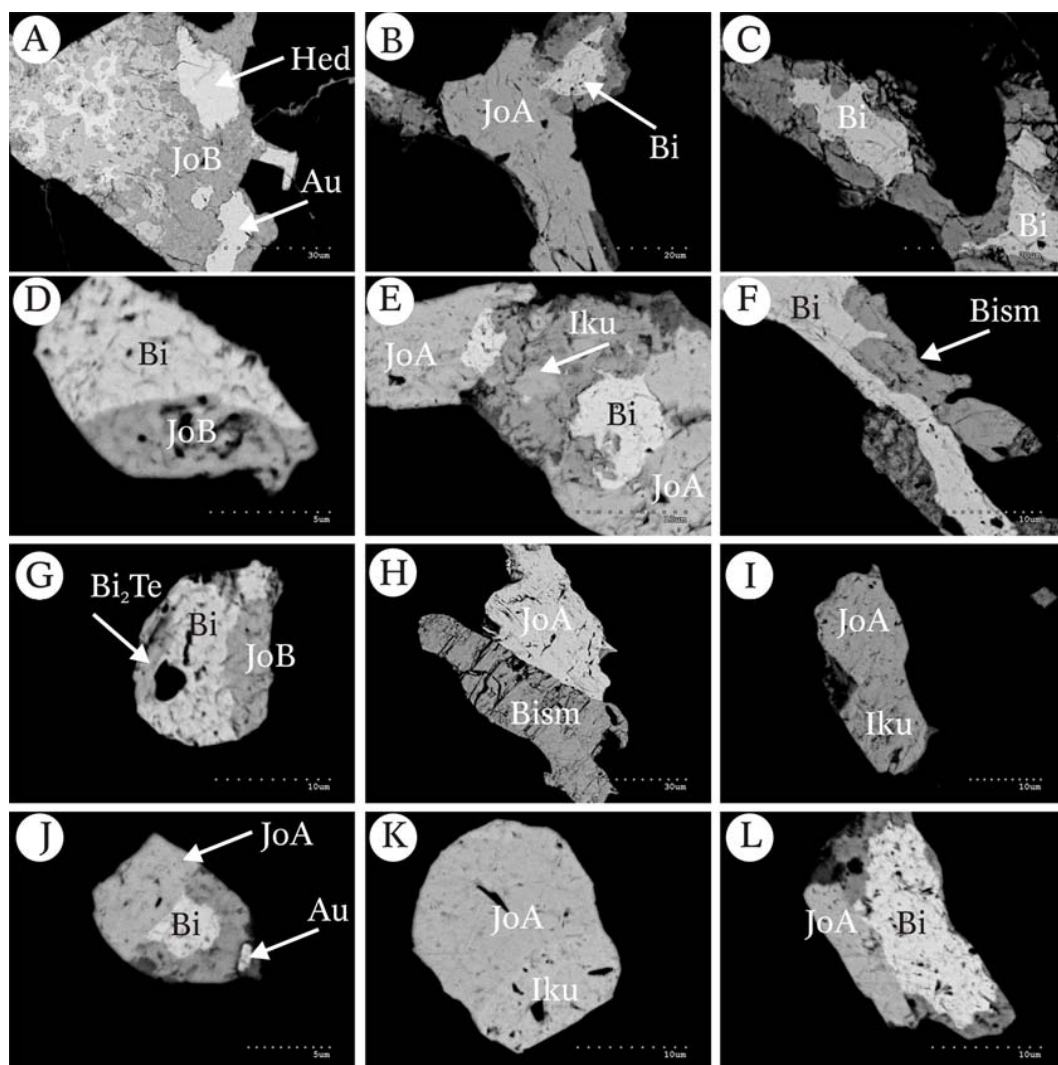


Fig. 8 Back-scattered electron images showing assemblages of GBT minerals in sample 0414 from the Blue Quartz Vein. **hedleyite** Hed, jositite-A JoA, jositite-B JoB, gold Au, native bismuth Bi, **ikunolite** Iku, bismuthinite Bism, unnamed mineral Bi_2Te . Dot scale in A & H is 20 microns; B & C 20 microns, E F G I K & L 10 microns, D & J 5 microns. From Cook & Ciobanu (2006) in Howard (2006a).

The first report Howard 2006a discusses some textural relationships in 12 microphotos of Bi-Te minerals in sample 0414 from the Blue Quartz Vein, Fig. 2 of Cook & Ciobanu 2006. There is “apparent eutectic crystallisation between [some] phases.” Re-investigating the textures,

Fig. 8A has **hedleyite** {now considered **unnamed Bi₂Te**} surrounding joséite–B and native gold grains. Grain boundaries are not smooth so it is inferred that the mineral assemblage did not form in equilibrium. The texture may record a sulphidation event.

Fig. 8D has joséite–B + native bismuth with curvilinear contact, Fig. 8G same pair also with **unnamed Bi₂Te**. Fig. 8J & 8L have joséite–A + native bismuth in textural equilibrium and ‘stable’; in Fig. 8L the pair also co-exists with native gold. Figs. 8I & 8K have joséite–A + **ikunolite** stably coexisting as interstitial blebs with curvilinear boundaries. Fig. 8H has the stable pair joséite–A + bismuthinite.

Fig. 8E shows two native bismuth cores surrounded by the pair joséite–A + **ikunolite** on each of their sides. This replacing texture shows joséite–A + **ikunolite** is younger than native bismuth [?]. Fig. 8F illustrates bismuthinite corroding native bismuth, same as in Fig. 8C though the surrounding bismuthinite is not labeled. This may indicate sulphidation with later-formed bismuthinite. Fig. 8B has joséite–A + native bismuth, again bismuthinite partially replaces native bismuth.

In 0414 “Most abundant are blebs containing an association of native Bi + bismuthinite. ... Joséite–B is found especially in blebs that contain native bismuth (Figs. 8D) and also **unnamed Bi₂Te** and/or **hedleyite** (Fig. 8A) or the pair with native gold (Fig. 8G). Sulphur-rich blebs dominated by joséite–A may occasionally also contain **ikunolite** (Fig. 8E). These Bi-rich associations are similar to those typically reported from gold skarns (Cook et al. 2007c)”.

In 0414 paired Bi–telluride associations have metal:chalcogen ratio Bi (+ minor Pb + trace Sb) / (Te + S + trace Se) > 1. Remembering joséite–A has more Sulphur than –B, stable mineral pairs observed are

- [1] joséite–B + **unnamed Bi₂Te** ± native gold
- [2] joséite–B + native bismuth ± native gold
- [3] **hedleyite** + native bismuth
- [4] joséite–A + **ikunolite**
- [5] joséite–A + native bismuth
- [6] joséite–A + bismuthinite
- [7] **ikunolite** + native bismuth

These may represent binary eutectics in the Bi–Te–(S) system. **Se is near absent.**

There are too many Bi-Te mineral phases in the Blue Quartz Vein for all to be in equilibrium. **Textures infer native bismuth is early**; it is partially replaced by any of the assemblages

joséite–B + **unnamed Bi₂Te**

joséite–A + **ikunolite**

ikunolite

joséite–A + bismuthinite

bismuthinite.

The processes are sulphidation and increase in tellurium chemical activity. One of these replacing textures noted above is also well displayed in:

Textures in microphotos Figs. 8E & 8F from the Blue Quartz Vein clearly indicate **ikunolite** corrodes first-formed native bismuth, discussed above. There is slight indication of bismuthinite replacing native Bi. The process is sulphidation.

12.9 Formation conditions of the Blue Quartz Vein inferred from mineral assemblages with **ikunolite**

Bi-Te minerals sample 0414 of the Blue Quartz Vein (Map 1) have metal:chalcogen ratios $\text{Bi} + \text{Pb} / \text{Te} + \text{S} (+\text{Se}) \geq 1$ (see fig. 8, Ciobanu & Cook 2003, Ciobanu et al. 2003). Both the Blue Qtz Vein and the Maiskoe deposit include **hedleyite** + joséite–B and native bismuth + **ikunolite** assemblages:

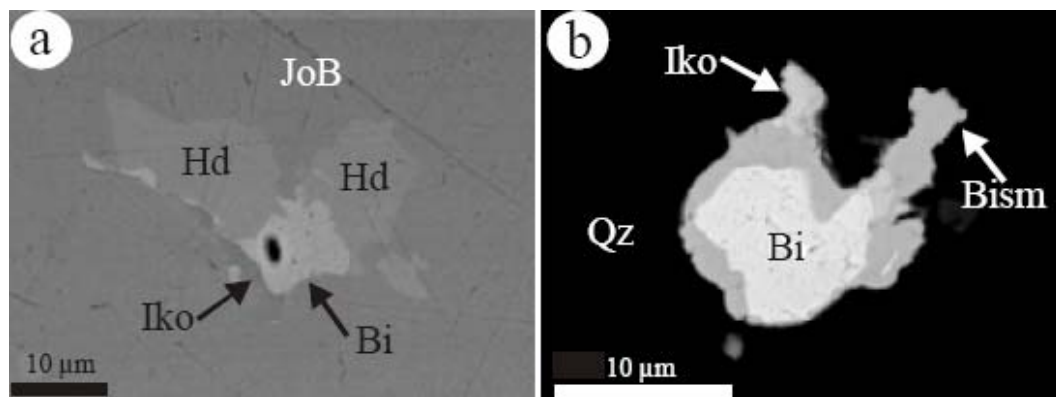


Fig. 9a & 9b Two back-scattered electron images of Maiskoe gold deposit GBT mineral assemblages from Cook et al. (2002). Fig 9a **ikunolite** border Iko on native bismuth Bi and **hedleyite** Hed, all enclosed in joséite–B. Strong textural evidence that joséite–B + native bismuth / joséite–B + **hedleyite** / **hedleyite** + native bismuth are equilibrium assemblages. Later sulfidation in part forms **ikunolite**. **Hedleyite** + native bismuth are a eutectic pair at 266 °C in the Bi-Te system (Elliot 1965), thus 266 °C is maximum temperature of formation. Fig. 9b Core of native bismuth Bi nearly completely rimmed by bismuthinite Bism. Part of this has altered to **ikunolite** Iko - find two spots in lighter grey, the second unlabelled one to left of Bism label. Later sulfidation formed bismuthinite and more uncommonly **ikunolite**.

Thus in the Blue Quartz Vein, as also proposed for the Maiskoe gold deposit in Ukraine,

“Scavenging of Au by Bi melt above 271°C (the Bi melting point) is evident. [Estimated formation] temperatures ~266 °C are indicated by paired Bi–telluride associations with $\text{Bi} / (\text{Te} + \text{S}) > 1^{30}$, representing binary eutectics in the Bi–Te–(S) system. ...An increase in $f\text{S}_2$ triggered Bi–Au–Te droplet precipitation (Mudrovskaya et al. 2004).”

Similar formation conditions are proposed for two other gold deposits with **ikunolite** - Ilijarvi in Finland (Ciobanu et al. 2002) and the Ortosa gold skarn in Spain (Cepedal et al. 2006).

Ore microscopy shows the “...Bi-rich associations are similar to those typically reported from gold skarns (Cook et al. 2007c).” Bi-Te mineral assemblages in the Blue Quartz Vein formed under ‘reduced’ conditions of low $f\text{S}_2$ and low $f\text{O}_2$. In other worldwide occurrences **ikunolite** “...is most stable where pyrrhotite is the stable Fe-sulfide (Cook et al. 2007b)” but no iron sulphide has been observed in the Blue Quartz Vein to date.

³⁰ An abbreviated Metal:Chalcogen ratio

13 Ingodite Bi₂TeS

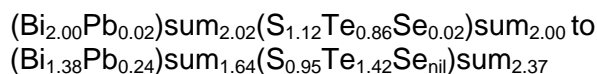
13.1 Ingodite: its rarity and compositional range

Ingodite is a rarely reported mineral (Shin et al. 2005). “Zav’yalov & Begizov (1981a) formally described **ingodite** as Bi(Te,S) (ideally Bi₂TeS)³¹, although the existence of the phase had been mentioned in several earlier studies (Zav’yalov & Begizov 1978). Their data and subsequent information from other occurrences (e.g., Ren 1986a, Ren 1986b, Shimizu et al. 1999) illustrate a degree of non-stoichiometry and also variable but roughly equal Te and S contents (Te:S ratio between 0.45 and 0.55) (Cook et al. 2007b).” Metal:Chalcogen ratio (Bi + Pb + Sb + Cd) / (S + Te + Se) ranges between 0.95 and 1.08; Te and S are roughly equal. Pb may be essential to the **ingodite** structure, with ~0.05 atoms per formula unit (op. cit. their fig. 12).

Fleischer et al. 1982 and Dunn et al. 1985 review the work of Zav’yalov & Begizov. Conditions of **ingodite** formation in the Pogo gold deposit [3.51 M. oz] is discussed below. Considering about equal Te & S the formula used herein is Bi₂(Te,S)₂. <http://www.mindat.org/min-2033.html> lists 10 localities.

13.2 Ingodite type locality – Verkhne-Ingodinskoye tin deposit, Russia

The type locality is the **Verkhne-Ingodinskoye tin deposit**, near the source of the Ingoda River, Transbaikalia (Zabaykalye), Far East Russia (Siberia). **Ingodite** formulae range “from



with quite variable Te / (Se + S) = 0.75 to 1.49 (Shin et al. 2005)”. The first analysis is near ideal, the second is non-stoichiometric. **Verkhne-Ingodinskoye** is a cassiterite-sulfide-silicate vein and stockwork deposit in volcanic complexes and replacements. Greisen-altered granite intrudes slate and metamorphosed sandstone. Albite cassiterite fluorite muscovite quartz topaz wolframite and sulfides occur (ref. <http://maurice.strahlen.org/transbaikal/transbaikal.htm>). The interpreted age of mineralization is Middle Jurassic to Early Cretaceous, related to Trans-Baikalian-Daxinganling transpressional arc magmatism (Rodionov et al. 2007).

13.3 Ingodite in some global RIRG deposits

EDAX {Energy Dispersive Analysis} identifies **ingodite** as a minor phase in the **Petráčkova hora gold deposit** [1.03 M. oz] in the Bohemian Massif SW of Prague in Czech Republic (Fig. 5 in Zachariáš et al. 2001, 2006, p.c. 2006). No analysis is given. **Petráčkova hora** is an *intrusion-hosted* RIRG gold deposit in a Variscan age porphyritic biotite-hornblende granodiorite stock. Quartz veins are “characterized by low sulfide content, native gold with auriferous bismuth telluride minerals and no visible alteration (Zachariáš et al. 2006).” Auriferous veins are “sheeted arrays of quartz veins and veinlets. Sulphides and other ore minerals form <5 volume % of the quartz veins... The most common sulphide minerals are pyrrhotite and chalcopyrite. ...Pyrite, arsenopyrite and molybdenite are present, but are relatively rare (op. cit.)”.

³¹ Bi(Te,S) means 1 atom of Bi with equal halves of Te & S atoms, better Bi₂(TeS)

In **Petráčkova hora** "...Gold within and associated with quartz veins occurs mainly as free grains ≤ 80 microns in size or as intergrowths with Bi-Te-S [younger] or Bi-S [older] minerals. ... Traces of electrum and Cu-Au alloy are present. Gold minerals, including maldonite, aurostibite, an unnamed AuBi_5S_4 phase [jonassonite see section 21], and Au-Hg amalgam are rare and intimately intergrown with native gold or Bi-Te-S minerals. Native bismuth, bismuthinite and **hedleyite** (Bi_7Te_3) are the most common bismuth-bearing minerals. Many other Bi-Te-S minerals were identified qualitatively (Zachariáš et al. 2001)". EDAX identifies **ingodite** (their fig. 5). ... In one case a veinlet of **unnamed** $\text{Bi}_2(\text{Te},\text{Se})$ cuts bismuthinite. No formula is given.

Ingodite from the Precambrian **Mazowe gold deposit**, Zimbabwe [0.99 M. oz] is lead-rich at $(\text{Bi}_{1.478}\text{Pb}_{0.319}\text{Fe}_{0.215})\text{sum}_{1.988}(\text{S}_{1.102}\text{Te}_{0.886})\text{sum}_{1.988}$ (Oberthür & Weiser 2008). "Seven main subparallel shear zones have ... 5-20 cm thick [auriferous] pyritic impregnations or quartz veins mainly hosted by the Jumbo granodiorite stock and quartz-feldspar porphyry. The individual ore bodies crop out between 100 and 300 m apart on the surface and can be followed for ~500 to 1500 m along strike. ...A late association of a number of Bi-minerals is notable in the ores, namely native bismuth, bismuthinite, **tetradymite** ($\text{Bi}_2\text{Te}_2\text{S}$), cosalite ($\text{Pb}_2\text{Bi}_2\text{S}_5$) with distinct Ag contents (0.49-1.95 wt %, n=10), joséite-A (Bi_4TeS_2) and **ingodite** (Oberthür et al. 2001)". But contradicting this Oberthür & Weiser (2008) write "Gold mineralization related to Bi-Te-S phases is of local interest only and was found in two of 150 polished sections... Native bismuth and bismuth tellurides are very rare at Mazowe. ...The Bi-Te-S phases at Mazowe reflect their sulphur-rich environment (elevated $f\text{S}_2$ buffered by pyrite combined with higher $f\text{Te}_2$), and have Bi / (Se + Te) ratios = 1".

Ingodite occurs with other bismuthian minerals in gold-bearing mineralization at **Kasejovice**, southwest Bohemia, Czech Republic (Litochleb et al. 1990, Litochleb & Šrein 1994, Litochleb 1998). It is in the gold-bearing stage with quartz, muscovite, chlorite, pyrite-2, pyrrhotite, chalcopyrite-1, molybdenite, native bismuth, bismuthinite, various other Bi-Te-S phases and gold-1. No formula is given.

Ingodite occurs in the **Săcărâmb epithermal gold-telluride deposit** [2.7 M. oz.] (formerly Nagyag) in the Metaliferi Mtns, **Romania** (Simon & Alderton 1995, Shimizu et al. 1999b). Mineralogy of this is described under **pilsenite**; **pilsenite** replaces **Pb-rich ingodite** along cleavage planes or surrounds **ingodite** blebs. No formula is available.

Ingodite occurs in the Brues gold deposit, Spain. One analyses is near-stoichiometric **ingodite** $(\text{Bi}_{1.40}\text{Pb}_{0.74})\text{sum}_{2.14}(\text{Te}_{0.72}\text{Se}_{0.02}\text{S}_{1.12})\text{sum}_{1.96}$. At Brues a set of Hercynian-age quartz + gold veins "is spatially associated with a regular network of granitic to aplitic-pegmatitic dykes and connected sills, also intrusive in the mica schist. ... Arsenopyrite forms large infillings (up to 10 cm wide) within quartz veins ... Bismuthinite is found within arsenopyrite as infillings of cavities and is associated with phengites [micas]. Gold (electrum $\text{Ag}_{0.15}\text{Au}_{0.85}$) mostly occurs within arsenopyrite ... from 1 to 50 μm in size, mostly within fractures affecting arsenopyrite, and is associated with bismuth, maldonite and Bi-tellurides [including **tetradymite**]. Boulangerite has only been observed within late quartz veinlets (Gloaguen 2006)." Pyrite, marcasite, chalcopyrite, sphalerite, bismuthinite, 'protojoseite' Bi_3TeS and maldonite also occur.

13.4 **Ingodite** in some polymetallic Sn W Mo Bi Cu Pb Zn Ag As deposits

Ingodite occurs in the important **Tyrnyaуз W + Mo deposit**, on the left bank of the Baksan River Valley in the northern Caucasus Mountains, Kabardino-Balkaria Republic in Russia (©2001-2005 Mineral Data Publishing, version 1; Jambor et al. 1997; Bindi & Cipriani 2003). This was “...the former Soviet Union’s largest producer of tungsten from tungsten skarns (0.14% WO₃), with an original annual capacity of 42,000 t of tungsten concentrate. Mining began in 1940, and surface mining was stopped in 1995. Only underground mining of the deepest and richest deposits (with an average WO₃ content 0.19%) remained profitable in the second half of the 1990s (Bindi & Cipriani 2003)”. **Tyrnyaуз is Russia’s largest tungsten producer** with “low-grade reserves estimated at 375 Million tonnes ore (Nokleberg et al. 2005).”

At **Tyrnyaуз** the rare bismuth sulphotelluride mineral **baksanite** **Bi₆Te₂S₃** occurs in altered magnetite-andradite skarn among voids in aggregates of andradite, calcite, chlorite, and stilpnomelane. “Associated minerals are bismuthinite, **tetradymite**, joséite–A and **ingodite**... gangue minerals are calcite and andradite. **Ingodite** occurs as anhedral grains up to 0.5 mm across, closely associated with bismuthinite (Bindi & Cipriani 2003).” Baksanite contains inclusions of native gold and, rarely, intergrowths of **ingodite** and joséite–A; all are separated from the host aggregates by a thin lining of bismuthinite. Baksanite is ideally Bi₆Te₂S₃; “electron-microprobe analyses gives the formula (Bi_{4.94}Pb_{0.96})sum_{5.90}Te_{2.03}S_{3.06} ...Analyses of **ingodite** and joséite–A associated with plumbian baksanite yield the following formulae (means of 5 analyses):

ingodite (Bi_{1.78}Pb_{0.32})sum_{2.10}(S_{1.01}Te_{0.95})sum_{1.96}

joséite–A (Bi_{3.64}Pb_{0.40})sum_{4.04}Te_{0.91}S_{1.94}

thus indicating a Pb-rich environment of formation for the baksanite (op. cit.).”

In the **Pangushan W + Bi vein-form deposit** Jiangxi Province, Ganzhou Prefecture in China, Shin et al. (2005) quote an **ingodite** formula, after work by Ren (1986b):

“(Bi_{2.00}Pb_{0.04})sum_{2.04}(S_{0.95}Te_{1.05})sum_{2.00} with Te / S = 1.11, which is close to the ideal composition.” Ren et al. 1986 discuss mineral and element zonation; see above under ikunolite.

The **Nakdong As + Bi deposit** in South Korea is a Cretaceous age intrusion-related deposit with some gold & silver content. In Nakdong **ingodite** has general composition

(Bi_{1.94}Sb_{0.01}Ag_{0.04})sum_{1.99}(S_{1.08}Te_{1.03}Se_{0.03})sum_{2.14} “regarded as **Te-rich ingodite**” by Shin et al. 2005, but the formula has only the expected *apfu* Te of one unit. **Nakdong ingodites may carry considerable gold to about ⅓ weight percent, section 13.8 below.** Nakdong also has **unnamed Bi₂Te**, see below.

Ingodite in the **Suehiro vein of the Otome Deposit**, Yamanashi Prefecture, Japan is found enclosed in cosalite in Stage II quartz veining formed at 330-150 °C with pyrrhotite, less arsenopyrite, common chalcopyrite, bismuthinite, native bismuth, sphalerite, galena, common Ag- and Sb-bearing cosalite Pb₂Bi₂S₅, galenobismutite PbBi₂S₄, Bi-bearing boulangerite Pb₅Sb₄S₁₁, izoklakeite Pb₂₇(Cu,Fe,Ag)₂(Sb,Bi)₁₉S₅₇, molybdenite and common pyrite (Tsunoda & Shimizu 1995). Suehiro **ingodite** has significant Pb, e.g. analysis no. 3 in their Table 3 is (Bi_{1.77}Pb_{0.23})sum_{2.00}(S_{0.99}Te_{1.01})sum_{2.00}. Stage I scheelite and ferberite are earlier. Sulphur activity *f*S₂ for stage II is estimated at -11 to -20 log units.

Ingodite also occurs in mesothermal Cu-Zn-Pb-Bi-Mo-W veins at the **Ohisawa mine** (Oizawa) Tochigi Prefecture, Japan (Shimizu et al. 1999). Quartz veins in “altered quartz porphyry-granite porphyry have small amounts of calcite muscovite clinozoisite chlorites and pyrite chalcopyrite galena sphalerite marcasite bismuthinite wolframite scheelite and molybdenite. **Ingodite** and joséite–A tend to occur together as anhedral grains up to 30 microns in size at the rim of bismuthinite grains”.

Third Mineralogical Report detailing the finding of two 'new' gold-associated bismuth sulphotelluride minerals and identifying other opaque minerals, namely native silver electrum **tetradymite** **pilsenite** **hessite** bismuthinite–aikinite pavonite and greenockite characterizing a RIRG system in claim # 516584 and the Bunker Hill & Mormon Girl Crown Grants, on Nox Fort Project south of Salmo in Nelson Mining Division, southernmost British Columbia p. 67

Their table 1 has the mean of 3 microprobe analyses $(\text{Pb}_{0.125}\text{Bi}_{1.858}\text{Sb}_{0.002})\text{sum}_{1.985}(\text{S}_{1.012}\text{Te}_{1.004})\text{sum}_{2.016}$ close to ideal excepting Pb content. Shimizu et al. considered minor Pb may be essential to the **ingodite** structure.

“**Ingodite** is described as the second most abundant Bi–Te–(S) phase after **tetradymite** in the **Băița Bihor skarn deposit (Rezbanya)**, Apuseni Mountains in Romania, as well as other deposits in the Upper Cretaceous ‘banatitic’ province (Ilinca & Makovicky 1999). Compositional ranges [of] the entire population varies ... with Bi / (S + Te) from ~0.7 to 1.25 and Te/S from ~0.4 to 0.6. Ilinca & Makovicky (1999) state their compositions contain Pb and plot along the same line as reported by Zav’yalov et al. (1984), i.e., from $(\text{Bi}_{2.00}\text{Pb}_{0.02})\text{sum}_{2.02}(\text{S}_{1.12}\text{Te}_{0.86})\text{sum}_{1.98}$ to $(\text{Bi}_{1.38}\text{Pb}_{0.24})\text{sum}_{1.62}(\text{S}_{0.95}\text{Te}_{1.42})\text{sum}_{2.37}$ (Cook et al. 2007b).” Individual formulae are not given.

At the **Highiş Massif Şoimuş Ilii copper vein prospect** in Romania “**Ingodite**, the most abundant sulfotelluride, displays a limited spread of compositions, with the (Te + Se) / (Te + S + Se) ratio varying from 0.42 to 0.54 and (Bi + Pb) / (Te + Se + S) ranging from 0.9 to 1.06 (Ciobanu et al. 2006a).” The metal: chalcogen ratio is near 1. Mean analysis of **ingodite** [n=8] from Highiş is $(\text{Bi}_{1.92}\text{Pb}_{0.06})\text{sum}_{1.98}(\text{S}_{1.06}\text{Te}_{0.72}\text{Se}_{0.24})\text{sum}_{2.02}$ (op. cit.).

“**Ingodite** from **Carrock Fell**³², Cumbria, U.K. ... is intimately associated with joséite–A, joséite–B, **tetradymite**, bismuthinite and **hedleyite**. Microanalytical data illustrate the variation in Bi / (Te + S) from 0.88 to 1.08 [between $\sim\text{Bi}_5(\text{S},\text{Te})_6$ and $\sim\text{Bi}_6(\text{S},\text{Te})_5$] and significant differences also in Te:S value. The Se contents are negligible (Cook et al. 2007b).” Baksanite $\text{Bi}_6\text{Te}_2\text{S}_3$ may be present. In one polished section the mean of 8 is $(\text{Bi}_{3.09}\text{Pb}_{\text{nil}})\text{sum}_{3.09}(\text{S}_{1.66}\text{Te}_{1.23}\text{Se}_{0.01})\text{sum}_{2.91}$, in another section the mean of 12 is $(\text{Bi}_{2.82}\text{Pb}_{0.04})\text{sum}_{2.86}(\text{S}_{1.55}\text{Te}_{1.59}\text{Se}_{0.01})\text{sum}_{3.14}$.

There is an occurrence in Arizona in Cochise Co. in the Little Dragoon Mts on the **Primos claims** (Primos Mine) aka **Bluebird Mine** (Anthony et al. 1995). **Ingodite** occurs as small silver-gray cleavable crystals with tabular habitat in scheelite-bearing garnetite (a metamorphic rock with more than 75% garnet by volume). Mineralization is hübnerite with minor scheelite, pyrite and chalcopyrite in irregular quartz veins in a fractured and altered Laramide-age quartz monzonite intrusion.

Ingodite also occurs at Kašperské Hory, Nepomuk (Pomuk), Pilzeň Region in Bohemia (Litochleb & Šrein 1994).

³² This is a historic locality with minimal production.

13.5 Composition of Eloise Vein **ingodites**

With a composition of near-equal Te & S, the formula **Bi(Te,S)** is doubled to use the formula **Bi₂TeS**. The average of 16 microprobe analyses of 0412 **ingodite** from Eloise Vein North (Cook et al. 2007c), recalculated to include trace Cd and Se gives a formula close to stoichiometric **ingodite**

$$(\text{Bi}_{1.85}\text{Pb}_{0.09}\text{Sb}_{0.01}\text{Cd}_{0.02})_{\text{sum}1.97}(\text{Te}_{0.98}\text{Se}_{\text{nil}}\text{S}_{1.05})_{\text{sum}2.03}$$

Metal:Chalcogens ratio (Bi + Pb + Sb + Cd) / (Te + Se + S) = 0.970

Grab rock sample 0412 of Eloise Vein North ran 23.10 g/t Au by FA, 27.03 g/t Au & 4.2 g/t Ag by ICP-MS, and 1,601 Bi / 84.1 Pb / 13.2 Mo / 95.4 Te / 1.0 Se (high) ppm. Calculated 'bulk' fineness is 867. 0412 has "mm-thick seams of dark grey-blue very fine to coarse (one mm-sized) Bi minerals, about 0.3% to 0.5% of the sample. Accompanying are many grains of coarse-grained visible gold. Rare microvugs are infilled by metallic-lustre Bi minerals with trace whitish green secondary Bi minerals (Howard 2005)."

The average of 10 microprobe analyses of 0441 **ingodite** from Eloise Vein South (Cook et al. 2007c) recalculated is also near-ideal

$$(\text{Bi}_{1.88}\text{Pb}_{0.05}\text{Sb}_{0.01}\text{Cd}_{0.01})_{\text{sum}1.94}(\text{Te}_{1.06}\text{Se}_{0.01}\text{S}_{0.99})_{\text{sum}2.06}$$

Metal:Chalcogens ratio = 0.942

Grab rock sample 0441 of Eloise Vein South ran 7.97 g/t Au by FA, 8.17 g/t Au & 1.43 g/t Ag by ICP-MS, and 564 Bi / 33.0 Te / 0.2 Se / 2.9 Cu / 4.8 Pb / 15.2 Zn / 30.1 Mo / 0.8 As and 37.1 W ppm. Calculated 'bulk' fineness is 851. 0441 was "a 0.3 m chip sample at the site of BHCK-24 limonite-stained quartz [with] about 0.5% Bi minerals (Howard 2005).

As the above two microprobe average analyses are near-identical **ingodite** appears compositionally uniform along the length of Eloise Vein.

Polished section EL-05 is collected very close to 0424, the site of Eloise Vein North where Clarissa Main Vein intersects it. EDS by N. Cook (Part II) determines EL-05 Bi-tellurides IV V VI & VIII as **ingodites** with respective formulae

$$(\text{Bi}_{1.66}\text{Pb}_{0.29}\text{Sb}_{0.04})_{\text{sum}1.98}(\text{Te}_{1.22}\text{Se}_{0.01}\text{S}_{0.79})_{\text{sum}2.02} \text{ but wt \% adds only to 97.62\%}$$

$$(\text{Bi}_{1.80}\text{Pb}_{0.21})_{\text{sum}2.01}(\text{Te}_{1.10}\text{S}_{0.89})_{\text{sum}1.99}$$

$$(\text{Bi}_{1.81}\text{Pb}_{0.15}\text{Sb}_{0.02})_{\text{sum}1.98}(\text{Te}_{1.14}\text{S}_{0.88})_{\text{sum}2.02}$$

$$(\text{Bi}_{1.73}\text{Pb}_{0.14}\text{Sb}_{0.09})_{\text{sum}1.95}(\text{Te}_{1.09}\text{S}_{0.96})_{\text{sum}2.05}$$

Not considering the first poor determination, the mean of 3 EDS analyses³³ for EL-05 gives **near-ideal ingodite**

$$(\text{Bi}_{1.78}\text{Pb}_{0.17}\text{Sb}_{0.04})_{\text{sum}1.99}(\text{Te}_{1.11}\text{Se}_{\text{nil}}\text{S}_{0.91})_{\text{sum}2.02}$$

Metal:Chalcogens ratio = 0.985

EL-05 **ingodite** has significant 0.17 *apfu* Pb substituting for Bi, slightly more than the former microprobe determinations. Sb is trace. **Lead content in Eloise Vein ingodite does not follow amounts in rock geochem analyses**, low 15.4 ppm Pb in 0424 vs. higher 84.1 ppm Pb in 0412.

³³ Cd was not analyzed by EDS

Grab rock sample 0424 of Eloise Vein North at its intersection with Clarissa Vein ran 9.94 g/t Au by FA, 10.29 g/t Au & 1.52 g/t Ag by ICP-MS, and 476 Bi / 15.4 Pb / 8.6 Mo / 55.8 Te / 0.2 Se (bkgd) ppm. Calculated 'bulk' fineness is 868. "Minor vugs are 1- 3 mm in size. Uncommon clots of dark grey blue bismuthoid minerals colour the quartz. Very fine sized grains of visible gold are set amongst weathered Bi minerals, there are rare traces of a straw yellow-green mineral (Howard 2005)."



Fig. 10 Typical hand specimen of Eloise Vein North with mm-sized seams of dark blue-grey Bi-Te-S-(Se) minerals, slightly weathered. Site 0424 with 9.94 g/t Au (on Map 1) is same as EL-05 site. Above 3 cm mark are traces of very pale yellow-green secondary Bi minerals along recently broken fractures. Orange-yellow limonite is common on weathered fractures. With a 14X lens trace native gold is infrequently seen in patches of the Bi-Te minerals. Magnified 1.5 times.

Concluding, Eloise Vein **ingodite is near-stoichiometric.** For **0424 ingodite** Te is slightly more abundant than S; all three compositional formula have only trace Se. Pb at 0.04 to 0.17 *apfu* ~0.1 is not exceptionally plumbian, c.f. **ingodite** in the Tyrnyauz W + Mo deposit or the Mazowe gold deposit both with 0.32 *apfu* (Table 4). Sb is a low trace.

Mean analyses for the three Eloise Vein **ingodites** give Metal:Chalcogen ratios 0.970 0.942 and 0.985 respectively. These are slightly lower than the expected 0.98-1.08 range Cook et al. 2007b specify. Metal ion content is slightly lower than chalcogens in the formulae.

13.6 Table of global **ingodite** formulae and that in Eloise Vein

Table 4 **Ingodite** formulae compared

Location	No. analyses	Method	Pb	Bi	Sb	Metal Sum	Te	Se	S	Chalc. Sum
RRIG deposits:										
^Mazowe	1	Mprobe	0.319	1.478	-	2.012	0.886	-	1.102	1.988
Brues	1	Mprobe	0.74	1.40	-	2.14	0.72	0.02	1.12	1.96
polymetallic deposits:										
Verkhne-Ingodinskoye 1 of 5	1	Mprobe	0.02	2.00	-	2.02	0.86	0.02	1.12	2.00
Tyrnyauz	5	Mprobe	0.32	1.78	-	2.10	0.95	-	1.01	1.96
*Nakdong	9	Mprobe	-	1.94	0.01	1.99	1.03	0.03	1.08	2.14
Pangushan	1	?	0.04	2.00	-	2.04	1.05	-	0.95	2.00
Ohisawa	3	Mprobe	0.125	1.858	0.002	1.985	1.004	-	1.012	2.016
Băița Bihor 1	1	?	0.02	2.00	-	2.02	0.86	-	1.12	1.98
Băița Bihor 2 [poor]	1	?	0.24	1.38	-	1.62	1.42	-	0.95	2.37
Suehiro vein Otome	4	Mprobe	0.23	1.77	-	2.00	1.01	-	0.99	2.00
Highiş	8	Mprobe	0.06	1.92	-	1.98	0.72	0.24	1.06	2.02
Nox Fort:										
♠Eloise Vein North 0412	16	Mprobe (2007)	0.09	1.85	0.01	1.97	0.98	-	1.06	2.03
§Eloise Vein South 0441	10	Mprobe (2007)	0.05	1.88	0.01	1.94	1.06	0.01	0.99	2.06
Eloise Vein North EL-05 near 0424	3	SEM	0.17	1.78	0.04	1.99	1.11	-	0.91	2.02

^from Oberthür & Weiser 2008; also Fe_{0.215}

*also Ag_{0.04}

♠also Cd_{0.02}

§also Cd_{0.01}

13.7 Interpretation: Compare conditions of formation of **ingodite** in the Fort Knox and Pogo deposit GBT mineral assemblages

In the **Pogo Alaska** RIRG deposit [3.51 M. oz] **ingodite** is sixth in abundance of twelve gold-associated bismuth and bismuth telluride minerals (Rombach et al. 2002). The formula is stated 'BiTeS'; no analyses are given. In only five microscopic sections the BiTel Knoll veins have 7 of 13 GBT minerals identified in a thorough research study of the Liese Zone at Pogo (see Rombach et al. 2002). All three Bi-Te mineral assemblages defined by Rombach et al. (2004) have **ingodite**. Furthermore, reading McCoy (Figs. 43A & 43C in 2000 thesis) **unnamed Bi₂Te** occurs in white/gray quartz veins in the **Pogo deposit**.

In both the Fort Knox and Pogo deposits

“Bi-Te mineralogy changes in kind with the gold composition and the sulphide-alteration assemblages. In general paragenetically early, high temperature, and very low fS_2 (loellingite³⁴–pyrrhotite stable) native bismuth, bismuth telluride and S-poor sulphotelluride [e.g. **ingodite**, joséite–B bearing] assemblages yield to late, lower temperature, higher relative fS_2 (pyrite stable) S-rich sulphotelluride [e.g. joséite–A], Sb-bearing bismuthinite and sulphosalt assemblages (Rombach et al. 2004).”

In general Central Nox Fort mineralization is paragenetically early, like that at Fort Knox and Pogo. Low Sb content of all analyzed bismuthinite grains in the BiTel Knoll quartz veins supports this conclusion. The interpretation is that increase in chemical activity of sulphur fS_2 , late stage sulphidation, is a key mechanism of gold deposition on Nox Fort. See the references for Rombach et al. (2002) and (2004) complete.

13.8 **Ingodite** carries gold and silver in solid solution in the Nakdong South Korea As + Bi deposit

Importantly Nakdong ingodites may carry considerable gold to about ⅓ weight percent: three of nine microprobe analyses have gold in solid solution 0.16, 0.29 and 0.31 wt % or 1,600 2,900 and 3,100 ppm Au (Table 1 in Shin et al. 2005). **The maximum recorded 3,100 ppm = 3.1 Kg/t = 90.5 oz/ton Au).** The highest silver value is even greater at ~1 wt %.

³⁴ Easily mistaken for arsenopyrite, a common associate which it closely resembles in hand specimen. They are difficult to distinguish; crystal forms, color, luster, streak and fracture are all very similar. Loellingite is somewhat softer and denser. Loellingite is steel-gray to silver-white, luster metallic; streak is gray black; hardness 5-5 1/2; specific gravity approx. 7.1-7.5; a basal cleavage is rarely distinct. Habits: Brittle with uneven fracture - flat surfaces (not cleavage) fractured in an uneven pattern; massive to granular, a common texture observed in granite and other igneous rock; prismatic; crystals are usually twinned and commonly striated lengthwise. (from webmineral.com & www.galleries.com/minerals/sulfides/lollingi/lollingi.htm)

13.9 Conclusion: Eloise Vein **ingodite** grains carry gold and silver that may have nucleated with formation of **unnamed Bi₂Te**

Laser ablation analyses of Eloise Vein North and South polished sections show “highest Au concentrations do not appear to be restricted to one telluride species in particular. **Ingodite** can be the most and least Au-enriched within individual patches (Cook et al. 2007c.)”, see their figs. 4 & 10. In Eloise Vein some **ingodite** carries gold like in the Nakdong As + Bi deposit, Eloise Vein **ingodite** is Au + Ag bearing.

In Eloise Vein South **unnamed Bi₂Te** (misabeled Hed) partly replaces **auriferous ingodite** grains (Ing) with native gold formed, a prominent ‘gold corona’ texture:

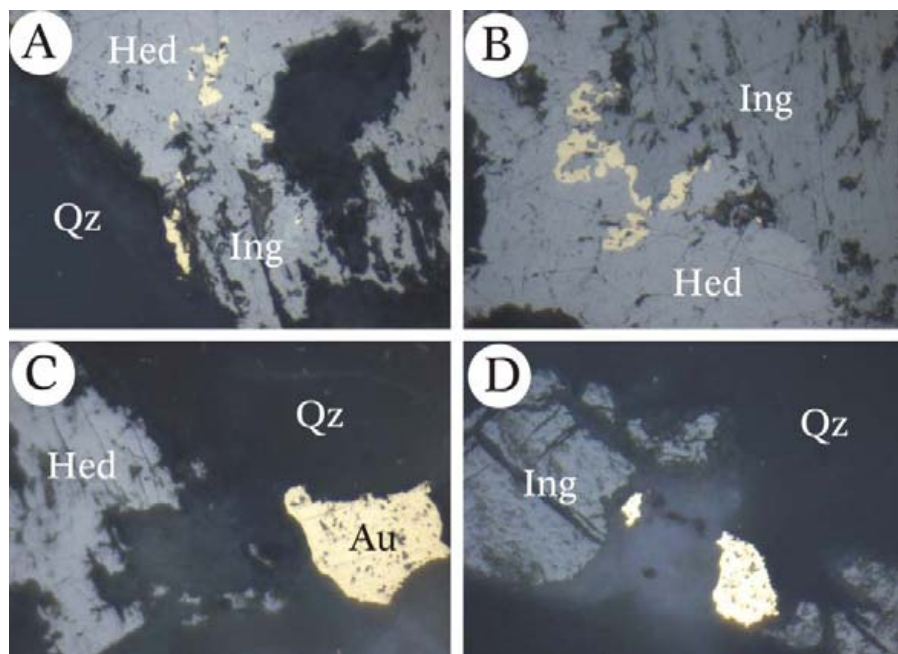


Fig. 11 Four reflected light microphotos showing assemblages of gold and Bi-minerals in Eloise Vein South sample 0441. Figs. 11A & 11B display a well developed ‘gold corona’ texture at **ingodite**–**unnamed Bi₂Te** grain boundaries. This reaction formed native gold or gold-rich electrum. Initially **hedleyite Hed** was identified; further work confirms it is near-ideal **unnamed Bi₂Te**. **Ing**: **ingodite**, **Au**: gold, **Qz**: quartz. Horizontal field of view is 50 µm. Fig. 3 from Cook & Ciobanu 2006.

“The mantling of **ingodite** by **Bi₂Te** and the rim of native gold formed at the boundary between the two (Fig. 2c, d) can be interpreted as replacement of **ingodite** that also may have released Au. This would explain the low values of Au in **ingodite** from this patch (0.05 ppm) relative to another in which no native gold is observed (9 ppm). ...The jump over an order of magnitude in the Au signal obtained during ablation of **Bi₂Te** is indicative of formation of sub-micron scale inclusions of gold (their fig. 5 in Cook et al. 2007c.).”

This may be the first report of the reaction

ingodite Bi₂TeS with sub-microscopic Au + Ag ► **unnamed Bi₂Te** + native gold or gold-rich electrum

Third Mineralogical Report detailing the finding of two 'new' gold-associated bismuth sulphotelluride minerals and identifying other opaque minerals, namely native silver electrum **tetradymite** **pilsenite** **hessite** bismuthinite–aikinite pavonite and greenockite characterizing a RIRG system in claim # 516584 and the Bunker Hill & Mormon Girl Crown Grants, on Nox Fort Project south of Salmo in Nelson Mining Division, southernmost British Columbia p. 73

Sulfur is released. The maximum gold content of 23 spots ablated by the LA-ICP-MS method is 57 ± 8 ppm Au in **unnamed** Bi_2Te in Eloise Vein South sample 0441. Two other **unnamed** Bi_2Te analyses ran 6.8 ± 1 and 3.6 ± 0.7 ppm Au (op. cit., their fig. 3). **Ingodite** ran 9 ± 1.8 ; joséite–A or –B 26 ± 5 ppm.

14 Unnamed Bi₂Te

14.1 Unnamed Bi₂Te – a partly characterized mineral

Unnamed Bi₂Te is especially rare, known at about 14 localities. The International Mineralogical Association has not formally approved it as a mineral and there is no type locality. **Its composition is certainly distinct from hedleyite.** “Bi₂Te has been reported by Gamyranin et al. (1980, 1982), Goncharov et al. (1984), Huang et al. (1991), Luukkonen (1994) and Gu et al. (2001) [also Shin et al. 2005 and Zachariáš et al. 2006, see below]. ...In the case of Bi₂Te, the observations of Gu et al. (2001) are to be noted: ‘...the consistent “2:1” stoichiometry and slight difference in optical properties compared to **hedleyite**, **joséite–B** or **pilsenite**, lead us to infer that this may be an independent mineral.’ ...Our own observations are similar: Bi₂Te is conspicuous within several of the Romanian skarn deposits, and in numerous other **reduced** gold deposits, but it rarely exceeds a few mm in diameter. We would further reason that the incidence of Bi₂Te in nature and in synthetic studies (Abrikosov & Bankina 1958, Okamoto & Tanner 1990) is sufficiently great to suggest that a discrete mineral with this composition exists (Cook et al. 2007b, see refs. quoted therein)”. Recalculation of three Ortosa gold skarn ‘**hedleyite**’ analyses show two of them are actually **unnamed Bi₂Te** (see below under **hedleyite**).

14.2 Unnamed Bi₂Te first described in Ergelyakh Au-W-Bi deposit Far East Russia

Gamyranin (1980, 1982) first described **unnamed Bi₂Te** in the **Ergelyakh Au-W-Bi deposit**, Indigirka River Basin in Saha Republic, Yakutia, Far East Russia. Fleischer & Pabst (1981) abstract the 1980 work and M. Fleischer (1982) provides a full translation. The following quotes are from M. Fleischer: “The [**Ergelyakh**] deposit is restricted to greisenized granodiorite, cut by a series of quartz and quartz + tourmaline veins and veinlets.” The first paragenetic stage comprises W-bearing minerals, the second complicated assemblages of bismuth minerals. **Unnamed Bi₂Te** occurs with bismuth sulphotellurides and native bismuth. “Bi₂Te occurs as a narrow 0.1-0.2 mm rim adjacent to muscovite, amid various Bi minerals, at the contact of these with quartz, and very rarely as inclusions in native bismuth (Fleischer 1982).” “Early deposits of bismuthinite ... alternate with close intergrowths of ... **joséite–A** and mineral [phases] K and L of Godovikov et al. (1971) and ... Bi₂Te and tellurobismuthite. The latest mineral is native bismuth.” Tellurobismuthite is considerably more common than Bi₂Te “and is usually associated with [unspecified] bismuth sulphotelluride...”

The formulae of two grains from 8-10 microprobe determinations on each are simply Bi_{2.02}Te_{0.98} and Bi_{2.04}Te_{0.96}. Metal:Chalcogen ratios are thus Bi/Te = 2.07 & 2.11.

Gamyranin (1968) describes Ergelyakh mineralization as “an association of **joséite–A** and **joséite–B** with **tetradymite** ... with native bismuth, bismuthinite and gold, representing a late stage of the ore formation.” Nokleberg et al. 1997 classify Ergelyakh as a ‘Granitoid-related Au’ deposit. Size is ‘small’ with average grade 0.1-90 g/t Au, 0.02-0.8% WO₃, locally to 1.37% Bi, to 0.4% Te, and to 2% As. **In C. Hart’s (2007) classification it is a RIRG deposit.** Various-oriented quartz veins and stringers occur along the contact of an Early Cretaceous granodiorite and Upper Triassic metasediments. “Quartz constitutes 90% of the veins, which also include tourmaline, muscovite, wolframite, arsenopyrite, cobaltite, niccolite, bismuth, bismuthinite, gold, **joséite** [both **joséite–A** and **–B**], and other Te and Bi minerals. Ore bodies are cut by [later] crush belts that contain comb quartz, galena, sphalerite, Ag-tetrahedrite, and pyrargyrite that are part of epithermal veins with high Ag grades, up to 200 g/t Ag (op. cit).” The latter compare to younger phase II Pb-Ag-Mo mineralization in the Moly Quartz Vein, just south of BiTel Knoll. Anthony et al. 1990 also have sulphotsumoite and tsumoite occurring.

14.3 Problem identifying **unnamed Bi₂Te** and **hedleyite** considering the minerals do not have uniform compositions

Ciobanu et al. (2008) discuss the problem of identifying a specimen of an inhomogeneous Bi-Te mineral as either **hedleyite** or **unnamed Bi₂Te** or another species:

“Recognizing which of the stacking sequences correspond to single phases is important for assessing equilibrium diagrams, e.g., for the systems Bi-Te or Bi-Se (Okamoto and Tanner 1990; Okamoto 1994), as much as for petrogenetic interpretations. Slower cooling rates ... are inherent to specific geologic environments. For example, the richest Bi-phase obtained experimentally in the system Bi-Te is Bi₇Te₃, whereas the results here show the existence of Bi₈Te₃, a phase still richer in Bi and not previously identified. [This in sample H2a from the Good Hope skarn deposit near Hedley] formed in a deep environment thus increasing the efficiency of slow cooling rates in stabilizing Bi-rich phases.

The laboratory results are nonetheless paralleled by the fact that the mineral corresponding to **Bi₇Te₃**, **hedleyite**, is relatively common, whereas the nearest phases with $i = 1$, [that is, phases built by a single type of Bi_{2k}X₃ module] i.e., **Bi₂Te** (= Bi₆Te₃) and Bi₈Te₃, are unnamed species, only occasionally reported (or inferred) from electron probe microanalysis data (e.g., Cook et al. 2007b). This is despite the fact that both Bi₂Te and Bi₈Te₃ have simpler stacking sequences ... than Bi₇Te₃ ... and should, presumably, be more stable. Why then are **Bi₂Te** or Bi₈Te₃ not more widely reported? Small chemical differences between Bi₇Te₃ and either **Bi₂Te** or Bi₈Te₃ (3 atomic % or 2 wt. % Te) may make them difficult to recognize on the scale of the microprobe beam. [But Oberthür and Weiser (2008) would disagree and show a full range of 50 Viceroy mine ‘**hedleyite**’ compositions in their Fig. 5 from 24.5% Te = **Bi₃Te** to 33.3% Te = **Bi₂Te**; these are homogeneous phases]. In any case, inhomogeneous material, containing intergrowths of **Bi₂Te**, Bi₈Te₃ and Bi₇Te₃ will inevitably give a “bulk” composition approximating to Bi₇Te₃. In fact, Cook et al. (2007b) note that the variety of published microanalytical data for **hedleyite** reflect a broad field from Bi₆Te₃ [= **unnamed Bi₂Te**] to Bi₈Te₃ (or even Bi₉Te₃). Small chemical variations can be assumed to occur at a local scale during crystallization. For example, in mixed-layer compounds, often occurring as lamellae stratified along [the crystallographic c axis] in a given package, compositional variation can be recognized from one lamella to another, e.g., **hedleyite** lamellae embedded within a patch of Bi₈Te₃... (Ciobanu et al. 2008).”

In the simple synthetic Bi-Te system the phase diagram has a triple point for the Bi₂Te phase at 66.6 wt % Bi at 585 K = 311.85 °C (Predel 1992). This is the maximum temperature for stability of **unnamed Bi₂Te** in this simple system. This fits with the paragenetic sequence of deposition described in the **Mokrsko deposit**: “**Bi₂Te** is younger than maldonite or native gold and older than **tetradymite**, **joséite–A**, **joséite–B** or bismuthinite (Zachariáš et al. 2006).”

14.4 Unnamed **Bi₂Te** in some global RIRG deposits

Upon re-reading D. McCoy’s (2000) thesis, the triangular plot of Bi:Te:S cation ratios fig. 43A has analyses of two grains of a mineral that can only be **unnamed Bi₂Te** plotting at ~63 atom % Bi. These are **from Pogo deposit white/gray veins**. Table B-4 p. 165 has the analyses. Furthermore on fig. 43C two grains ‘circled 8’ included in arsenopyrite plot close to ideal **Bi₂Te**; these carry some Au + Ag. Concluding, **some Pogo deposit GBT assemblages also include unnamed Bi₂Te**.

Three **Ortosa gold skarn ‘hedleyite’** analyses are actually **unnamed Bi₂Te**, determined by recalculating compositions in Fuertes-Fuente et al. (2000) and Cepedal et al. (2006), see under **hedleyite** below.

Third Mineralogical Report detailing the finding of two 'new' gold-associated bismuth sulphotelluride minerals and identifying other opaque minerals, namely native silver electrum **tetradymite** **pilsenite** **hessite** bismuthinite–aikinite pavonite and greenockite characterizing a RIRG system in claim # 516584 and the Bunker Hill & Mormon Girl Crown Grants, on Nox Fort Project south of Salmo in Nelson Mining Division, southernmost British Columbia p. 76

In the 1.03 M. oz **Petráčkova hora deposit**, Czech Republic (Zachariáš et al. 2001 and p.c. 2006) in one polished section “a veinlet of an [unnamed] $\text{Bi}_2(\text{Te}, \text{Se})$ cuts bismuthinite (their fig. 7C). The formula is given as $\text{Bi}_{2.3}\text{Te}$ (?). Jonassonite $\text{Au}(\text{Bi}, \text{Pb})_5\text{S}_4$ (Paar et al. 2006) also occurs (op. cit. p. 524).

Three microprobe analyses of unnamed Bi_2Te grains from the intrusion-hosted **Mokrsko deposit** in Czech Republic [3.08 M. oz], samples Mo-10, Mo-13/1 & Mo-11/1, give the formula $\text{Bi}_{2.02}\text{Te}_{0.98}$ for the first two and $\text{Bi}_{2.03}\text{Te}_{0.97}$ for the third (Zachariáš p.c. 2006). Sb and S contents are nil. Unnamed Bi_2Te and other little-characterized Bi-Te minerals are “younger than maldonite or native gold and older than **tetradymite**, joséite–A, joséite–B or bismuthinite. Joséite–A and –B are always younger than **tetradymite**. Bismuthinite is younger than both gold and bismuth telluride or bismuth sulphotelluride minerals (Zachariáš et al. 2006).”

At **Mokrsko** “gold concentration reaches economically important tonnages (several tons of gold) with grades from 0.2 to 30 g/t and averaging 2 g/t in the whole mineralised block. Minerals of Bi (bismuth, bismuthinite, Te (**hedleyite** and joséite–B) and Au (native gold, maldonite AuBi_2 and aurostibite AuSb_2) occur as very small particles ... observed by scanning electron microscopy (Boiron et al. 2001)”.

Nekrasov (1996, Table 52) gives formulae of minerals associated with maldonite, gold and gold-silver bearing deposits in north-eastern Russia. Three deposits have unnamed Bi_2Te :

Chuguluksoe has maldonite, gold, **tetradymite**, joséite–A, joséite–B, native bismuth and ‘bismuth telluride’, near-stoichiometric unnamed Bi_2Te
 $(\text{Bi}_{2.02}\text{Pb}_{\text{nil}}\text{Sb}_{0.04})\text{sum}_{2.06}\text{Te}_{0.93}\text{Se}_{\text{nil}}\text{S}_{\text{nil}}\text{sum}(\text{Te} + \text{Se} + \text{S})_{0.93}$.

Dybinskoe has maldonite, gold, **tetradymite**, and ‘bismuth telluride’ or near-stoichiometric unnamed Bi_2Te
 $(\text{Bi}_{1.90}\text{Pb}_{0.01}\text{Sb}_{0.01})\text{sum}_{1.93}\text{Te}_{1.05}\text{Se}_{0.02}\text{S}_{0.03}\text{sum}(\text{Te} + \text{Se} + \text{S})_{1.10}$

Kuchugei-Yuryakhskoe has maldonite, sulphide, jonassonite AuBi_5S_4 then unnamed, gold with maldonite, native gold, **hedleyite**, joséite–B, ‘joséite–E’ & ‘joséite–K’ both not established species, bismuthinite and ‘bismuth telluride’, that is near-ideal unnamed Bi_2Te
 $(\text{Bi}_{1.96}\text{Pb}_{\text{nil}}\text{Sb}_{0.02})\text{sum}_{1.98}\text{Te}_{0.89}\text{Se}_{\text{nil}}\text{S}_{0.13}\text{sum}(\text{Te} + \text{Se} + \text{S})_{1.02}$

14.5 Unnamed Bi_2Te in some global polymetallic deposits

Gu et al. 2001 researched Bi-Te-S-(Se) minerals from various ore deposits genetically related to Jurassic [Yanshanian 132-148 Ma] granites. Notable is the large-scale **Huangshaping polymetallic Pb-Zn-Cu-Ag-Fe-W-Mo-Sn deposits** in Hunan Province, south China. These are skarn and mesothermal vein-type deposits in Lower Carboniferous carbonates and sandstones about small Jurassic plugs of felsic porphyries. It is operated by Hunan Nonferrous Metals Corp. Ltd. with significant reserves. The Bi-Te-S-(Se) minerals occur in the Cu-Ag orebody with chalcopyrite and “minor marcasite pyrite bornite molybdenite sphalerite and galena. The Bi-Te-S-(Se) minerals, 10 micron to 1.5 mm in size, include **tetradymite** tsumoite sulphotsumoite **pilsenite** joséite–B **hedleyite** and unnamed Bi_2Te ... in close association with wittichenite emplectite bismuthinite hodrushite unnamed $\text{AgCu}_4\text{Bi}_7\text{S}_{13}$ native bismuth and Ag-Te series minerals (Gu et al. 2001)”.

Unnamed Bi_2Te grains of 2-10 μm in size occur as veinlets along **pilsenite** grain boundaries in a matrix of either joséite–B (text) or **hessite** (note in fig. 5B the label Hs = hessite). Jambor (2002) briefly reviews Gu et al.’s research. The mean of 3 microprobe analyses is
 $(\text{Bi}_{2.003}\text{Pb}_{\text{nil}}\text{Sb}_{\text{nil}}\text{Ag}_{\text{nil}})\text{sum}_{2.01}\text{Te}_{0.983}\text{Se}_{\text{nil}}\text{S}_{\text{nil}}\text{sum}(\text{Te} + \text{Se} + \text{S})_{0.983}$, near-stoichiometric unnamed Bi_2Te .

In the **Nakdong South Korea As + Bi deposit** five electron microprobe analyses of unnamed Bi_2Te have a compositional range $(\text{Bi}_{1.95-1.97}\text{Sb}_{0.02-0.03})\text{sum}_{-1.97}(\text{Te}_{0.79-0.86}\text{Se}_{0.11-0.13})\text{sum}_{-0.90}$ (Shin et al. 2005).

Third Mineralogical Report detailing the finding of two 'new' gold-associated bismuth sulphotelluride minerals and identifying other opaque minerals, namely native silver electrum **tetradymite** **pilsenite** **hessite** bismuthinite–aikinite pavonite and greenockite characterizing a RIRG system in claim # 516584 and the Bunker Hill & Mormon Girl Crown Grants, on Nox Fort Project south of Salmo in Nelson Mining Division, southernmost British Columbia p. 77

The mineral has “a relatively constant Bi / (Te + Se + S) ration close to 2 (1.99-2.11) but a variable Te/ (Se + S) ratio from 5.68-8.18 with Se contents 1.6-1.9 wt %. ...**unnamed** Bi_2Te is “placed in the intermediate compositional range **between** Bi_2Te and $\text{Bi}_2(\text{Te},\text{Se})$ (op. cit.).” The mean of 5 analyses is $(\text{Bi}_{1.97}\text{Sb}_{0.02})\text{sum}_{1.99}\text{Te}_{0.83}\text{Se}_{0.12}\text{S}_{0.01}\text{sum}(\text{Te} + \text{Se} + \text{S})_{0.96}$ with no Fe or Pb, near-stoichiometric.

Trace **unnamed** Bi_2Te occurs in the high grade zinc and gold **Caijiaying mine** in Hebei Province, China (Huang et al. 1991). In Zone III, one of five identified mineralized zones, the current Zn resource is 23.6 Mt @ 8.08% and Au resource 2.61 Mt @ 6.78 g / t (Chang et al. 2006).

Cook & Ciobanu (Aug. 2006) find **unnamed** Bi_2Te in the **Good Hope skarn in the Hedley district B.C.** [2.18 M. oz].

Unnamed Bi_2Te is reported in the Bi-Au association in pyrrhotite-rich undersea massive sulfide deposits, **Esanaba Trough, Southern Gorda Ridge** (Törmänen & Koski 2005). The given microprobe formula is near-stoichiometric $\text{Bi}_{2.004}\text{Te}$ (their Table 3 p. 1,144). **Ikunolite** (?) may also occur (see above).

14.6 Near-stoichiometric **unnamed** Bi_2Te in three Nox Fort occurrences

Unnamed Bi_2Te is **near** near-stoichiometric in three Nox Fort occurrences.

unnamed Bi_2Te in Eloise Vein South (Map 1):

0441, mean of 12 microprobe analyses in two sections 0441a & 0441b recalculated from Cook et al. 2007c

$(\text{Bi}_{1.96}\text{Pb}_{0.02}\text{Sb}_{0.01}\text{Cd}_{0.01})\text{sum}_{2.01}\text{Te}_{0.92}\text{Se}_{0.01}\text{S}_{0.06}\text{sum}(\text{Te} + \text{Se} + \text{S})_{0.99}$

Pb Sb Cd Se & S are near absent.

The following are by EDS analyses:

unnamed Bi_2Te in Eloise Vein South EL-02 mean of 2

$(\text{Bi}_{1.89}\text{Pb}_{0.11})\text{sum}_{2.005}\text{Te}_{0.99}\text{Se}_{0.015}\text{S}_{\text{nil}}\text{sum}(\text{Te} + \text{Se} + \text{S})_{1.00}$

unnamed Bi_2Te in Lefevre skarn / hornfels (Map 2):

L-11 skn one analysis of a grain labelled 'hedleyite 2'

$(\text{Bi}_{2.04}\text{Pb}_{\text{nil}})\text{sum}_{2.04}\text{Te}_{0.91}\text{Se}_{0.01}\text{S}_{0.05}\text{sum}(\text{Te} + \text{Se} + \text{S})_{0.96}$

unnamed Bi_2Te in Lefevre arsenopyrite + pyrite quartz vein, E side of the pit in trench 5:

L-04QVXtry arsenopyrite vein mean of 5³⁵

$(\text{Cu}_{0.018}\text{Ag}_{0.008}\text{Bi}_{1.932}\text{Pb}_{\text{nil}}\text{Sb}_{0.054})\text{sum}_{2.012}\text{Te}_{0.958}\text{Se}_{0.016}\text{S}_{0.012}\text{sum}(\text{Te} + \text{Se} + \text{S})_{0.984}$

Sb is in trace quantities; five analyses give a nil value, min. 0.02 and max. 0.11 *apfu*. Table 5 compares other global **unnamed** Bi_2Te localities.

³⁵ Cu Ag Pb and S determined only in individual analyses

14.7 Table of global **unnamed Bi₂Te** formulae, in Eloise Vein and in Lefevre skarn and vein mineralization

Table 5 **Unnamed Bi₂Te** formulae compared

Location	No. analyses	Method	Pb	Bi	Sb	SUM	Te	Se	S	SUM
RRIG deposits:										
Ergelyakh 1	8-10	Mprobe	-	2.02	-	2.02	0.98	-	-	0.98
Ergelyakh 2	8-10	Mprobe	-	2.04	-	2.04	0.96	-	-	0.96
§Ortosa [2] Cepedal et al. 2006	1	Mprobe	-	2.00	0.01	2.04	0.94	0.02	-	0.96
»Ortosa [3] Cepedal et al. 2006	1	Mprobe	0.01	1.97	0.01	2.01	0.98	0.01	-	0.99
¬Ortosa [6] Fuentes-Fuente et al. 2000	1	Mprobe	0.01	1.96	0.01	2.03	0.96	0.01	-	0.97
Mokrsko	3	Mprobe	-	2.02	-	2.02	0.98	-	-	0.98
Chuguluksoe	1	?	-	2.02	0.04	2.06	0.93	-	-	0.93
Dybinskoe	1	?	0.01	1.90	0.01	1.93	1.05	0.02	0.03	1.10
Kuchugei-Yuryakhskoe	1	?	-	1.96	0.02	1.98	0.89	-	0.13	1.02
polymetallic deposits:										
Huangshaping	3	Mprobe	-	2.003	-	2.003	0.983	-	-	0.983
Nakdong	5	Mprobe	-	1.97	0.02	1.99	0.83	0.12	0.01	0.96
Escanaba Trough (?)	1	Mprobe	-	2.004	-	2.004	1.000	-	-	1.000
Nox Fort:										
¤Eloise Vein South 0441a & 0441b (Cook et al. 2007c)	12	Mprobe	0.02	1.96	0.01	2.01	0.92	0.01	0.06	0.99
Eloise Vein South EL-02	2	SEM	0.11	1.89	-	2.005	0.99	0.015	-	1.00
L-11 skn Lefevre hornfels/skarn 'hedleyite 2'	1	SEM	-	2.04	-	2.04	0.91	0.01	0.05	0.96
L-04QVXtry Arsenopyrite – Qtz Vein cutting Lefevre hornfels/skarn	5	SEM	-	1.932	0.054	2.012	0.958	0.016	0.012	0.984

§ with Zn 0.01 As 0.01 and 0.46 wt % gold corresponding to 0.01 apfu Au

» with Hg 0.01 As 0.01 Fe 0.01 apfu

¬ with Fe 0.05 and 0.34 wt % gold corresponding to 0.01 apfu Au

¤ with trace Sb & Cd, both 0.01 apfu

14.8 In Eloise Vein early-formed **ingodite** may react to form **unnamed Bi₂Te** with native gold (or electrum) deposited

The reaction

ingodite Bi₂TeS with sub-microscopic Au + Ag ► **unnamed Bi₂Te** + native gold or gold-rich electrum

is inferred by textures in Eloise Vein South (see discussion above under **ingodite**). Sulfur is released. The maximum gold content of 23 spots ablated in **unnamed Bi₂Te** in Eloise Vein South sample 0441 by the LA-ICP-MS method is 57 ± 8 ppm Au. Two other **unnamed Bi₂Te** spots illustrated ran 6.8 ± 1 and 3.6 ± 0.7 ppm Au (op. cit., their fig. 3). Clearly **unnamed Bi₂Te** is a direct gold associate and carrier in Eloise Vein.

15 Hedleyite Bi_7Te_3 or $\text{Bi}_{2+x}\text{Te}_{1-x}$

15.1 Hedleyite type locality – former Good Hope mine in BC, properties and associated minerals

The type locality is the former **Good Hope mine** MINFILE 092HSE060, sited 4 km SE of the Nickel Plate mine near Hedley, BC. There **hedleyite** occurs in plates up to 6 mm wide and 1 mm thick with hexagonal outline, often with trigonal growth features. Separating these gives “flexible and slightly elastic folia; occasionally a hint of crystal form. **Hedleyite** is tin-white with an iron-black tarnish; perfect basal cleavage, hardness 2 (Warren & Peacock 1945)”. The country rock is garnet-epidote-pyroxene skarn cut by irregular veins and stringers of quartz. Most of the **hedleyite** is in these quartz bodies, but some also occurs in the skarn. Associated minerals include bismuth, joséite–A, pyrrhotite, arsenopyrite, calcite, and gold. **Hedleyite** is often intercalated with joséite–B, native bismuth, and gold, associated with arsenopyrite, molybdenite, and pyrrhotite (op. cit.). Cook & Ciobanu (Aug. 2006) also tentatively identify unnamed Bi_2Te .

Good Hope **hedleyite** has formula $\text{Bi}_{2.19}(\text{Te}_{0.80}\text{S}_{0.01})\text{sum}_{0.81}$, the average of two analyses (© 2001-2005 Mineral Data Publishing, version 1). With $x = 0.19$ this is just in the range of the formula $\text{Bi}_{2+x}\text{Te}_{1-x}$ $x = 0.13$ to 0.19 . For ionic charge neutrality a surplus of Bi or Metals necessarily coincides with a deficit of Te.

Hedleyite is “impossible to visually identify. All species in the tetradymite / tellurobismuthinite / pilsenite family must be analysed for positive identification.” <http://www.mindat.org/min-1843.html>
This lists 43 **hedleyite** occurrences.

15.2 Hedleyite – its formula and compositional range

Cook et al. (2007b) in their review of Bi-Te-Se-S minerals of the tetradymite group note “**Hedleyite** is attributed the formula Bi_7Te_3 ...some give the formula as Bi_8Te_3 or $\text{Bi}_{2+x}\text{Te}_{1-x}$, stressing the range of natural compositions. The literature data for **hedleyite** ... indicate that natural compositions may extend beyond Bi_7Te_3 (30 atom % Te) to Bi_8Te_3 (27.2 atom % Te) and may approach Bi_3Te (25 atom % Te) and even Bi_7Te_2 in some cases. ...Other compositions with lower values of the Bi:Te ratio have also been ascribed to **hedleyite**. ...Our own experience is that **hedleyite** compositions are generally consistent over a certain range of Bi:Te within a given deposit, but tend to vary among deposits [but not in Viceroy gold mine Bi-Te, see below]. ...Sum Metal divided by Sum Chalcogens (Te + Se + S) in **hedleyite** [is ideally $7/3=$] 2.33. Selenium substitution in **hedleyite** appears to be low ... contents slightly above the 1 wt % level in the data from Maiskoe appear to be the highest reported. The extent of Pb substitution for Bi in **hedleyite** seldom exceeds 1 wt %.”

Warren and Peacock (1945) give the formula Bi_7Te_3 but Bayliss (1991) notes “both Bi_5Te_2 and Bi_8Te_3 are in better agreement with the chemical analyses”. See section 14.3 ‘Problem identifying unnamed Bi_2Te and **hedleyite** considering these Bi-Te minerals are inhomogeneous’.

15.3 Three other **hedleyite** localities in the Hedley district

The Hedley district in BC produced 2.18 M. oz. gold. In addition to the type locality the former Good Hope mine claim **hedleyite** also occurs at {1} the abandoned **French mine / Oregon claim** MINFILE 092HSE059, 5 km S of the Nickel Plate mine near Hedley.

"The mineralization here is similar to that of the Good Hope claim, about 2 miles north, and consists of massive garnet, hedenbergite, wollastonite, calcite, and minor quartz with sparsely disseminated sulphides. **Hedleyite** and joséite-B are seen together in polished sections as rounded grains with smooth boundaries. When the two minerals are in contact, **hedleyite** is distinguished by its slightly lighter colour. Native bismuth, molybdenite, and gold are closely associated ... while bornite, chalcopyrite, cobaltite, and safflorite occur apart and are locally abundant (Thompson 1951)." Characteristic are "arsenopyrite chalcopyrite covellite bornite and pyrrhotite with sporadic pyrite, molybdenite and minor scheelite. In the lower parts of the deposit rare coarse visible gold and visible tellurides are present (Ray & Dawson 1994).

{2} At the former **Nickel Plate mine** near Hedley MINFILE 092HSE036 "The sulfide minerals associated with garnet and pyroxene skarn are dominantly arsenopyrite, loellingite, and pyrrhotite. Other sulfides, in decreasing order of abundance, are chalcopyrite, pyrite, sphalerite, **hedleyite**, native bismuth, gold, galena, and maldonite (Ettlinger 1990). This latter group of minerals is mostly associated with lower temperature alteration including amphibole, ferroan wollastonite, scapolite, and prehnite (Meinert 1992)." Ray & Dawson (1994 p. 51) mention "less common to rare opaques include electrum tetrahedrite native copper magnetite bismuthinite gersdorffite marcasite covellite molybdenite **tetradymite** ... cobaltite erythrite pyrrargyrite lollingite and breithauptite."

{3} Recently a Goldcliff Resource Corporation (GCN TSX-V) news release reports minerals in a sample with 17.368 oz. per ton gold [or 596 g/t] from the **Bonanza Trench on the Panorama Ridge property** near Hedley. These are **hedleyite**, joseite (*sic* presumably joséite-A) and native gold. "The minerals were identified by electron microprobe ... and scanning electron microscope ... by Cannon Microprobe, Seattle, WA (Saleken 2008)." These minerals are "important contributors to the high-grade gold values in the Bonanza Trench on the Panorama Ridge property and other gold mines in the Hedley gold mining district (op. cit.)."

15.4 **Hedleyite** in two other RIRG deposits in Canada

In the **Tillicum Mtn gold skarn** MINFILE 082FNW234 north of Nelson BC "native gold, native bismuth, and bismuthinite occur in fractures in garnet, gold occurs along cleavage planes in pyroxene, and massive sulfide locally replaces calc-silicate skarn. ... Sulfide minerals include major pyrrhotite and pyrite. Minor to trace minerals are native gold, marcasite, native bismuth, bismuthinite, **hedleyite**, and joséite-B (Peterson 1996)." No analyses are given.

Like in the Bunker Hill mine veins "Native gold is associated with marcasite and locally pyrite that has almost completely replaced pyrrhotite", well displayed in a microphoto of a specimen from the high grade Heino pit (Kwong 1984). Tillicum Mtn is a 'reduced' gold skarn, considered RIRG mineralization as the "Triassic Goatcanyon-Halifax Creek and mela-diorite stocks" are spatially, and likely genetically, related. The stock is "a medium-grained, equigranular quartz monzonite with an ilmenite to magnetite ratio of 5:1 (Peterson 1996)", in other words a reduced granitoid.

At the **Beaver Dam gold deposit** in the Meguma Terrane of Nova Scotia "Arsenopyrite-absent quartz - feldspar - muscovite ± tourmaline veins ... contain co-existing electrum, native bismuth, galena, **hedleyite**, joséite-A, galenobismutite and bismuthinite. So far as we know, this unusual mineral paragenesis in the Au-Ag-Bi-Te-Pb-S system is unknown in mesothermal lode gold deposits... The association of native bismuth plus **hedleyite** in veins implies a temperature < 266 °C (Chatterjee & Smith 2000)." Beaver Dam may have a component of overprinting RIRG mineralization(?)

15.5 Hedleyite in some global RIRG deposits

Rombach et al. 2002 find **hedleyite** the seventh most abundant Bi-Te mineral in the 3.51 M. oz **Pogo deposit**. This is discussed in the ingodite section above. Briefly, in Pogo "Early joséite-B, sulphotsumoite, native bismuth, **hedleyite**, **ingodite**, and **pilsenite** occur with an arsenopyrite - loellingite ± pyrrhotite assemblage (450-600 °C), and 850-1000 fineness gold (other phases include maldonite, K-feldspar, and Mn-siderite) (Rombach et al. 2004)." No individual analyses are given.

In the **Mokrsko gold deposit** Czech Republic Zachariáš (2006) identifies trace **hedleyite** by microprobe analysis. See above under unnamed Bi₂Te.

The 'reduced' **Ortosa Au-Bi-Te skarn deposit** in Asturias Spain has **ikunolite** and other GBT minerals, see discussion under **ikunolite**. "...the typical assemblage (native bismuth-gold-**hedleyite**-joséite-B) limits conditions ... within the pyrrhotite stability field. ...The occurrence of **hessite**, bismuthinite and joséite-A may indicate an increase in f_{S_2} as suggested by the replacement of pyrrhotite by pyrite. ...This fact is confirmed by ... Bi-tellurides and selenides (**hedleyite**, joséite-B, joséite-A, **ikunolite**-laitakarite) with $Bi / Te + (Se + S) \geq 1$ (Cepedal et al. 2006)."

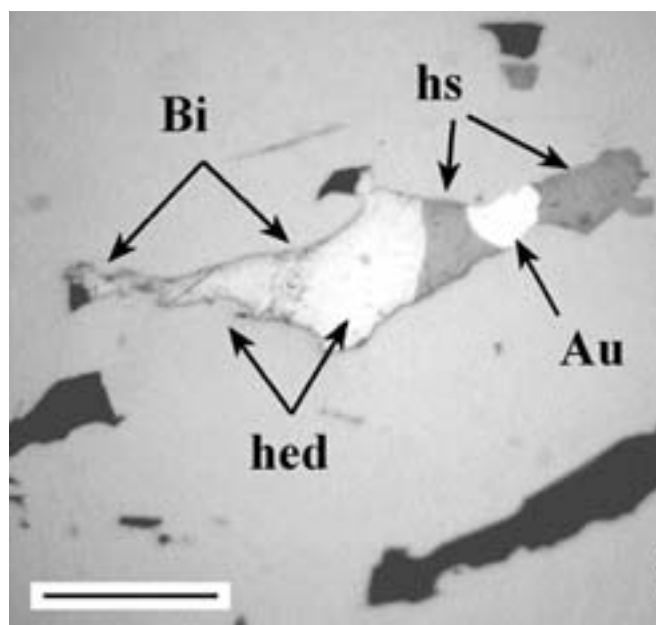


Fig. 12 Back-scattered electron image of Ortosa gold skarn Bi-Te-Ag-Au patch with native bismuth Bi + **hedleyite** hed (or is it correctly **unnamed Bi₂Te**, see below), possibly an equilibrium assemblage, and **hessite** hs surrounding native gold. All enclosed in arsenopyrite. Scale bar is 60 microns. Fig. 6(f) of Cepedal et al. 2006.

Hedleyite occurs in the **Maiskoe gold deposit** in Ukraine, the **Osikonmäki (Osikko) gold prospect** in Finland and the **Darasun gold deposit** in Far East Russia, see above under **ikunolite** for discussion of the GBT parageneses.

Björkdal gold mine near Skellefteå Kåge in Sweden has **hedleyite** with electrum **hessite** nickeline scheelite tellurobismuthite and tsumoite amongst others; see below under **pilsenite**.

Hedleyite occurs in the **Ocna de Fier-Dognecea iron skarn deposits**, Banat, SW Romania, see below under **tetradymite**.

15.6 Composition of Nox Fort **hedleyites**

Hedleyite $\text{Bi}_{2+x}\text{Te}_{1-x}$ ($x = 0.13$ to 0.19) occurs in three Bunker Hill mine veins and once in the Lefevre skarn, there also with **unnamed** Bi_2Te :

BH UHS 1 from Adit 2 Underhand Stope Vein, 2 analyses:

[1] $(\text{Bi}_{2.15}\text{Pb}_{\text{nil}}\text{Sb}_{0.01})\text{sum}_{2.16}\text{Te}_{0.84}\text{Se}_{\text{nil}}\text{S}_{\text{nil}}\text{sum}(\text{Te} + \text{Se} + \text{S})_{0.84}$

hedleyite with $x = 0.16$, middle of the $x = 0.13$ to 0.19 range

Sum Metal:Chalcogens = $2.16/0.84 = 2.57$

[2] $(\text{Bi}_{2.16}\text{Pb}_{\text{nil}}\text{Sb}_{0.02})\text{sum}_{2.17}\text{Te}_{0.83}\text{Se}_{\text{nil}}\text{S}_{\text{nil}}\text{sum}(\text{Te} + \text{Se} + \text{S})_{0.83}$

hedleyite with $x = 0.17$, nearly same as [1]

Sum Metal:Chalcogens = $2.17/0.83 = 2.61$

[3] **BHA-1-8 from Adit 1 Crush Vein** one analysis of 'Hedleyite Fig. 2A' with excess wt % total 102.52%

$(\text{Bi}_{2.12}\text{Pb}_{0.04}\text{Sb}_{0.03})\text{sum}_{2.18}\text{Te}_{0.82}\text{Se}_{\text{nil}}\text{S}_{\text{nil}}\text{sum}(\text{Te} + \text{Se} + \text{S})_{0.82}$

hedleyite, $x = 0.18$ in the $x = 0.13$ to 0.19 range

Sum Metal:Chalcogens = $2.18/0.82 = 2.56$

[4] **BH-0567 from dump close to Adit 1, uncertain vein**

Near-ideal Bi_7Te_3 but the single analysis has low wt % total 97.61% and is suspect:

$(\text{Bi}_{2.08}\text{Pb}_{0.01}\text{Sb}_{0.01})\text{sum}_{2.10}\text{Te}_{0.89}\text{Se}_{0.01}\text{S}_{\text{nil}}\text{sum}(\text{Te} + \text{Se} + \text{S})_{0.90}$

$x = 0.10$, *not* in the $x = 0.13$ to 0.19 range *suspect analyses*

Sum Metal:Chalcogens = $2.10/0.90 = 2.33$

[5] **Lefevre skarn / hornfels L-11 skn** one analysis of grain labelled '**hedleyite 1**' Total 98.88 wt %

$\text{Bi}_{2.04}\text{Pb}_{0.02}\text{Sb}_{0.04})\text{sum}_{2.11}\text{Te}_{0.88}\text{Se}_{0.01}\text{S}_{\text{nil}}\text{sum}(\text{Te} + \text{Se} + \text{S})_{0.89}$

$X = 0.11$, *not* in the $x = 0.13$ to 0.19 range

Sum Metal:Chalcogens = $2.11/0.89 = 2.37$

Using formula **Bi_7Te_3** :

$\text{Bi}_{6.81}\text{Pb}_{0.07}\text{Sb}_{0.16})\text{sum}_{7.03}\text{Te}_{2.92}\text{Se}_{0.05}\text{S}_{0.05}\text{sum}(\text{Te} + \text{Se} + \text{S})_{2.97}$

near-ideal Bi_7Te_3 .

Sum Metal:Chalcogens = $7.03/2.97 = 2.37$, *same*



Fig. 13 SEM back-scattered image showing a smooth curvilinear triple-junction between three bismuth minerals in L-11 skarn suggesting they formed at equilibrium conditions. Both **hedleyite** and **unnamed Bi₂Te** are identified by SEM analyses in L-11 skarn. Bi native bismuth; JoB joséite-B; Hed either hedleyite or **unnamed Bi₂Te**. Fig. 3 in Lefevre section Part II

Metal:Chalcogen ratios for the first three Bunker Hill mine vein **hedleyites** exceed the ideal 7/3 ratio 2.33. **Bunker Hill mine vein hedleyites have excess metal cations Bi Pb and/or Sb, and deficient chalcogens Te & Se.** Analysis [4] is suspect. **Hedleyite** [5] in Lefevre skarn / hornfels specimen L-11 skn is **near-ideal Bi₇Te₃**.

15.7 Recalculating Ortosa gold skarn **hedleyite** analyses finds some are **unnamed Bi₂Te**

In the **Ortosa Au–Bi–Te skarn deposit** 15 **hedleyite** analyses “show significant compositional variation in both Te (from 18.0 to 23.1 wt %) and Bi (from 75.3 to 78.3 wt %); typical impurities are Sb and Se. Formulae calculations were done on the basis of 10 atoms (Bi₇Te₃), but ... excess or deficiency of Te gives an apparent **non-stoichiometric** formula. ... **Bi_{2+x}Te_{1-x}** is a more appropriate formula, where **x varies ...** (Table 5 in Cepedal et al. 2006).”

Re-calculating the three given ‘Cepedal’ Ortosa **hedleyite** analyses using the formulae **Bi_{2+x}Te_{1-x}** **x = 0.13 to 0.19** finds **x** considerably lower:

$$[1] (\text{Bi}_{2.12}\text{Pb}_{\text{nil}}\text{Sb}_{0.05})\text{sum}_{2.17}\text{Te}_{0.83}\text{Se}_{\text{nil}}\text{S}_{\text{nil}}\text{sum}(\text{Te} + \text{Se} + \text{S})_{0.83} \mathbf{x = 0.17}$$

$$[2] (\text{Bi}_{2.00}\text{Pb}_{\text{nil}}\text{Sb}_{0.01}\text{Zn}_{0.01}\text{Hg}_{\text{nil}}\text{As}_{0.01}\text{Au}_{0.01})\text{sum}_{2.04}\text{Te}_{0.94}\text{Se}_{0.02}\text{S}_{\text{nil}}\text{sum}(\text{Te} + \text{Se} + \text{S})_{0.96} \mathbf{x = 0.04}$$

This second mineral has **0.46 wt % gold** corresponding to 0.01 *apfu*. **x** is outside the **0.13 to 0.19** range and this phase is more correctly **unnamed Bi₂Te**, **not hedleyite**. Compare other **unnamed Bi₂Te** sites in Table 5.

$$[3] (\text{Bi}_{1.97}\text{Pb}_{0.01}\text{Sb}_{0.01}\text{Hg}_{0.01}\text{As}_{0.01}\text{Fe}_{0.01})\text{sum}_{2.01}\text{Te}_{0.98}\text{Se}_{0.01}\text{S}_{\text{nil}}\text{sum}(\text{Te} + \text{Se} + \text{S})_{0.99} \mathbf{x = 0.01}$$

Again x is outside the **0.13 to 0.19** range and this phase is **unnamed Bi₂Te**, **not hedleyite**. See Table 5.

Mean of the above 3 'Cepedal' Ortosa '**hedleyite**' is

$$(\text{Bi}_{2.03}\text{Pb}_{\text{nil}}\text{Sb}_{0.02}\text{Hg}_{\text{nil}}\text{As}_{0.01}\text{Fe}_{\text{nil}})\text{sum}_{2.07}\text{Te}_{0.92}\text{Se}_{0.01}\text{S}_{\text{nil}}\text{sum}(\text{Te} + \text{Se} + \text{S})_{0.93} \text{ x} = 0.04$$

✦ This mean formula is near ideal **unnamed Bi₂Te**, not **hedleyite**. Mineral [1] corresponds to **hedleyite Bi_{2+x}Te_{1-x} x = 0.17**. Minerals [2] and [3] are near-stoichiometric **unnamed Bi₂Te**.

The mean 'Cepedal' Ortosa '**hedleyite**' has Sum Metal:Chalcogens ratio = 2.07/0.93 = 2.2 meaning chalcogens Te & Se are slightly deficient.

Three representative Ortosa **hedleyite** analyses in Fuertes-Fuente et al. (Table 3, 2000) give formulae calculated with MS Excel:

$$[4] (\text{Bi}_{2.03}\text{Pb}_{\text{nil}}\text{Sb}_{0.03}\text{Fe}_{0.05}\text{Co}_{\text{nil}}\text{Au}_{0.01}\text{Ag}_{0.03}\text{Pt}_{0.03})\text{sum}_{2.19}\text{Te}_{0.79}\text{Se}_{0.02}\text{sum}(\text{Te} + \text{Se})_{0.81} \text{ x} = 0.19$$

with 0.27% Au and 0.90% Pt

$$[5] (\text{Bi}_{2.00}\text{Pb}_{0.02}\text{Sb}_{\text{nil}}\text{Fe}_{0.06}\text{Co}_{0.01}\text{Au}_{0.01}\text{Ag}_{0.03}\text{Pt}_{\text{nil}})\text{sum}_{2.11}\text{Te}_{0.89}\text{Se}_{\text{nil}}\text{sum}(\text{Te} + \text{Se})_{0.89} \text{ x} = 0.11$$

with 0.35% gold

$$[6] (\text{Bi}_{1.96}\text{Pb}_{0.01}\text{Sb}_{0.01}\text{Fe}_{0.05}\text{Co}_{\text{nil}}\text{Au}_{0.01}\text{Ag}_{\text{nil}}\text{Pt}_{\text{nil}})\text{sum}_{2.03}\text{Te}_{0.96}\text{Se}_{0.01}\text{sum}(\text{Te} + \text{Se})_{0.97} \text{ x} = 0.03$$

with 0.34% gold

Analysis [6] has x outside the 0.13 to 0.19 range and is correctly near-stoichiometric **unnamed Bi₂Te**, like 'Cepedal' analyses [2] and [3]. Compare other **unnamed Bi₂Te** sites in Table 5.

Concluding, **hedleyite** and **unnamed Bi₂Te** both occur as separate minerals in the Ortosa gold skarn. This is confirmed by analyses by two researchers at different times. Both **phases** may carry ~0.3% **gold**, and **hedleyite** also to 0.9% platinum.

15.8 '**Hedleyite**' composition varies between Bi₃Te and **unnamed Bi₂Te** in the Viceroy gold mine

In the **Viceroy gold mine** in Zimbabwe “**Hedleyite**” is the only Bi-Te phase present. ... It is relatively common and occurs intergrown with other phases of the Au-Bi-Te-S system or in rarer instances in small veinlets in gangue. Microprobe analyses showed that this mineral only occasionally carries elevated contents of Fe (up to 1.91 wt. %), Pb (up to 1.15 wt. %), Sb (up to 0.31 wt. %) and Se (up to 0.71 wt. %). However, a plot of Bi-Te ratios, expressed in atomic % Te (their Fig. 5 plots 50 **hedleyite** analyses), indicates a larger spread of compositions with **a complete solid solution series between Bi₃Te and unnamed Bi₂Te** [both one analysis], and a bimodal distribution of the analytical data. Most compositions (Fig. 5) approximate to the composition Bi₈Te₃ [n=13] and only a smaller set of data [2] plots close to the ideal **hedleyite** composition Bi₇Te₃... (Oberthür & Weiser 2008)”. Unfortunately individual analyses are not given. Similar to Viceroy, many **hedleyite-like** Bi-Te minerals may occur on Nox Fort; some may preferentially concentrate gold (and platinum?).

16 Pilsenite Bi_4Te_3

16.1 Pilsenite – type locality Nagybörzsöny in Hungary and its compositional range

Pilsenite was ... first described by Kenngott (1853) from Deutschpilsen, then in Germany, now named Nagybörzsöny and in Hungary. It is lead-gray with hardness $1\frac{1}{2}$ - $2\frac{1}{2}$. <http://www.mindat.org/min-3921.html> lists 25 occurrences.

“Topotype wehrlite was re-examined and found to be a mixture of Bi_4Te_3 and **hessite** Ag_2Te . **Pilsenite** is redefined as Bi_4Te_3 ... Microprobe analysis of **pilsenite** yielded: Bi 65.2 wt % (64.7-66.0), Pb 1.1 (0.9-1.3), Ag 0.1 (0.0-0.3), Fe nil to trace, Te 31.0(30.6-31.2), S 0.1(0.1-trace) corresponding to $(\text{Bi}_{3.87}\text{Pb}_{0.07}\text{Ag}_{0.1})\text{sum}_{3.95}(\text{Te}_{3.01}\text{S}_{0.04})\text{sum}_{3.05}$ or ideally Bi_4Te_3 (Dunn et al. 1984).” The new mineral jonassonite also occurs at Nagybörzsöny (see under jonassonite).

“Like other members of the Bi_4X_3 isoseries, **pilsenite** shows little variation in Bi / (Te + S + Se), and the common presence of minor Pb. Some S and Se may be present, although generally ... extremely low.” **Pilsenite** is relative rare compared to other binary tellurides of Bi. ... Compositions are invariably close to end-member Bi_4Te_3 , with no compositional data to support solid solution toward joséite–B $\text{Bi}_4\text{Te}_2\text{S}$ or $\text{Bi}_4\text{Te}_2\text{Se}$ (Cook et al. 2007b)”.

16.2 Pilsenite and other Ag-Pb-Bi-Te-Se bearing minerals in the ‘Bismuth Gold Zone’ on the Jersey-Emerald property near Salmo

Pilsenite occurs in sulphide rich samples of the ‘**Bismuth Gold Zone**’ on the **Jersey-Emerald property** of Sultan Minerals Inc., 13 km E of Nox Fort. Development of tungsten + molybdenum reserves is presently in progress (section 9). The ‘Bismuth Gold Zone’ has abundant pyrrhotite, arsenopyrite, quartz, native bismuth and stibnite (Troup 1994). Samples are anomalous in any of Au As Pb Bi Te and Se (Table 3 in Cathro & Lefebure 2000); the geochemistry differs from Nox Fort (section 9.1).

“Microprobe analyses ... indicate ... native bismuth, Ni and Co-bearing arsenopyrite, an Mg-rich sideritic carbonate, as well as a number of bismuth tellurides, bismuth selenides and several minerals containing various quantities of Pb, Ag, Sb, Cu, Bi, Te, Se and S {S.B. Cornelius p.c. 1995}. A preliminary examination of the microprobe data (L.A. Groat, p.c. 1996) suggests the alteration contains several unusual minerals including **tetradymite** $\text{Bi}_2\text{Te}_2\text{S}$, **pilsenite** Bi_4Te_3 , bismuthinite Bi_2S_3 and joséite–B $\text{Bi}_4\text{Te}_2\text{S}$. In addition, a number of exotic minerals may be present, including csiklovaite $\text{Bi}_2\text{Te}(\text{S},\text{Se})_2^{36}$, laitakarite $\text{Bi}_4(\text{Se},\text{S})_3$, paraganajuatite $\text{Bi}_2(\text{Se},\text{S})_3$, eskimoite $\text{Ag}_7\text{Pb}_{10}\text{Bi}_{15}\text{S}_{36}$, schirmerite $\text{Ag}_3\text{Pb}_3\text{Bi}_9\text{S}_{18}^{37}$, vikingite $\text{Ag}_5\text{Pb}_8\text{Bi}_{13}\text{S}_{30}$ and heteromorphite $\text{Pb}_7\text{Sb}_8\text{S}_{19}$. No gold-bearing minerals have yet been identified in either polished thin sections or by microprobe analysis (Ray & Webster 1997)”.

R.M. Thompson (1954) identified Sb-bearing kobellite $\text{Pb}_{22}\text{Cu}_4(\text{Bi},\text{Sb})_{30}\text{S}_{69}$ by XRD in a specimen from the then-productive Dodger Tungsten Mine. This was “in milky quartz [as] lead gray capillary crystals protruding from a vug and embedded in quartz [with] coarse crystals of scheelite, abundant sericite mica, some molybdenite and minor pyrite, [collected] about three feet above a flat-lying granite contact. The same mineral has been noted in a specimen from a quartz-calcite vein at the granite contact.”

³⁶ Csiklovaite was discredited in 1991, it is a mixture of bismuthinite, galenobismutite and **tetradymite**

³⁷ empirical formula $\text{Ag}_3\text{Pb}_3\text{Bi}_9\text{S}_{18}$ to $\text{Ag}_3\text{Pb}_6\text{Bi}_7\text{S}_{18}$

Contrast these Ag, Pb, Sb and often Se -bearing Bi minerals in the 'Bismuth Gold Zone' with the Pb & Sb poor Bi-Te minerals on Nox Fort. Se is near absent on Nox Fort. **Some of the exotic 'Bismuth Gold Zone' minerals are selenides, not tellurides.** Furthermore, presence of **tetradymite** indicates 'oxidized' depositional conditions; confirming this the Metal:Chalcogen ratios are generally < 1 for many of the rare Pb-Se-Bi minerals identified.

16.3 **Pilsenite** in the Buckhorn Mountain [Crown Jewel] RIRG gold skarn in northern Washington State

M. Gaspar in a recent thesis (2005) on the **Buckhorn Mountain gold skarn deposit** of Kinross Gold Corp. in northern Washington State (location on fig. 3), formerly Crown Jewel [0.984 M. oz. reserves] describes both 'reduced' and 'oxidized' GBT mineralization in this mid Jurassic age [Nelson-suite] gold skarn. Some of the bismuth (sulpho)tellurides present have metal:chalcogen ratios 1 (tsumoite BiTe) or < 1 (**tetradymite** $\text{Bi}_2\text{Te}_2\text{S}$) defining 'oxidized' formation conditions.

The Buckhorn Mountain South West Ore Zone has 70% of the reserves. It "contains on average 6-15% total sulfides, 3-6% magnetite at the marble/basalt contact, and 6-19% magnetite in the "nose" zone (Jones, 1993). Opaque minerals occur in all skarn assemblages with magnetite as the most abundant oxide and pyrrhotite as the dominant sulfide, reflecting a relatively reduced environment. Other opaque minerals present in decreasing order of abundance are pyrite, chalcopyrite, marcasite, Bi-minerals, gold, arsenopyrite-cobaltite, galena, sphalerite, covellite, and digenite.

"Textural evidence (Figs. II.16i, II.19, A2.14) shows that gold, Bi-minerals, and minor galena formed together in equilibrium with pyrrhotite and chalcopyrite, immediately before or in part during the alteration of pyrrhotite to marcasite / pyrite [sulfidation is described]. This Au-Bi-Pb assemblage, together with pyrrhotite and chalcopyrite, commonly forms intergrowth textures with amphibole along grain boundaries and cleavage planes (Fig. II.19b-c). Au-Bi-Pb are also associated with the late hydrated Fe-silicate assemblage. ... Bi minerals include, in decreasing order of abundance: ✓ bismuthinite Bi_2S_3 , ✓ joseite-A Bi_4TeS_2 , ✓ **pilsenite** Bi_4Te_3 , sulphotsumoite $\text{Bi}_3\text{Te}_2\text{S}$, ✓ native bismuth, ✓ **tetradymite** $\text{Bi}_2\text{Te}_2\text{S}$, ✓ joseite-B $\text{Bi}_4\text{Te}_2\text{S}$, and tsumoite BiTe. Minor cobaltite was found associated with the Au-Bi assemblage as well as arsenopyrite included in native bismuth." Checked minerals ✓ also occur in Nox Fort. Cannon (2004) identifies **hedleyite**.

"...Bi-tellurides and Bi-sulfosalts show textural evidence for both intergrowth in equilibrium with sulfide minerals (pyrrhotite, chalcopyrite, and galena) at skarn [prograde] temperatures and later unmixing as stability of individual phases are reached. Bismuthinite intergrown with pyrrhotite, immediately preceding pyrite replacement of pyrrhotite [sulfidation], indicates a narrow range of log $f\text{S}_2$ between -11.8 and -11.0, again consistent with pyrrhotite compositions. ...**the replacement of pyrrhotite by marcasite / pyrite requires an increase of $f\text{O}_2$ and/or $f\text{S}_2$** (op. cit.)."

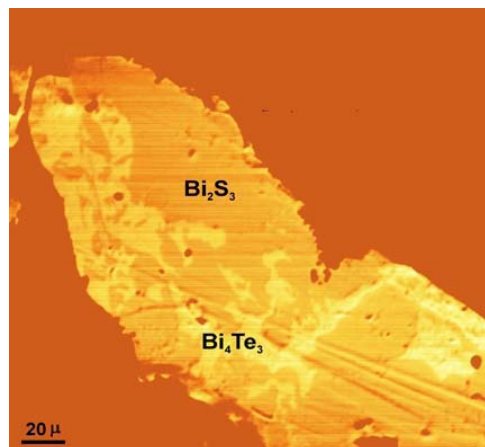


Fig. 14 False-coloured image of a polished section of the Buckhorn Mountain gold skarn, from the South West Ore Zone. Enveloping dental-caries texture infers bismuthinite Bi_2S_3 partly replaces earlier formed **pilsenite** Bi_4Te_3 ; the process is latter-stage sulfidation. Figure A2.13 of Gaspar (2005); bar scale is 20 microns

16.4 **Pilsenite** occurrence in some global RIRG systems

In the **Pogo deposit** [3.51 M. oz] in Alaska C. Rombach et al. (2002) find **pilsenite** more abundant than native bismuth, bismuthinite, **ingodite** and **hedleyite** and scarcer than **joséite**–B, gold (fineness 850-1000) and **tetradymite**, discussed above in the ingodite section. “Early **joséite**–B, **sulphotsumoite**, native bismuth, **hedleyite**, **ingodite**, and **pilsenite** occur with an arsenopyrite - **loellingite** ± **pyrrhotite** assemblage (450-600 °C), and 850-1000 fineness gold (other phases include **maldonite**, **K-feldspar**, and **Mn-siderite**) (Rombach et al. 2004).” Latter stages are **pilsenite**-absent.

The **Petráčkova hora RIRG deposit** in Czech Republic [1.03 M. oz] has **pilsenite** as an accessory phase in Au mineralization, identified by microprobe EDAX analysis (Zachariáš et al. 2001); see above under ingodite.

Pertoldová & Scharmová (1990, 1991) describe **pilsenite** in the **Mokrsko RIRG deposit** [3.08 M. oz], also in Czech Republic. For description see above under unnamed Bi_2Te .

The arsenical **Osikonmäki (Osikko) gold prospect** in Finland and the **Darasun gold deposit** in Far East Russia have **pilsenite**, see above under **ikunolite** section.

Björkdal gold mine near Skellefteå Kåge in Sweden has **pilsenite** with electrum **hedleyite** **hessite** **nickeline** **scheelite** **tellurobismuthite** and **tsumoite** amongst others. “Sulfides, mostly **pyrite**, **pyrrhotite**, **chalcopyrite**, and **galena**, are common in the quartz veins. **Galena** appears to be the last phase to crystallize, as it is commonly found infilling fractures in earlier sulfides. **Pyrrhotite** shows a strong association with quartz, calcite, and gold and is common within fractures that cut large **scheelite** crystals (their Fig. 2B). A bismuth telluride (**tsumoite**?) is observed infilling brecciated **tourmaline** grains with abundant inclusions of **pyrrhotite** (Fig. 2D). Gold occurs with sulfides and **scheelite** and is particularly evident within quartz-calcite-filled fractures within **scheelite**, either as a discrete phase or at the margins of **pyrrhotite** grains (Fig. 2B) (Roberts et al. 2006).”

Pilsenite occurs at **Săcărâmb (formerly Nagyg)** in **classic epithermal gold veins** in the Metaliferi Mtns, Romania [2.7 M. oz.]. This gold-telluride deposit has **Pb-rich ingodite** **pilsenite** galena and chalcopyrite (Simon & Alderton 1995, Shimizu et al. 1999b). Pilsenite always replace **Pb-rich ingodite** along cleavages or surrounds it forming irregular grains (Simon & Alderton 1995). The assemblage is **Pb-rich ingodite** **pilsenite** galena chalcopyrite and unidentified 'mineral A' in calcite ankerite and minor quartz. The calculated **pilsenite** formula is near-ideal $(\text{Bi}_{3.97}\text{Pb}_{0.13})\text{sum}_{4.10}(\text{Te}_{2.88}\text{S}_{0.03})\text{sum}_{2.91}$. **Săcărâmb pilsenite** may have formed by the reaction of Te-rich hydrothermal solutions with **Pb-rich ingodite** (op. cit).

16.5 **Pilsenite** occurrence in two polymetallic deposits

Pilsenite occurs in the Bi-Te-S-(Se) assemblage in the **Huangshaping polymetallic Pb-Zn-Cu-Ag-Fe-W-Mo-Sn deposits** in Hunan Province, south China. **Tetradymite** + sulphotsumoite + joséite–B + unnamed Bi_2Te + hessite are associated (Gu et al. 2001 their Fig. 5). Calculated formula from 5 analyses is $(\text{Bi}_{4.05}\text{Ag}_{0.01})\text{sum}_{4.06}(\text{Te}_{2.93}\text{Se}_{0.01})\text{sum}_{2.94}$ close to ideal **pilsenite** Bi_4Te_3 . See above under unnamed Bi_2Te for other Huangshaping Bi-Te-S-(Se) minerals.

Pilsenite occurs at **Košický Kraj**, Gemerská Poloma, in the Slovenské Rudohorie Mtns (eastern part), Slovak Republic with many other minerals including bismuth, bismuthinite, cosalite, joséite [joséite–A], joséite–B, gold, galenobismutite, scheelite & sulphotsumoite (Koděra et al. 1986 a 1990).

16.6 Occurrence of **Pilsenite** in Adit 1 Crush Vein

Pilsenite occurs twice in polished section BHA-1-8 of Adit 1 Crush Vein of Bunker Hill mine. In Fig. 2D **pilsenite** occurs with native bismuth and joséite–B adjacent on its sides. The **pilsenite** texture in Fig. 3D infers it “replaces joséite–B; possibly the released sulphur formed **ikunolite**. The association is unusual and atypical as **ikunolite** and **pilsenite** are unlikely to be stable together; this cannot be a 'primary' assemblage (Part II). Fig. 3D **pilsenite** is non-stoichiometric $\text{Bi}_{4.35}(\text{Te}_{2.34}\text{Se}_{0.07}\text{S}_{0.23})\text{sum}_{2.64}$.

17 Pavonite

17.1 Pavonite – type locality Bolivar Mine in Bolivia, properties

Pavonite is a rare sulphosalt mineral originally named alaskaite (benjaminite); the type locality is the Bolivar Mine in Potosí Department, Bolivia (Nuffield 1954). The ideal formula is **AgBi₃S₅**. Pavonite is and steel-gray with hardness 2 and indistinct cleavage. The crystal system is monoclinic; the habit is as tiny bladed crystals elongated parallel to [010] (©2001-2005 Mineral Data Publishing version 1). Typically crystals intergrow to form felted masses with other mineral species, or it occurs as bladed aggregates of thin lath-like crystals. "Crystallographic characterisation is generally required in order to identify pavonite homologues with any certainty (Cook 1998)." <http://www.mindat.org/min-3136.html> lists 39 sites.

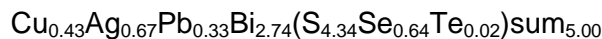
17.2 Pavonite – sole other Canadian locality

The only Canadian locality is at the Canadian Keeley Mine (Frontier Mine), Timiskaming District in the Cobalt-Gowganda region Ontario (Sabina 1973). No formula is available.

17.3 Pavonite some international localities

Pavonite occurs in the **Rędziny dolomite quarry** in Lower Silesia Poland (Gołębiowska et al. 2006) this site described above under ikunolite.

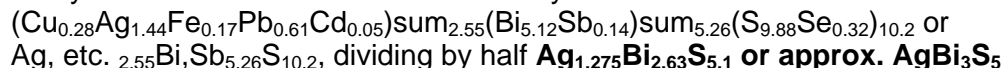
In the **Darwin mining district** in Inyo County California pavonite occurs "as the Cu-Se-rich variety associated with exsolved cupropavonite, junote and **Se-rich tetradymite** in the first specimen from the Lucky Lucy mine. The pavonite constitutes most of the specimen. It is moderately anisotropic and the grains are generally elongated parallel to the vein direction. Microprobe analysis of two grains gives a near-ideal formula



...In the sulfosalts of the pavonite series, which always have a high Bi/Pb ratio, Mumme (1990) indicates no limit in the Se-for-S substitution ... This explains the highest Se content encountered in the pavonite-cupropavonite inter-growth from Lucky Lucy mine (Dunning et al. 2006)."

Pavonite is identified in intermediate mine levels of the **Larga-Fata Băii gold ore field**, Metaliferi Mtns. in Romania, discussed below under tetradymite section. "Within the Padina skarn mineralization [a body of garnet-epidote skarn hosting Zn-Pb-(Cu)]... we note a pavonite homologue as a minor component in a single sample. The mineral occurs as inclusions in pyrite, associated with lillianite (their Fig. 9). ...Compositions of the pavonite homologue are given in Table 3. Members of this mineral group are difficult to identify on the basis of microprobe analyses alone {e.g. Karup-Møller & Makovicky, 1979}. Nevertheless, the relatively low Cu and Pb contents and tight cluster on the compositional plot in Bi-Ag-(Pb+Cu) space (their Fig. 9) give us confidence to consider the mineral in question the 5P homologue, pavonite (Cook et al. 2004)."

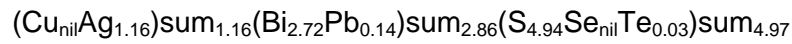
Analysis of c163 in their Table 3 with analytical total 100.10 wt % is



17.4 Composition of Pavonite in Lefevre vein

Trace pavonite occurs in the polished section of L-04QVXtry a quartz + arsenopyrite vein crosscutting the Lefevre tungsten + gold skarn / hornfels. In Fig. 2E pavonite may have crystallised out of joséite–A, all enclosed in matrix arsenopyrite.

Only the second analysis of this 'Pavonite 2' is valid with low total wt % 97.00% and formula



This is very close to ideal AgBi_3S_5 .

18 Tetradymite $\text{Bi}_2\text{Te}_2\text{S}$

18.1 Tetradymite – type locality Župkov in Slovakia

The type locality is Župkov (Zsubko or Schubkau) in the Vtáčnik Mts, Slovakia, discovered in 1831 (Sejkora & Litochleb et al. 2004). It occurs in highly altered andesite and pyroclastic rocks with minor sulphides.

18.2 Tetradymite properties and compositional range

Tetradymite $\text{Bi}_2\text{Te}_2\text{S}$ is **common** as an accessory mineral in many telluride-bearing precious metal deposits (Cook et al. 2007b). The name is from the Greek "tetra", four, and "didymos", twin, alluding to its usual occurrence as twin crystals of four individuals. **Tetradymite** is bright steel-gray or tin-white and tarnishes with iridescence to a dull gray. Hardness is $1\frac{1}{2}$ - 2. Common impurities are Se Au Cu and Pb. <http://www.mindat.org/min-3921.html> lists 269 localities.

“Despite the fact that **tetradymite** is widespread, there is some continuing ... uncertainty about the structural formula, which is now almost universally accepted as $\text{Bi}_2\text{Te}_2\text{S}$ (e.g., Bayliss 1991). Nevertheless, **sulfur-rich tetradymite** appears more chemically stable than stoichiometric $\text{Bi}_2\text{Te}_2\text{S}$, and the formula $\text{Bi}_{14}\text{Te}_{13}\text{S}_8$ given by Pauling (1975) appears valid for most examples of natural **tetradymite**. ... An extensive compositional range is supported by experimental work in the system Bi_2S_3 – Bi_2Te_3 at higher temperature... (Cook et al. 2007b)”. Se substitutes for S and Pb for Bi; galena is a common associate. “Pauling (1975) considered that **S-rich tetradymite** ($\text{Bi}_{14}\text{Te}_{13}\text{S}_8$) is chemically more stable than **ideal** $\text{Bi}_2\text{Te}_2\text{S}$ (Cook & Ciobanu 2001)”. Bayliss (1991) proposed limited Se-for-Te substitution.

18.3 Tetradymite is stable at more oxidizing formation conditions

Tetradymite $\text{Bi}_2\text{Te}_2\text{S}$ is stable at more oxidizing conditions - higher $f\text{O}_2$ and/or $f\text{S}_2$ - than those hypothesized for most all the ‘reduced’ Nox Fort bismuth (sulpho)telluride assemblages. Chemical conditions importantly determine the mineralogy, and depositional conditions can be inferred by mineral assemblages. “Co-existing ... **tetradymite**, tsumoite have metal:chalcogen ratio ≤ 1 . Such assemblages indicate relatively high $f\text{S}_2$ conditions, coupled with still relatively high $f\text{Te}_2$ (Cook & Ciobanu 2004).

“The buffering host [iron oxide + iron sulphide mineral] assemblage and its position in $f\text{O}_2$ - $f\text{S}_2$ space constrains the assemblage of Bi-tellurides / sulphotellurides (\pm selenides, selenosulphides) in each field. At higher $f\text{O}_2$ - $f\text{S}_2$ hematite and pyrite [are stable], approaching the stability field of native-Te [and] Bi-tellurides / sulphotellurides with $\text{Bi} / (\text{Te} + \text{Se} + \text{S}) = 1$... (for example, the relatively widespread assemblage tellurobismuthite-**tetradymite** (\pm kawazulite, if Se is available). In such systems ... an affinity between **tetradymite** and various Bi-sulphosalts (aikinite-bismuthinite and lillianite series) is not uncommon... Cook et al. 2003)”.

Examples formed under these conditions are “Porphyry and epithermal Cu deposits (both high sulphidation & low sulphidation) in the Banatitic Belt (in SE Europe, especially Romania, of Late Cretaceous age) with gold-enriched ores with Bi-telluride signature $\text{Bi} / (\text{Te} + \text{Se} + \text{S}) < 1$; here **tetradymite**, tellurobismuthite \pm native Te \pm Au-(Ag)-tellurides) ... formed ... at $T \geq 400^\circ\text{C}$ at the magnetite / pyrite \pm hematite buffer {e.g. Ciobanu et al. 2003} (Ciobanu et al. 2005). These conditions are surmised for bornite- and chalcopyrite-rich Cu-Fe ores from **Ocna de Fier - Dognecea [iron skarn] deposit in Romania**.

Ag-Bi-Se-Te mineral assemblages are restricted to chalcopyrite ores [and] include kawazulite $\text{Bi}_2(\text{Te}, \text{Se}, \text{S})_3$, bohdanowiczite AgBiSe_2 , **hessite** Ag_2Te , **hedleyite** Bi_7Te_3 or $\text{Bi}_{2+x}\text{Te}_{1-x}$ and volynskite AgBiTe_2 (Cook & Ciobanu 2001)".

18.4 Tetradymite some BC localities

Sulphide-rich samples from the **Emerald Tungsten - Dodger tungsten + molybdenum deposits** near Salmo, 13 km E of Nox Fort Project, have **tetradymite** $\text{Bi}_2\text{Te}_2\text{S}$ with other bismuth tellurides and selenides. See above under **pilsenite**.

At the **Jumbo Mine** MINFILE 082FSW111 near **Rosslund**, not far west of Nox Fort, a thin film of **tetradymite** and gold was found on a working in Rosslund monzonite (Thompson 1949). There "A vein along a minor shear, ranging up to 9 m or more in width, is mineralized with pyrrhotite, arsenopyrite, molybdenite, bismuthinite and native gold in mainly quartz, ankerite and calcite gangue. ...Bismuthinite occurs in particles or aggregates up to a few cm in diameter. ...Pyrrhotite and other sulphides are associated with native bismuth and bismuthinite... Visible free gold is frequently found with native bismuth (MINFILE)".

The former **Nickel Plate mine gold skarn deposits** MINFILE 092HSE038 in the Hedley district include trace minerals "galena, native bismuth, gold, electrum, tetrahedrite, native copper, gersdorffite, marcasite, molybdenite, titanite, bismuth tellurides (**hedleyite**, **tetradymite**), cobaltite, erythrite, pyrrargyrite, breithauptite and maldonite (after Ray & Dawson 1994)." See hedleyite section for more description.

The past producing **White Elephant mine**, 25 km WSW of Vernon, Vernon Mining Division MINFILE 082LSW042 mined a large quartz vein or lens in granodiorite. Pyrrhotite, pyrite, chalcopyrite and **tetradymite** (ID by Warren 1946 p. 77) occur as lens-like bodies within the vein. Stringers and segregations of bismuth telluride, free gold and scheelite are reported.

Tetradymite occurs at the **Taylor Windfall Mine**, Clinton Mining Division MINFILE 092O 028, (Thompson 1949). This polymetallic vein prospect is hosted by Upper Cretaceous Powell Creek Formation propylitically altered and silicified dacitic and andesitic tuffs. Gold was present as coarse angular crystalline fragments in both a tourmaline-rich and a sulphide-rich vein. The tourmaline vein has chlorite, pyrite, tennantite, sphalerite and chalcopyrite, with lesser galena, **tetradymite**, native gold and enargite. The sulphide vein has similar mineralogy with greater amounts of sphalerite, tennantite and coarse siderite. Thompson (1951) identified tetrahedrite-tennantite.

Several small showings of auriferous **tetradymite** are known at **Glacier Gulch Gold (Bismuth) occurrence** on Hudson Bay Mountain near Smithers, Omineca Mining Division MINFILE 093L 109. It occurs in shears and quartz veins in silicified andesite and sheared andesitic tuff. There are silver "and some platinum values (MINFILE)". The **tetradymite** is usually found with native gold along shear planes. Joséite–A also occurs as coarse plates up to ½ x 2 inches, sometimes intergrown with bismuth and joséite–B (Warren & Davis 1940, Thompson 1949). Pratt (1931 p. 56) identifies calaverite.

The former **Pellaire mine** in Clinton Mining Division MINFILE 092O 045 had some high grade gold ore. Auriferous quartz veins primarily within a lobe of granodiorite extend northwards into both flows and pyroclastics, well altered to a siliceous hornfels. "The veins are composed of limonite and occasionally malachite-stained friable quartz with voids of weathered-out sulphides, dominantly pyrite and lesser chalcopyrite. ...The veins carry less than 3% metallic minerals ... in approximate order of abundance, pyrite, chalcopyrite, galena, sphalerite, arsenopyrite, tetrahedrite, **hessite**, altaite, pyrrhotite, magnetite, bornite, gold, **tetradymite**, cosalite, and antimony....

The **hessite**, which carries the bulk of the precious metal, occurs veining quartz, pyrite and chalcopyrite, and as disseminations in these minerals and in galena, **tetradymite** and wehrlite. Some of the gold is residual and has been left behind in veins and pockets after **hessite** Warren (1947) (MINFILE)".

18.5 **Tetradymite** in Dublin Gulch, an 'oxidized' IRG deposit

Tetradymite was found at **Dublin Gulch central Yukon** in placer workings as "a small placer pebble with an embedded subhedral crystal of gold (Thompson 1949)". This is an example of **tetradymite's** direct association with gold. **Tetradymite** $\text{Bi}_2\text{Te}_2\text{S}$ occurs in place in the **Dublin Gulch Eagle Zone 'RIRG' deposit** with GBT minerals native gold, native bismuth, bismuthinite and **tellurobismuthite** Bi_2Te_3 (Hitchens & Orssich 1995). It can be well surmised that this mineralogy formed at $T \geq 400^\circ\text{C}$ at $f\text{O}_2$, $f\text{S}_2$ conditions at about the magnetite / pyrite \pm hematite buffer (after Ciobanu et al. 2005). Dublin Gulch Eagle Zone is 'oxidized' IRG mineralization; correspondingly the Metal:Chalcogen ratios of the two bismuth (sulpho)tellurides in the deposit are < 1 .

Maloof et al. (2001) identify trace undetermined Pb–Bi \pm Sb sulphosalts in the Eagle Zone; most common are pyrite scheelite arsenopyrite sphalerite bismuthinite and galena. Galenobismutite PbBi_2S_4 is expected in place; in gravels at Dublin Gulch this rare mineral "was found surrounding a small nugget of gold from the placer workings... (Thompson 1950)." Wolframite occurs in quartz veins cutting argillites near granite and also in the gold placers (Cockfield 1920). "There are numerous quartz stringers carrying wolframite and scheelite in the granitic rocks and their contact zone, a cassiterite-tourmaline zone and several NE-striking gold-bearing quartz-arsenopyrite-pyrite-sulphosalt veins. [In placer gravels in addition to gold,] scheelite, some wolframite and a little cassiterite ... there are a number of heavy minerals including magnetite ... arsenopyrite nodules, jamesonite nodules, bismuth, galenobismutite, **rarely bismuth tellurides**, pyrite, tourmaline and garnet (Boyle 1979)."

18.6 **Tetradymite** in some global RIRG deposits

In the **Pogo Alaska deposit** [3.51 M. oz] "**tetradymite** and **pilsenite** are associated with gold of 780-879 fineness (Rombach 2002)." Rombach et al. 2002 find **tetradymite** more common than **pilsenite**, native bismuth, bismuthinite, **ingodite** and **hedleyite** and less common than joséite–B and gold (fineness 850-1000). Rombach et al. 2004 observe "Early joséite–B, sulphotsumoite, native bismuth, **hedleyite**, **ingodite**, and **pilsenite** occur with an arsenopyrite - loellingite \pm pyrrhotite assemblage ($450\text{--}600^\circ\text{C}$), and 850-1000 fineness gold (other phases include maldonite, K-feldspar, and Mn-siderite). This is followed by joséite–B, **tetradymite**, tsumoite, and **ingodite** with an arsenopyrite-pyrite assemblage ($350\text{--}500^\circ\text{C}$), and 850-950 fineness gold. Later **tetradymite (S-enriched)**, bismuthinite (Sb-bearing), joséite–B, joséite–A, **ingodite** and various (Ag–Bi–Sb–Pb) sulfosalts are found with pyrite (no arsenopyrite) and < 850 fine electrum.

"**Fort Knox** contains early joséite–A, joséite–B, and **tetradymite (S-enriched)** with an arsenopyrite-pyrite assemblage ($300\text{--}490^\circ\text{C}$), >900 gold finesses, and feldspathic alteration (other phases include native bismuth, maldonite, and bismuthinite (Rombach et al. 2004)." McCoy et al. 1997 & McCoy 2000 describe Fort Knox further.

The SW ore zone of **Buckhorn Mtn gold skarn** in Washington State (formerly Crown Jewel) has **tetradymite**, see above under pilsenite.

The **Petráčkova hora RIRG deposit** in Czech Republic [1.03 M. oz] has accessory **tetradymite** with Au mineralization, identified by EDAX (Zachariáš et al. 2001); see above under ingodite.

At **Mokrsko RIRG deposit** [3.08 M. oz] in Czech Republic **unnamed** Bi_2Te and other, little-characterized, Bi-Te phases are “younger than maldonite or native gold and older than **tetradymite**, joséite–A, joséite–B or bismuthinite (Zachariáš et al. 2006).” **Tetradymite**, joséite–A(?) and joséite–B replace the Bi-Te minerals, or are intergrown with them without any signs of replacement. **Tetradymite** is always older than joséite–A or joséite–B (op. cit.). See above under unnamed Bi_2Te .

The **Darasun gold deposit** in Transbaikalia Far East Russia and the **Maiskoe gold deposit** in Ukraine have **tetradymite**, see above under ikunolite.

In the Precambrian **Mazowe gold deposit** in Zimbabwe [resource 0.99 M. oz] **tetradymite** occurs in “A late association of a number of Bi-minerals ... namely native bismuth, bismuthinite, cosalite ($\text{Pb}_2\text{Bi}_2\text{S}_5$) with distinct Ag contents (0.49-1.95 wt % Ag, $n=10$), joséite–A (Bi_4TeS_2) and **ingodite** (Oberthür et al. 2000).” From Oberthür & Weiser (2008) the average of 4 **tetradymite** analyses is $\text{Bi}_{1.912}\text{Pb}_{0.151}\text{sum}_{2.063}\text{S}_{1.129}\text{Te}_{1.808}\text{sum}_{2.937}$. See above under ingodite.

Tetradymite from the **Clogau gold mine** in the Dolgellau gold belt in Gwynedd, Wales has Pb <1 wt % to as much as 8 wt % (Cook et al. 2007a). “Published electron-microprobe data for **tetradymite** commonly show the presence of several wt % Pb.... The presence of lead may be caused by the presence of sub-mm inclusions of galena or other lead minerals, but could ... be real (op. cit.).”

In the **Larga-Fata Băii gold ore field** in the Metaliferi Mtns of Romania rich epithermal veins and skarn in altered andesite have “Silver-Pb-Bi sulphosalts, some with Sb and/or Se, intimately associated with **hessite** and a range of Bi-tellurides with $\text{Bi} / (\text{Te} + \text{S} + \text{Se}) \leq 1$ (**tetradymite**, tellurobismuthite, tsumoite, Pb-free rucklidgeite) ... Lillianite and gustavite [are] most abundant ... with subordinate bismuthinite derivatives (aikinite, krupkaite, bismuthinite).... All **tetradymite** analyses display the same slight enrichment of (S + Se) relative to Te that is seen in almost all published analyses for the mineral (Cook et al. 2007b). **Analysed tetradymite compositions contain up to 0.3 apfu Se**, and plot along the **tetradymite-kawazulite** join (their Fig. 6b). Some **tetradymite** contains several wt % Pb, attributable to sub-mm inclusions of galena (Cook et al. 2004).”

18.7 **Tetradymite** in some global polymetallic Sn W Bi Au Fe Pb Zn Ag and Cu deposits

The **Verkhne-Ingodinskoye tin deposit** in Far East Russia, the type locality for **ingodite**, the **Vostok-2 skarn scheelite–sulphide deposit** in northern Primo'rye, Far East Russia and the **Tyrnyauz W + Mo deposit** in northern Caucasus, Kabardino-Balkaria Republic, Russia all have **tetradymite**; see above under ingodite.

Tetradymite occurs in the bismuth-bearing “large **Berezovsk gold deposit** located 12 km northeast of Yekaterinburg Far East Russia. Since its discovery in 1745, 160 minerals have been identified.... Quartz, calcite, ankerite, pyrite, galena, fahlore, chalcopyrite, aikinite, native gold, and sphalerite are the most abundant ... **Bismuth reserves at the deposit are estimated at more than 1,000 tonnes ... a significant share of world reserves**. In the sulfide–quartz veins of the deposit, bismuth occurs on its own or as an admixture in galena, fahlore, and native gold. Bismuth minerals are native bismuth; simple sulfides (bismuthinite); selenides (guanajuatite); sulfotellurides (**tetradymite**); and sulfobismuthides of Pb (cosalite) Pb–Cu (aikinite) and Cu (wittichenite, emplectite). The major part of bismuth is related to aikinite and fahlore. Matildite (AgBiS_2) grains were identified by microprobe... (Vikent'eva et al. 2008).”

Third Mineralogical Report detailing the finding of two 'new' gold-associated bismuth sulphotelluride minerals and identifying other opaque minerals, namely native silver electrum **tetradymite** **pilsenite** **hessite** bismuthinite–aikinite pavonite and greenockite characterizing a RIRG system in claim # 516584 and the Bunker Hill & Mormon Girl Crown Grants, on Nox Fort Project south of Salmo in Nelson Mining Division, southernmost British Columbia p. 96

Tetradymite occurs in the Bi-Te-S-(Se) mineral assemblages with tsumoite sulphotsumoite **pilsenite** joséite–B **hedleyite** and **unnamed** Bi_2Te in the large-scale **Huangshaping polymetallic Pb-Zn-Cu-Ag-Fe-W-Mo-Sn deposits** in Hunan Province, south China (Fig. 5 in Gu et al. 2001)". See above under **unnamed** Bi_2Te .

The **Pangushan W + Bi vein-form deposit** in Jiangxi Province, Ganzhou Prefecture China and the **Kingsgate Mo-Bi deposits** in NSW Australia both have **tetradymite**, see above under ikunolite.

Tetradymite, **hedleyite** and **hessite** occur in the **Ocna de Fier - Dognecea [iron skarn] deposit** in Romania. Ag-Bi-Se-Te mineral assemblages are restricted to chalcopyrite ores, Fe Pb Zn and Cu were produced.

Tetradymite is the second most abundant Bi–Te–(S) phase after **ingodite** in the “**Băița Bihor skarn deposit**, (Rezbanya) Apuseni Mountains in Romania as well as others in the Upper Cretaceous ‘banatitic’ province {Ilinca & Makovicky 1999}, (Cook et al. 2007b).”

18.8 Occurrence of **Tetradymite** in Adit 1 Crush Vein

N. Cook (Part II) observes three grains of **tetradymite** $\text{Bi}_2\text{Te}_2\text{S}$ in polished section BHA-1-8 of Adit 1 Crush Vein of Bunker Hill mine. Fig. 2B has three very small electrum grains adjacent to **tetradymite** encased in pyrite. Fig. 1F has two grains enclosed in pyrite. The pyrite buffers the local $f\text{S}_2$ conditions allowing it s formation. Fig. 2B **tetradymite** is deficient in Te with surplus S ($\text{Bi}_{1.96}\text{Pb}_{0.01}\text{Sb}_{0.02}$)sum_{2.07} ($\text{Te}_{1.70}\text{S}_{1.21}\text{Se}_{0.02}$)sum_{2.93} but the analysis is suspect at low 96.3 wt %.

19 Hessite Ag₂Te

19.1 Hessite properties

Hessite Ag₂Te is lead-grey or steel-grey, has hardness 2-3, monoclinic crystal form and poor indistinct [001] cleavage. It occurs as well-formed crystals or more commonly subhedral grains in matrix. <http://www.mindat.org/min-1881.html> lists 318 sites.

19.2 Hessite – type locality in eastern Kazakhstan

Hessite was first described by G. Rose in 1830. The type locality is the Koz'modem'yanskii shaft, Second Zavodinsk Mine, Altai Mtns in eastern Kazakhstan. There it occurs with pyrite chalcopryrite and sphalerite.

19.3 Hessite some localities in BC

The **Kena** MINFILE 082FSW379 and **Gold Mtn Zones** MINFILE 082FSW237 five km S of Nelson have pyrite ± chalcopryrite + rare pyrrhotite + trace native gold & electrum sphalerite galena and tetrahedrite; **hessite** occurs as micro inclusions at pyrite grain boundaries (Logan 2003, Logan et al. 2003). Together gold reserves are 0.77 M. oz. (Sultan Minerals Inc.).

The former **Snip Mine** near Iskut River, Liard Mining Division MINFILE 104B 250 is 100 km NW of Stewart. In this early Jurassic age intrusion-related vein deposit gold mineralization occurs in 1 cm to 1 m alternating bands of massive (streaky) calcite, heavily disseminated to massive pyrite, biotite-calcite as thin bands or streaks, or in quartz with sulphides in crackle breccia or pyritic to non-pyritic fault gouge. "Abundant calcite occurs throughout the mineralized zone with sulphides consisting of pyrite, pyrrhotite, chalcopryrite, sphalerite, galena, molybdenite and arsenopyrite. Minor/trace amounts of bismuth and lead tellurides, including tellurobismuthite, cosalite, **hessite** and volynskite have been noted in thin sections. From 1991 to 1999 Snip produced 32.093 Million grams of gold, 12.183 Million grams of silver and 249,276 kg of copper from about 1.2 Mt (MINFILE)."

The **Red Mountain intrusion-related gold deposits** are in Skeena Mining Division MINFILE 103P 086. "Gold-silver mineralization (1992 resource 2.5 Mt grading 12.8 g/t Au and 38.1 g/t Ag) occurs within several discrete zones within a folded sequence of Middle to Late Triassic sedimentary rocks, Early Jurassic volcanoclastic and pyroclastic rocks, and Early Jurassic intrusions (Rhys 1996)." Deposits are "spatially related to the contact of the Goldslide Intrusion and surrounding pyroclastic and sedimentary rocks. Mineralization occurs both within the intrusion as well as in surrounding country rocks. Marc Zone mineralization consists of densely disseminated to massive (> 60%) pyrite and/or pyrite stringers and veinlets, variable amounts of associated pyrrhotite and sphalerite as well as minor chalcopryrite, arsenopyrite, galena, tetrahedrite and various tellurides. Several phases of mineralization and deformation are indicated by the presence of different generations of pyrite as well as breccia fragments consisting of pyrite. High grade gold values are usually associated with the semi-massive, coarse-grained pyrite aggregates, but also occur with stockwork pyrite stringers and veinlets. Gold occurs as native gold, electrum and as tellurides. Visible gold is rare. Native gold, as observed in polished thin sections, ranges in size from 10 to 500 microns and occurs as threads, interstitial pockets, and partial networks within the pyrite as well as moulded on to the periphery of pyrite fragments within gangue and altered wall rock.

Hessite Ag_2Te altaite PbTe petzite Ag_3AuTe_2 calaverite AuTe_2 sylvanite $(\text{Au},\text{Ag})_2\text{Te}_4$ native tellurium aurostibite AuSb bournonite PbCuSbS_3 **hedleyite(?)** Bi_7Te_3 native bismuth and bismuthinite Bi_2S_3 contain a significant amount of the gold and are closely associated with native gold and electrum (Bray 1992)."

The **Sweetner Vein on the Hedley Monarch Property**, Olalla, Osoyoos Mining Division MINFILE 082ESW015 "varies in width from 1/4 inch to 1 ½ inches and is sparsely mineralized with pyrite, chalcopyrite, sphalerite, galena, tetrahedrite, gold, petzite, **hessite**, and altaite for 130 feet. The erratic distribution of the microscopic telluride minerals and gold leads to erratic gold and silver values (Thompson 1949)".

19.4 **Hessite** occurrence in some global RIRG deposits

Hessite Ag_2Te is an accessory phase in the **Petráčkova hora RIRG gold deposit** in Czech Republic [1.03 M. oz], identified by EDAX (Zachariáš et al. 2001); see above under ingodite.

The 'reduced' **Ortosa gold skarn** in the Rio Narcea Gold Belt in Asturias Spain has **hessite** associated with Ag-rich electrum, **hedleyite** and native bismuth (see Fig. 12 above) in "pyrite-bearing ore in those samples **where pyrrhotite appears partially replaced by pyrite and marcasite...** [with] galena [as] coarse grains that fill cavities in arsenopyrite crystals, commonly associated with chalcopyrite... In both the El Valle and Ortosa deposits, the field of **hessite** stability with respect to Ag-rich electrum or argentite defines the minimum $f\text{S}_2 - f\text{Te}_2$ conditions required for the stability of the other telluride minerals {Afifi et al., 1988}... The occurrence of **hessite**, bismuthinite and joséite–A may indicate an increase in $f\text{S}_2$ as suggested by the replacement of pyrrhotite by pyrite (Cepedal et al. 2004)." See above under hedleyite.

The **Björkdal gold mine** near Skellefteå Kåge in Sweden has copper breithauptite covellite cubanite ferberite frobergite native gold bismuth **hedleyite** electrum **pilsenite** **hessite** nickeline scheelite tellurobismuthite and tsumoite amongst others, see under hedleyite.

Hessite occurs with **tetradymite** in the **Maiskoe gold deposit** in Ukraine, apparently restricted to '**oxidized**' hematite-dominant environments (Cook et al. 2002)". See above under ikunolite for discussion of the GBT parageneses.

Nagybörzsöny in Hungary has **hessite** with **pilsenite** and the new mineral jonassonite amongst others, see under pilsenite and jonassonite.

Hessite occurs in the **Kontaktovyi Stock RIRG** mineralization in Northeast Russia described by Sidorov et al. 2007, see Appendix 7.

Intermediate mine levels of the **Larga-Fata Băii gold field** in the Metaliferi Mtns. in Romania have **hessite** (Cook et al. 2004), see tetradymite section.

19.5 Hessite occurrence in two global polymetallic deposits

Hessite occurs in the Bi-Te-S-(Se) assemblage in the **Huangshaping polymetallic Pb-Zn-Cu-Ag-Fe-W-Mo-Sn deposits** in Hunan Province, south China. Hessite occurs with **bismuthian pilsenite** tsumoite **pilsenite** unnamed **Bi₂Te** and joséite–B (Gu et al. 2001 their Fig. 5). See section above on unnamed Bi₂Te.

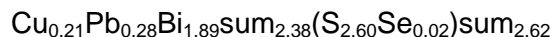
The **Ocna de Fier-Dognecea iron skarn deposits** at Banat in SW Romania produced Fe Pb Zn Cu and minor gold & silver. Two analyses of hessite are Ag_{1.97}Te_{1.03} and Ag_{1.95}(Cu + Fe)_{0.15}Te_{1.05} from Table 2 in Cook & Ciobanu (2001). See above under tetradymite; **hedleyite** also occurs.

19.6 Composition of hessite in Adit 2 Underhand Stope Vein

Hessite occurs in BH UHS 1 from Adit 2 Underhand Stope Vein, Bunker Hill mine. Fig. 2C shows joséite–B exsolved out of hessite. Fig. 2E shows a minute grain of hessite exsolved out of native bismuth and bismuthinite. Two analyses give formula Ag_{1.86}Sb_{0.04}sum_{1.90}Te_{1.07}Se_{0.03} and Ag_{1.95}Sb_{0.02}sum_{1.97}Te_{1.03}Se_{0.01}, both close to stoichiometric Ag₂Te.

20 Bismuthinite–aikinite series mineral in a Lefevre quartz + arsenopyrite vein cross-cutting the Lefevre skarn / hornfels

In **Lefevre quartz + arsenopyrite vein L-04QVXtry** cross-cutting the Lefevre skarn / hornfels a bismuthinite derivative mineral in the bismuthinite–aikinite solid-solution series $\text{Bi}_2\text{S}_3 - \text{CuPbBiS}_3$ (Topa et al. 2002) may occur. With ikonolite this replaces earlier formed native bismuth, all enclosed in arsenopyrite (figs. 2A, 2D & 2F in Lefevre section Part II). The single analysis has excess total wt % 102.00; the formula is



Using the formula $\text{Cu}_x\text{Pb}_x\text{Bi}_{2-x}\text{S}_3$ and $\text{Cu} = x = 0.21$ the formula is **non-stoichiometric** as apfu Bi should be 1.79 and it is 1.89. Sulphur is also deficient by a very high ~0.4 apfu. There is no Sb. The phase is uncertainly bismuthinite–aikinite.

Polished section BHA-1-8 of Adit 1 Crush Vein of Bunker Hill mine has common bismuthinite–aikinite grains replacing earlier formed native bismuth (fig. 3A, 3B & 3C) and also bismuthinite–aikinite adjacent to **hedleyite** (fig. 3D) in quartz or pyrite. The Fig. 3D phase was analyzed.

The first analysis with total wt % 99.33 has formula $\text{Cu}_{0.03}\text{Pb}_{0.27}\text{Bi}_{1.90}\text{sum}_{2.19}(\text{S}_{2.79}\text{Se}_{0.02})\text{sum}_{2.81}$. Using the formula $\text{Cu}_x\text{Pb}_x\text{Bi}_{2-x}\text{S}_3$ and $\text{Pb} = x = 0.27$ the formula is **non-stoichiometric** as apfu Bi should be 1.73 and it is 1.90. Sulphur is also deficient by ~0.2 apfu.

The second analysis with total wt % 101.99 is $\text{Cu}_{0.07}\text{Pb}_{0.42}\text{Bi}_{1.86}\text{Sb}_{0.01}\text{sum}_{2.38}(\text{S}_{2.62}\text{Se}_{\text{nil}})\text{sum}_{2.62}$. Using $\text{Cu}_x\text{Pb}_x\text{Bi}_{2-x}\text{S}_3$ and $\text{Pb} = x = 0.42$ the formula is **non-stoichiometric** as apfu Bi should be 1.58 and it is 1.86. Sulphur is also deficient by a high ~0.4 apfu.

Concluding, SEM-EDS analyses give **non-stoichiometric formulae** for three Nox Fort bismuthinite–aikinite grains. Microprobe analyses may be needed for characterization.

Bismuthinite–aikinite occurs in polymetallic mineralization in the Rędziny quarry in Poland (Golebiowska et al. 2005), discussed above under ikonolite.

21 Does Jonassonite $\text{Au}(\text{Bi,Pb})_5\text{S}_4$ a new gold + bismuth mineral occur on Nox Fort?

Jonassonite is a newly named and characterized gold + bismuth sulphosalt mineral $\text{Au}(\text{Bi,Pb})_5\text{S}_4$ (Paar et al. 2006). It is found in old mining dumps of the abandoned Nagyörzsöny deposit in the Börzsöny Mountains, northern Hungary. "Mineralization is hosted by Miocene calc-alkaline volcanic rocks and occurs as a stockwork in a pyroclitic dacite breccia pipe (op. cit.).

"In [five] occurrences, jonassonite is part of a pronounced Bi association: either Bi-sulfosalts (e.g. Nagyörzsöny northern Hungary), Bi-tellurides (Yakutia Russia), or both sulfosalts and tellurides (Highiş Romania occurrence). Although the phase is generally only present as a trace constituent, **it can also form mineable concentrations**, for example in the New Occidental deposit, Cobar District, NSW, Australia (called 'newoccidentallite' by Stegman 2001). We note that in these occurrences, both native bismuth and native gold are present (Ciobanu et al. 2006a)."

In the Cobar deposits stage 2 gold-bismuth mineralization is overprinted by stage 3 fine-grained gold (850-900 fineness), bismuthinite (Bi_2S_3) and "newoccidentallite" (Bi_5AuS_4), properly the new mineral jonassonite. The latter two bismuth-bearing minerals may replace and rim earlier formed stage 2 gold, maldonite and native bismuth (Stegman 2001).

Jonassonite also occurs at Crown Jewel [Buckhorn Mtn] (N. Cook p.c. 2008, interpretation of analytical data in Gaspar 2005). As Nox Fort has abundant bismuth, approx. 70 times the abundance of gold (Howard 2006b), and a reduced bismuth telluride mineralogy, could jonassonite occur?

22 Blue Quartz Vein has similar ‘fracture-trails’ of bismuth minerals as in secondary ‘Type III’ two-phase liquid and vapour fluid inclusions in the Batman gold orebody, Australia

N. Cook observes a key texture in Blue Quartz Vein BQ-02 polished section, evidence of the formation process of the Nox Fort gold + bismuth (sulpho)telluride mineralization: “an abundance of fine swarms of bismuth minerals (and omnipresent galena) throughout parts of the section (Fig. 15). These swarms consist of numerous blebs, from <5 µm up to a maximum of ca. 100 µm in size, commonly interconnected with one another as well as other bodies of Bi-minerals infilling fractures in the quartz. **The abundant oriented arrays of blebs ... or ‘fracture-trails’ are visually spectacular.** These characteristic trails of Bi-minerals as blebs in quartz are, in the author’s experience, very typical of intrusion-related gold deposits (Hart, 2007). Formation of the Blue Quartz vein may have taken place under high-volatile, CO₂-rich conditions with sudden catastrophic and erratic release of volatiles from hydrothermal fluids (Blue Quartz Vein section in Part II).”

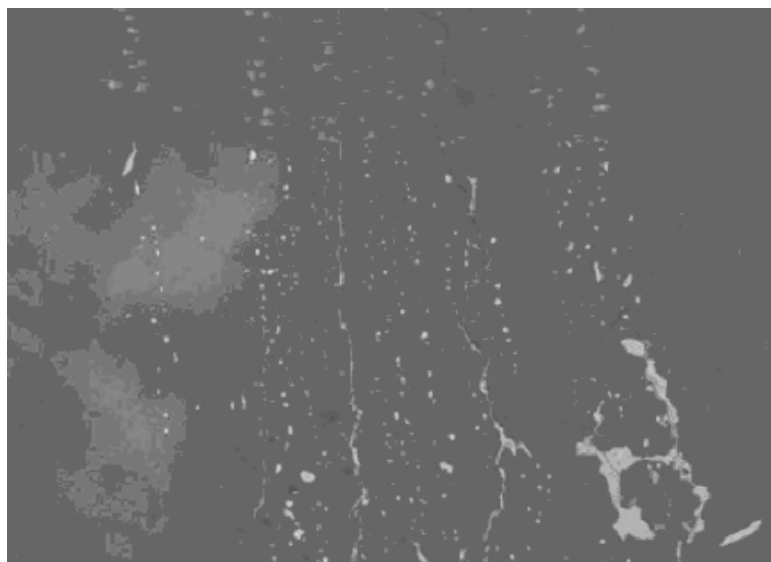


Fig. 15 Back-scattered electron image showing array of oriented blebs of “various bismuth minerals (bismuthinite, joséite–A and native bismuth) plus galena within quartz” in polished section BQ-02 from the Blue Quartz Vein. “Many of the individual blebs interconnect ... along fine fractures, infilling the quartz matrix (N. Cook).” Horizontal scale about 1.5 mm. Fig. 1B in Blue Quartz Vein section, Part II.

A similar micro-fracturing texture is well-researched in the Batman gold orebody in the Northern Territory of Australia. This is the largest gold deposit in the Mt. Todd mine with recorded production 0.3 M. oz. gold (Hein et al. 2006). Sheeted extensional veins “have quartz, pyrrhotite, chalcopyrite, loellingite, cubanite, pyrite, marcasite, arsenopyrite, native gold, native bismuth, bismuthinite, talnakhite Cu₉Fe₈S₁₀, pavonite Ag₃Bi₃S₅, **hedleyite** Bi₇Te₃, Bi-rich galena, sphalerite, galena, calcite and chlorite {Hein, 2003b}. **Gold is associated with bismuth in vapour-rich fluid inclusions** {England, 1990; Hein, 1994}. The alteration selvage surrounding quartz veins has biotite, rare muscovite, sericite, chlorite, and **accessory tourmaline**. Detailed paragenetic and textural studies by Hein {2003b} have established a sequence in sulphide and silicate precipitation (their Fig. 2): formation of sulphides; replacement of pyrrhotite by pyrite and marcasite; Bi–Te ± Pb ± Ag mineralisation; Bi–Au mineralisation. Micro-fracturing interrupted vein formation and new sulphides were precipitated during each micro-fracture event (Hein et al. 2006)”.

Study of the fluid inclusions along the micro-fractures definitively supports the 'liquid bismuth gold collector' model of Douglas et al. (2000). "In gold-bearing quartz–sulphide veins ... Type III fluid inclusions are secondary 2-phase liquid and vapour fluid inclusions. They are accompanied by gold, maldonite and bismuth grains in the same healed fracture, or they wet those grains (their Fig. 3E). Liquid /Vapour proportions are 70–95% vapour in vapour-rich inclusions, and rarely 1-2% vapour in liquid-rich inclusions. The inclusions are smooth, but irregular in shape with max. size 5 x 4 microns ... Type III liquid and vapour secondary fluid inclusions (28 to 34 or 17 to 18 wt.% NaCl equivalent) [have] CH₄ vapour and discrete gold and bismuth grains and associated growth zones...

The mineral paragenesis has been linked to the trapping chronology of Types I–IV fluid inclusions in order to constrain the fluid conditions during (micro)-tectonism and the mineralising process. **Gold is intimately associated with bismuth in Type III vapour–liquid fluid inclusions**, either as discrete inclusions within the trails, or wetting the inclusions. The progressive change in the composition of Types I–IV is consistent with the evolution of a retrograde contact metamorphic fluid in wall rock lithologies.

Maldonite and native bismuth-only grains are observed in intimate association with Type III inclusions in the same healed fracture [photo].... Temperatures of first melting of native bismuth grains range from 241.9 - 259.9 °C, which broadly agrees with the maldonite–bismuth eutectic in the two component gold–bismuth system (op. cit.)". For 81% atomic percent bismuth (and 19% alloyed gold) this is 241.0 °C. "The proportion of gold and bismuth in grains can be estimated from the phase diagram for the bismuth–gold system (their Fig. 5). Using the observed upper temperature of first melting of Bi of 259.9 °C, the mole fraction of bismuth in the gold–bismuth grains range from ~ 0.79 to 0.96 (Hein et al. 2006)" or 79 to 96% bismuth.

A very similar genesis is proposed for Nox Fort, from N. Cook's observation of characteristic fluid inclusion trails of Bi-minerals as blebs in fractured vein quartz in the Blue Quartz Vein.

23 Conclusions

Investigation of the opaque mineralogy in 18 polished sections of gold-mineralized specimens from the Nox Fort property by Nigel J. Cook has been very successful in identifying rare minerals and advancing the further understanding of the formation conditions of this gold + bismuth + tellurium bearing, granite-related mineralization. The research has also been cost-effective, considering the abundance of information obtained.

Mineralization on Knox Fort may form a mineable gold deposit. Consider that there are only so many occurrences known worldwide of these especially rare, to at least uncommon, gold-associated Bi-Te-S bearing minerals! Most are in past or presently producing gold deposits. Generally they have been identified only by more thorough academic research on higher numbers of prepared polished sections (microscope mounts). This report summarizes global occurrences of these Bi-Te-S-(Se) minerals, concentrating on those most thoroughly researched, in the public domain to Dec. 2008.

Two 'new' minerals have been identified in Eloise Vein, **Bi₈Te₅S₄** and **Bi₄Te₃S₂** in 2 polished sections; these await further characterization.

The Scanning Electron Microscope – Energy Dispersive Spectrographic micro-analyses in Part II are considered only slightly less reliable than electron microprobe analyses from 2006. The SEM-EDS method is quite sufficient for bismuth (sulpho)telluride identification as the number of elements present in the mineral formulae are low, and excepting sulphur, they are all have high atomic weights, that is they are heavy elements. Some mineral formulae presented herein provide some direct comparison of the accuracy of the different methods.

C. Hart's RIRG system model (2005 & 2007) has been used to further understand the property. The present study reinforces this interpretation with additional confirming evidence, e.g. "the comparable mineralogy in veins and skarn, identification of arsenopyrite and broad distribution of reduced Bi-mineral assemblages across the deposit. The study has proven that gold is associated, paragenetically, with bismuth minerals in all ore types on the property. CLY [Nox Fort] is demonstrated to be a single mineralised system, with mineralization consisting of both veins and skarns, all closely tied to the [Bunker Hill Sill] granite which is the likely source of metals (Conclusion of N. Cook in Part II)."

In the investigated central Nox Fort occurrences early-stage minerals are 'reduced' minerals with Metal:Chalcogen ratios ≥ 1 (Cook et al. 2002) including native bismuth **hedleyite** **Bi₇Te₃** **unnamed** **Bi₂Te** **ingodite** **Bi₂(Te,S)** **joséite–B** **Bi₄Te₂S** and **joséite–A** **Bi₄TeS₂** with more sulphur. These are stable with magnetite (with **hessite** **Ag₂Te** in BH UHS-1 from the Adit 2 Underhand Stope Vein), pyrrhotite and/or arsenopyrite. Maldonite and löllingite have not been observed; minor galena molybdenite accompanies. The gold mineral is native gold with low silver content. These mineral assemblages formed in the pyrrhotite / magnetite stability fields. This is compatible with the setting of their host quartz veins and skarn in reduced graphitic metasediments, situated near intrusive contacts with a 'reduced' ilmenite-bearing felsic granitoid – the Bunker Hill Sill.

Latter stage minerals are more 'oxidized', actually meaning the minerals present have more sulphur and chalcogen (Te, Se) content in their formulae, with Metal:Chalcogen ratios < 1 . These include bismuthinite **Bi₂S₃** **tetradymite** **Bi₂Te₂S** **pilsenite** **Bi₄Te₃** and two 'new' unnamed minerals, the phases **Bi₄Te₃S₂** and **Bi₈Te₅S₄** found in Eloise Vein. Some of these Bi-Te-S minerals may have formed by sulfidation of the early-stage minerals, e.g. textures show bismuthinite **Bi₂S₃** commonly replaces native bismuth Bi. Silver is more abundant: electrum is the gold mineral rather than native gold.

Tetradymite **pilsenite** and base metal-bearing minerals of Pb and Sb are more abundant in this latter stage mineralization, as in other well-documented occurrences discussed in the report. This formed under conditions of higher sulphur chemical activity, the process sulfidation.

Sulfidation is commonly incomplete, allowing for the observation of relict early-stage mineralization. Late stage sulphidation may be one mechanism of gold deposition. **Tetradymite** and **pilsenite** are very scarce in the examined microscope mounts.

The gold mineral in the **Bunker Hill mine veins** is **silver-rich electrum** as 5-30 micron-sized grains included in pyrite. Very practically pyrite content may be a reliable indicator of gold and silver content there.

The gold mineral in **Eloise Vein** is **native gold to gold-rich electrum**. Polished sections have common generally 5-20 micron-sized grains. These are isolated in matrix quartz or spatially associated with patches of Bi-Te-S minerals. The latter may be larger. Grains are very abundant in Eloise Vein Bi-Te-S minerals, spectacularly in joséite–B as aligned 'gold trails' (fig. 6).

Laser ablation analysis of polished sections BHUS-01 from Adit 1 of the Bunker Hill mine and L-11 from the Lefevre skarn finds **no 'invisible gold'** (a term for both gold in the pyrite lattice itself and sub-microscopic gold inclusions) in the iron sulphides pyrite pyrrhotite and marcasite.

In all examine polished sections **gold tellurides are completely absent**. This indicates the chemical concentration (fugacity) of tellurium, abbreviated fTe_2 , was not sufficient to reach the stability field of calaverite $AuTe_2$. It was sufficient to form the silver telluride **hessite** Ag_2Te , observed in the polished section of BH UHS 1 from Adit 2 Underhand Stope Vein of the Bunker Hill mine.

SEM analyses show the bismuth telluride and sulphotelluride minerals in showings in the central area are near stoichiometric, that is the mineral formulae have atomic proportions close to integer numbers.

Ikunolite in Adit 1 Crush Vein is the most tellurium-rich known, comparing 11 other worldwide localities. **Ikunolite** in Lefevre vein L-04QVXtry is the second-richest (Table 3). Lead content is ~0.2 atoms per formula unit [apfu], typical for **ikunolite**. **Unnamed Bi_2Te is near** near-stoichiometric in three Nox Fort occurrences. **Ingodite** solely found in Eloise Vein is near-stoichiometric with typical Pb at ~0.1 apfu. Sb & Se are trace.

Occurrences of early-stage bismuth telluride minerals appear to be spatially zoned w.r.t. the Bunker Hill Sill granite. Two occurrences of **unnamed Bi_2Te** in *proximal*-placed Eloise and Lefevre quartz + arsenopyrite veins contrast with **hedleyite** occurrence in three *intermediate*-placed Bunker Hill mine veins. The formula used for **hedleyite** herein is **$Bi_{2+x}Te_{1-x}$ with $x = 0.13$ to 0.19** .

Mineralogical research suggests that the gold-bearing blebs or patches of native bismuth and Bi-Te-S minerals in the BiTel Knoll quartz veins exsolved (crystallized) from cooling, gold-bearing, Bi + Te (+ S) melts. These 'sloshed about' cooling Bunker Hill Sill granitic magma and solidified at temperatures ~277 °C (after Ciobanu et al. 2003). Oriented blebs or trails, micro-inclusions of "various bismuth minerals (bismuthinite, joséite–A and native bismuth) plus galena within quartz" are prominent in polished section BQ-02 of the Blue Quartz Vein (fig. 15). Many of the individual blebs interconnect along fine micro-fractures in the quartz matrix. The inference is that gold is intimately associated with bismuth in vapour-rich (carbon dioxide-rich) fluid inclusions in the Blue Quartz Vein and elsewhere on Nox Fort.

Similar physical-chemical conditions experienced at Nox Fort formed these six RIRG deposits:

Fort Knox [5.4 M. oz] and Pogo [3.51] (but less arsenic and base metal sulphides)
both in Alaska

Petráčkova hora [1.01] and Mokrsko [3.08]

both in Czech Republic

Ortosa gold skarn in Spain

Maiskoe gold deposit in Ukraine (but little Cu and no Ni minerals)

Nine of 13 GBT minerals that characterize the Pogo deposit (Rombach et al. 2002) occur in central Nox Fort. Petráčkova hora has Bi-Te mineralogy similar to Nox Fort with trace **ingodite** and **unnamed Bi₂Te** (Zachariáš et al. 2001, 2006, p.c. 2006).

The geochemistry and mineralogy of the 'Bismuth Gold Zone' on the Jersey-Emerald property of Sultan Minerals Inc., 13 km east, (fig. 3) is considerably different than Nox Fort. Bismuth minerals there are Ag, Pb, Sb and often Se -bearing; some of the minerals present are selenides, not tellurides. Contrast these with the Pb poor bismuth (sulpho)telluride minerals directly associated with native gold or electrum on Nox Fort. Sb and Se are near absent. Practically the differing geochemistry and mineralogy reflects which elements are possibly concentrated in economic deposits at the property scale: Mo W Pb Zn on Sultan Minerals' Jersey-Emerald property vs. Au (Ag) Bi Te W on Nox Fort, at least about the central part investigated herein.

Further mineralogical work, a fluid inclusion study and characterization of the two 'new' minerals found in Eloise Vein is recommended. Because showings in the central area of the property have high bismuth contents with gold, more analytical work may find other rare gold or gold-associated Bi-Te minerals. Newly characterized jonassonite³⁸ Au(Bi,Pb)₅S₄ (Paar et al. 2006) may occur. This is found in the Petráčkova hora (Zachariáš et al. 2001) and Buckhorn Mtn (Cook, p.c. 2008), both Reduced Intrusion-Related Gold deposits applying the mineral deposit model of C. Hart (2007).

³⁸ Jonassonite is mined in Australia (Stegman 2001).

24 Appendices

24.1 Appendix 1 Bismuth

Bismuth is a silver-gray, reddish-tinged, brittle and heavy metallic element atomic number 83. It is usually produced as a by-product of processing of lead ores. Bismuth melts at 271.4 °C and unusually for a liquid expands on solidifying. “Bismuth, at an estimated **8 parts per billion** by weight, is the 69th element in order of abundance in the Earth’s crust, **about twice as abundant as gold**. World reserves of bismuth are usually based on bismuth content of lead resources because bismuth production is most often a by-product of processing lead ores; in China, bismuth production is a by-product of tungsten and other metal ore processing. Bismuth minerals rarely occur in sufficient quantities to be mined as principal products; the Tasna Mine in Bolivia and a mine in China are the only mines that produced bismuth from a bismuth ore. ... Several bismuth-containing deposits are in varying stages of mining feasibility review. These polymetallic deposits include NICO in Canada, Nui Phao in Vietnam, and Bonfim in Brazil (USGS 2006).” Its insoluble compounds are non-poisonous and used in medicine.

24.2 Appendix 2 Tellurium

Tellurium was discovered in gold ores in Transylvania Romania in 1782. It is a rare element, 73rd in order of crustal abundance, **1 to 2 parts per billion**. “Estimates of the mean Te content of the Earth’s crust range from 0.36 to 10 ppb, with 1 to 2 ppb [0.001-0.002 ppm] being the most commonly cited estimates of mean content (see refs in Hein et al. 2003, Brown et al. 2000).” “Tellurium is enriched more than any other element (up to about 50,000 times) relative to its Earth’s crustal mean ...” in ocean floor Fe-Mn crusts (Hein et al. 2003). Tellurium is about as rare as platinum and **about four times rarer than gold**.

Crystalline tellurium is silvery-white with a metallic luster but industrial tellurium is usually a dark gray powder. It is brittle and a p-type semiconductor. Many telluride-bearing minerals occur with sulfides of the chalcophile metals Cu Ag Au Zn Cd Hg Fe Co Ni Pb As & Bi. The mineral native tellurium is very rare. Tellurium is obtained from anode slime as a byproduct of electrolytic copper refining (Klapotke & Crawford 2004). It has an affinity to gold in nature as shown by the existence of several gold telluride minerals. Tellurium and bismuth are specific geochemical pathfinders for gold concentrations (Boyle 1979).

24.3 Appendix 3 Claim list

Table 1A: Details on the new tenure mineral claim #516584 in Nelson Mining District, southernmost British Columbia owned by Clarke Gold Inc.

New Tenure Numbers	(Legacy) Claim Name	Owner number	[⊖] Work recorded, Good to Date	Area, hectares
--------------------------	---------------------------	-----------------	--	-------------------

516584	(CLY 2)	210814	2012/Jun/13	740.853
--------	---------	--------	-------------	---------

516584 Partially surrounds the 2 Crown Grants (Table 1B following)

[⊖] After approval of this report

Table 1B: Details on the Crown Grant Mineral Claims in the Pend d'Oreille River area, Kootenay Land district, British Columbia owned by Clarke Gold Inc.

Lot name	Lot number	area (hectares)	NTS map sheet	BCGS map sheet	Land district
Bunker Hill	2939	12.08	082F03W	082F.004	Kootenay
Mormon Girl	1949	17.65	082F03W	082F.004	Kootenay

Crown Granted. **Both administered from Kamloops, B.C.**, subject to annual taxes (current).

Crown Grants state, in so many words, that one quarter of each claim surface area can be used for road building for mining purposes.

24.4 Appendix 4 Itemized Cost Statement

Expenses incurred by B Howard for expert rock & mineralogical sampling on central CLY claims by Nigel J. Cook (of Norway), C.L. Ciobanu (of Australia), A. Koffyberg and B. Howard in period Oct. 16 2007 - Oct. 15 2008:

Small Equipment

Field notebooks, 30m tape, pin flags	Butler Survey Supplies	52.84
bear spray, holster for spray, batteries	Mtn Equipment Co-op Calgary	44.26
bags	Superstore in	4.43
15 plastic 5 gal. pails for rk packaging	Rona Home & Garden hardware Calgary	84.51
refund for overcharge for 3 plastic 5 gal. pails for rk packaging	Rona Home & Garden hardware Calgary	-15.74
replace cotter pin on Thunderbolt tool	Bolt Supply House	5.00
15 lids for plastic 5 gal. pails for rk packaging	Rona Home & Garden Calgary	43.57

Office

Copies	UPS Store in Calgary	3.25
rebind Field Trip Guide Book	UPS Store in Calgary	6.34

Meals – travel

coffee	Café in Invermere	2.50
lunch for BH	Castlegar Airport	5.14
lunch for 3	in Rossland	7.50
bkfeast for 3	A&W in Castlegar	15.88

Parking

NC & CC arrival	Castlegar Airport	0.50
B Howard	Castlegar Airport	0.50
B Howard 5 days	Castlegar Airport	25.00

Site Meals

lunches for 3	Superstore in Calgary	32.72
bkfeast for BH	Subway Salmo	7.93
supper for 3	Salmo Hotel	52.00
bkfeast for 3	Charlie's Café in Salmo	40.00
lunch for 3	Subway Salmo	22.53
supper for 3	Ymir Hotel	47.31
lunch for 3	Subway Salmo	17.13
bkfeast for 3	Charlie's Café in Salmo	37.00
supper for 3	Fruitvale Kitchen	40.00
bkfeast for 3	Whiteline Truck Stop in Erie	26.00
supper for 3	Salmo Hotel	41.00
bkfeast for 3	Charlie's Café in Salmo	26.00
supper for 3	Dragon Fly Café Salmo	37.00

Third Mineralogical Report detailing the finding of two 'new' gold-associated bismuth sulphotelluride minerals and identifying other opaque minerals, namely native silver electrum **tetradymite** **pilsenite** **hessite** bismuthinite–aikinite pavonite and greenockite characterizing a RIRG system in claim # 516584 and the Bunker Hill & Mormon Girl Crown Grants, on Nox Fort Project south of Salmo in Nelson Mining Division, southernmost British Columbia p. 110

Accommodation

A Koffyberg 2 nites	Reno Motel Salmo	148.20
N Cook & C Ciobanu 5 nites	Reno Motel Salmo	427.50
B Howard 6 nites	Reno Motel Salmo	444.60

Kilometerage

B Howard 4th trip 1760 km at 0.45 per km	1760 km in BC, 337.5 km in AB not charged	792.00
---	---	--------

Field Work

B Howard 6 days @ \$450/day	Oct. 21 – 26 2007	2,700.00
-----------------------------	-------------------	----------

De-mobilization

B Howard 2 days @ \$400/day	Oct. 20 & Oct. 30 2007	800.00
-----------------------------	------------------------	--------

Microscopical Mineralogical Research

Converted from Norwegian Kroner currency to N. Cook, TD Bank Dec. 1 2007	6,866.16
--	----------

Bank fee

Foreign currency draft to N. Cook	TD Bank Dec. 1 2007	30.00
-----------------------------------	---------------------	-------

Air Cargo

Mineral specimens to Oslo Norway	Shenker or Bax Global Air Cargo Dec. 6 2007	223.80
----------------------------------	---	--------

Misc. office expenses incurred but not charged

Subtotal		\$13,144.36
Report writing costs 3 days @400/day	B Howard	<u>1,200.00</u>
Subtotal		\$14,344.36
Clarke Gold Inc.	Management fee 10%	<u>1,434.44</u>
Total		\$15,778.80

1/5th (20%) apportioned work as work on claim # 516584	\$3,155.76
--	-------------------

Filed for Assessment Credit on claim # 516584	\$3,100.00
Previously discussed with A. Wilcox.	
Only travel in BC is accounted for and no airfare.	

Third Mineralogical Report detailing the finding of two 'new' gold-associated bismuth sulphotelluride minerals and identifying other opaque minerals, namely native silver electrum **tetradymite** **pilsenite** **hessite** bismuthinite–aikinite pavonite and greenockite characterizing a RIRG system in claim # 516584 and the Bunker Hill & Mormon Girl Crown Grants, on Nox Fort Project south of Salmo in Nelson Mining Division, southernmost British Columbia
p. 111

From above:

Microscopical Mineralogical Research in total \$6,866.16

The letter below apportions **more** than 20% of this expense = \$1,373.23 to work on mineral specimens from claim # 516584; less or \$1,373.23 is claimed as work on claim # 516584 in the above tally.

Attn. Clarke Gold Inc.
c/o Wm Howard VP Operations
Calgary AB Canada
by email to wm.howard@shaw.ca

Oct. 10 2008

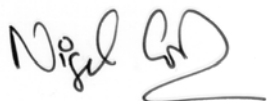
Mineralogical investigation by microanalysis of mineralized rock (ore) samples from CLY project collected from tenure claim 516584:
EL-01, EL-02, EL-05, EL-06, EL-07, EL-08, C-01, CLS-0446, Ella-01, BQ-01 and BQ-02
(Total 11 samples)

Priced in Norwegian kroner (NOK)

Sample slicing	NOK	550.00
Preparation of polished blocks	NOK	800.00
Binocular and optical (reflected light) microscopy 5 hrs @ NOK 400/hr	NOK	2,000.00
Scanning electron microscopy 3 hrs. @ NOK 750/hr	NOK	2,250.00
Report preparation 6 hrs. @ NOK 400/hr	NOK	2,400.00
Total	NOK	8,000.00

Currency equivalence 1 Norwegian Kroner = 0.178 CDN \$ [Oct. 10 2008]

Total **CDN\$ 1,430.14**



Prof. Nigel J. Cook
Natural History Museum (Geology)
University of Oslo,
Oslo, Norway

nigelc@nhm.uio.no

24.5 Appendix 5 Statement of Qualifications for Prof. Nigel J. Cook

Nigel John Cook, a British citizen, was born in 1960 and is based at the Natural History Museum (Geology section), University of Oslo in Oslo Norway. After receiving his B.Sc. and Ph.D. degrees from the University of London, he worked as postdoctoral researcher in Canada (1987-1990) and later (1991-1998) in Germany, where he also obtained his Habilitation. He joined the Geological Survey of Norway in 1998, serving as leader of the Mineral Resources Section until 2001. He joined the University of Oslo in 2004 as Assistant Professor and was awarded a full professorship in 2005.

His research interests span both mineralogy and ore deposit studies and he is particularly interested in using detailed mineralogical investigation at the micro- and nanoscopic scales to understand ore-forming processes. Field work has taken him to many parts of the world, but he has been most active in Scandinavia and Southeastern Europe, investigating massive sulphide, skarn and epithermal deposits. More recently, he has developed a number of research projects addressing mineral systematics, structures and, in particular, non-stoichiometric minerals.

Nigel has been Secretary General of IAGOD since 2000 and Editor-in-Chief of the IAGOD journal, 'Ore Geology Reviews' since 2003. He is currently also Chairman of the International Mineralogical Association 'IMA' Commission on Ore Mineralogy 'COM', leader of International Geological Correlation Programme (IGCP) project 486 (2004-2008) and non-permanent Associate Professor at the University of Turku, Finland.

IGCP project 486 "focuses on studies of all types of Au-Ag-telluride-selenide mineralizations and their ore deposits and attempts to bridge the gap between scientists working in the laboratory and those working in the field from the microscopic- to orogen-scales. The project aimed to understand geological processes causing accumulations of Au (\pm Ag) with Te and Se over space and time, the mineralogy of these deposits and the internal and external controls on metal and mineral distributions."

Nigel is the author of ca. 70 publications and more than 125 conference contributions on subjects ranging from nanoscale mineralogy to regional metallogenesis, and from platinum group elements to industrial minerals.

Nigel Cook is the lead author of two recent review papers 'Compositional data for Bi-Pb tellurosulfides' and 'Minerals of the system Bi-Te-Se-S related to the tetradymite archetype: review of classification and compositional variation' published in 2007 in volume 45 of the Canadian Mineralogist.

24.6 Appendix 6 Statement of Qualifications for William R. Howard

I graduated in 1978 from the University of Alberta with a B.Sc. Honours with distinction in Geology. Thereafter I prospected at Dublin Gulch, Yukon for Canada Tungsten Mining Corp. in 1980 in the area of the Ray Gulch tungsten skarn during its exploratory drilling. This was before the discovery of the M. oz Eagle Zone gold deposit (StrataGold Corp.). A few years later I worked briefly for Noranda at the intrusion-related Marn gold skarn NE of Dawson City Yukon.

In 1997 I purchased the Bunker Hill and Mormon Girl Crown Grants. In 1999 the Bunker Hill project on the present central area CLY1 and CLY2 claims was awarded a BC Prospectors Assistance Program grant for \$10,000 (Howard 2000). I have attended numerous conferences, field trips and courses on mineral exploration including

1997 Numerical techniques and strategies for evaluation of geochemical data by E.C Grunsky, 145 pp. Part of Exploration '97 Workshop: Current topics in GIS and Integration of Exploration Datasets Sept. 9 - 13 1997, Ottawa, Ont.

1999 Short Course on Intrusion-related Gold by Kamloops Exploration Group [KEG] April in Kamloops BC

2004 Short Course 'Gold Vein Deposits: Turning Geology into Discovery' by D. Rhys & P. Lewis. Cordilleran Exploration Round-up Jan. 24 – 25 2004 Vancouver BC

2005 Short Course 'Orogenic vs. Intrusion-Related gold' with emphasis on Yukon and Alaska deposits by C. Hart of Yukon Geological Survey & R. Goldfarb of USGS. at Minerals South 2005 Conference Oct. 25 - 27 2005, Cranbrook BC

2006 Private field trip to RIRG gold deposits in the Czech Republic near Prague: Mokrsko [3.08 M. oz] and Petrůvka hora [1.03 M. oz] with Dr. J. Zachariáš

2007 August 26-31 attended the International IGCP-486 Field Workshop on Au-Ag telluride-selenide deposits at GTK, Espoo Finland. Presented paper 'Structural setting and geochemical correlations in bismuth (sulfo)telluride - native gold-bearing veins, CLY group, British Columbia, Canada: A reduced intrusion-related gold system' at Symposium & Field trip

2007 Oct. 28-31 attended the Geological Society of America Denver Annual Meeting October 2007. Symposium & Field trip to the Cripple Creek gold mine, leaders E. Jensen & P. Spry in conjunction with IGCP-486

2008 Jan. 28-31 Mineral Exploration Round-up 2008 Vancouver BC and February 1-2 Short Course 'Understanding Mineralization Controls: Applied Structural Geology to 3D Modelling and Mining'

2008 April 15-18 Poster Presentation at 17th Annual Calgary Mining Forum, Calgary Mineral Exploration Group

I have been involved in prospecting in the Canadian Cordillera since 1976 and the Nelson Mining Division since 1988.

24.7 Appendix 7 Mineralogy of the Kontaktovyi Stock *intrusion-hosted* RIRG system deposit in Far Northeast Russia

'**Hedleyite**' with formula ' Bi_2Te ' is a gold carrier in the RIRG mineralization of the **Kontaktovyi Stock, Far Northeast Russia** (Sidorov et al. 2007). **No precise analyses are given - the mineral may actually be unnamed Bi_2Te .** The following are excerpts of Sidorov et al.'s paper on this **well-described *intrusion-hosted* RIRG deposit:**

"Major pyrite and arsenopyrite, secondary [minor] molybdenite and galena and rare native gold, native bismuth and pyrrhotite occur with '**hedleyite Bi_2Te** ' (?), hessite Ag_2Te and very rare bismuth oxide-fluoride minerals. "The Kontaktovyi stock (1500 x 1300 m in size) is composed of [Early Mesozoic] granite porphyries and quartz diorites. The central part of the intrusive dome hosts an aureole of a stockwork-stringer system ... developed in the beresitized granite porphyries, which are transformed into fine crystalline albite–quartz metasomatic rocks with a relict porphyritic texture. They are crosscut by a dense network of differently oriented albite–quartz and quartz veinlets ranging in thickness from 0.5–1 mm to 1–2 cm. Generally, the thickness varies from 4 to 5 mm. The veinlets are characterized by inconsistent sinuous forms with several pinch outs and offshoots. ... The quartz grains have a rim of fine-flaky sericite, which is also confined to lenticular relicts of host rocks. Thin albite fringes are developed along the selvage of veinlets. [Their] Table 1 presents contents of trace elements in metasomatic rocks...

Clusters of veinlets are confined to zones with a high degree of jointing and maximal metasomatic alteration. Based on the size of colluvial debris, such zones are up to 20 m thick. Based on the size of chalcedony-type quartz fragments in [talus of altered granitoids], some veins of massive quartz are up to 20 cm thick. They have a vaguely banded structure owing to the alternation of white, yellowish white, and gray quartz bands, as well as the irregular distribution of ore mineralization. Only pyrite is identified reliably. The maximal contents of elements recorded in the veins are: Sb 3,000 / Bi 2,000, Ag 3–4, and Te 100 [all in ppm]. Au content varies from 0.006 - 0.01 g/t.

The results of the mineralogical analysis revealed new data on the Au–Bi–Te mineralization of the Kontaktovyi ore occurrence. The mineralization is irregularly developed mainly near the selvages of veinlets. At present, 19 ore minerals have been identified (their Table 2). The major minerals are ... coarse-grained disseminations of pyrite, arsenopyrite, galena, and molybdenite (up to 1–2 mm). Arsenopyrite grains include a very fine (30–40 μm) emulsion dissemination of native bismuth and gold. The development of fine dissemination of bismuth, tellurides, and gold is an indicator of hypabyssal gold–rare metal mineralization (Volkov et al. 2007). In general, gold occurs as intergrowths with native bismuth and '**hedleyite**' (?) (see their Fig. 3c). Results of microprobe analysis show that the fineness of gold varies from 480 to 670–760 and 870–920. The purest gold includes a significant Cu admixture (up to 0.3%). The '**hedleyite**' includes tiny arsenopyrite crystals (Fig. 3d). Many ore minerals on the granitoid surface are commonly oxidized. The microprobe analysis made it possible to identify a great number of rare secondary Te-bearing minerals (see Sidorov et al. 2007, their Table 2 & Figs. 3a, 3b)."

Dedication

This report is dedicated to Morris Butler of Calgary, founder, owner and President and of Butler Survey Supplies with five stores in western Canada, for his encouraging personality and excellent service supplying field equipment for various prospecting ventures.

25 References in chronological order

Cockfield, W.E. 1920 Mayo area, Yukon GSC Summary Report 1919, Part B

Pratt, G.M. 1931 An occurrence of tellurides near Smithers, B.C.
p. 55-56 in Contr. Can. Min., Geological Series No. 30. pub. University of Toronto, Toronto Ontario

Annual Report of the Minister of Mines 1934 Bunker Hill p. E24-E25

Waneta Gold Mines Ltd. (operator of Bunker Hill mine) May 13 1936a Survey underground plan of 3 adits. Shows "best ore shipped" was from Underhand Stope Vein in Adit No. 2. Scale 1"=40'. Archive Map # 53B Ministry of Energy & Mines, Cranbrook B.C.

Waneta Gold Mines Ltd. Sept. 13 1936b Bunker Hill Group underground plan of three adits.
Compiled by H. Sargent from surveys by A.H. Green & Co. 1934 and H.D. Dawson 1936. Scale 1"=20'.
Archive Map # 60175 Ministry of Energy & Mines, Cranbrook B.C.

Annual Report of the Minister of Mines 1936
p. E18-E21 Waneta Gold Mines Ltd. (operator of Bunker Hill mine) includes underground plan map
http://www.em.gov.bc.ca/DL/GSBPubs/AnnualReports/AR_1936.pdf

Warren, H.V. & Davis, P. 1940 Some Bismuth minerals from British Columbia.
p. 107-111 in Contr. Can. Min., Geological Series No. 44. pub. University of Toronto, Toronto Ontario

Peacock, M.A. 1941 On joseite, grüningite, orueteite.
p. 83-105 in Contr. Can. Min., Geological Series No. 46. pub. University of Toronto, Toronto Ontario
p. 92 joséite–A, "**auriferous tetradymite**" from Glacier Gulch.

Warren, H.V., & Peacock, M.A. 1945 Hedleyite, a new bismuth telluride from British Columbia, with notes on wehrilite and some bismuth-tellurium alloys.
p. 55-69 in Contr. Can. Min., Geological Series No. 49. pub. University of Toronto, Toronto Ontario

Warren, H.V. 1946 Bismuth tellurides from the White Elephant claim, British Columbia.
p. 75-77 in Contr. Can. Min., Geological Series No. 50. pub. University of Toronto, Toronto Ontario

Warren, H.V. 1947 A New Type of Gold Deposit in British Columbia.
Transactions of the Royal Society of Canada, Third Series; Section IV, Vol. XLI Ottawa

Thompson, R.M. 1949 The telluride minerals and their occurrence in Canada.
p. 342-382 in American Mineralogist, Vol. 34

Thompson, R.M. 1951 Mineral Occurrences in Western Canada.
p. 504-508 in American Mineralogist, Vol. 36

Nuffield, E.W. 1954 Studies of mineral sulphosalts: XVIII-pavonite, a new mineral.
p. 409-415 in American Mineralogist, Vol. 39

Thompson, R.M. 1954 Mineral occurrences in Western Canada
p. 525-526 in American Mineralogist, Vol. 39

Third Mineralogical Report detailing the finding of two 'new' gold-associated bismuth sulphotelluride minerals and identifying other opaque minerals, namely native silver electrum **tetradymite** **pilsenite** **hessite** bismuthinite–aikinite pavonite and greenockite characterizing a RIRG system in claim # 516584 and the Bunker Hill & Mormon Girl Crown Grants, on Nox Fort Project south of Salmo in Nelson Mining Division, southernmost British Columbia p. 117

Abrikosov, N.K. & Bankina, V.F. 1958 Study of phase diagram of the system Bi–Te.
p. 659-667J. Inorg. Chem. USSR [N. Kh. Zhur.] Vol. 3 [in Russian]

Kato, A. 1959 **ikunolite**, a new bismuth mineral from the Ikuno mine, Japan.
p. 397-407 in Mineralogical Journal (Japan), Vol. 2

Lawrence, L.J., & Markham, N.L. 1962 A contribution to the study of the molybdenite pipes of Kingsgate, NSW, with special reference to ore mineralogy.

p. 67-94 Proceedings of the Australasian Institute of Mining and Metallurgy, Vol. 203

Quote from S.S. Augustithis 1995 p. 121

“The Mo-Bi bearing quartz pipes in the Kingsgate area occur within and show gradations to irregular intrusive masses of granitoid quartz, which probably represents the extreme magmatic differentiate of highly acidic granites. The pipes may be classified as epi-magmatic plutonic offshoots grading into hydrothermal bodies. The complex relationship of ore minerals include two main assemblages: pyrrhotite–chalcopyrite–iron-rich sphalerite in galena, and molybdenite with Pb, Bi and Te-bearing minerals; also co-existing assemblages not necessarily in equilibrium, in the Pb–Bi–S system include bismuthinite–bismuth, galena–bismuth, bismuthinite–galenobismutite, and cosalite–galenobismutite–bismuthinite. In the Bi–Te–S system bismuth–**ikunolite**, **ikunolite**–joseite-A, **ikunolite**–bismuth–joseite-A, **ikunolite**–joseite-A–bismuthinite, bismuth–joseite-A–joseite-B, and bismuth–**ikunolite**–joseite-A–joseite-B assemblages have been observed.

The occurrence of apparently stable pyrite–pyrrhotite and bismuth–bismuthinite assemblages suggests that deposition took place in a system closed with respect to sulphur [?]. Arsenopyrite, gudmundite (FeSbS), cassiterite, wolframite, gold and pyrrargyrite occur.”

Markham, N.L. 1962 Plumbian **ikunolite** from Kingsgate, New South Wales.
p. 1431-1434 in Amer. Mineral., Vol. 47 No. 11-12

Abstract

The second occurrence of **ikunolite** (Bi_4S_3) is recorded. It has been found in bismuth-molybdenite pipes at Kingsgate, New South Wales, in association with bismuth, bismuthinite, joseite A, molybdenite, and gold. Its properties are reported. The chemical analysis shows 83.24 Bi, 5.49 Pb, 10.41 S, 0.27 Se, 0.78 Te, 0.04 Fe wt %. It is suggested that **ikunolite** forms under very special conditions and may be stable only over a limited pressure- temperature range or in the presence of significant Se and Te.

Little, H.W. 1965 Geology, Salmo Map Area, B.C.
GSC Map 1145A 1:63,360 scale

Gamyranin, G.N. 1968 Sul'fotelluridy vismuta severo-vostochnoy Yakutii. Bismuth sulfotellurides from northeastern Yakutia.

pp. 679-682 in Doklady Akademii Nauk SSSR Vol. 178 (3) [in Russian with English abstract]
from abstract

An association of joseite–A and joseite–B with **tetradymite** is described, for the first time in the world, from the gold deposit at the contact of granodiorites in Ergelyakh (Yakutia, USSR). The bismuth sulfotellurides occur with native bismuth, bismuthinite, and gold, representing a late stage of the ore formation.... intensively intergrown ... [Mineral abundance] changes gradually from joseite–A through **tetradymite** to joseite–B, presumably due to the decrease in sulfur content in this direction.

Godovikov, A.A., Kochetkova, K.V. & Lavrent'ev, Yu.G. 1971 Systematization of bismuth sulfotellurides and tellurides.

pp. 417-428 in Zapiski Vsesoyuznogo Mineralogicheskogo Obshchestva Vol. 100 (4) [in Russian]

Third Mineralogical Report detailing the finding of two 'new' gold-associated bismuth sulphotelluride minerals and identifying other opaque minerals, namely native silver electrum **tetradymite** **pilsenite** **hessite** bismuthinite-aikinite pavonite and greenockite characterizing a RIRG system in claim # 516584 and the Bunker Hill & Mormon Girl Crown Grants, on Nox Fort Project south of Salmo in Nelson Mining Division, southernmost British Columbia p. 118

Sabina, A.P. 1973 Cobalt-Belleterre-Timmins; Ontario and Quebec.
[Canadian] Rocks and Minerals for the Collector. GSC Paper 73-13 199 pp.

Imai, H., et al., 1975 Geologic structure and mineralization of the xenothermal vein-type deposits in Japan.
p. 647-676 in Economic Geology July 1975 vol. 70 no. 4

Pauling, L. 1975 The formula, structure, and chemical bonding of **tetradymite**, $\text{Bi}_{14}\text{Te}_{13}\text{S}_8$, and the phase $\text{Bi}_{14}\text{Te}_{15}\text{S}_6$.
p. 994-997 in Amer. Mineral. Vol. 60

Zav'yalov, Y.N. & Begizov, V.D. 1978 New types of bismuth sulfotellurides.
p. 91-100 in Izvestia Vysshikh Uchebnykh Zavedniy, Geologiya i Razvedka Vol. 10 [in Russian]
*a new phase to be named **ingodite** identified*

Nechelyustov, G.N., et al. 1978 **Ikunolite**, Bi_4S_3 from the Kara-Obo tungsten deposit, central Kazakhstan; the first discovery in the USSR. (**Ikunolit**- Bi_4S_3 iz vol'framovogo mestorozhdeniya Kara-Oba (Tsentral'nyy Kazakhstan)-pervaya nakhodka v SSSR).
p.105-111 in Novye Dannye o Mineralah. SSSR, No. 26 [in Russian]

Boyle, R.W. 1979 The geochemistry of gold and its deposits.
GSC Bulletin 280, 584 pp.

Finashin, V.K., Litavrina, R.F., Romanenko, I.M. & Chubarov, V.M. 1979 **Ikunolite** from the Vysokogora Deposit, Primor'ye [Russian Federation, USSR]. (**Ikunolit** Vysokogorskogo mestorozhdeniya (Primor'ye)).
p. 337-339 in Zap. Vses. Mineral. Obshch. Vol. 108 No. 3 [in Russian with English abstract] ISSN 0044-1805
abstract

Ikunolite, $\text{Bi}_4(\text{S},\text{Se})_3$, occurs in the Vysokogora [alternate sp. Vysokogorsk] Sn deposit in sericite-quartz metasomatic rocks, sulphide ores intergrown with bismuthinite and also with native bismuth in arsenopyrite and quartz. **Ikunolite** differs from bismuthinite in having very weak birefringence and anisotropism. Microprobe analyses (6) show Pb 2.3-11.4, Te 0.10-3.0%; a specimen with composition Bi 79.3, Pb 6.7, S 9.7, Te 1.1, Se 1.3 [calculated formula $(\text{Bi}_{3.59}\text{Pb}_{0.31})\text{sum}_{3.90}(\text{S}_{2.86}\text{Se}_{0.16}\text{Te}_{0.08})\text{sum}_{3.10}$] has [unit cell dimensions] a 4.16, c 39.44 Å. The dispersion of the reflectance is tabulated.

Fleischer, M. & Pabst, A. 1981 'New Mineral Names' **Unnamed Bi_2Te** .
p. 439 in Am. Mineral. Vol. 66
review of

Gamyanin, G.N., et al., 1980 Bismuth tellurides - Bi_2Te and BiTe in deposits of northeastern USSR.
p. 230-235 in Zapiski Vses. Mineralog. Obsh. Vol. 109 [in Russian]

http://www.minsocam.org/ammin/AM66/AM66_436.pdf

"The mineral Bi_2Te was found associated with wehrlite⁴¹, tellurobismuthite, and joséite-A in the Ergelyakh deposit, Yakutia. Probe analyses gave Bi 76.8, 76.44; Te 22.6, 22.04; sum 99.4, 98.48%; ratio Bi/Te = 2.07, 2.11. ... [by M. Fleischer.]" Keywords Indigirka River Basin, Saha Republic (Sakha Republic; Yakutia), Eastern-Siberian Region, Russia

Third Mineralogical Report detailing the finding of two 'new' gold-associated bismuth sulphotelluride minerals and identifying other opaque minerals, namely native silver electrum **tetradymite** **pilsenite** **hessite** bismuthinite–aikinite pavonite and greenockite characterizing a RIRG system in claim # 516584 and the Bunker Hill & Mormon Girl Crown Grants, on Nox Fort Project south of Salmo in Nelson Mining Division, southernmost British Columbia p. 119

Fleischer, M. in Fleischer, M., Chao, G.Y. & Mandarino, J.A. 1982 New Mineral Names – **Ingodite**.
p. 855 in Am. Mineral. Vol. 67 p. 854-860

http://www.minsocam.org/ammin/AM67/AM67_854.pdf

reviews of:

Ingodite (Grünlingite discredited)

1981a The new bismuth mineral **ingodite**, Bi_2TeS .

p. 594-600 in Zapiski Vses. Mineralog. Obsh. Vol. 110 [in Russian]

and

E.N. Zav'yalov and V.D. Begizov 1981b Once again on the problem of grünlingite.

p. 633-635 in Zapiski Vses. Mineralog. Obsh. Vol. 110 [in Russian]

During the study of numerous museum samples labeled "grünlingite", all were found to consist of joséite–A or bismuthinite. A sample from the type locality, Brandy Gill, Cumberland, England, and one from the Ingoda deposit, central Transbaikalia, also contained a new mineral [**ingodite**].

Electron microprobe analyses of 5 samples from the 2 localities gave Bi 68.8-73.3, Pb 0-1.2, Sb 0-0.15, Te 19.3-25.3, S 5.1-6.3, Se 0-0.4, sum 99.1-100.3%, giving the formula above. ... **Ingodite** is silver-white, luster metallic, cleavage perfect, nonmagnetic, brittle, soft. ...The name is for the locality (this review does not give precise formulae).

Bortnikov, N.S., Mozgova, N.N., Nekrasov, I.Ya, Rozov, D.N., Tupyakov, V.Y. & Tsepin, A.I. 1982 Particularities of bismuth mineralization in gold ores of eastern Transbaikalia.

p. 45-58 in Mineralogicheskii Zhurnal Vol. 4(4) [in Russ. with English abstract]

abstract with English edited

X-ray methods have revealed a high Bi content in ores from one of the medium-depth gold-ore deposits in E Transbaikalia (locality is not specified – secrecy of Communists). Gold in this deposit is associated with native bismuth, bismuthinite, **ikunolite**, and Bi- and Sb-Bi-sulphosalts of lead (galenobismutite, cosalite, kobellite and a $\text{Pb}_5(\text{Sb,Bi})_4\text{S}_{11}$ (?) mineral), Bi-bearing bournonite and Bi-sulphotellurides (joséite–A, joséite–B and **tetradymite**). A characteristic feature of the [unspecified] deposit is the combination of sulphosalt and sulphotelluride bismuth mineral associations. Isomorphous elements occur in the Bi minerals (Ag, Sb and Se in the Bi-sulphosalts; Pb, Sb, Cu and Se in the Bi-sulphotellurides; and Pb, Sb and Te in the Bi-sulphides). The Bi-sulphosalts were deposited in a sequence from those with high Bi content to those with high Pb content. Pb-bearing sulphoantimonides (boulangerite, jamesonite and zinkenite $\text{Pb}_9\text{Sb}_{22}\text{S}_{42}$) formed throughout. Au-Bi mineralization formed at temperatures 425-470 °C and sulphur fugacities from 10^{-12} to 10^{-6} (lower limit) to 10^{-8} to 10^{-5} (upper limit).

Gamyranin, G.N., N.V. Leskova, L.N. Vyal'sova, & I.P. Laputina 1982 Bismuth tellurides – **Bi₂Te** and **BiTe** – in deposits of northeast USSR.

p. 451-457 in International Geology Review Vol. 24, complete translation by M. Fleischer of Gamyranin, G.N., et al., 1980 Telluridy bismuta - **Bi₂Te** i **BiTe** – v mestorozhdeniyakh Severo-Vostoka SSSR.

p. 230-235 in Zapiski Vses. Mineralog. Obsh. vyp. 2 Vol. 109 [in Russian]

Dunn, P.J., et al. 1984 New Mineral Names.

p 210-215 in American Mineralogist Vol. 69:

Review of T. Ozawa and H. Shimazaki 1982 **Pilsenite** redefined and wehrnite discredited.

p. 291-294 in Proc. Japan Acad., Vol. 58

Kaufman, M. 1984 PCMI (BC) Project, Bunker Prospect area.

B.C. EMPR Assessment Report #12,758. Work by M. Harris

<http://aris.empr.gov.bc.ca/ArisReports/12758.PDF>

Third Mineralogical Report detailing the finding of two 'new' gold-associated bismuth sulphotelluride minerals and identifying other opaque minerals, namely native silver electrum **tetradymite** **pilsenite** **hessite** bismuthinite–aikinite pavonite and greenockite characterizing a RIRG system in claim # 516584 and the Bunker Hill & Mormon Girl Crown Grants, on Nox Fort Project south of Salmo in Nelson Mining Division, southernmost British Columbia p. 120

Kwong, Y.T.J. 1984 The Tillicum Mountain Gold Prospect – A Petrologic Update (82F/13).
p. 23-34 in GF 1984 Paper 1985-1 pub. BC EMPR

Dunn, P.J., et al., 1985 New Mineral Names – **Ingodite**.

p. 220 in Am. Mineral. Vol. 70 p. 214-221

http://www.minsocam.org/ammin/AM70/AM70_214.pdf

review of:

Zav'yalov, E.N., Begizov, V.D. & Tedchuk, V.Ya. 1984 Additional data on the chemical composition of **ingodite**.

p. 31-35 in Zapiski Vses. Mineralog. Obsh. Vol. 113 [in Russian]

"The composition of **ingodite** (Fleischer 1982) was given as Bi_2TeS , based on 5 microprobe analyses (Bi 68.8-73.3, Pb, 0-1.2, Sb 0-0.15, Te 19.3-25.3, S 5.1-6.3, Se 0-0.4 wt %. Twelve new analyses (samples verified by X-ray study) from Ingoda, Transbaikalia; Cumberland, England; Kamchatka; and southern Urals gave Bi 51.1-73.3, Pb 0.6-10.6, Te 19.3-32.1, S 5.2-6.3, Se 0-0.4 %, giving formulas ranging from $(\text{Bi}_{2.00}\text{Pb}_{0.02})\text{Te}_{0.86}(\text{S}_{1.12}\text{Se}_{0.02})$ to $(\text{Bi}_{1.38}\text{Pb}_{0.24})\text{Te}_{1.42}\text{S}_{0.95}\text{Se}_{\text{nil}}$; the ratio Bi:(Te,S) ranges from 3:4 to 5:7" by M. Fleischer

Goncharov, V.I., Alshevskiy, A.V., Vortsepnev, V.V., Sergeyeva, N.I., & Savva, N.Y. 1984 New find of bismuth telluride, **Bi₂Te**, in northeastern USSR.

p. 111-113 in Doklady Acad. Nauk. SSSR, Earth Sci. Sec. Vol. 275 [in Russian]

Little, H.W. 1985 Geological Notes Nelson West Half (82F, W1/2) Map Area

GSC Open File 1195 47 p.

The CS Unit is "a thick assemblage of black argillite and grey massive limestone, with minor chert, greenstone, and phyllite. The age ... is assumed to be Silurian (?), Lower and Middle Devonian, and Carboniferous (?) "

Imai, N. & Chung, J.I. 1986 The first Korean occurrence of **ikunolite**.

p. 65-74 in Mineralogical Journal ISSN 0544-2540 Vol. 13 No. 2 (8 ref.) in English.

Pub. Japan Publications Trading, Tokyo

Ognyanov, N.V. 1986 Geology of tin-bearing districts and deposition of the Khingan-Okhotsk tin-bearing area.

p. 340-399 in Lugov, S.F., ed., Geology of tin deposits of the U.S.S.R. Nedra, no.1 [in Russian]

Ren, Yingchen 1986a Tellurobismuthinides from Pangushan, China.

p. 277-279 in Geochemistry ISSN 0253-486X Vol. 5 No 3 (4 ref.) in English. pub. Science Press, Beijing

from p. 277 "South of Jiangxi, S China metamorphosed Devonian sandstones and slates are underlain by a biotite granite stock. Alterations are silicification, sericitization and tourmalinization. Wolframite occurs in quartz veins; this and cassiterite zinnwaldite and tourmaline are characteristic of upper zone ones, wolframite scheelite molybdenite pyrrhotite and arsenopyrite lower zone quartz veins. Bi-Te minerals include joséite, **tetradymite** and **ingodite**."

An unnamed mineral "gave a chemical analysis with Bi 75.42, Te 19.2, and S 6.65 wt %. ...chemical formula is $(\text{Bi}_{3.5}\text{Te}_{0.5})(\text{S}_{2.0}\text{Te}_{1.0})$; i.e., this phase is **tellurian ikunolite** (Bayliss 1991)."

Ren, Yingchen 1986b Tellurobismuthinides from Pangushan, China.

p. 209 in Abstracts with program; the Fourteenth general meeting of the International Mineralogical Association (in English). ISSN 0579-5559. Keywords bismuthides; **ingodite**; joséite; tellurides; tellurobismuthite

Ren, Yingchen, Cheng, Mingqing, & Wang, Cunchang 1986 Characteristics and vertical zoning of tungsten-bismuth minerals in the Pangushan quartz vein type tungsten deposit of Jiangxi province. 63-74 in Mineral Deposits [Kuangchuang Dizhi] Vol. 5 (2), ISSN 0258-7106. In Chinese with English summary:

"The Pangushan quartz-vein type tungsten deposit has great vertical extension and complicated ore mineral constituents characterized by obvious vertical zoning which finds expression in the following aspects:

1. From top to bottom tungsten-bismuth quartz veins show regular variations in texture and structure. ...
2. Mineral assemblages show regular variation in space, with minerals of high temperature assemblage such as zinnwaldite, tourmaline and cassiterite in the upper part of the deposit, whereas lower temperature assemblage with bismuth sulfosalt minerals and tellurobismuthite in the lower part.
3. Wolframite in the lower part contains more manganese than in the upper part...
4. The spatial variations in $\text{Bi}_2\text{S}_3\text{-PbS}$ series and tellurobismuthite group are characterized by downward depletion in sulfur."

Bakharev, A.G., Gamyagin, G.N., Goryachev, N.A. & Polovinkin, V.L. 1988 Magmatic complexes and mineral assemblages of the Ulakhan-Tas Range, the northeast Yakutia. pub. U.S.S.R. Academy of Sciences, Siberian Branch, Institute of Geology, Yakutsk. 199 pp. [in Russian].

Morávek, P., Janatka, J., Pertoldová, J., Straka, E., Ďurišová, J. & Pudilová, M. 1989 Mokrsko gold deposit - the largest gold deposit in the Bohemian Massif, Czechoslovakia. p. 252-259 in Economic Geology Monograph vol. 6

Anthony, J.W., Bideaux, R.A., Bladh, K.W. and Nichols, M.C. 1990 Handbook of Mineralogy, Volume I. Elements, Sulfides, Sulfosalts. Mineral Data Publishing, Tucson, AZ 588 pp.

Ettlinger, A.D., 1990 A geological analysis of gold skarns and precious metal enriched iron and copper skarns in British Columbia, Canada. unpub. PhD thesis, Washington State University, 246 pp.

Höy, T. & Andrew, K.P.E. 1990a Structure and Tectonics of the Rossland Group, Mount Kelly - Hellroaring Creek Map Area, southeastern British Columbia. p. 11-17 in GF 1989 Paper 1990-1 pub. B.C. EMPR <http://www.em.gov.bc.ca/DL/GSBPubs/GeoFldWk/1989/010-018-hoy.pdf>

Höy, T. & Andrew, K.P.E. 1990b Geology of the Mount Kelly - Hellroaring Creek Map Area, southeastern British Columbia. Open File Map 1990-8 pub. BC MEMPR 1:20,000 scale

Jambor, J.L. & Puziewicz, J. 1990 New Mineral Names p. 431-438 in Am. Mineral. Vol. 75 review of:

Dobosi, G. & Nagy, B. 1989 The occurrence of an Au-Bi sulfide in the Nagyörzsöny hydrothermal ore deposit, Northern Hungary. p. 8-14 in Neues Jahrbuch für Mineralogie, Monatshefte, 1989, Heft 1, p. 8-14

"Electron-microprobe analyses of two of three grains found in core from a drillhole at the former gold-producing Nagyörzsöny deposit, Börzsöny Mountains, Hungary, gave Au 14.81, 14.87; Ag 0.12, 0.28; Bi 68.39, 71.11; Pb 5.95, 4.31; S 9.81, 9.75; sum 99.08, 100.32 wt %, corresponding to $\text{Au}_{1.02}\text{Ag}_{0.3}(\text{Bi}_{4.58}\text{Pb}_{0.28})_{\Sigma 4.86}\text{S}_{4.09}$, or $\text{Au}(\text{Bi,Pb})_5\text{S}_4$. The grains are intergrown with native gold and a bismuth sulfide tentatively identified as **Se-free ikunolite**; grain size not stated (but a photo indicates a

probable maximum of about 8 by 25 μm). Reflectance higher than those of bismuthinite and **ikunolite(?)**, less than that of arsenopyrite. Occurs with chalcopyrite, pyrite, arsenopyrite, lillianite(?), native bismuth, bismuthinite, **ikunolite(?)**, and native gold in a stockwork zone in a propylitized dacite breccia pipe in Miocene calc-alkaline volcanics. The polished section containing the three grains of the unnamed mineral is the Laboratory for Geochemical Research of the Hungarian Academy of Science". This is the new mineral jonassonite AuBi_5S_4 discussed by Ciobanu et al. (2006a) and Paar et al. (2006).

Litochleb, J., Křištin, J. & Šrein, V. 1990 Bismutové minerály zlatonosného zrudnění z Kasejovic v jz. Čechách (Bismuthian minerals from gold-bearing mineralization at Kasejovice, southwest Bohemia). p. 279-289 in Věst. Ústř. Úst. geol., Vol. 65 (5) [in Czech]

Mumme, W.G. 1990 A note on the occurrence, composition and crystal structures of pavonite homologous series members 4P, 6P, and 8P. p. 193-204 in Neues Jahrb. Mineral. Monatsh.

Nysten, P. 1990 Tsumoite from the Björkdal gold deposit, Västerbotten County, Northern Sweden. 59-60 in Geologiska Föreningens I Stockholm Förhandlingar Vol. 112 ISSN 0016-786X

Pertoldová, J., & Scharmová, M. 1990 Vazba zlata na sulfidy na ložisku Mokrsko 'Relationship of gold sulfides in the Mokrsko Deposit'.

Geoindustria, S. p., Prague, Czechoslovakia (CSK)

p. 89-93 in Monograph 'Prinos mineralogie k reseni prumyslovych a ekologickych problemu; Seminaire. Contribution of mineralogy to industrial and ecological problems; Seminars. Conference Prinos mineralogie k reseni prumyslovych a ekologickych problemu, Usti. pub. Dum techniky CSVTS, Usti nad Labem, Czechoslovakia [in Czech]

Descriptors arsenides; arsenopyrite; aurostibite; bismuthinite; Bohemian Massif; gold; inclusions; maldonite; sulfides; technology.

Roberts, W.L., Campbell, T.J. & Rapp, G.R. Jr. 1990 Encyclopedia of Minerals. 2nd ed. pub. Van Nostrand Reinhold N.Y., N.Y. 979 pp.

Bayliss, P. 1991 Crystal chemistry and crystallography of some minerals in the tetradymite group. 257-265 in Am. Mineral. Vol. 76

Huang, D., Ding, X., Wu, C. & Zhang, C. 1991 Mineral characteristics and occurrence of gold, silver and bismuth of the Caijaying lead – zinc – silver deposit, Hebei Province. p. 127-140 in Acta Geologica Sinica Vol. 65 (in Chinese with English abstract)

Pertoldová, J., & Scharmová, M. 1991 Ore mineralization of the sample VM-31, 292.1m (A, B, C) Mokrsko-East. p. 10, Geoindustria GMS Praha [Prague] special paper [in Czech]

Bray, D. 1992 Assessment Report on Survey Program on the Red Mountain and Sarah Properties Skeena Mining Division. Owner Lac Minerals Ltd. BC MEMPR Assessment Report #22,598 <http://aris.empr.gov.bc.ca/ARISReports/22598a.pdf>

Hollister, V.F. 1992 On a Proposed Plutonic Porphyry Gold Deposit Model.
p. 293-302 in Nonrenewable Resources Vol. 1 pub. Oxford University Press
<http://www.springerlink.com/index/M252372384625672.pdf>
abstract

“A plutonic porphyry gold deposit model is proposed that is similar to the plutonic porphyry copper deposit model. However, unlike the plutonic porphyry copper deposit model, the proposed model is deficient in copper and contains less than 1% total sulfides. In the proposed model, gold is accompanied by scheelite, molybdenite, arsenopyrite, a variety of bismuth sulfides, tellurides, and native bismuth. The host rock varies from granite to granodiorite stock. Most of the ore is in the pluton. Deposits cited as examples of the proposed model are the Mokrsko deposit in Czechoslovakia, the Fort Knox deposit in the United States, and the Dublin Gulch deposit in Canada. In each of these deposits, pervasive potassic or phyllic alteration zones accompany the gold ore, which is disseminated in quartz-rich stockworks, veinlet swarms, and veins. Tonnages of gold-bearing material are large, but grades are low in the cited deposits. The proposed model is distinct from other gold deposit models because of the low Cu to Au ratio and the association of Au, Bi, W, and Mo.”

Meinert, L. 1992 Skarns and Skarn Deposits - section on Hedley District, British Columbia
<http://www.earthscience.org/t1/mel01/#Gold%20Skarns>

Predel, B. 1992 Landolt-Börnstein Bi-Te (Bismuth-Tellurium).
Book Series - Volume 5b. Subvolume B 'B-Ba – C-Zr' of Volume 5 'Phase Equilibria, Crystallographic and Thermodynamic Data of Binary Alloys' of Landolt-Börnstein - Group IV Physical Chemistry.
Publisher Springer-Verlag ISSN 1615-2018 (Print)
ISBN 978-3-540-55115-7 (on-line)

Dobbe, R. 1993 Bismuth tellurides (joseite–B, bismuthian tsumoite) in a Pb-Zn deposit from Tunaberg, Sweden.
p 165-170 in Eur. J. Mineral. Vol. 5 ©1993. pub. E. Schweizerbart'sche Verlagsbuchhandlung, D-7000 Stuttgart 1 Germany

Scharmová, M. & Pertoldová, J. 1993 The mineral “AuBi₅S₄” from Kašperské Hory and Petráčkova Hora near Rožmitálu pod Třemšínem.
p. 24-26 in Proc. V. Mineralogical Cyclic Meeting. Česká společnost průmyslové chemie ČSVTS Pracovní skupina aplikované mineralogie. Horní Bečva [in Czech]

Stinson, P. & D.R.M. Pattison 1993 Petrology of the Evening Star claim, Rossland, B.C. (82F/4).
p. 249-254 in GF 1992 Paper 1993-1 BC MEMPR
<http://www.em.gov.bc.ca/DL/GSBPubs/GeoFldWk/1992/249-254-stinson.pdf>

Litochleb, J. & Šrein, V. 1994 Minerály bismutu a telluru z ložisek a výskytů zlata v České republice. [Bismuth and tellurium minerals from the gold deposits and occurrences in the Czech Republic.]
p. 89-105 in Bulletin mineralogicko-petrologického oddělení Národního muzea v Praze (Journal ISSN 1211-0329) Vol. 2 1994 [in Czech]
Table 2 p. 92 lists rare and unnamed Bi-Te minerals from the Petráčkova hora (Vacikov) deposit:
AuBi₅S₄ / Ag_{2-x}Te_{1+x} empressite / Ag_{5-x}Te₃ stützite / unnamed Bi₂Te / Bi₃Te / Bi₃Te₂ / Bi₅Te₂ / Bi₇Te₅ [also occurs in Mokrsko deposit] / Bi₃TeS 'protojoseite' / Bi₃Te₂S sulphotsumoite / Bi₃Te₂S₂ / Bi₄(S,Te)₃ / Bi₅TeS₂ and Bi₄Se₂S laitakarite. Also see Table 4 p. 95

Ray, G.E. & Dawson, G.L. 1994 The Geology and Mineral Deposits of the Hedley Gold Skarn District, Southern British Columbia.
Bulletin 87 BC MEMPR 156 pp.

Third Mineralogical Report detailing the finding of two 'new' gold-associated bismuth sulphotelluride minerals and identifying other opaque minerals, namely native silver electrum **tetradymite** **pilsenite** **hessite** bismuthinite–aikinite pavonite and greenockite characterizing a RIRG system in claim # 516584 and the Bunker Hill & Mormon Girl Crown Grants, on Nox Fort Project south of Salmo in Nelson Mining Division, southernmost British Columbia p. 124

Anthony, J.W., et al., 1995 Mineralogy of Arizona. 3rd. ed., 259 pp.

Bakke, A.A. 1995 The Fort Knox 'porphyry' gold deposit – Structurally controlled stockwork and shear quartz vein, sulphide-poor mineralization hosted by a Late Cretaceous pluton, east-central Alaska. p. 795-802 in Porphyry Deposits of the Northwestern Cordillera of North America. pub. Canadian Institute of Mining, Metallurgy and Petroleum, Special Vol. 46, ed. T.G. Schroeter

Einarsen, J.M. 1995 Structural Geology of the Pend d'Oreille area and tectonic evolution of the southern Kootenay Arc. unpub. Ph.D. Thesis, University of Calgary, Calgary AB 4 plates (maps), 172 pp.

Gamyanin, G.N. 1995 Granitoid-related gold deposits in the Russian Far East. p. 20 in Abstracts with Programs Vol. 27 (5), pub. Geological Society of America. Cordilleran Section, 91st annual meeting Abstract 38762

"Granitoid-related gold deposits in the Russian Far East include three major deposit types: [1] gold skarns [2] gold-rare metal {bismuth, lead, copper, tin [Note: and tungsten & tellurium]} veins and greisens and [3] disseminated gold-quartz sulphide veinlets and stockworks. ... [For all] native gold in early paragenetic stages is frequently associated with arsenopyrite, loellingite, nicolite and cobaltite. Native gold of later paragenetic stages occurs with bismuthinite **ikunolite** **hedleyite** **joséite** and native bismuth. ... Type 2 deposits often have coarse gold formed in later paragenetic stages: examples include the Ergelyak, Levo-Dybin, Chistoe and Khalali deposits. Many sulphide-sulphosalt minerals occur.

For all deposit types gold fineness ranges from 400-950. Gold content varies widely, and generally ranges from 1-30 g/t and averages 10 g/t in many deposits. Granitic host rocks for all deposit types have greisen, potassic and beresite alteration. Gold mineralization formed 200-400 °C at 0.5-1.5 kb. The presence of **ikunolite**, native gold, native bismuth and maldonite [suggest] reduced conditions of ore formation in these granitoid-related gold deposits. These are associated with both magmatic Mo-W deposit and gold-quartz deposits [meaning the mesothermal-type or 'orogenic gold' veins] formed in accretionary metallogenic belts and hosted in sialic crust [as for the Tintina Gold Belt]."

Levo-Dybin in South Verkhoyansk Metallogenic Belt has Au, W, Bi (Nokleberg et al. 1997). "Ranges up to 3% As, 7-13 g/t Au, up to 2.5% WO₃, up to 1% Bi, up to 0.6% Te. Consists of abundant quartz stringers 0.2 to 0.3 m thick that form peculiar sheet stockworks in contact metamorphosed Late Permian sandstone beds 5 to 20 m thick. Stringers consists of 90-95% quartz, muscovite and potassium feldspar {Kokin, written commun. 1978; Zubkov 1984; N.A. Goryachev, written commun. 1993} (in Ariunbileg et al. 2003).

Rhys, D. 1996 Red Mountain, Northwestern British Columbia: auriferous pyrite stockworks in a zoned, porphyry-like system. 1996 Cordilleran Roundup Short Course <http://www.empr.gov.bc.ca/Mining/Geoscience/MetallicMinerals/NewModelsCordillera/Pages/IntrusiveandPorphyryrelatedGold.aspx#n>

Hitchens, A.C. & Orssich, C.N. 1995 The Eagle zone gold - tungsten sheeted vein porphyry deposit and related mineralization, Dublin Gulch, Yukon Territory. p. 803-810 in Porphyry Deposits of the Northwestern Cordillera of North America. pub. Canadian Institute of Mining, Metallurgy and Petroleum, Special Vol. 46, ed. T.G. Schroeter

Third Mineralogical Report detailing the finding of two 'new' gold-associated bismuth sulphotelluride minerals and identifying other opaque minerals, namely native silver electrum **tetradymite** **pilsenite** **hessite** bismuthinite–aikinite pavonite and greenockite characterizing a RIRG system in claim # 516584 and the Bunker Hill & Mormon Girl Crown Grants, on Nox Fort Project south of Salmo in Nelson Mining Division, southernmost British Columbia p. 125

Naciuk, T.M. & Hawkins, T.G. 1995 The Katie copper-gold porphyry deposit, southeastern British Columbia.

p. 666-673 in Porphyry Deposits of the Northwestern Cordillera of North America. Canadian Institute of Mining, Metallurgy and Petroleum, Special Vol. 46, ed. T.G. Schroeter

Kotlyar, B.B., Ludington, S. & Mosier, D.L. 1995 Descriptive, grade, and tonnage models for molybdenum-tungsten greisen deposits.

U.S. Geological Survey Open-File Report 95-584, 17 p.

Simon, S.G. & Alderton, D.H.M. 1995 **Pilsenite**, Bi_4Te_3 from the Săcărîmb gold-telluride deposit, Metaliferi Mts; first occurrence in Romania.

p. 111-113 in Romanian Journal of Mineralogy, Vol. 76 (2) **ingodite** present

Tsunoda, K. & Shimizu, M. 1995 Mineralization of the Suehiro vein of the Otome Deposit, Yamanashi Prefecture, Japan.

p. 111-120 in Resource Geology Vol. 45 (2). In Japanese with English abstract, figures & tables.

Ingodite is found enclosed in cosalite (their Fig. 4) in quartz veining with pyrrhotite chalcopyrite and galena (Fig. 5). It has significant Pb, e.g. an analysis in their Table 3 is $(\text{Bi}_{1.77}\text{Pb}_{0.23})\Sigma 2.00\text{Te}_{1.01}\text{S}_{0.99}$. It occurs in Stage II mineralization formed at 330-150 °C with pyrrhotite, less pyrite, bismuthinite, native bismuth, sphalerite, galena, cosalite, galenobismutite, Bi-bearing boulangerite and molybdenite. Log activity (fugacity) of sulphur $f\text{S}_2$ is estimated as -11 to -20 log units.

Alldrick, D.A. 1996 Intrusion-related Au Pyrrhotite Veins.

p. 57-58 in Selected British Columbia Mineral Deposit Profiles, Volume 2 - Metallic Deposits. D.V. Lefebure & T. Höy, Editors, Open File 1996-13, BC Ministry of Employment and Investment

<http://www.em.gov.bc.ca/Mining/Geolsurv/MetallicMinerals/MineralDepositProfiles/profiles/i02.htm>

Zachariáš, J., et al. 1995 Porphyry–Au Mineralization in the Bohemian Massif [Czech Republic]: its magmatic and hydrothermal evolution.

p. 211-214 in Mineral Deposits: From Their Origin to Their Environmental Impacts ... Society for Geology Applied to Mineral Deposits. pub. Balkema Rotterdam

Morávek, P. 1996 The Mokrsko gold deposit.

p. 1-17 in Morávek, P., editor Gold deposits in Bohemia. pub. Czech Geological Survey, Praha.

Nekrasov, I.Ya. 1996 Geochemistry, Mineralogy and Genesis of Gold Deposits.

iv + 344 pp. pub. AA Balkema or Taylor & Francis, Inc. Rotterdam or Brookfield

ISBN-13: 978-9054107231 'A study of the behavior of gold in sedimentary, magmatic and post-magmatic processes, describing 40 gold-bearing minerals, including 10 recently discovered ones. The results are presented of experimental studies on phase relations in gold-sulphide systems...'

Peterson, 1996 unfinished thesis at Washington State University on Tillicum Mtn gold skarn, supervisor Prof. L. Meinert. See <http://www.wsu.edu:8080/~meinert/aboutskarn.html>

Jambor, J.L., et al., 1997 New Mineral Names – Baksanite.

p. 1038-1041 in Amer. Mineral. Vol. 82

Review of Baksanite, $\text{Bi}_6(\text{Te}_2\text{S}_3)$, a new mineral from Tyrny'auz (northern Caucasus). By I.V. Pekov et al., p. 787–791 in Doklady Akad. Sci., 1996 Vol. 347 No. 6 (in Russian).

Electron microprobe analysis of several grains that were checked by X-ray powder patterns gave a mean of Bi 76.40, Pb 2.15, Sb 0.12, Te 14.33, Se 0.00, S 6.64, sum 99.64 wt%, corresponding to

$(\text{Bi}_{5.78}\text{Pb}_{0.16}\text{Sb}_{0.02})_{\Sigma 5.96}(\text{Te}_{1.77}\text{S}_{3.27})$. The composition is uniform. The mineral occurs as spherical to droplet-like single grains and aggregates up to 13 mm across; steel-gray color, metallic lustre, black streak, perfect basal cleavage, $H = 1\frac{1}{2}$ –2. ... The mineral occurs among voids in aggregates of andradite, calcite, chlorite, and stilpnomelane in altered magnetite-andradite skarn at the Tyrny'auz W-Mo deposit, Kabardino-Balkaria Republic, Russian Federation. Baksanite contains inclusions of native gold and, rarely, intergrowths of **ingodite** and **joséite**–A; all are separated from the host aggregates by a thin lining of bismuthinite. The new name refers to the type locality, the Baksan River valley. Type material is in the Fersman Mineralogical Museum, Moscow, Russia. By N.N. Pertsev.

McCoy, D. & Olsen, I. 1997 Thermochronology, mineralogy, elemental and microprobe analysis of the Fort Knox, Dolphin and selected Golden Summit deposits.

In: Newberry, R., & McCoy, D. (eds) Geology of bulk-mineable, plutonic-hosted and plutonic related gold deposits of the north Pacific: Short Course Notes, Alaska Miner's Association Annual Convention and Trade Fair, Anchorage Alaska, 15 pp.

McCoy, D., et al., 1997 Plutonic-Related Gold Deposits of Interior Alaska.

p. 191-241 in Mineral Deposits of Alaska. eds. R.J. Goldfarb & L.D. Miller, Economic Geology Monograph 9

"Plutonic-related gold deposits in interior Alaska occur in apexes of middle Cretaceous (mostly 93-86 Ma) reduced plutons and in spatially associated sedimentary and metamorphic rocks. The gold is typically present in and around the tops of intrusions. It occurs in closely spaced anastomosing or planar quartz veins ... most predominant in brittlely deformed planar quartz-sericite (carbonate) shear zones and veins. Tourmaline is common in systems associated with smaller intrusions. Arsenopyrite and stibnite (a Sb bearing sulphosalt) are the most common sulphides. Bismuthinite, bismuth telluride, and bismuth-lead-antimony sulphosalt are common gold associates; a Bi-Au correlation is significant at many deposits. The relatively low oxidation state associated with gold-favourable intrusions allows for gold fractionation into magmatic hydrothermal fluids and favours efficient gold transport ... Because of the brittle nature of ore-hosting structures, competency contrasts between hosting lithologies control the geometry of plutonic-related deposits. [Ore-hosting shear structures are preferentially located in mechanically brittle lithologies – note veins in the central Nox Fort area are in argillaceous metaquartzite and garnet skarn near Bunker Hill Sill leucogranitoids.] The last intrusive phase in multiphase systems contains the bulk of the alteration, veining and gold mineralization. It is always the most porphyritic and most felsic intrusive phase and often consists of biotite granite (Fort Knox), granodiorite-granite or quartz monzonite (?)."

Newberry, R.J., et al., 1997 Skarn Deposits of Alaska.

p. 355-395 in Mineral Deposits of Alaska. eds. R.J. Goldfarb & L.D. Miller, Economic Geology Monograph 9

Nokleberg, W.J., et al., 1997 Significant Metalliferous and Selected Non-Metalliferous Lode Deposits and Placer Districts for the Russian Far East, Alaska, and the Canadian Cordillera.

USGS Open-File Report 96-513-B

<http://pubs.usgs.gov/of/1996/of96-513-b/>

Ray, G. E. and I. C. L. Webster 1997 Skarns in British Columbia

Bulletin 101 GSB B.C. Ministry of Employment & Investment 260 p.

Third Mineralogical Report detailing the finding of two 'new' gold-associated bismuth sulphotelluride minerals and identifying other opaque minerals, namely native silver electrum **tetradymite** **pilsenite** **hessite** bismuthinite–aikinite pavonite and greenockite characterizing a RIRG system in claim # 516584 and the Bunker Hill & Mormon Girl Crown Grants, on Nox Fort Project south of Salmo in Nelson Mining Division, southernmost British Columbia p. 127

Bakke, A., et al., 1998 The Fort Knox porphyry gold deposit, east-central Alaska; an overview and update.

p. 89-98 in Porphyry and hydrothermal copper & gold deposits; a global perspective.

Conference Proceedings. Ed. T.M. Porter. pub. Australian Mineral Foundation, Glenside, Australia.

abstract

The Fort Knox gold mine near Fairbanks, Alaska, began commercial production in 1997. Gold mineralisation is hosted by the Late Cretaceous Fort Knox Pluton, a granitic intrusive suite. Gold occurs within, and along the margins of pegmatite vein swarms and quartz veins and veinlets. Numerous northwest-southeast trending shear zones influence the orientation of the vein swarms and the geometry of ore zones. Weak to moderate development of vein controlled phyllic, potassic, albitic, and argillic alteration styles are present. Gold is closely associated with trace amounts of bismuth and tellurium. The overall sulphide content of the orebody is very low.

Cook, N.J. 1998 Bismuth sulphosalts from hydrothermal vein deposits of Neogene age, N.W. Romania.

pp. 19- 39 in Mitt. Österr. Miner. Ges., Vol. 143

Gamyranin, G.N., Goncharov, V.I. & Goryachev, N.A. 1998 Gold and rare-metal deposits of Northeast Russia.

p. 94-103 in Geology of the Pacific Ocean, Volume 17, № 3, English translation of Tikhookeanskaya Geologiya (in Russ.) pub. Harwood Academic Publishers GmbH. ISSN 0207-4028 70985

http://itig.as.khb.ru/POG/17_3.html#9

abstract, revised for its English:

A large group of gold-ore deposits genetically related to the Late Mesozoic granitoids is analyzed. Three genetic types of such deposits are distinguished: {1} gold-skarn {2} gold-greisen and {3} gold and rare-metal quartz vein deposits. Ore bodies are represented by veins, stockworks and metasomatic impregnated massive deposits of various forms. Early gold is closely associated with sulphoarsenides and arsenides of iron, nickel and cobalt, and late gold with bismuth minerals (native bismuth, bismuthinite, **ikunolite**, tellurides and sulphotellurides) in the ores.

Gold in the ores is small and submicroscopic. In {1} gold-skarn and {2} gold-greisen deposits 90% is less than 0.1 mm; in {3} gold and rare-metal quartz vein deposits 60% is less than 0.1 mm. The fineness of gold varies from 400-950 fine. The distribution of gold in the ores is irregular; often type {3} may have bonanza grade ores. Gold resources are small (1-30 tonnes) with average grade 7-15 g/t Au. Gold and rare-metal mineralization was formed at gradational temperatures 200-360 °C and pressures 0.5-2.0 kb from predominantly chloride and relatively concentrated solutions with high arsenic potential in a reduced environment. Geological, mineralogical-geochemical, and thermobar-geochemical data show gold and rare-metal mineralization are genetically related to I-type ilmenite and magnetite series granitoids in collisional and continental margin magmatic arcs.

Lawrence, L.J., Ramsden, A.R. & Munro-Smith, V. 1998 Maldonite and its paragenesis at Kingsgate, New South Wales.

p. 13-18 Journal and Proceedings of the Royal Society of New South Wales Vol. 131

Leppinen, J. & Kontoniemi, O. 1998 Beneficiation study of the Osikonmäki refractory-type gold ore at Rantasalmi, southeastern Finland.

p. 101-110 in Special Paper of the Geological Survey of Finland, Issue 25 in English ISSN 0782-8535

abstract

Osikonmäki is a Paleoproterozoic, epigenetic, tonalite-hosted and shear zone related gold deposit. The ore minerals: pyrrhotite, arsenopyrite, lollingite and chalcopyrite and the accessories: sphalerite, galena and ilmenite or rutile, occur as uneven or banded disseminations throughout the ~3 km long shear zone. Gold or electrum and associated minerals occur as inclusions in and also on the grain boundaries

of sulphide, arsenide and silicate phases. The most common associated minerals are native bismuth, **hedleyite** and **ikunolite**. Beneficiation studies on the refractory-type Osikonmäki ore were carried out with a composite sample made of three subsamples taken from the study pit. Froth-flotation, cyanide leaching and pressure oxidation were used to test the recovery of gold from the ore. In conventional bulk-flotation, gold recovery was only 70% although sulphides and arsenides were almost completely recovered. The arsenic content in the bulk concentrate is 10 - 25%. Depending on the grinding fineness, the maximum recovery of gold by cyanide leaching was 75 - 80%. Pressure oxidation increased gold recovery from the cyanide leaching by 10 - 25%, the maximum recovery then being about 93%. Conventional processes may not provide satisfactory gold recovery or acceptable arsenic content. More sophisticated technologies and/or new process options must therefore be considered in processing the Osikonmäki ore.

Litochleb, J. 1998 Mineralogie zlatonosného zrudnění z dolu Jakub u Kasejovic (jz. Čechy). p. 102-112 in Bulletin mineralogicko-petrografického oddělení Národního muzea v Praze, roč. Vol. 6 [in Czech]

Meinert, L.D. 1998a A review of skarns that contain gold. p. 359-414 in Mineralized porphyry / skarn systems. D.R. Lentz, ed., Min. Assoc. Can. Short Course Series Vol. 26.

Meinert, L.D. 1998b Washington State University Geology 470 Fall Field Trip Guidebook, Oct. 2-4 1998.

Stein, H.J., Morgan, J.W., Markey, R.J., Sundblad, K., Sivoronov, A.A., Bobrov, A.B., Malyuk, B.I. & Pavlun, M.M. 1998 ^{187}Re - ^{187}Os ages for molybdenites from the Archean Maiske [sp. Maiskoe] and Sergeevske Au deposits, Ukraine. p. F-933 in EOS, *Transactions, American Geophysical Union*, v. 79, no. 45 <http://airie.warnercnr.colostate.edu/documents/Publications102007.pdf>

Höy, T. & Dunne, K.P.E. 1999 Geological compilation of the Trail map-area, southeastern British Columbia (082F/3,4,5,6) B.C. Ministry of Energy and Mines B.C. ME&M Geoscience Map 1998-1 colour compilation map at 1:100,000 scale

Ilinca, G. & Makovicky, E. 1999 Bismuth sulphotellurides in the Banatitic Province, Romania. p. 40-41 in International Symposium "Mineralogy in the System of Earth Sciences", Abstract vol., Univ. Bucharest, Romania.

Lefebure, D.V. & Cathro, M. 1999 Plutonic-related gold-quartz veins and their potential in British Columbia. p. 185-221 in Short Course on Intrusion-Related Gold, April 9 1999. pub. Kamloops Exploration Group

Lefebure, D.V., Fournier, M.A. & Jackaman, W. 1999 Prospective Areas in British Columbia for Intrusion - related Gold - Tungsten - Bismuth Veins. Open File 1999-3 B.C. ME&M <http://www.em.gov.bc.ca/Mining/Geolsurv/Publications/OpenFiles/OF1999-03/toc.htm>

Mutschler, F.E., et al., 1999 Giant Porphyry-Related Metal Camps of the World—A Database. U.S. Geological Survey Open-File Report 99-556, Online Version 1.0 <http://geopubs.wr.usgs.gov/open-file/of99-556/>

Third Mineralogical Report detailing the finding of two 'new' gold-associated bismuth sulphotelluride minerals and identifying other opaque minerals, namely native silver electrum **tetradymite** **pilsenite** **hessite** bismuthinite–aikinite pavonite and greenockite characterizing a RIRG system in claim # 516584 and the Bunker Hill & Mormon Girl Crown Grants, on Nox Fort Project south of Salmo in Nelson Mining Division, southernmost British Columbia p. 129

Pratico, V. Oct. 26 1999 Review of the Bunker Hill Area Gold Showings.
12 p. private report for W. Howard

Shimizu, Masaaki, Shimizu, Marina, et al., 1999 **Ingodite** $(\text{Bi,Pb})_2\text{TeS}$, joséite— $\text{A Bi}_4\text{TeS}_2$, galenobismutite PbBi_2S_4 , and lillianite–gustavite solid solution $\sim\text{Ag}_{0.67}\text{Pb}_{1.67}\text{Bi}_{2.67}\text{S}_6$, from mesothermal Cu-Zn-Pb-Bi-Mo-W veins of the Oizawa mine, Tochigi Prefecture, Japan and its ore genesis.
p. 89-101 in Bulletin of the Tochigi Prefectural Museum - Natural History, No. 16. Pub. Tochigi Prefectural Museum, Japan
*Note the formula is written differently; it emphasizes minor Pb may be essential to the **ingodite** structure*

Smith, M., et al., 1999 Geology of the Liese Zone, Pogo property, east central Alaska.
p. 1, 12-21 SEG Newsletter No. 38
abstract

The Liese zone is a recently discovered high-grade gold deposit on the Pogo claims, approximately 90 miles (145 km) southeast of Fairbanks. A conservative geologic resource for the Liese zone is 9.98 million tons at an average grade of 0.52 oz/t, for a total of 5.2 million contained ounces. The region is underlain by highly deformed, amphibolite-grade paragneiss and minor orthogneiss of the Late Proterozoic(?) to middle Paleozoic Yukon-Tanana terrane, which has been intruded by Cretaceous felsic granitoid bodies thought to be related to gold mineralization in the Fairbanks area and elsewhere along the Tintina gold belt. The Liese zone is hosted primarily in gneiss, and lies approximately 1.5 km south of the southern margin of the Late Cretaceous Goodpaster batholith. Mineralization occurs in three or more tabular, gently dipping quartz bodies, designated L1 (uppermost), L2, and L3 (lowermost). The thickness of the quartz bodies ranges from 1 to 20 m, averaging approximately 7 m. The quartz contains approximately 3 percent ore minerals, including pyrite, pyrrhotite, loellingite, arsenopyrite, chalcopyrite, bismuthinite, various Ag-Pb-Bi \pm S minerals, maldonite, native bismuth, and native gold. Early biotite and later quartz-sericite-stockwork and sericite-dolomite alteration are spatially associated with the Liese zone, which shows characteristics of both vein and replacement styles of mineralization. Geochemical data indicate a strong correlation between gold and bismuth, and weaker correlations between gold, silver, and arsenic. Based on U-Pb dating of intrusive rocks, the Liese zone was formed between 107 and 94.5 m.a., although $^{40}\text{Ar} / ^{39}\text{Ar}$ cooling ages on alteration minerals return younger ages of 91 Ma, suggesting a protracted or multiphase thermal history. The Liese zone may represent a deep-seated manifestation of the "intrusion-related" gold deposit type.

Zhao, Yiming, et al., 1999 Geology of gold-bearing skarn deposits in the middle and lower Yangtze River Valley and adjacent regions.
p. 227–249 in Ore Geology Reviews Vol. 14

Brown, R.D. 2000 Selenium, tellurium, and bismuth: Supply, demand, and progress.
p. 307–321 in Minor Elements 2000: Processing and Environmental Aspects of As, Sb, Se, Te, and Bi. ed. C. Young, pub. Society for Mining, Metallurgy and Exploration

Chatterjee, A.K., & Smith, P.K. 2000 Co-existing Electrum, Bismuth, Galena and Plumbian Bismuth Sulfotellurides, Beaver Dam Gold Deposit: Implication for Thermometry of Hydrothermal Veins.
abstract in Mining Matters for Nova Scotia 2000 - Opportunities for Economic Development Report ME 2000-2 ed. D.R. MacDonald Nova Scotia Department of Natural Resources, Mineral Resources Branch
<http://www.gov.ns.ca/NATR/meb/00re2/00re2.htm#08>

Cathro, M.S. & Lefebvre, D.V. 2000 Several New Plutonic-related Gold, Bismuth and Tungsten Occurrences in Southern British Columbia
p. 207-224 in B.C. Ministry of Energy and Mines Geological Fieldwork 1999 Paper 2000-1
http://www.em.gov.bc.ca/DL/GSBPubs/GeoFldWk/1999/GF14_Cathro_207-224.pdf

Third Mineralogical Report detailing the finding of two 'new' gold-associated bismuth sulphotelluride minerals and identifying other opaque minerals, namely native silver electrum **tetradymite** **pilsenite** **hessite** bismuthinite-aikinite pavonite and greenockite characterizing a RIRG system in claim # 516584 and the Bunker Hill & Mormon Girl Crown Grants, on Nox Fort Project south of Salmo in Nelson Mining Division, southernmost British Columbia p. 130

Douglas, N., Mavrogenes, J., Hack, A. & England, R. 2000 The liquid bismuth collector model: an alternative gold deposition mechanism.

p. 135 in Understanding planet Earth; searching for a sustainable future; on the starting blocks of the third millennium. Eds. Skilbeck, C.G. and Hubble, T.C.T. Geological Society of Australia, 15th Australian Geological Convention, Sydney, Abstracts

Flanigan, B., Freeman, C., Newberry, R., McCoy, D. & Hart, C. 2000 Exploration models for mid and Late Cretaceous intrusion-related gold deposits in Alaska and the Yukon Territory, Canada.

p. 591-614 in Cluer, J.K. et al. editors Geology and Ore Deposits 2000: The Great Basin and Beyond Geological Society of Nevada Symposium Proceedings May 15-18 2000

<http://www.avalonalaska.com/pub/TGTpap4web.pdf>

excerpt

"This paper looks at Bi/Au as a function of formation depth and distance from known or suspected causative intrusions. It relates this variable to the gold-associative mineralogy present in the different deposits. The data indicate that the strongest Bi-Au correlation and highest Bi/Au in the Fairbanks district are at Fort Knox, which in relation to other deposits ****is hosted in the largest, deepest-emplaced intrusion; contains the most early higher temperature sheeted and/or stockwork veins****; and has the least shear-hosted gold ore contained in the surrounding schist.

Early high-temperature stockwork veins at the Fort Knox and Dolphin deposits contain the mineral maldonite Au_2Bi as well as wormy Bi-Au intergrowths suggestive of maldonite exsolution. **Because bismuth is nonrefractory as pertains to cyanide, the associated gold is thus highly amenable to cyanide leach.** *This suggests that a high Bi-Au correlation, together with a low arsenic content, may be predictive of ore that is more easily beneficiated".

abstract

"Plutonic-related" gold deposits in Interior and SW Alaska (Tintina Gold Belt) vary significantly in size, grade, vein/deposit morphology, depth of emplacement, distance from causative pluton and metal association. Metal associations such as Au-Bi and Au-As-(Sb-Hg) are a good empirical indicator of the depth of emplacement and distance from causative pluton. These associations have been used successfully in exploration. Results from several analytical techniques also suggest a phenomenological cause for these metal associations. Gold and bismuth have paired mineralogy at high temperatures and, thus, are best correlated (i.e. highly associated) at deposits that are deep and/or close to causative intrusions.

Fuertes-Fuente M., et al., 2000 Preliminary mineralogical and petrological study of the Ortosa Au-Bi-Te ore deposit: a reduced gold skarn in the northern part of the Río Narcea Gold Belt, Asturias, Spain. p. 177-190 in Journal of Geochemical Exploration Vol. 71

Hart, C.J.R., Baker, T. & Burke, M. 2000 New Exploration Concepts for Country-Rock-Hosted, Intrusion-Related Gold Systems: Tintina Gold Belt in Yukon.

p. 145-171 in Tintina Gold Belt: Concepts, Exploration, and Discoveries, Special Volume 2, British Columbia and Yukon Chamber of Mines, Cordilleran Roundup Jan. 2000, eds. T. L. Tucker & M. T. Smith

Howard, W.R. 2000 CLY Group Total Field VLF-EM Geophysical, Soil / Rock Geochemical, and detailed Geologic Surveys, Bunker Hill Mine area, NTS 082F03 W ½ Nelson Mining Division, B.C.

BC MEMPR Assessment Report #26,159

36 pp., 8 fig., 21 drawings, 5 maps and 1 section.

<http://aris.empr.gov.bc.ca/ArisReports/26159.PDF>

Lang, J.R., Baker, T., Hart, C.J.R. & Mortensen, J.K. 2000 An exploration model for intrusion-related gold systems.

p. 1-11 in Society of Economic Geologists Newsletter Vol. 40

Logan, J.M. 2000 Plutonic-Related Gold-Quartz Veins in Southern British Columbia.

p. 193-206 in GF 1999 B.C. MEMPR Paper 2000-1

http://www.em.gov.bc.ca/DL/GSBPubs/GeoFldWk/1999/GF13_Logan_193-206.pdf

McCoy, D.T. 2000 Mid-Cretaceous plutonic-related gold deposits of interior Alaska: metallogenesis, characteristics, gold associative mineralogy and geochronology.

unpub. Ph.D. thesis, University of Alaska, Fairbanks, AK 245 pp.

Meinert, L.D. 2000 Gold in Skarns related to Epizonal Intrusions.

p. 347-375 Chapter 10 in Gold in 2000. Reviews in Economic Geology Vol. 13, pub. SEG

Moore, K.H. 2000 Geology of the gold-bearing L1 and L2 Liese quartz zones, Pogo Deposit, East-Central Alaska.

M.Sc. thesis Colorado School of Mines, Golden CO USA 108 pp.

abstract

"Gold mineralization at Pogo is hosted within the subhorizontal, subparallel L1 and L2 Liese quartz zones, which crosscut Proterozoic to Paleozoic para- and orthogneisses of the Yukon-Tanana terrane. Intrusion of granite and diorite brackets quartz vein emplacement and mineralization between 107 and 94.5 Ma.

Detailed core logging and petrography have identified mappable quartz vein types within the Liese zones. These types have been related to alteration and mineralization through definition of a paragenetic sequence for formation and mineralization of the Liese zones. Formation of the Liese zones consisted of precipitation of granular quartz (Type 1) and then massive white quartz (Type 2A). As the granular quartz is similar in mineralogy to pegmatite bodies and locally displays igneous textures, it is probably related to granitic intrusions. The massive white quartz records a major episode of fracturing and quartz precipitation. Both granular and massive white quartz are accompanied by weak potassic alteration of surrounding wallrocks and were probably initially non-mineralized. The "Liese event" followed emplacement of the granular and massive white quartz veins and includes the following stages:

- 1) precipitation of iron-arsenic sulfides (arsenopyrite, pyrite, and pyrrhotite) along fractures
- 2) formation of ankerite veins with haloes of white mica ("sericite") and precipitation of chalcopyrite, gold, and bismuth
- 3) deformation
- 4) formation of minor base metal veins (sphalerite, galena). Sulfides, ankerite, gold, and bismuth occur in fractures in both granular and massive quartz.

Deformation following stages 1 and 2 resulted in both massive gray, strained quartz (Type 2B) and dark gray to black, recrystallized quartz (Type 3). Type 2B quartz is gradational with massive white quartz (Type 2A). Type 3 quartz forms thin zones that typically follow the lower contacts of the Liese zones. Limited fluid inclusion studies and the presence of abundant carbonate indicate that the fluids responsible for mineralization were probably CO₂ -rich. These fluids appear to have been related to magmatic processes, as evidenced by mineralogical and morphological similarities between the quartz veins and granite and pegmatite bodies, the timing of Liese zone emplacement (postdates peak metamorphism), sulfur isotopic values (around zero per mil), and the strong correlation between gold and bismuth."

Third Mineralogical Report detailing the finding of two 'new' gold-associated bismuth sulphotelluride minerals and identifying other opaque minerals, namely native silver electrum **tetradymite** **pilsenite** **hessite** bismuthinite–aikinite pavonite and greenockite characterizing a RIRG system in claim # 516584 and the Bunker Hill & Mormon Girl Crown Grants, on Nox Fort Project south of Salmo in Nelson Mining Division, southernmost British Columbia
p. 132

Oberthür, T., et al., 2000 Gold mineralization in the Mazowe area, Harare-Bindura-Shamva greenstone belt, Zimbabwe: II. Genetic relationships deduced from mineralogical, fluid inclusion and stable isotope studies, and the Sm-Nd isotopic composition of scheelites.
p. 138-156 in Mineralium Deposita Vol. 35

<http://www.springerlink.com/content/tr78ykhc09reg140/>

"A late association of a number of Bi-minerals is notable in the ores, namely native bismuth, bismuthinite, **tetradymite** ($\text{Bi}_2\text{Te}_2\text{S}$), cosalite ($\text{Pb}_2\text{Bi}_2\text{S}_5$) with distinct Ag contents (0.49-1.95 wt % Ag, $n=10$), **joséite-A** (Bi_4TeS_2) and **ingodite** (Bi_2TeS)", plumbian with analytical formula ($\text{Bi}_{1.476}\text{Pb}_{0.319}\text{Fe}_{0.215}\text{S}_{2.009}\text{Te}_{0.885}\text{S}_{1.100}\text{S}_{1.985}$) (from their Table 2).

Rombach, C.S. 2000 Genesis and Mineralization of the Shotgun Deposit, southwestern Alaska.
p. 181-196 in Tintina Gold Belt: Concepts, Exploration, and Discoveries. Special Volume 2, British Columbia and Yukon Chamber of Mines, eds. T.L. Tucker & M.T. Smith

Smith, M., et al. 2000 Gold mineralization on the Pogo Claims, east-central Alaska.
p. 3 in GSN Newsletter October 2000, Vol. 14, No. 8 pub. Geological Society of Nevada

Thompson, J.F.H. & Newberry, R. 2000 Gold deposits Related to Reduced Granitic Intrusions.
p. 377-400 in 'Gold in 2000' Reviews in Economic Geology Vol. 13, pub. SEG

Baker, T. & Lang, J.R. 2001 Fluid inclusion characteristics of intrusion-related gold mineralization, Tombstone-Tungsten magmatic belt, Yukon Territory, Canada.
p. 563–582 in Mineralium Deposita Vol. 36

Boiron, M.-C., et al., 2001 Geometry and P–V–T–X conditions of microfissural ore fluid migration: the Mokrsko gold deposit (Bohemia).
p. 207–225 in Chemical Geology Vol. 173
<http://linkinghub.elsevier.com/retrieve/pii/S000925410000276X>

Cook, N.J., & Ciobanu, C.L. 2001 Paragenesis of Cu-Fe ores from Ocna de Fier-Dognecea (Romania), typifying fluid plume mineralization in a proximal skarn setting.
p. 351-372 in Mineralogical Magazine, June 2001 Vol. 65 (3)

Gu, X., Watanabe, M., Hoshino, K. & Shibata, Y. 2001 Mineral chemistry and associations of Bi–Te(S,Se) minerals from China.
p. 289-309 in Neues Jahrbuch für Mineralogie – Monatshefte. [N.Jb.Mineral.Mh] Vol. 7 July pub. E. Schweizerbart Science Publishers. Stuttgart Germany ISSN 0028-3649

Höy, T. & Dunne, K.P.E. 2001 Metallogeny and Mineral Deposits of the Nelson-Rossland Map Area: Part II: The Early Jurassic Rossland Group Southeastern British Columbia.
Bulletin 109 B.C. MEMPR 195 pp.
<http://www.em.gov.bc.ca/Mining/Geolsurv/Publications/Bulletins/Bull109/toc.htm>

Lang, J.R. & Baker, T. 2001 Intrusion-related gold deposits: the present level of understanding.
p. 477-489 in Mineralium Deposita Vol. 36

Lang, J.R., et al., 2001 Ch. 2 Tombstone-Tungsten Magmatic Belt.
p. 7-48 in Regional and System-Scale Controls on the Formation of Copper and/or Gold Magmatic-Hydrothermal Mineralization. MDRU Special Publication Number 2, ed. by J. R. Lang. pub. The Mineral Deposit Research Unit at The University of BC

Third Mineralogical Report detailing the finding of two 'new' gold-associated bismuth sulphotelluride minerals and identifying other opaque minerals, namely native silver electrum **tetradymite** **pilsenite** **hessite** bismuthinite–aikinite pavonite and greenockite characterizing a RIRG system in claim # 516584 and the Bunker Hill & Mormon Girl Crown Grants, on Nox Fort Project south of Salmo in Nelson Mining Division, southernmost British Columbia p. 133

Logan, J.M. 2001 Prospective Areas for Intrusion-Related Gold-Quartz Veins in Southern British Columbia.

p. 231-252 in GF 2000, B.C. MEMPR, Paper 2001-1

http://www.em.gov.bc.ca/DL/GSBPubs/GeoFldWk/2000/Logan_p231-252.pdf

Maloof, T.L., et al., 2001 The Dublin Gulch intrusion-hosted gold deposit, Tombstone plutonic Suite, Yukon Territory, Canada.

p. 583-593 in Mineralium Deposita Vol. 36

Mustard, R. 2001 Granite-hosted Gold Mineralisation at Timbarra, northern New South Wales, Australia.

p. 542-562 in Mineralium Deposita Vol. 36

Rombach, C.S. & Newberry, R.J. 2001 Shotgun Deposit: granite-hosted porphyry gold-arsenic mineralization in southwestern Alaska, USA.

p. 607-621 in Mineralium Deposita Vol. 36

Stegman, C.L. 2001 Cobar deposits - Still Defying Classification!

SEG Newsletter Jan. 2001 No. 44

Wagner, T. & Jonsson, E. 2001 MINERALOGY OF SULFOSALT-RICH VEIN-TYPE ORES, BOLIDEN MASSIVE SULFIDE DEPOSIT, SKELLEFTE DISTRICT, NORTHERN SWEDEN

pp. 855-872 in the Canadian Mineralogist Vol. 39

Zachariáš, J., et al., 2001 Geology and Genesis of Variscan porphyry-style gold mineralization, Petráčková hora deposit, Bohemian Massif, Czech Republic.

p. 517-541 in Mineralium Deposita Vol. 36

[http://www.springerlink.com/\(wlbzjl55lfwne3flsbbp4sj55\)/app/home/contribution.asp?referrer=parent&backto=searcharticlesresults,3,3](http://www.springerlink.com/(wlbzjl55lfwne3flsbbp4sj55)/app/home/contribution.asp?referrer=parent&backto=searcharticlesresults,3,3)

Ciobanu, C.L., Cook, N.J. & Sundblad, K. 2002 Genetic insights from exotic trace mineral associations at Orijarvi and Ilijarvi, S.W. Finland.

abstract in International Symposium 'Metallogeny of Precambrian Shields', Sept. 18-20 Kyiv, Ukraine, September 13-26 2002

<http://www.geofuel.lviv.net/MISCEL/MPSab/sab054.htm>

Cook, N.J., Ciobanu, C.L., Nechaev, S.V. & Mudrovskaja, I.V. 2002 Genetic Constraints from Bi-mineral Associations in the Maiskoe Au-Deposit, Ukrainian Shield.

abstract in International Symposium 'Metallogeny of Precambrian Shields', Sept. 18-20 Kyiv, Ukraine, September 13-26 2002

<http://www.geofuel.lviv.net/MISCEL/MPSab/sab048.htm>

"Recent experiments on the partitioning of Au between hydrothermal solutions and liquid bismuth show that, above its melting point (271 °C), liquid Bi is a powerful scavenger for gold from gold-undersaturated hydrothermal solutions, especially when fS_2 is below the pyrrhotite / pyrite buffer (Douglas et al. 2000)... We believe that liquid Bi may scavenge other chalcogenides (e.g. Te) in a comparable way as for Au, precipitating them as blebs of {gold – bismuth tellurides}. The resulting assemblages, in which minerals of the Bi–Te–Se–S system typically have Metal / (Te + S + Se) >1 (e.g. **hedleyite** Bi_7Te_3 , **joséite**–B Bi_4Te_2S and **ikunolite** $Bi_4(S,Se)_3$), are characteristic for Au in which pyrrhotite is the stable sulphide at the time of deposition, not uncommonly also with selenides and other, e.g. Ag, tellurides (Ciobanu & Cook 2002). Similar gold-bismuth tellurides associations occur ... in Au skarns worldwide (Meinert 2000). The presence of gold [with] bismuth tellurides can therefore be considered

Third Mineralogical Report detailing the finding of two 'new' gold-associated bismuth sulphotelluride minerals and identifying other opaque minerals, namely native silver electrum **tetradymite** **pilsenite** **hessite** bismuthinite-aikinite pavonite and greenockite characterizing a RIRG system in claim # 516584 and the Bunker Hill & Mormon Girl Crown Grants, on Nox Fort Project south of Salmo in Nelson Mining Division, southernmost British Columbia p. 134

highly indicative for Au enrichment in deposits in which bismuth can be precipitated at higher temperatures than its melting point, even in the absence of boiling processes (Cook et al. 2002)".

"The absence of maldonite Au_2Bi ... constrains the temperature range for the episode of Au-Bi precipitation from the fluids at between ~ 370-240 °C ... Te-bearing Bi-rich melts crystallize at the point of metallic bismuth stability (271 °C), or closely thereafter ..."

Freeman, C. 2002 (Avalon Development Corp.) SUMMARY REPORT FOR THE SHOTGUN GOLD PROSPECT, KUSKOKWIM MINERAL BELT, ALASKA GEOLOGIC REPORT SH02EXE-1 prepared for (and from) NovaGold Resources Inc. and TNR Resources Ltd.

<http://www.infomine.com/index/pr/Pa101108.PDF>

Hart, C.J., et al., 2002 Geology, Exploration and Discovery in the Tintina Gold Province, Alaska and Yukon.

p. 241-274 in Society of Economic Geologists Special Publication 9 Integrated Methods for Discovery: Global Exploration in the 21st Century

Editors: Goldfarb, R.J. and Nielsen, R.L. ISBN 1-887483-91-8 392 pp.

<http://store.agiweb.org/seg/pubdetail.html?item=SP09>

Jambor, J.L. 2002 New Mineral Names section Bi_2Te , $\text{Bi}_4\text{Te}_2\text{Se}$, $\text{Bi}_6(\text{Te},\text{Se})_3$ (all unnamed).

p. 181-184 in Am. Mineral. Vol. 87

Review of paper by 'X. Gu, M. Watanabe, K. Hoshino, Y. Shibata (2001) Mineral chemistry and associations of Bi-Te(S,Se) minerals from China' p. 289-309 in Neues Jahrb. Mineral. Mon.

Unnamed Bi_2Te

"One of three listed electron microprobe analyses has Bi 75.60, Sb 0.16, Ag 0.03, Fe 0.01, Te 24.01, sum 99.81 wt %, giving Bi / (Te+S) = 1.93; for the other two analyses, the ratio is 2.09 and 2.11, ideally **Bi_2Te** . Grains are 2-10 μm in size, occurring as veinlets along the grain boundaries of **pilsenite** and joséite-B in material from the Huangshaping Pb-Zn polymetallic deposit, about 45 km west of the city of Chengzhou, Hunan Province, China. Bright white color with a yellowish tint in reflected light, distinct birefractance and anisotropism, optically similar to **pilsenite**."

Logan, J.M. 2002a Intrusion-Related Gold Mineral Occurrences of the Bayonne Magmatic Belt.

p. 237-246 in GF 2001, B.C. MEMPR, Paper 2002-1

<http://www.em.gov.bc.ca/DL/GSBPubs/GeoFldWk/2001/17-JL-p237-246.pdf>

Logan, J.M. 2002b Intrusion - Related Mineral Occurrences of the Cretaceous Bayonne Magmatic Belt, Southeast British Columbia (NTS 82/E,F,G,J,K,L,M,N).

Geoscience Map 2002-1

<http://www.em.gov.bc.ca/mining/Geolsurv/bedrock/maponline/dwfs/GM2002-1.htm>

McCoy, D., Newberry, R., Severin, K., Marion, P., Flanigan, B. & Freeman, C. 2002 Paragenesis and metal associations in interior Alaska gold deposits: an example from the Fairbanks district.

p. 33-38 in Mining Engineering Vol. 54 No. 1 also Preprint number 00-036, presented at the SME Annual Meeting, Feb. 28-Mar. 1 2001, Salt Lake City, UT

http://me.smenet.org/200201/pdf/min0201_33.pdf

excerpt

"This paper looks at Bi/Au as a function of formation depth and distance from known or suspected causative intrusions.

It relates this variable to the gold-associative mineralogy present in the different deposits. The data indicate that the strongest Bi-Au correlation and highest Bi/Au ratio in the Fairbanks district are at Fort Knox, which in relation to other deposits * is hosted in the largest, deepest-emplaced intrusion;

contains the most early higher temperature sheeted and/or stockwork veins; and has the least shear-hosted gold ore contained in the surrounding schist.

Early high-temperature stockwork veins at the Fort Knox and Dolphin deposits contain the mineral maldonite (Au_2Bi) as well as wormy Bi-Au intergrowths suggestive of maldonite exsolution. Because bismuth is nonrefractory as pertains to cyanide, the associated gold is thus highly amenable to cyanide leach.

This suggests that a high Bi-Au correlation, together with a low arsenic content, may be predictive of ore that is more easily beneficiated."

abstract

'Plutonic-related' gold deposits in Interior and SW Alaska (Tintina Gold Belt) vary significantly in size, grade, vein/deposit morphology, depth of emplacement, distance from causative pluton and metal association. Metal associations such as Au-Bi and Au-As-(Sb-Hg) are a good empirical indicator of the depth of emplacement and distance from causative pluton.

These associations have been used successfully in exploration. Results from several analytical techniques also suggest a phenomenological cause for these metal associations. Gold and bismuth have paired mineralogy at high temperatures and, thus, are best correlated (i.e. highly associated) at deposits that are deep and/or close to causative intrusions.

Schwarz-Schampera, U., & Herzig, P.M. 2002 Indium: geology, mineralogy, and economics. Springer, Heidelberg, Germany 257 pp.

Rombach, C.S. 2002 Geochemical and geochronological constraints on genesis of gold-bearing quartz veins of the Pogo deposit, east central Alaska.

abstract from segweb.org/AB-Rombach.htm [formerly]:

The Pogo deposit, located ~145 km southeast of Fairbanks, Alaska, consists of Au-As-Bi-Te mineralization in at least two sub-parallel, quartz veins (Liese zones) that cut gneissic units of the Yukon-Tanana terrane. The veins are continuous for as much as 0.8 km along strike, and average ~3.5 m in thickness. The resource estimate is 10.7 Mt at an average grade of 0.52 opt Au, for a total of 5.6 M. oz.

Two main generations of quartz-sulfide veins have been recognized; early, semi-ductile, planar veins and later, brittle, fracture-hosted veins. Arsenopyrite, pyrite, and pyrrhotite are the most common sulfides, typically forming about 3 vol. % of the veins. Although gold occurs within and proximal to sulfides, it is commonly observed as discrete grains in quartz with Bi-minerals. ...Petrographic and electron microprobe investigations show that:

- 1) arsenopyrite compositions yield a range of formation temperatures from 350-650 °C;
- 2) **tetradymite** and **pilsenite** are associated with gold of 780-879 fineness;
- 3) joséite-B is associated with gold of >930 fineness and temperatures >400 °C; and
- 4) native bismuth, bismuthinite, **hedleyite**, maldonite, and several unknown bismuth telluride minerals are also present. ...

Rombach, C.S., Newberry, R.J., Goldfarb, R. & Smith, M. 2002 Geochronology and Mineralization of the Liese Zones, Pogo Deposit, Alaska.

The Geological Society of America (GSA) 2002 Denver Annual Meeting (October 27-30 2002) Session No. 52

http://gsa.confex.com/gsa/2002AM/finalprogram/abstract_45183.htm

abstract

Checked ✓ occur on central Nox Fort in surface samples, 9 of 13 minerals:

"The Pogo deposit, located 145 km east of Fairbanks in east-central Alaska, consists of Au-As-Bi-Te mineralization in four or more stacked, sub-parallel, low-angle, shear zone-hosted, quartz veins (termed Liese zones) that cut Paleozoic and older gneiss and schist of the Yukon-Tanana terrane. The current

resource estimate is 10.7 Mt at an average grade of 0.52 oz/t, for a resource of 5.6 M. oz Au. Liese quartz veins contain ~3% sulfide minerals (arsenopyrite-pyrite-pyrrhotite) [all in Lefevre skarn ✓], with the majority as linear bands that are sub-parallel to the vein-wallrock contact and define multiple fluid pulses. The bismuth-gold mineralogy includes (in order of abundance): joséite-B ($\text{Bi}_4\text{Te}_2\text{S}$) ✓, gold (fineness 850-1000) ✓, **tetradymite** ($\text{Bi}_2\text{Te}_2\text{S}$) ✓, **pilsenite** (Bi_4Te_3) ✓, native bismuth Bi ✓, bismuthinite (Bi_2S_3) ✓, **ingodite** (BiTeS) ✓, **hedleyite** (Bi_7Te_3) ✓, sulphotsumoite ($\text{Bi}_3\text{Te}_2\text{S}$), joséite-A (Bi_4TeS_2) ✓, maldonite (Au_2Bi), tsumoite (BiTe), and baksanite ($\text{Bi}_6\text{Te}_2\text{S}_3$).

Measured arsenic compositions of arsenopyrite vary from 30.4-37.2 atomic %; most are 35-37. The high-arsenic arsenopyrites occur with loellingite and pyrrhotite ($T = 450\text{-}600\text{ }^\circ\text{C}$). The low-arsenic arsenopyrites occur with pyrite ($T = <450\text{ }^\circ\text{C}$).

Along with evidence for some arsenopyrites in disequilibrium with pyrite, and alteration of pyrrhotite to pyrite and marcasite [yes], these data indicate a change from very low $f\text{S}_2$ and/or high T (loellingite-pyrrhotite stable) to higher $f\text{S}_2$ and/or lower T (pyrite stable) over time.

Fluid inclusions in quartz from the main Liese veins are low salinity, liquid- and vapor-rich aqueous ($T_h = 174\text{-}247\text{ }^\circ\text{C}$; 2-5 wt% NaCl eq.), saline aqueous ($T_h = 188\text{-}348\text{ }^\circ\text{C}$; 14-18 wt% NaCl eq.), and aqueous-carbonic ($T_h = 140\text{-}340\text{ }^\circ\text{C}$; 3-46 mol% $\text{CO}_2 \gg \text{CH}_4$). Several extension veins that splay off of the Liese veins contain more saline inclusions ($T_h = 175\text{-}328\text{ }^\circ\text{C}$; 30-34 wt% NaCl eq.), with one or two daughter minerals and coexisting inclusions that exhibit properties of pure CH_4 . (Note T_h is uncorrected for pressure). MoS_2 ✓ from the Liese vein has a Re/Os age of 104 Ma, which is 5-12 Ma younger than the age of last metamorphism (U-Pb, zircon) and constrained by Ar/Ar (hornblende) and U-Pb (zircon) ages of nearby intrusions (~107 Ma and 95-92 Ma). Biotites from intrusions, gneiss, and wall rock in quartz yield Ar/Ar ages of ~92 Ma, presumably due to thermal reset from the former intrusions.

Ariunbileg, S., et al., 2003 Significant Metalliferous and Selected Non-Metalliferous Lode Deposits, and Selected Placer Districts of Northeast Asia.

U.S. Geological Survey Open-File Report 03-220

<http://pubs.usgs.gov/of/2003/of03-220/>

Baker, T. 2003a Intrusion-related Gold deposits: Explorable Characteristics. Gold Short Course at Cordilleran Exploration Roundup Jan. 26 2003. 10 pp.

Baker, T. 2003b Intrusion related gold deposits; Classification, characterization and exploration: Society of Economic Geologists Regional VIP Lecturer Presentation

http://www.smedg.org.au/jul03BakerSEG_files/frame.htm

Bindi, L. & Cipriani, C. 2003 Plumbian baksanite from Tyrnyauz W-Mo deposit, Baksan River valley, northern Caucasus, Russian Federation.

p. 1475-1479 in Can. Mineral. Volume 41, Number 6

<http://pubs.nrc-cnrc.gc.ca/mineral/tcm-147541-6.html>

Baksanite is ideally $\text{Bi}_6\text{Te}_2\text{S}_3$. "A sample of Pb-rich baksanite was recovered in a magnetite-andradite skarn from the Tyrnyauz W-Mo deposit, in the northern Caucasus ... Russian Federation. Associated minerals are bismuthinite, **tetradymite**, joséite-A and **ingodite**; gangue minerals are calcite and andradite".

Caron, L., M.Sc., P. Eng. 2003 Technical Report on the BURNT BASIN PROPERTY, BOUNDARY DISTRICT, NTS 82E/1, Lat: 49° 10' 00"N Long: 118° 07' 30"W (at approximate centre of property), Greenwood Mining Division, British Columbia Canada.

Prepared for: Newport Gold Inc. 43 pp.

Ciobanu, C.L. & Cook, N.J. 2003 Tellurides and/or selenides in Au-ores: Examples from Shield and orogenic areas.

Extended abstract in Uzbekistan Gold 2003: 'Problems of Ore Deposits and Maximizing Prospecting Efficiency'. Tashkent, Uzbekistan, 21st - 24th October 2003

http://www.ngu.no/igcp486/Gold_enrichment_and_Bi-mineral_assemblages_in_ores.htm

...telluride speciation can be readily predicted from the local redox environment at the time of crystallisation, as reflected by the observed host minerals. Modelling of trace mineralogy can therefore assist in identifying formation conditions and deposition during processes characterised by abrupt changes in physical-chemical fluid parameters.

Investigations have allowed construction of a qualitative diagram for stability of Bi tellurides in fS_2 - fO_2 space, on the basis of Bi / (Te + Se + S) ratios. This diagram has implications for discriminating overprinting events in metamorphosed terranes within shield areas, with emphasis on the behaviour of Au during remobilisation and associated Au enrichment. Bi-tellurides / tellurosulphides, in particular, are commonly found closely associated with gold, due to their incorporation within bismuth melt at temperatures >295 °C. They may thus occur in association with native bismuth, Au and/or maldonite, reinforcing experimental work showing that Bi melt acts as a powerful 'scavenger' for Au in ore-forming systems, especially when buffered by evolving fS_2 / fO_2 conditions. The overall composition of the melt / fluids and the resultant Bi-tellurides and selenides, and their Bi / (Te + Se + S) ratios, reflect the reducing / oxidizing character of the melts / fluids that introduced or modified them.

Ciobanu, C.L., Cook, N. & Pring, A. 2003 Gold Enrichment and Bi-mineral Assemblages in ores: examples from Shield and Orogenic areas.

Geophysical Research Abstracts, Vol. 5, 13549, 2003 European Geophysical Society

<http://www.cosis.net/abstracts/EAE03/13549/EAE03-J-13549.pdf>

Part of abstract:

"A systematic study of the distribution of bismuth tellurides / selenides in gold-enriched ores from 25 deposits in the Fennoscandian / Ukrainian Shields and in European Phanerozoic orogenic belts allows comparison of telluride [mineral] speciation and association and **construction of a qualitative diagram for bismuth telluride stability in fugacity S_2 - fugacity O_2 space on the basis of Bi^{42} / (Te + Se + S) {abbreviated $R_{Bi/Te}$ }**. Tsumoite (the mineral $BiTe$) stability separates reducing environments where bismuth tellurides with $R_{Bi/Te} > 1$ are associated with native Bi and maldonite Au_2Bi , and oxidizing environments where bismuth tellurides with $R_{Bi/Te} < 1$ are associated with Au–Ag-bearing tellurides and native tellurium. Bismuth tellurides / selenides are closely associated with gold, due to incorporation within bismuth melt above 271° C. Such melts are powerful "scavengers" for gold, especially at the main fS_2 / fO_2 buffers. Overall compositions of Bi–Te–Se–Au melts, as seen in resultant bismuth telluride/selenide [mineral] associations, reflect the reducing or oxidizing character of source fluids. Telluride speciation has implications for discriminating overprinting events, with focus on local gold-enrichment at metamorphic peaks, during retrograde stages in skarn and secondary boiling in porphyry, irrespective of age or deposit type. ..."

Cook, N.J. & Ciobanu, C.L. 2003 Telluride and selenide mineralogy as a tool in understanding gold deposits.

Extended abstract in Uzbekistan Gold 2003: 'Problems of Ore Deposits and Maximizing Prospecting Efficiency'. Tashkent, Uzbekistan, 21st - 24th October 2003

http://www.ngu.no/igcp486/Telluride_and_selenide_mineralogy_as_a_tool_in_understanding_gold_dep osits.html

extract:

"Non-stoichiometry and disordering of Bi and Te atoms in the structure appears a common and characteristic feature of tsumoite (also nevskite, **ingodite**). The implications for interpretation of analyses in the extended Bi–S–Te and Bi–S–Te–Se systems are therefore considerable. ... Tellurides,

⁴² includes Pb content

Third Mineralogical Report detailing the finding of two 'new' gold-associated bismuth sulphotelluride minerals and identifying other opaque minerals, namely native silver electrum **tetradymite** **pilsenite** **hessite** bismuthinite-aikinite pavonite and greenockite characterizing a RIRG system in claim # 516584 and the Bunker Hill & Mormon Girl Crown Grants, on Nox Fort Project south of Salmo in Nelson Mining Division, southernmost British Columbia p. 138

selenides and related compounds are good tracers of fO_2 / fS_2 buffered reactions during ore formation (e.g. magnetite-hematite, pyrrhotite-pyrite)."

Dilworth, K., Ebert, S., Mortensen, J. & Tosdal, R. 2003 Gold-bearing quartz veins related to reduced intrusions at the 4021 Prospect, Goodpaster district, east-central Alaska.

Chapter 3, unpublished M.Sc. thesis by Katherine Dilworth, The University of British Columbia 2003 p. 167-218 Ch. 4-2 in Intrusive Gold Final Report. pub. MDRU Vancouver BC

Ebert, S., Dilworth, K., et al., 2003 Quartz veins and gold prospects in the Goodpaster Mining district. p. 256-281 Ch. 4-5 in Intrusive Gold Final Report. pub. MDRU Vancouver BC

Gamyanin, G.N., Goryachev, N.A., Bakharev, A.G., et al., 2003 Genesis and Evolution of Gold-bearing Granitoid Magmatic Systems in the Mesozoids of Northeast Asia. (Magadan, 2003) [in Russian]

Hart, C.J.R. & Burke, M. 2003 The Tombstone Gold Belt: An Emerging Gold Camp.

Yukon Geological Survey Yukon Energy, Mines and Resources

72 x 48 inch poster

http://geology.gov.yk.ca/publications/miscellaneous/placemats/tombstone_placemat.pdf

Hein, J.R., et al., 2003 Global occurrence of tellurium-rich ferromanganese crusts and a model for the enrichment of tellurium.

p. 1117–1127 in *Geochimica et Cosmochimica Acta*, Vol. 67 No. 6

doi:10.1016/S0016-7037(00)01279-6

http://walrus.wr.usgs.gov/reports/reprints/Hein_GCA_67.pdf

Jensen, P.W., Odden, J., Frantz, P.S. & Newberry, R. 2003 The Gil Hornfels Gold System, Fairbanks District, Alaska.

In Mining Infrastructure – A Key to Alaska's Mineral Future, abstracts of Alaska Miners Association 2003 Annual Convention

<http://www.alaskaminers.org/abstracts2003.pdf>

Kennedy, C. 2003 Assessment Report Rock Geochemistry Program CLY Property NTS Map sheets 082F.004 - 082F.003.

BC MEMPR Assessment Report #27,231

<http://aris.empr.gov.bc.ca/ArisReports/27231.PDF>

Logan, J.M. 2003 Kena Mountain Gold Zone, Southern British Columbia.

p. 133-152 in *Geological Fieldwork 2002*, B.C. Ministry of Energy, Mines and Petroleum Resources,

Paper 2003-1 http://www.em.gov.bc.ca/DL/GSBPubs/GeoFldWk/2002/11_JLp133-152.pdf

Logan, J.M., Laflamme, G. & Dandy, L. 2003 Kena Gold Mountain Zone - Early Middle Jurassic Porphyry Au +/- Cu Mineralization, SE British Columbia.

GeoFile 2003-6 poster

<http://www.em.gov.bc.ca/DL/GSBPubs/GeoFile/GF2003-6/GF2003-6.pdf>

Cannon, B. 2004 The Skarns of Washington State.

p. 8-9 in September 2004 Bulletin of Friends of Mineralogy, Pacific Northwest Chapter

http://www.pnwfm.org/newsletters/PNWFM_newsletter_0409.pdf

Third Mineralogical Report detailing the finding of two 'new' gold-associated bismuth sulphotelluride minerals and identifying other opaque minerals, namely native silver electrum **tetradymite** **pilsenite** **hessite** bismuthinite–aikinite pavonite and greenockite characterizing a RIRG system in claim # 516584 and the Bunker Hill & Mormon Girl Crown Grants, on Nox Fort Project south of Salmo in Nelson Mining Division, southernmost British Columbia p. 139

Cook, N.J. & Ciobanu, C.L. 2004 Bismuth tellurides and sulphosalts from the Larga hydrothermal system, Metaliferi Mts., Romania: Paragenesis and genetic significance. pp. 301–321 in Mineralogical Magazine, April 2004 Vol. 68 (2)

Giroux, G. & Dandy, L. 2004 Technical Report Preliminary Resource Calculations for Gold Mountain and Kena Gold zones, Kena Property, BC for Sultan Minerals Inc. [using 43-101 guidelines]

Jackaman, W. & Höy, T. 2004 Gold Exploration, Rossland-Nelson Area, Southeastern B.C. p. 195 - 198 in GF 2004, Paper 2004-1 BC Ministry of Energy and Mines
<http://www.em.gov.bc.ca/DL/GSBPubs/GeoFldWk/2003/18-Jackaman-195-198-w.pdf>
INAA gold-in-stream-sediment data is colour-gridded at a regional scale.

Klapotke, T.M. & Crawford, M.J. 2004 "Tellurium" in Chemistry: Foundations and Applications.

Mudrovskaya, I., Cook, N.J., Ciobanu, C.L., et al., 2004 Bi-Tellurides and Orogenic Gold: Examples from the Ukrainian Shield.

Poster Presentation in session: "G14.07 - Telluride and selenide minerals related to gold- and platinum-group element deposits" 32nd Int. Geol. Congr., Florence Italy, 2004 electronic version posted on-line on July 20, 2004, Abstract. Vol., part 54, abstract 54-29

<http://www.32igc.info/igc32/search/>

From abstract

In the low-sulphide Mayske [sp. Maiskoe] gold deposit "Scavenging of Au by Bi melt above 271°C (the Bi melting point) is evident. Temperatures ~266 °C are indicated by paired Bi–telluride associations with Bi / (Te + S) > 1 [e.g. **hedleyite**–joseite–Bi; native bismuth–**ikunolite**], representing binary eutectics in the Bi–Te–(S) system. This can be correlated with pyrrhotite inversion and late pyrite formation. An increase in fS_2 triggered Bi–Au–Te droplet precipitation."

Ray, G.E. 2004 Assessment Report on the Geology & Mineral Potential of the CLY 1 & 2 Claims (including the Bunker Hill & Mormon Girl Crown Grants), southeastern BC, Canada (NTS 082F03).

BC MEMPR AR #27,513 Includes Map 1 Geology of part of the Bunker Hill Claims 1:5,000 scale & Map 2 Geology of part of the Bunker Hill Claims 1:2,000 scale

<http://aris.empr.gov.bc.ca/ArisReports/27513.PDF>

Ren Yunsheng, Liu Liandeng, Wan Xiangzong, & Chen Guohua 2004 Relationship between bismuth minerals and gold mineralization in skarn-type gold deposits in the Shizishan Orefield, Tongling, Anhui, China.

p. 41-45 in Kuangwu Yanshi = Journal of Mineralogy and Petrology Vol. 24 no. 2 ISSN 1001-6872. in Chinese with English Summary:

"Located in the Shizishan orefield, both Baocun and Chaoshan gold deposits are of the skarn type. Bismuth minerals and their relationship with gold mineralization are studied by reflecting light microscope and electron microscope. The results show that native bismuth and bismuthinite are the main bismuth minerals in the two mines. As the main minerals holding native gold [they] closely coexist with native gold. The correlation coefficient of Bi and Au is 0.69 in the Baocun deposit, which proves the close paragenetic relationship between bismuth minerals and gold mineralization. The decreasing of fS_2 , due to phase separation of ore-forming fluid, may cause maldonite to separate into gold and bismuth.

Rombach, C.S., McCoy, D.T., Newberry, R.J. & Smith, M. 2004 Telluride-bearing deposits of the Tintina Gold Province, Alaska: Investigations of the Fort Knox and Pogo gold deposits.

Oral Presentation in session: "G14.07 - Telluride and selenide minerals related to gold- and platinum-group element deposits" 32nd Int. Geol. Congr., Florence Italy, 2004 electronic version posted on-line on July 20, 2004, Abstract. Vol., part 54, abstract 54-11

<http://www.32igc.info/igc32/search/>

abstract

The Fort Knox (~5 M. oz) and Pogo (~6 M. oz) gold deposits are located in the Tintina Gold Province in interior Alaska. Mineralization at Fort Knox occurs in pegmatite, stockwork, and sheeted veins in a granite stock, while Pogo is comprised of several, sub-parallel, shear-hosted, quartz veins in schist and gneiss. Both of these deposits contain telluride minerals in close association with gold mineralization. Despite the different deposit styles, the telluride mineralization at both deposits consists of Bi-tellurides and -sulfotellurides. Au-Ag tellurides are notably absent. The deposits share a reduced geochemistry ($\text{CO}_2\text{-CH}_4$) and are arsenopyrite-bearing (rare at Fort Knox), thus allowing an estimate of Temperature- $f\text{S}_2$ conditions through the mineral paragenesis.

Fort Knox contains early joséite–A, joséite–B, and **tetradymite (S-enriched)** with an arsenopyrite-pyrite assemblage (300-490 °C), >900 gold finesses, and feldspathic alteration (other phases include native bismuth, maldonite, and bismuthinite). Only joséite–A is found among the later arsenopyrite-pyrite assemblage (<380 °C), <900 fineness electrum, and sericitic alteration. Native bismuth is commonly coated with bismuthinite.

Pogo is host to numerous telluride minerals, typically as composite grains. Early joséite–B, sulphotsumoite, native bismuth, **hedleyite**, **ingodite**, and **pilsenite** occur with an arsenopyrite - loellingite \pm pyrrhotite assemblage (450-600 °C), and 850-1000 fineness gold (other phases include maldonite, K-feldspar, and Mn-siderite). This is followed by joséite–B, **tetradymite**, tsumoite, and **ingodite** with an arsenopyrite-pyrite assemblage (350-500 °C), and 850-950 fineness gold.

Later **tetradymite (S-enriched)**, bismuthinite (Sb-bearing), joséite–B, joséite–A, **ingodite** and various (Ag-Bi-Sb-Pb) sulfosalts are found with pyrite (no arsenopyrite) and < 850 fine electrum. Variably Sb-rich bismuthinite commonly corrodes or rims other Bi-mineral grains. This and the texture of composite grains imply disequilibrium among the telluride minerals.

At both deposits, these observations suggest that the telluride mineralogy changes in kind with the gold composition, and the sulfide-alteration assemblages. ★In general, paragenetically early, high temperature, and very low $f\text{S}_2$ (loellingite-pyrrhotite stable), native bismuth, Bi-telluride and S-poor sulfotelluride assemblages yield to late, lower temperature, higher relative $f\text{S}_2$ (pyrite stable) S-rich sulfotelluride, Sb-bearing bismuthinite and sulfosalt assemblages

Ciobanu, C.L., Cook, N.J., Sundblad, K. & Kojonen, K. 2004 Tellurides and selenides in Au ores from the Fennoscandian Shield: a status report.

Poster Presentation in session: "G14.07 - Telluride and selenide minerals related to gold- and platinum-group element deposits" 32nd Int. Geol. Congr., Florence Italy, 2004 electronic version posted on-line on July 20, 2004, Abstract. Vol., part 54, abstract 54-12

<http://www.32igc.info/igc32/search/>

from abstract

Bi / (Te + S + Se) ratios of BTS indicate reduced (>1) or oxidised (<1) fluids. Our compilation suggests that orogenic-Au fluids in greenstone belts and gneissic terrains are predominantly oxidised, with the exception of Au in the Svecofennian Domain ... with VHMS deposits. ...**Telluride speciation respects regional and temporal trends.**

Third Mineralogical Report detailing the finding of two 'new' gold-associated bismuth sulphotelluride minerals and identifying other opaque minerals, namely native silver electrum **tetradymite** **pilsenite** **hessite** bismuthinite–aikinite pavonite and greenockite characterizing a RIRG system in claim # 516584 and the Bunker Hill & Mormon Girl Crown Grants, on Nox Fort Project south of Salmo in Nelson Mining Division, southernmost British Columbia p. 141

Rhys, D. & Lewis, P. Jan. 2004 Short Course 'Gold Vein Deposits: Turning Geology into Discovery' BC& Yukon Chamber of Mines Cordilleran Exploration Round-up Jan. 24 – 25, Vancouver B.C. 190 p.

Schroeter, T.G., Pardy, J.W. & Cathro, M. June 2004 Significant British Columbia Porphyry Cu-Au Resources.

BC MEMPR GeoFile 2004-11

<http://www.em.gov.bc.ca/mining/Geolsurv/Publications/GeoFiles/Gf2004-11/toc.htm>

Sejkora J., Litochleb J., Černý P. & Ozdín D., 2004 Bi-Te minerálna asociácia zo Župkova (Vtáčnik, Slovenská republika).

p. 303-315 in Mineralia Slovaca Vol. 36, 3-4 (in Slovak with English abstract)

Shedd, K.B. 2004 Tungsten in USGS Minerals Yearbook – 2004

<http://minerals.usgs.gov/minerals/pubs/commodity/tungsten/tungsmbyb04.pdf>

Shin, D., Park, H.I., Lee, I., Lee, K.S. & Hwang, J., 2004 Hydrothermal arsenic and bismuth mineralization in the Nakdong deposits, South Korea: Fluid inclusion and stable isotope studies.

p. 1465-1481 in The Canadian Mineralogist Vol. 42

Baker, T., Pollard, P.J., Mustard, R., Mark, G. & Graham, J.L. 2005 A comparison of granite-related tin, tungsten, and gold-bismuth deposits: implications for exploration.

Society of Economic Geologists Newsletter, No. 61 p. 5-17

Ciobanu, C.L., Cook, N.J. & Pring, A. 2005 Bismuth tellurides as gold scavengers.

p. 1383-1386 in Mao, J.W., Bierlein, F.P. (eds.) Mineral Deposit Research: Meeting the Global Challenge, pub. Springer Berlin-Heidelberg-New York, 1613 pp. ISBN13: 9783540279457

Cook, N.J. & Ciobanu, C.L. 2005 Tellurides in Au deposits: Implications for modeling.

p. 1387-1390 in Mao, J.W., Bierlein, F.P. (eds.) Mineral Deposit Research: Meeting the Global Challenge, pub. Springer Berlin-Heidelberg-New York, 1613 pp. ISBN13: 9783540279457

Hart, C.J.R., Mair, J.L., Goldfarb, R.J. & Groves, D.I. 2005 Source and redox controls on metallogenic variations in intrusion-related ore systems, Tombstone-Tungsten Belt, Yukon Territory, Canada.

pp. 339-356 in Transactions: Earth Sciences Vol. 95 No. 1-2. pub. Royal Society of Edinburgh.

Gaspar, L.M.G.G. 2005 The Crown Jewel gold skarn deposit.

Ph.D. thesis, Washington State University

Golebiowska, B., Pieczka, A., & Parafiniuk, J. 2005 Minerals of the Bismuthinite – Aikinite Series from Rędziny (Western Sudetes).

pub. Mineralogical Society of Poland – Special Papers Vol. 26, 2005

<http://www.geo.uw.edu.pl/PTMINSP/2005/167.pdf>

At Rędziny in Poland hydrothermal polymetallic mineralization occurs in the Rędziny dolostones quarry several hundred meters distant from the Karkonosze granite intrusion. Dolomitic marbles in schist are intruded by Hercynian granites. Within arsenopyrite-quartz-chlorite veins "Besides dominating arsenopyrite and cassiterite ... chalcopyrite, pyrite, pyrrhotite, sphalerite, galena, various Pb, Bi(Sb), Cu and Ag sulphosalts, and others [occur]. ... In the polymetallic veins another type of aikinite can also be found, occurring in the form of large grains reaching 1 mm and associated with a slightly different association (chalcopyrite, bismuth, Bi sulphides). In the outer parts of such aikinite grains as well as in

Third Mineralogical Report detailing the finding of two 'new' gold-associated bismuth sulphotelluride minerals and identifying other opaque minerals, namely native silver electrum **tetradymite** **pilsenite** **hessite** bismuthinite-aikinite pavonite and greenockite characterizing a RIRG system in claim # 516584 and the Bunker Hill & Mormon Girl Crown Grants, on Nox Fort Project south of Salmo in Nelson Mining Division, southernmost British Columbia p. 142

their fractures were found tiny inclusions of bismuthinite, **ikunolite** and bismuth with sizes not exceeding 10 µm." These crystallized at ~ 270-260 °C.

Gvozdev, V.I. & Tsepin, A.I. 2005 Bismuth Mineralization in the Ores of the Vostok-2 Deposit (Primor'ye Region, Russia).

pp. 132-145 in Geology of Ore Deposits Vol. 47 No. 2, March-April 2005

<http://www.maiconline.com/maik/showArticle.do?pii=S1075701505020030>

abstract

"The ore composition was studied in the underground workings (levels 720–560 m) at the Vostok-2 skarn scheelite–sulfide deposit. These ores are similar to those that have been mined from the open pit. Bismuth, lead, silver, gold, tellurium, and selenium are extracted from the ores. The ores with an increased content of these metals consist of galena, native Bi and Au, kobellite, Bi-containing jamesonite, **tetradymite**, and some other minerals.

Some new minerals for the deposit were found with electron microprobe analysis: jaskolskiite, cosalite with a high Sb content, **ikunolite**, **hessite**, bismuth sulfotellurides (joseite group), sulfotellurides with complex composition (with Pb and Ag), and some others. The relation between minerals, the chemical composition of minerals, and some problems of the zonation and genesis of the Pb–Sb–Bi mineralization are discussed."

Ren, Yunsheng, Liu, Liandeng & Zhang, Huihuang 2005 Gold deposits rich in bismuth minerals: An important type of gold deposits.

Ch. 5-16 in Mao, J.W., Bierlein, F.P. (eds.) Mineral Deposit Research: Meeting the Global Challenge, pub. Springer Berlin-Heidelberg-New York, 1613 pp. ISBN13: 9783540279457

abstract

"Several gold deposits both in China and abroad [have] abundant bismuth minerals. [They are] structurally controlled, with gold or rich in bismuth minerals most of which are major gold-bearing minerals. ...there is a prominent positive correlation of Au with Bi".

Goldfarb, R. of USGS, Denver Colorado

Nov. 2005 email re XRD Identification of **ingodite** in Eloise vein: "the signature in the area of obvious Bi mineralization is a very distinct Bi-Te-S signature with no trace of other species. The XRD analysis indicated **ingodite**, bismuthinite, and, yes, native bismuth. Also, although not 100% certain, there is likely a trace of **tetradymite**."

Hart, C.J.R. 2005 Classifying, Distinguishing and Exploring for Intrusion-Related Gold Systems.

p.1, 4-9 in Issue 87 'The Gangue' newsletter of GAC Mineral Deposits Group

<http://www.gac.ca/SECTIONS/GANGUE/Gang87.pdf>

Hart, C.J.R. & Goldfarb, R. 2005 Short Course 'Orogenic vs. Intrusion-Related gold' with emphasis on Yukon and Alaska deposits.

Minerals South 2005 Conference Oct. 25 - 27 2005, Cranbrook BC

Howard, W.R. 2005 BiTel Knoll Mineralized Rock Geochemical Survey on CLY Group, Bunker Hill Mine Area, Salmo Sheet NTS 082F03 W ½, Nelson Mining District B.C. 2005 Assessment Report.

70 pp., includes 2 maps, 21 tables, 19 figs., 5 appendices. BC Assessment Report #27,893

<http://aris.empr.gov.bc.ca/ArisReports/27893.PDF>

Lefebure, D. & Hart, C. 2005 Plutonic-Related Au Qtz Veins & Veinlets 'L02'

B.C. Mineral Deposit Profiles

http://www.geology.gov.yk.ca/metallogeny/mineral_deposit_profiles/of2005_5/l02_plutonic_related_au_quartz_veins_and_veinlets.pdf

Third Mineralogical Report detailing the finding of two 'new' gold-associated bismuth sulphotelluride minerals and identifying other opaque minerals, namely native silver electrum **tetradymite** **pilsenite** **hessite** bismuthinite–aikinite pavonite and greenockite characterizing a RIRG system in claim # 516584 and the Bunker Hill & Mormon Girl Crown Grants, on Nox Fort Project south of Salmo in Nelson Mining Division, southernmost British Columbia p. 143

Meinert, L.D., Dipple, G.M. & Nicolescu, S. 2005 World Skarn Deposits.
p. 299-336 in Economic Geology 100th Anniversary Volume
Editors J.W. Hedenquist, J.F.H. Thompson, R.J. Goldfarb and J.P. Richards
ISBN 978-1-887483-01-8 1146 pp.
<http://store.agiweb.org/seg/pubdetail.html?item=EG100Ann>

Nokleberg, W.J., et al., 2005 Geology and Nonfuel Mineral Deposits of Greenland, Europe, Russia, and Northern Central Asia.
USGS Open File Report 2005–1294D
<http://pubs.usgs.gov/of/2005/1294/d/of2005-1294d.pdf>

Rumsey, M. & Savage, M. 2005 The First British Occurrence of Parkerite at North Devon United Mine, Peter Tavy, Devon.
in UK Journal of Mines and Minerals vol. 25
<http://www.ukjmm.co.uk/no25.htm>
abs

A complex assemblage of minerals including arsenopyrite, cobaltite, chalcopyrite, scheelite, bismuth, erythrite, quartz, fluorite, stannite, bismuth, bismuthinite, aikinite, cosalite, gersdorffite, **ikunolite** and various bismuth-bearing supergene minerals is present on the dumps of the North Devon United Mine at Peter Tavy, Devon. The rare nickel bismuth sulphide parkerite (ideally $\text{Ni}_3\text{Bi}_2\text{S}_2$) has been identified as grains up to 50 μm across in quartz-fluorite veinstone associated with sphalerite, ullmannite, bismuth, bismite, gersdorffite, an unknown lead copper sulphide selenide and cassiterite. Quantitative analyses record significant substitution of antimony for bismuth and include the most highly antimonian parkerite composition yet described, with 5.3 wt. % Sb. This is the first report of parkerite in the British Isles.

Shin, D.B., Lee, C.H. & Lee, K.S. 2005 Occurrence and mineral chemistry of bismuth sulfide–telluride–selenide solid solutions (**ingodite**, joséite, and unnamed phase) in the Nakdong deposit, South Korea.
p. 293-333 in Neues Jahrbuch für Mineralogie - Abhandlungen, Vol. 181, No. 3
<http://www.ingentaconnect.com/content/schweiz/njma/2005/00000181/00000003/art00008>
abstract

“Bismuth sulfide – telluride – selenide solid solutions, such as **ingodite** $\text{Bi}_2(\text{S},\text{Te})$, joséite–A Bi_4TeS_2 , selenian joséite–B $\text{Bi}_4(\text{Te},\text{Se},\text{S})_3$, and an **unnamed phase** $\text{Bi}_2(\text{Te},\text{Se})$ were formed during the As–Bi mineralization in the Nakdong deposits, South Korea.

Ingodite, a rarely reported mineral, has the general composition $(\text{Bi}_{1.94}\text{Sb}_{0.01}\text{Ag}_{0.04})\text{sum}_{1.99}(\text{Te}_{1.03}\text{Se}_{0.03}\text{S}_{1.08})\text{sum}_{2.14}$, which is regarded as **Te-rich ingodite** [No – Te and S are almost same, one *apfu*]. Compiled data of previous work indicates that joséite–A from the Nakdong deposits extends its compositional range toward joséite–B and there still remains an obvious compositional gap in the range of 19.7-24.6 atomic % S + Se and 16.4-21.9 atomic % Te between the two phases.

Selenian joséite–B has an intermediate compositional range between $\text{Bi}_4\text{Te}_2\text{S}$ and $\text{Bi}_4\text{Te}_2\text{Se}$ through the exchange between S and Se. The unnamed phase $\text{Bi}_{1.97}\text{Sb}_{0.02}\text{Te}_{0.83}\text{Se}_{0.12}\text{S}_{0.01}$, with constant Bi / (Te + Se + S) ratio close to 2 but variable Te / (Se + S) ratio from 5.7 to 8.2, is placed in the compositionally intermediate range between the **two unnamed phases of Bi_2Te and $\text{Bi}_2(\text{Te},\text{Se})$** of Gu et al. (2001). Coexistence of native bismuth with joséite–B and the unnamed phase constrains their formation temperature below 266 °C.”

Törmänen, T.O. & Koski, R.A. 2005 Gold Enrichment and the Bi-Au Association in Pyrrhotite-Rich Massive Sulfide Deposits, Escanaba Trough, Southern Gorda Ridge.
pp. 1135-1150 in Economic Geology Vol. 100

Third Mineralogical Report detailing the finding of two 'new' gold-associated bismuth sulphotelluride minerals and identifying other opaque minerals, namely native silver electrum **tetradymite** **pilsenite** **hessite** bismuthinite–aikinite pavonite and greenockite characterizing a RIRG system in claim # 516584 and the Bunker Hill & Mormon Girl Crown Grants, on Nox Fort Project south of Salmo in Nelson Mining Division, southernmost British Columbia p. 144

Borisenko, A.S., et al., 2006 Stages of formation of gold mineralization in the Central Viet Nam. In Journal of Geology, Series B, No. 28 pub. Department of Geology and Minerals of Vietnam http://www.idm.gov.vn/nguon_luc/Xuat_ban/2006/B28/b71.htm excerpt

“... the porphyry Cu-Mo (Au), gold-skarn, gold-sulfide-quartz, gold-silver, Mo-W (Cu, Bi) greisen and tungsten types of mineralization are related to the Triassic metallogenic stage... example the Khâm Đức ore cluster... . The ore bodies and zones at the Đắk Ripen and Đắk Roong deposits, at the Sa Thầy porphyry Cu-Mo (Au) and Ngọc Tụ Cu-Mo-W-Bi occurrences ...is characterized by the geochemical specialization which is expressed in the increased Bi and Te content in all types of ores, Mo and W in ores from gold-ore deposits, Au in Mo-W (Cu, Bi) greisen and porphyry Cu-Mo (Au). For gold mineralization tellurides, bismuthinite, native bismuth, **ikunolite**, rosvietite (AuBiS – a new mineral established by the authors from the Đắk Ripen deposit), scheelite and molybdenite are mineral forms for Bi, Te, Mo and W.”

Caron, L., M.Sc., P.Eng. Oct. 3 2006 CLY Property, NTS 82F/02, Salmo Area, SE British Columbia. Evaluation Report for Kinross Gold Corp. 9 p. + 2 p. tables + map

Cepedal, A., et al., 2006 Tellurides, selenides and Bi-mineral assemblages from the Río Narcea Gold Belt, Asturias, Spain: genetic implications in Cu–Au and Au skarns. p. 277-304 in Mineralogy and Petrology, pub. Springer Wein, Austria Vol. 87 Nos. 3-4 <http://www.springerlink.com/content/75nu845m52639t6m/?p=3781d1a8625a44748a00f69f13250f45&pi=5>

Summary

Gold ores in skarns from the Río Narcea Gold Belt are associated with Bi-Te-(Se) -bearing minerals. These mineral assemblages have been used to compare two different skarns from this belt, a Cu–Au skarn (calcic and magnesian) from the El Valle deposit, and a Au-reduced calcic skarn from the Ortosa deposit ... In Ortosa deposit gold essentially occurs as native gold and maldonite and is commonly related to pyrrhotite and to the replacement of löllingite by arsenopyrite, indicating lower fO_2 conditions for gold mineralization than those for El Valle deposit. This fact is confirmed by the speciation of Bi-tellurides and selenides (**hedleyite**, joséite–B, joséite–A, **ikunolite**–laitakarite) with $Bi / Te + (Se + S) \geq 1$. “At the Ortosa deposit, the typical assemblage (native bismuth–gold–**hedleyite**–joséite–B) limits the conditions ... within the pyrrhotite stability field. The $PbTe$ – PbS reaction constrains the fTe_2 and fS_2 values due to the presence of galena and the absence of altaite [$PbTe$]. The occurrence of **hessite**, bismuthinite and joséite–A may indicate an increase in fS_2 as suggested by the replacement of pyrrhotite by pyrite.”

Chang, Zhaoshan, et al., 2006 Caijiaying Mine, Hebei, China: An unusual Zn-Au deposit. abstract 2006 Australian Earth Sciences Convention 2006, Melbourne, Australia <http://www.earth2006.org.au/papers/new1aug/extendedabstracts/Chang%20Zhaoshan.pdf>

Ciobanu, C.L., Cook, N.J., Damian, F. & Damian, G. 2006a Gold scavenged by bismuth melts: An example from Alpine shear-remobilizates in the Highiş Massif, Romania. p. 351–384 in Mineralogy and Petrology, Austria Vol. 87 June 2006 Nos. 3-4 pub. Springer Wien, <http://www.springerlink.com/content/n4k06883534195qr/?p=3781d1a8625a44748a00f69f13250f45&pi=8>

Summary

Gold mineralization occurs in the Şoimuş Iliei vein, the main Cu prospect in the Highiş Massif, Western Apuseni Mtns., Romania. The Highiş Massif is part of the Highiş Biharia Shear Zone, a 320–300 Ma Variscan greenschist belt, with a 114–100 Ma Alpine overprint. In Highiş, phyllonites enclose an igneous core consisting of an Early Permian basic complex intruded by Middle Permian granitoids. The vein is hosted within basalt hornfels at its contact with the 264 Ma Jernova granite. Gold is not only

present as native gold, but also as jonassonite (ideally AuBi_5S_4). The latter occurs as inclusions 1-30 μm in size in chalcopyrite; microanalysis gives the empirical formulae $\text{Au}_{1.02}(\text{Pb}_{0.47}\text{Bi}_{4.51})_{4.98}\text{S}_4$. The two Au minerals are spatially associated with Bi-(Pb) sulfosalts (over substituted bismuthinite, cosalite) and sulfotellurides / selenides (**ingodite**, **ikunolite** and laitakarite) in blebs/patches, mainly hosted in chalcopyrite. This Au-Bi-Te association overprints an earlier, chalcopyrite-quartz assemblage, occurring as trails along discrete zones of brecciation that crosscut former mineral boundaries. Curvilinear and cusped boundary textures within the blebs/patches suggest deposition in a molten form. Mineral associations in combination with phase relations indicate that the Au-Bi-Te association formed as a result of melting of pre-existing native bismuth Bi (and possibly sulfosalts) at 400 °C under sulfidation conditions. These melts incorporated Au, Pb, Te and S as they moved in the vein during shearing and were locked within dilational sites. Native Bi occurs as coarse aggregates along vein margins, but in the Au-Bi-Te association, it is present only as small droplets in shear gashes, never together with other Bi- and Au-minerals. The Bi-derived melts are part of an internal remobilizate which also includes chlorite and adularia. Minerals in the system Au-Bi-Te were deposited from a neutral low reducing fluid during Alpine shearing in the Early Cretaceous. The fluid also assisted solid-state mobilisation of chalcopyrite and cobaltite. This study illustrates the significant potential of Bi, a low melting-point chalcophile element (LMCE), to act as Au scavenger at temperatures as low as 400 °C.

Ciobanu, C.L., Cook, N.J., Pring, A., Brugger, J., Netting, A. & Danushevskiy, L. 2006b LA-ICP-MS Evidence for the role of Bi-Minerals in Controlling Gold Distribution in Ores. Extended abstract Aug. 23 2006 in Session I-4 Au-Ag-Te-Se deposits: modern methods of studying their genesis, 12th Quadrennial IAGOD Symposium - 2006 'Understanding the Genesis of Ore Deposits to meet the demands of the 21st Century'. Moscow, Russia, 21-24 August 2006

Cook, N.J. & Ciobanu, C.L. Nov. 12 2006 Short report on electron probe microanalysis on samples [from BiTel Knoll veins] 2 p. In Part II of Howard 2008

Cook, N.J. & Ciobanu, C.L. 2006 Mineralogical investigation of polished sections from CLY Group, Southeastern B.C., Canada – Prelim. Report. 9 p. with colour plates Aug. 10 2006 [Part II of Howard 2006a AR]

Dunning, G.E. 2006 Ag-Cu-Pb-Bi Sulfosalts New to Darwin, Inyo County, California. Axis, Vol. 2 No. 4 www.MineralogicalRecord.com

Gloaguen, E. 2006 Apports d'une étude intégrée sur les relations entre granites et minéralisations filoniennes (Au et Sn-W) en contexte tardi orogénique (Chaîne Hercynienne, Galice centrale, Espagne). Contribution of an integrated study to the relationships between vein-type deposits (Au and Sn-W) in late orogenic settings (Hercynian belt, central Galicia, Spain).

PhD thesis Université d'Orléans France 574 pp.

From abstract

"Mineralizations were formed in favour of mechanical instabilities developed on top of the granite. Indeed, granites play a thermal, rheological and also chemical role in ore concentration, as the nature of the granite infers the nature of the mineralization (i.e., Au or Sn-W)."

From 2003 paper "The Bruès gold deposit takes place on the top of the two-mica Boborás 'G3' granite intruding Palaeozoic mica schists. The set of parallel ENE-WSW trending gold bearing veins is focused on the west dipping granite-mica schist contact."

Giroux, G., P.Eng., & Grunenberg, P., P.Geo. 2006 Sultan Minerals Ltd. news release Nov. 8 2006

Third Mineralogical Report detailing the finding of two 'new' gold-associated bismuth sulphotelluride minerals and identifying other opaque minerals, namely native silver electrum **tetradymite** **pilsenite** **hessite** bismuthinite–aikinite pavonite and greenockite characterizing a RIRG system in claim # 516584 and the Bunker Hill & Mormon Girl Crown Grants, on Nox Fort Project south of Salmo in Nelson Mining Division, southernmost British Columbia p. 146

Gołębiowska B., Pieczka A., Parafiniuk J. 2006 Cu(Ag)-Pb-Bi(Sb) sulphosalts from Rędziny (Western Sudetes, Poland).

Mineralogia Polonica - Special Papers, vol. 28, 78-80

Hart, C.J.R. 2006 Tombstone Gold Belt.

YGS brochure 2006-6, two 11x17" pages

Yukon Geological Survey Yukon Energy, Mines and Resources

http://www.geology.gov.yk.ca/publications/brochures/explorationists/ygs_brochure_6_tombstone_gold_belt.pdf

Hein, K.A.A., et al., (2006) Linking mineral and fluid inclusion paragenetic studies: The Batman deposit, Mt. Todd (Yimuyn Manjerr) goldfield, Australia.

Ore Geology Reviews Vol. 28 p. 180–200

Howard, W.R. 2006a Assessment Report Part I: 'Rare to exceptionally rare Gold-associated Bi–Te–S–(Se) ore minerals new to Canada: **ingodite** **ikunolite** **unnamed Bi₂Te** associated with **hedleyite** **joséite–A** **joséite–B** native gold...' 93+ pp. 2 tables, 8 figs., 1 map. Part II: 'Mineralogical investigation of polished sections from CLY Group, Southeastern B.C., Canada – Preliminary Report' by N. Cook and C. Ciobanu, 11 pp., Aug. 10 2006.

2006a Assessment Report – Mineralogical research. AR #28,748

95+ pp., 2 tables, 9 figs., map.

<http://aris.empr.gov.bc.ca/ArisReports/28748.pdf>

Howard, W.R. 2006b Assessment Report 'Geochemistry and Structural Geology of Reduced Intrusion Related gold [RIRG] showings on CLY Group claim # 516584, notably the Pogo-like Eloise Vein and the Fort Knox-like Clarissa Sheeted Veins on BiTel Knoll and the five Clease Quartz Veins and Shears. Auriferous bismuth telluride-bearing mineralization including especially rare **ingodite** **ikunolite** **unnamed Bi₂Te** **hedleyite** **joséite–B** and **joséite–A**, with native gold grains native bismuth and bismuthinite defining deposit type L-02 'Plutonic-Related Au Quartz Veins & Veinlets' in Salmo Sheet NTS 082F03 W 1/2, Nelson Mining Division B.C.'

2006b Assessment Report – Geochemistry and Structural Geology. AR #28,749

129+ pp., 11 tables, 24 figs., 3 maps.

<http://aris.empr.gov.bc.ca/ArisReports/28749.pdf>

Howard, W.R. 2006c Letter report to L. Caron 'CLY Group Au–Bi–Te prospect – List of Five Exploratory Drill Targets' (six as Adit 1 Gallery Quartz Vein added)

Howard, W.R. 2006d Letter to G. Schellenberg, B.Sc. Geol., President TNR Gold Corp. March 6 2006 11 p.

Baker, T., Ebert, S., et al., 2006 Chemical Compositions of Fluid Inclusions in Intrusion-Related Gold Systems, Alaska and Yukon, Using PIXE Microanalysis.

pp. 311–327 in Economic Geology, Vol. 101

Mair, J.L., Goldfarb, R.J., Johnson, C.A., Hart, C.J.R. & Marsh, E.E. 2006 Geochemical Constraints on the Genesis of the Scheelite Dome Intrusion-Related Gold Deposit, Tombstone Gold Belt, Yukon, Canada.

p. 523–553 in Ec. Geol. Vol. 101

<http://econgeol.geoscienceworld.org/cgi/reprint/101/3/523>

Third Mineralogical Report detailing the finding of two 'new' gold-associated bismuth sulphotelluride minerals and identifying other opaque minerals, namely native silver electrum **tetradymite** **pilsenite** **hessite** bismuthinite–aikinite pavonite and greenockite characterizing a RIRG system in claim # 516584 and the Bunker Hill & Mormon Girl Crown Grants, on Nox Fort Project south of Salmo in Nelson Mining Division, southernmost British Columbia p. 147

Mustard, R., Ulrich, T., Kamenetsky, V.S. & Mernagh, T. 2006 Gold and metal enrichment in natural granitic melts during fractional crystallization.

p. 85-88 in *Geology*, Vol. 34 No. 2

<http://eprints.comp.utas.edu.au:81/archive/00000304/01/Geology-Timbarra.pdf>

Paar, W.H., Putz H., Roberts, A.C., Stanley, C.J., & Culetto, F.J. 2006 Jonassonite, Au(Bi,Pb)₅S₄, a new mineral species from Nagybörzsöny, Hungary.

p. 1127-1136 in *Can. Mineral.* vol. 44 no. 5 DOI: 10.2113/gscanmin.44.5.1127

<http://canmin.geoscienceworld.org/cgi/content/abstract/44/5/1127>

Roberts, S. et al. 2006 Sm-Nd and REE Characteristics of Tourmaline and Scheelite from the Björkdal Gold Deposit, Northern Sweden: Evidence of an Intrusion-Related Gold Deposit?

p. 1415-1425 in *Econ. Geol.*, Vol. 101

Yudovskaya, M.A. 2006 Gaseous transport and deposition of gold in magmatic fluid: evidence from the active Kudryavy volcano, Kurile Islands.

pp. 828–848 in *Miner Deposita* Vol. 40

Zachariáš, J., Morávek, P. & Pertoldová, J. 2006 The Mokrsko-West gold deposit in the Bohemian Massif, Czech Republic: mineralogy, structure and classification.

unpub. V 5.0 draft, English edited by W. Howard

Caron, L. M.Sc., P.Eng. April 13 2007 Memo 'Proposed Work Program and Budget – CLY Property' a private report for Wm. R. Howard, 3 p.

Chen, Yan-Jing, et al., 2007 Geodynamic settings and tectonic model of skarn gold deposits in China: An overview

139–169 in *Ore Geology Reviews* Vol. 31

Cook, N.J., Ciobanu, C.L., Stanley, C.J., Paar, W.H. & Sundblad, K. 2007a Compositional data for Bi-Pb tellurosulfides.

p. 417-435 in *Can. Mineral.* vol. 45 no. 3 DOI: 10.2113 /gscanmin.45.3.417

<http://canmin.geoscienceworld.org/cgi/content/abstract/45/3/417>

Cook, N.J., Ciobanu, C.L., Wagner, T. & Stanley, C.J., 2007b Minerals of the system Bi-Te-Se-S related to the tetradymite archetype: review of classification and compositional variation.

p. 665-708 in *Can. Mineral.* vol. 45 no. 4 DOI: 10.2113/gscanmin.45.4.665

<http://canmin.geoscienceworld.org/cgi/content/abstract/45/4/665>

Cook, N.J., Ciobanu, C.L. & Howard, W. 2007c Bi-tellurides in gold veins, BiTel Knoll (CLY prospect), southeastern British Columbia, Canada.

p. 31-37 in Kojonen, K., Cook, N.J. & Ojala, V.J. (eds.) 2007: Au-Ag telluride-selenide deposits. pub. Geological Survey of Finland, Guide 53. 94 pp., 62 figs. and 14 tables.

Proceedings volume of Field Workshop of IGCP-486, Espoo Finland August 26-31 2007

in Part II below

<http://arkisto.gtk.fi/op/op53.pdf>

Third Mineralogical Report detailing the finding of two 'new' gold-associated bismuth sulphotelluride minerals and identifying other opaque minerals, namely native silver electrum **tetradymite** **pilsenite** **hessite** bismuthinite-aikinite pavonite and greenockite characterizing a RIRG system in claim # 516584 and the Bunker Hill & Mormon Girl Crown Grants, on Nox Fort Project south of Salmo in Nelson Mining Division, southernmost British Columbia p. 148

Cook, N.J., Ciobanu, C.L. & Spry, P.G. 2007d What makes a Gold-telluride deposit?
GSA Denver Annual Meeting 28–31 October 2007 Paper #72-1
Session No. 72 Au-Ag-Te-Se Deposits and Other Precious Metal Deposits
pub. Geological Society of America Abstracts with Programs, Vol. 39 No. 6 p. 196
http://gsa.confex.com/gsa/2007AM/finalprogram/abstract_131060.htm

de Graff, M.L.D. 2007 Minerals of Russia
<http://maurice.strahlen.org/>

Dilworth, K.M., Mortensen, J.K., Ebert, S., Tosdal, R.M., Smith, M.T., & Roberts, P. 2007 Cretaceous reduced granitoids in the Goodpaster Mining District, east central Alaska.
pp. 1347-1373 in Canadian Journal of Earth Sciences, Vol. 44, No. 9 September 2007
“Limited data indicate granitoid emplacement at 5-9 km depths, consistent with formation of the auriferous quartz veins based upon published fluid inclusion data.”

Hart, C.J.R. 2007 Reduced intrusion-related gold systems.
p. 95-112 in Mineral deposits of Canada: A Synthesis of Major Deposit Types, District Metallogeny, the Evolution of Geological Provinces, and Exploration Methods.
Ed. Goodfellow, W.D., Geological Association of Canada, Mineral Deposits Division, Special Publication No. 5

Howard, W. 2007 Structural setting and geochemical correlations in bismuth (sulfo)telluride - native gold-bearing veins, CLY group, British Columbia, Canada: A reduced intrusion-related gold system.
p. 45-50 in Kojonen, K., Cook, N.J. & Ojala, V.J. (eds.) 2007: Au-Ag telluride-selenide deposits. pub. Geological Survey of Finland, Guide 53. 94 pp., 62 figs. and 14 tables.
Proceedings volume of Field Workshop of IGCP-486, Espoo Finland August 26-31 2007
<http://arkisto.gtk.fi/op/op53.pdf>

Howard, W., Cook, N.J. & Ciobanu, C.L. 2007 Telluride assemblages in a Reduced Intrusion-Related Gold (RIRG) Deposit, CLY Group prospect, southeastern British Columbia, Canada.
GSA Denver Annual Meeting 28–31 October 2007 Paper #72-4
Session No. 72 Au-Ag-Te-Se Deposits and Other Precious Metal Deposits
pub. Geological Society of America Abstracts with Programs, Vol. 39 No. 6 p. 196
http://gsa.confex.com/gsa/2007AM/finalprogram/abstract_130211.htm In Part III below

Tooth, B.A, Brügger, J., Liu, W. & Ciobanu, C.L. 2007 Modelling Melts in Hydrothermal Systems – The Liquid Bismuth Collector Model.
GSA Denver Annual Meeting 28–31 October 2007 Paper #72-4
Session No. 72 Au-Ag-Te-Se Deposits and Other Precious Metal Deposits
pub. Geological Society of America Abstracts with Programs, Vol. 39, No. 6, p. 196
http://gsa.confex.com/gsa/2007AM/finalprogram/abstract_127915.htm

Petrov, A. 2006-2007 Encyclopedia of Japanese Minerals
© Petrov Rare Minerals
<http://www.petrovrareminerals.com/articles02i.html>

Rodionov, S.M., et al., 2007 Appendix C – Summary of Major Metallogenic Belts for Northeast Asia (Russian Far East, Yakutia, Eastern Siberia, Transbaikalia, Northern China, Mongolia, South Korea, and Japan).
USGS Open-File Report 2007-1183-Appendix C.
http://pubs.usgs.gov/of/2007/1183/appendix-c/of2007-1183_appendix-c.pdf

Third Mineralogical Report detailing the finding of two 'new' gold-associated bismuth sulphotelluride minerals and identifying other opaque minerals, namely native silver electrum **tetradymite** **pilsenite** **hessite** bismuthinite–aikinite pavonite and greenockite characterizing a RIRG system in claim # 516584 and the Bunker Hill & Mormon Girl Crown Grants, on Nox Fort Project south of Salmo in Nelson Mining Division, southernmost British Columbia p. 149

Sidorov, V. A., Volkov A. V., Wolfson, A.A. 2007 Au–Bi–Te Mineralization of the Kontaktovyi Stock in Northeast Russia.

pp. 1164–1168 in Doklady Earth Sciences Vol. 417 No. 8, ISSN 1028-334X ©Pleiades Publishing, Ltd., 2007 DOI:10.1134/S1028334X07080065

U.S. Geological Survey, January 2007 Mineral Commodity Summaries

p. 36 -37 'BISMUTH'

<http://minerals.usgs.gov/minerals/pubs/commodity/bismuth/bismumcs07.pdf>

U.S. Geological Survey, January 2007 Mineral Commodity Summaries

p. 166-167 'TELLURIUM'

<http://minerals.usgs.gov/minerals/pubs/commodity/selenium/tellumcs07.pdf>

Ciobanu, C.L., et al., 2008 Chemical-structural modularity in the tetradymite group: a HRTEM study. Paper accepted by Amer. Miner.

Howard, W. 2008 Continuing Mineralogical Research on rare to exceptionally rare gold-associated Bi–Te–S–(Se) ore minerals new to Canada ... in claim # 516584, central CLY Group, Salmo map sheet NTS 082F03 W1/2, Nelson Mining Division, southernmost British Columbia. 2007 Assessment Report – Research on Mineral Compositions.

Kaye, C., Challiner, G. & Inwood, N. 2008 Readdressed Technical Report Peak Mine New South Wales, Australia. Prepared by Mine and Quarry Engineering Services, Inc. Readdressed to GPJ Ventures Ltd. (Peak Gold) & others. US Securities & Exchange Commission Form 6-K

Krivitskaya, N.N., et al., 2008 Jonassonite AuBi_5S_4 : The First Find in Transbaikalia.

pp. 576–579 in, Doklady Earth Sciences Vol. 420 No. 4. ISSN 1028-334X ©Pleiades Publishing, Ltd., 2008

Oberthür, T. & Weiser, T.W. 2008 Gold-bismuth-telluride-sulphide assemblages at the Viceroy Mine, Harare-Bindura-Shamva greenstone belt, Zimbabwe.

p. 953-970 in Mineralogical Magazine Vol. 72 No. 4 Dec. 2008

DOI 10.1180/minmag.2008.072.4.953

abstract

"Gold mineralization at the Viceroy Mine is hosted in extensional veins in steep shear zones that transect metabasalts of the Archaean Arcturus Formation. The gold mineralization is generally made up of banded or massive quartz carrying abundant coarse arsenopyrite. However, most striking is a distinct suite of Au-Bi-Te-S minerals, namely joséite–A (Bi_4TeS_2), joséite–B ($\text{Bi}_4\text{Te}_2\text{S}$), **hedleyite** (Bi_7Te_3), **ikunolite** (Bi_4S_3), 'protojoseite' (Bi_3TeS), an unnamed mineral ($\text{Bi}_6\text{Te}_2\text{S}$), bismuthinite (Bi_2S_3), native Bi, native gold, maldonite (Au_2Bi), and jonassonite (AuBi_5S_4).

The majority of the Bi-Te-S phases is characterized by Bi / (Se + Te) ratios of <1. Accordingly, this assemblage formed at reduced conditions at relatively low $f\text{S}_2$ and $f\text{Te}_2$. Fluid-inclusion thermometry indicates depositional temperatures of the main stage of mineralization of up to 342 °C, in the normal range of mesothermal, orogenic gold deposits worldwide. However, melting temperatures of Au-Bi-Te phases down to at least 235 °C (assemblage maldonite + native Bi + **hedleyite**) imply that the Au-Bi-Te phases have been present as liquids or melt droplets. Furthermore, the close association of native gold, native bismuth and other Bi-Te-S phases suggests that gold was scavenged from the hydrothermal fluids by Bi-Te-S liquids or melts. It is concluded that a liquid/melt-collecting mechanism was probably active at Viceroy Mine, where the distinct Au-Bi-Te-S assemblage either formed late as part of the main, arsenopyrite-dominated mineralization, or it represents a different mineralization event, related to

rejuvenation of the shear system. In either case, some of the gold may have been extracted from pre-existing, gold-bearing arsenopyrite by Bi-Te-S melts, thus leading to an upgrade of the gold ores at Viceroy. The Au-Bi-Te-S assemblage represents an epithermal-style mineralization overprinted on an otherwise mesothermal (orogenic) gold mineralization.

KEYWORDS: gold mineralization, bismuth-tellurides-sulphides, Archaean, Viceroy and Mazowe Mines, Zimbabwe, Passagem de Mariana Mine, Brazil"

Parafiniuk, J, Pieczka, A. & Golbiowska, B. 2008 Compositional data for **ikunolite** from Rędziny Rudawy Janowickie, Lower Silesia, Poland

p. 1305-1315 Can. Mineral. Vol. 46 No. 5 DOI: 10.3749/canmin.46.5.1305

"The chemical composition of **ikunolite** and the distribution of Se among various sulfides and sulfosalts at Rędziny, in the metamorphic cover of the Variscan Karkonosze pluton, in Lower Silesia, Poland, have been documented by electron-microprobe analysis. At Rędziny, selenium becomes concentrated at the lower-temperature stages of mineralization. Its main carrier is **ikunolite**, $\text{Bi}_4(\text{S},\text{Se})_3$, with Se contents up to ca. 11 wt %. Some grains of Ag-bearing galena and aikinite also may be enriched in Se (above 1 wt %). The chemical composition of **ikunolite** shows a wide variability, never reported from any other locality. Results of our analyses document a full range of Se-for-S substitution in **ikunolite** and the existence of a complete solid-solution series from the sulfur end-member to a composition with a S:Se ratio ca. 1:1. According to data available in the literature, **ikunolite** also forms a continuous solid-solution series with laitarite, $\text{Bi}_4(\text{Se},\text{S})_3$. Some **ikunolite** compositions reveal substantial amounts of Pb substituting for Bi, in the range 0–0.46 apfu. One sample has the composition $\text{PbBi}_3(\text{S},\text{Se})_3$, indicating a compositional trend towards babkinite, $\text{Pb}_2\text{Bi}_2(\text{S},\text{Se})_3$ "

Keywords: **ikunolite**, selenium, Se-for-S substitution, Pb-for-Bi substitution, Rędziny, Poland.

Saleken, L.W. PGeo. Goldcliff Resource Corporation (GCN.TSXV) new release May 20 2008: 'HIGH-GRADE GOLD MINERALS IDENTIFIED AT BONANZA TRENCH'

Vikent'eva, O.V., et al., 2008 Finding of Matildite in Veins of the Berezovsk Gold Deposit, Ural Mountains.

pp. 5–8 in Doklady Earth Sciences, 2008, Vol. 418 No. 1 ISSN 1028-334X ©Pleiades Publishing, Ltd., 2008

Pieczka, A., Gołbiowska, B. & Parafiniuk, J. 2009 Formation conditions of polymetallic mineralization in the eastern envelope of the Karkonosze granite: the case of Rędziny, southwestern Poland. Can. Mineral. 47 (in press).

Korostelev, P.G., et al., no date. Some features of ore matter composition in Tin Deposits of Khingan-Olonoi (sp. Olono) District (Russia).

Far East Geological Institute of RAS

<http://www.fegi.ru/FEGI/sbornik2/art10/art10.htm>

(©2001-2005 Mineral Data Publishing, version 1)

<http://handbookofmineralogy.org/pdfs/ingodite.pdf>

mindat.org - the mineral and locality database <http://www.mindat.org/index.php>

Minerals of Hungary Herman Ottó Museum, Exhibition Building

Papszer Street 1, H-3530 Miskolc Hungary Post - P.O. Box 4, H-3501 Miskolc Hungary

http://www.mineral.hermuz.hu/nyito_a.htm#teteje

[END REFERENCES]

Third Mineralogical Report detailing the finding of two 'new' gold-associated bismuth sulphotelluride minerals and identifying other opaque minerals, namely native silver electrum **tetradymite** **pilsenite** **hessite** bismuthinite–aikinite pavonite and greenockite characterizing a RIRG system in claim # 516584 and the Bunker Hill & Mormon Girl Crown Grants, on Nox Fort Project south of Salmo in Nelson Mining Division, southernmost British Columbia

p. 151

Part II Mineralogical report on the CLY property

Dec. 11 2008 by Nigel J. Cook (Prof.) Natural History Museum (Geology section), University of Oslo, Oslo Norway. 94 pp.

A photograph of a light-colored, fractured rock surface, likely limestone or marble, showing a network of cracks and small-scale folding. The rock is covered with dry, brown pine needles and some green moss. A geological hammer with a wooden handle and a black head is positioned diagonally in the lower right corner, providing a sense of scale. The text "Mineralogical report on the CLY property" is overlaid in yellow in the center of the image.

Mineralogical report on the CLY property

Nigel J. Cook (Prof.)
Natural History Museum
University of Oslo, Norway

Contents

Summary	page 1
Objectives and methodology	page 2
Descriptions of polished sections:	
Lefevre skarn workings	page 3
Bunker Hill mine veins	page 28
M-01 Moly Quartz Vein	page 49
Blue Quartz Vein	page 52
Cleave 0446 shear vein	page 64
Laser ablation analysis of Fe sulphides for ‘invisible gold’ in samples L-11 from the Lefevre workings and BHUS-01 from Adit 1 of the Bunker Hill mine	page 68
Eloise Vein	page 71
Conclusions and recommendations	page 89
References	page 91

Summary

Polished sections were prepared with the aim of investigating ore mineralogy, by optical and scanning electron methods, in a number of representative samples from different ore types on the CLY property. The sample suite represents skarns and veins from the Lefevre skarn workings, the Bunker Hill mine veins, Moly Quartz Vein, Blue Quartz Vein, Cleave 0446 shear-vein and Eloise Vein.

Visible gold is widely distributed within the studied samples, typically as small (<50 µm) to very small (<10 µm) grains of variable fineness. The strong geochemical and mineralogical association between gold and bismuth noted in previous reports is maintained. Gold occurs together with a number of bismuth tellurides (most commonly joséite-B, joséite-A, hedleyite, unnamed Bi₂Te), as well as bismuthinite, and, rarely, also with native bismuth. There is only a weak correlation between the volume of sulphide in the sample and the abundance of gold grains; there is, however, a much stronger correlation between the gold and tellurium contents. Most observed gold occurs within quartz, often combined with the Bi-bearing phases.

In total, the observations made during these course of these investigations do not contradict a RIRG (reduced intrusion-related gold)-type model for the deposit. All observations can be explained within this model, albeit with abundant evidence for a superimposed event that has led to sulphidation of some assemblages, and likely local-scale redistribution of gold. Moreover, the observations, particularly those relating to the presence of gold together with bismuth minerals in all parts of the deposit, show that CLY represents a single mineralised system, with mineralization consisting of both veins and skarns, all closely tied to the granite which is the likely source of metals.

The observations confirm my earlier opinion that the property is interesting from a scientific as well as economic perspective, in that it represents an archetypal example of a RIRG deposit. This study, and any others that follow, can help increase understanding of how such mineralised systems form, and how gold may be distributed within them.

Further exploration work is enthusiastically recommended in order to better establish geological relationships below surface and to identify potential ore volumes and gold reserves. Although minor quantities of base metals are present (notably Zn in skarn) and the tungsten mineral scheelite is also identified, CLY remains, in my opinion, a gold target.

A small number of laser ablation analyses of pyrite shows that refractory or “invisible gold” within the sulphides is negligible and that the arsenic content of the ores (with the exception of minor arsenopyrite) is also low.

Objectives and methodology

The objectives of the study were to identify the major, minor and trace minerals present, with emphasis on the mineralogical distribution of gold, and on the distribution and speciation of bismuth minerals with which gold is commonly paragenetically associated in the mineralisation on the CLY property. This information can provide useful information about the genesis of the deposit and its evolution. In turn, improved genetic models will help local-scale exploration. Focus was also placed on comparing the ore mineralogy in different locations on the property, which would enable connections to be drawn between them. In addition, information on ore textures and gangue mineralogy was to be given. This can also be used to support the models. The mineralogy of the deposit has been investigated in the context of a working model for the deposit as a reduced intrusion-related gold deposit (Hart, 2007).

After the samples were shipped to Oslo, they were cut with a diamond saw and circular pieces mounted into one-inch epoxy blocks using standard routines, and polished using diamond paste to 0.1 μm . It was attempted to prepare sections from parts of the sample that contained visible ore minerals.

Polished blocks were investigated using a reflected light microscope at the Natural History Museum (University of Oslo) using air-immersion objectives (5, 10, 20, 40x magnifications). The microscope is fitted with a digital camera.

Scanning electron microscopy was undertaken using the Hitachi E-SEM at Natural History Museum (University of Oslo) under vacuum and carbon-coating the samples. Most of the investigation was conducted using back-scattered imaging. The instrument is equipped with an Oxford Instruments wavelength-dispersive spectrometer allowing minerals to be identified and analysed. While the data quality is slightly less than using an electron microprobe (due to the routine being standardless), past experience by the author has shown the data to be reliable for the type of minerals under investigation here. Analytical conditions were typically an acceleration voltage of 15 kV and 30 second count times.

Many of the illustrations in this report are back-scattered electron images. This means that the shades of grey in the images correspond to the average atomic mass of each mineral – i.e., sphalerite (ZnS) will appear brighter than chalcopyrite (CuFeS_2), which in turn is brighter than pyrite (FeS_2), and so forth. Contrast and brightness differ, however, from image to image.

In situ laser-ablation analysis was carried out on three samples to identify trace element contents of pyrite and sphalerite. Methodologies and analytical details are given within those sections of this report.

Sample L-11 skn from Lefevre tungsten + gold skarn / hornfels

Background

The sample was collected from a pit at the south end of trench #3 of the Lefevre workings, a mineralized skarn or hornfels. Site is at UMT 471,595 m E 5,434,124 mN \pm 10 m, the field label was L-11. From Trench # 3 BW-0111 a composite bulk sample of skarn ran 0.675 g/t Au, 46 ppm Bi and 9 ppm Te (Howard 2000). Kennedy's (2003) re-samples gave (ppm):

Sample	Au g/t	Ag g/t	Bi	Te	Se	Fe %	Cu	Mo	Pb	Zn	As	W
LS-13	1.582	1.0	108	2.2	3.0	15.83	170	142	9	28	25	>200
LS-14	0.980	0.9	93	1.9	3.2	11.61	294	62	<3	56	33	>200
LS-15	1.542	1.1	129	2.6	3.1	13.75	284	108	<3	39	24	>200

Te & Se values are re-assays from Howard (2005). Descriptions:

LS-13 – sample from intersecting fractures in ‘rotted’ sulfide

LS-14 – composite of skarn material across pit face with pods of pyrrhotite pyrite and some chalcopyrite

LS-15 – from zone of narrow quartz veins with same sulphides crosscutting the skarn at the W end of pit (op. cit.).

In trench #3 “garnet-pyroxene-scheelite skarn is largely overprinted by abundant and widespread quartz-sulphide mineralization. The latter includes thin veins of white to gray quartz as well as pods and veins of massive pyrite with lesser pyrrhotite and minor arsenopyrite (Ray 2004 p. 22)”.

Polished section description

L-11 skn is a weakly mineralized skarn with max. 5% by vol. sulfides in a silicate (quartz dominant) matrix. The polished block is from an area of the sample with sulfides (dominantly pyrite) ca. 15% by volume.

Reflected light microscopy of the polished section reveals dominant **pyrite** (Fig. 1) and small amounts of **sphalerite**, **galena**, **chalcopyrite** and **scheelite** (Fig. 4). The matrix is a mixture of quartz and a Ca-Fe carbonate in approximately equal amounts; two grains of Ca-Mg pyroxene (**diopside**) occur (Fig. 1D). Minor amounts of bismuth minerals include **native bismuth** and trace amounts of the bismuth tellurides **joséite-B** **Bi₄Te₂S**, **hedleyite** **Bi₇Te₃** and **unnamed** **Bi₂Te**. No gold minerals were observed. The sample is highly altered – pyrite has changed to goethite and other secondary oxides/hydroxides (Fig. 1a-c).

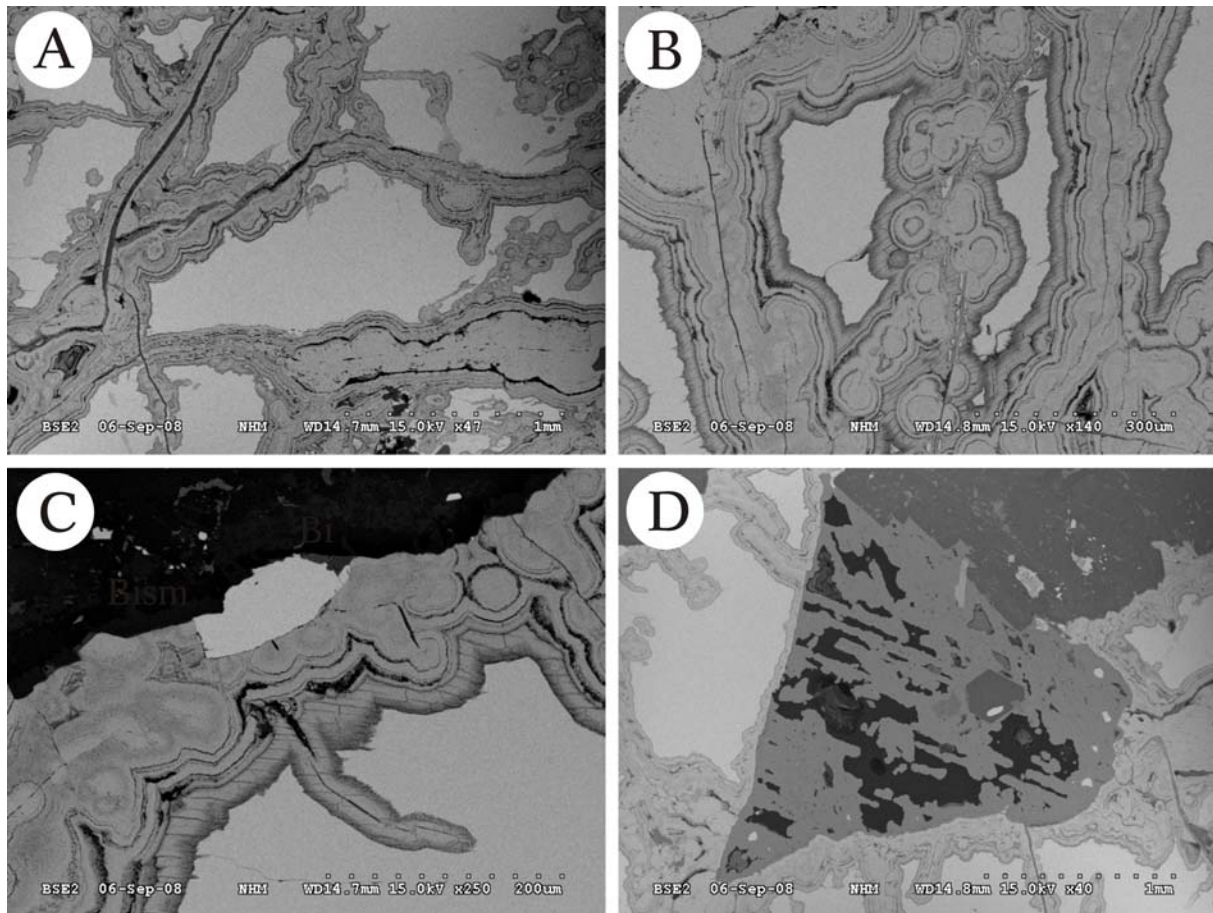


Fig. 1 SEM back-scattered images showing typical textures in sample L-11 skn. (A), (B) and (C): Pyrite (pale grey) undergoing alteration along grain boundaries and cleavage planes to an intergrowth of goethite and unspecified secondary hydroxides giving a boxwork-like appearance. In (C) a small grain of **chalcopyrite** (slightly brighter grey) lies within alteration surrounding pyrite. (D) Coarse grain of diopside of the skarn matrix (central in the image) within altered pyrite. Darker mineral at top is quartz.

Isolated grains of **native bismuth**, never exceeding ca. 10 μm in diameter, occur throughout the altered pyrite or the quartz-carbonate matrix (Fig. 2).

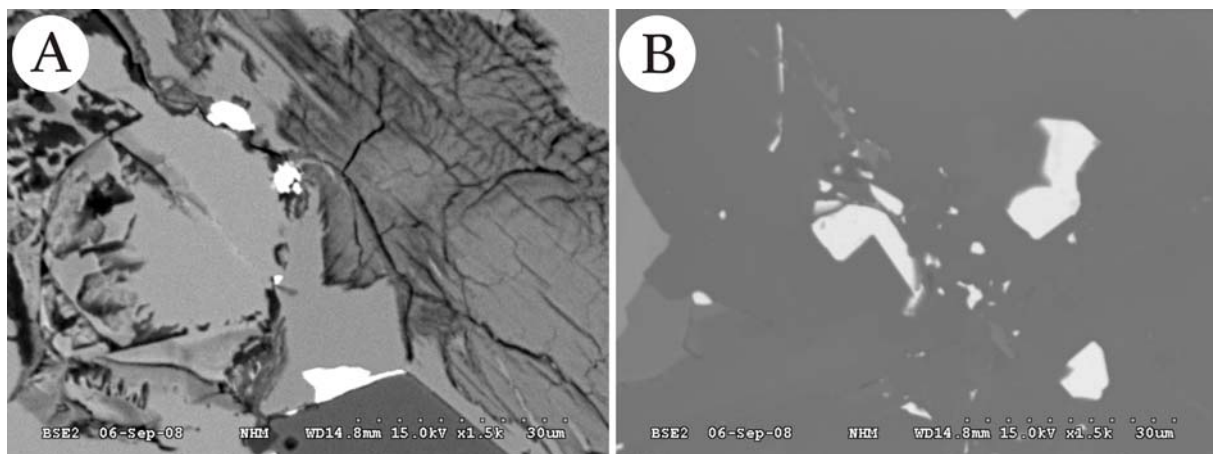


Fig. 2 SEM back-scattered images of small grains of native bismuth in partially altered pyrite (A) and quartz (B).

Other bismuth minerals are rather rare and were only observed in a single patch, ca. 50 μm in diameter (Fig. 3) where native bismuth coexists with hedleyite and joséite-B; textures suggest their formation at equilibrium conditions

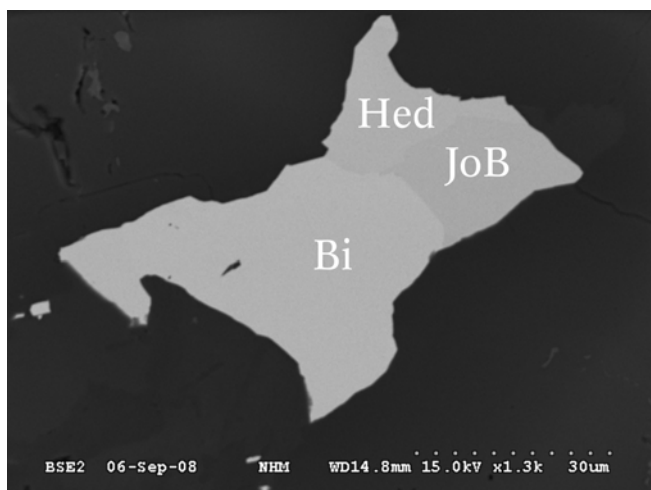


Fig. 3 SEM back-scattered image showing Note a neat triple-junction between the three bismuth minerals suggesting formation at equilibrium conditions. Bi – native bismuth; JoB – joséite-B; Hed – either hedleyite or unnamed Bi_2Te .

Scheelite occurs as isolated grains, typically ca. 50 μm in diameter within the quartz-calcite matrix (Fig. 2). It is, however, a relatively abundant phase and probably the most common opaque mineral after pyrite and its secondary alteration products. No molybdenite was observed in the polished block.

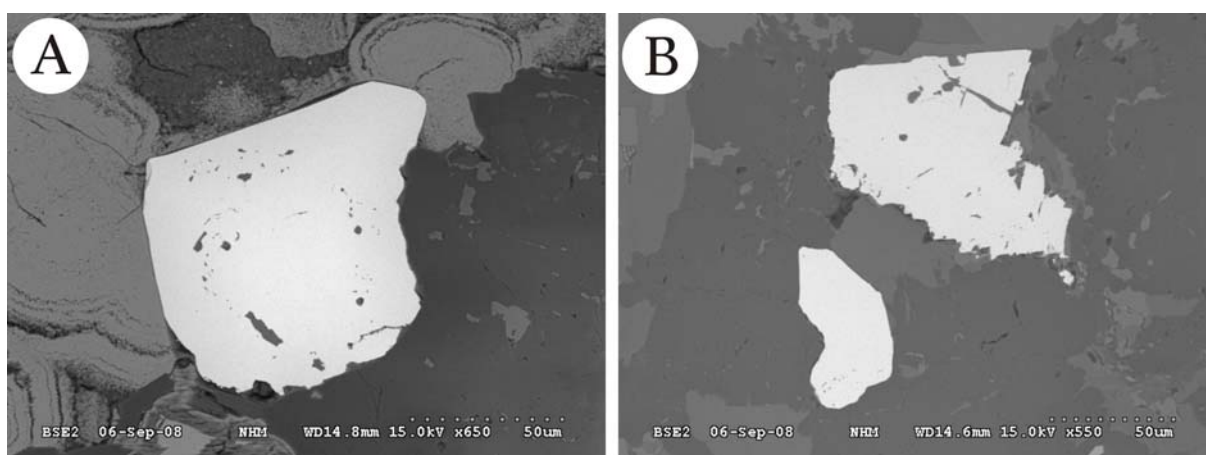


Fig. 4. Back-scattered scanning electron microscope images showing small grains of scheelite (white mineral) in matrix of quartz (dark) & pyrite (grey and colloform in A), and quartz & carbonates (in B).

Semi-quantitative Energy-Dispersive Spectroscopic (SEM-EDS) analyses of sample L-11 skn, elements in wt. %:

Phase	Cu	Ag	Bi	Pb	Sb	Te	Se	S	Total
joséite-B	-	-	70.92	-	-	23.87	0.66	3.26	98.71
hedleyite 1	-	-	76.77	0.75	1.06	20.09	0.21	-	98.88
hedleyite 2 [rather, near- stoichiometric unnamed Bi_2Te]	-	-	78.17	-	-	21.23	0.13	0.27	99.80

Joséite-B ideally $\text{Bi}_4\text{Te}_2\text{S}$, near-stoichiometric formula with sums

Phase	Cu	Ag	Bi	Pb	Sb	Metal Sum	Te	S	Se	S + Se Sum
joséite-B	-	-	3.73	-	-	3.73	2.06	1.12	0.09	1.21

Hedleyite 1 - near-stoichiometric Bi_7Te_3 , formula with sums

Phase	Cu	Ag	Bi	Pb	Sb	Metal Sum	Te	Se	S	Chalcogen Sum
hedleyite 1 Bi_7Te_3	-	-	6.81	0.07	0.16	7.03	2.92	0.05	-	2.97

Hedleyite 2 - actually near-stoichiometric unnamed Bi_2Te , formula with sums

Phase	Cu	Ag	Bi	Pb	Sb	Metal Sum	Te	Se	S	Chalcogen Sum
hedleyite 2 actually unnamed Bi_2Te	-	-	2.04	-	-	2.04	0.91	0.01	0.05	0.96

Only in this polished section are both hedleyite and unnamed Bi_2Te identified; that both phases are very close to their ideal formulae substantiates their mutual occurrence. The occurrence of bismuth minerals in sample L-11 skn (and the same bismuth tellurides very common in most all polished sections of the CLY veins) allows one to premise a genetic connection between the Lefevre vein and skarn mineralization. The presence of scheelite, a classic “high temperature” mineral, ties mineralization to the causative granite.

Sample L-04QVXtry from Lefevre tungsten + gold skarn / hornfels

Background

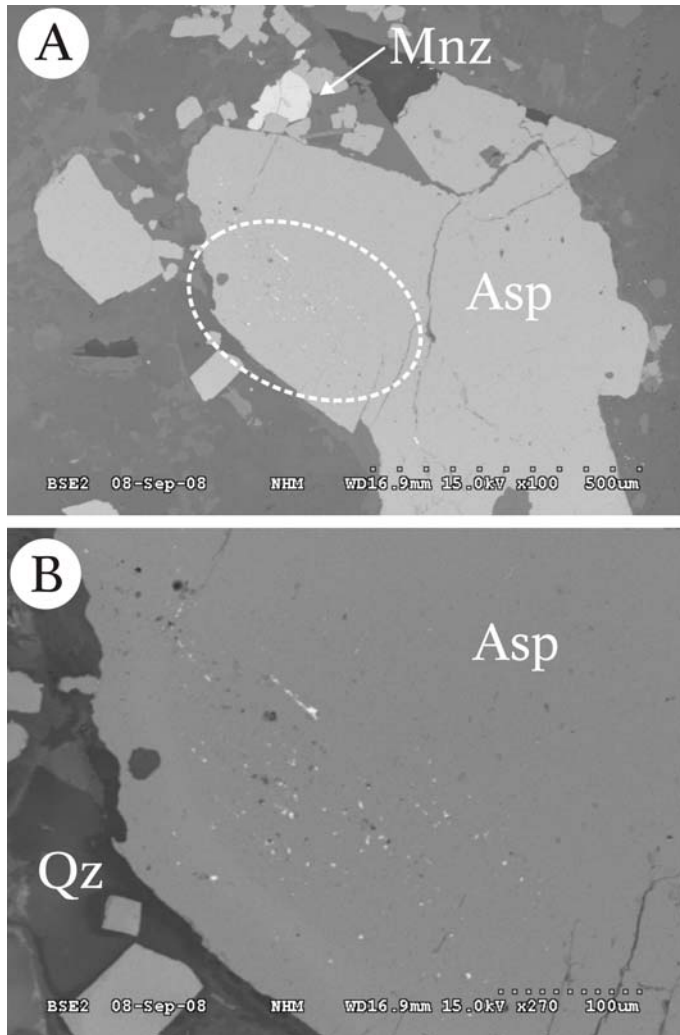
L-04QVXtry was collected from the east side of the pit in trench 5 in the quartz-veined Lefevre tungsten + gold skarn. The Lefevre skarn is a reduced, pyrrhotite-rich pyroxene (actinolite?) - garnet - scheelite skarn and hornfels with minor sphalerite, minor arsenopyrite and trace bismuth telluride minerals and gold. Further description is in Howard (2000) p. 24-27, (2005) p. 42-45 and (2006b) p. 46-49. Site is at UTM 471,597 mE 5,434,136 mN \pm 5 m; the field label is L-4. LS-12 a grab sample from Kennedy (2003) ran 14.17g/t Au and 343.5 ppm Bi, but this is likely from the differently oriented vein on the N side of the pit. This sample L-04QVXtry is from 'Vein 2' on the pit's east side. Part of the contact with the hornfelsed Harcourt Creek Assemblage Metaquartzite + Tuff Unit country rock (Howard 2006b) is included in the sample.

Polished section description

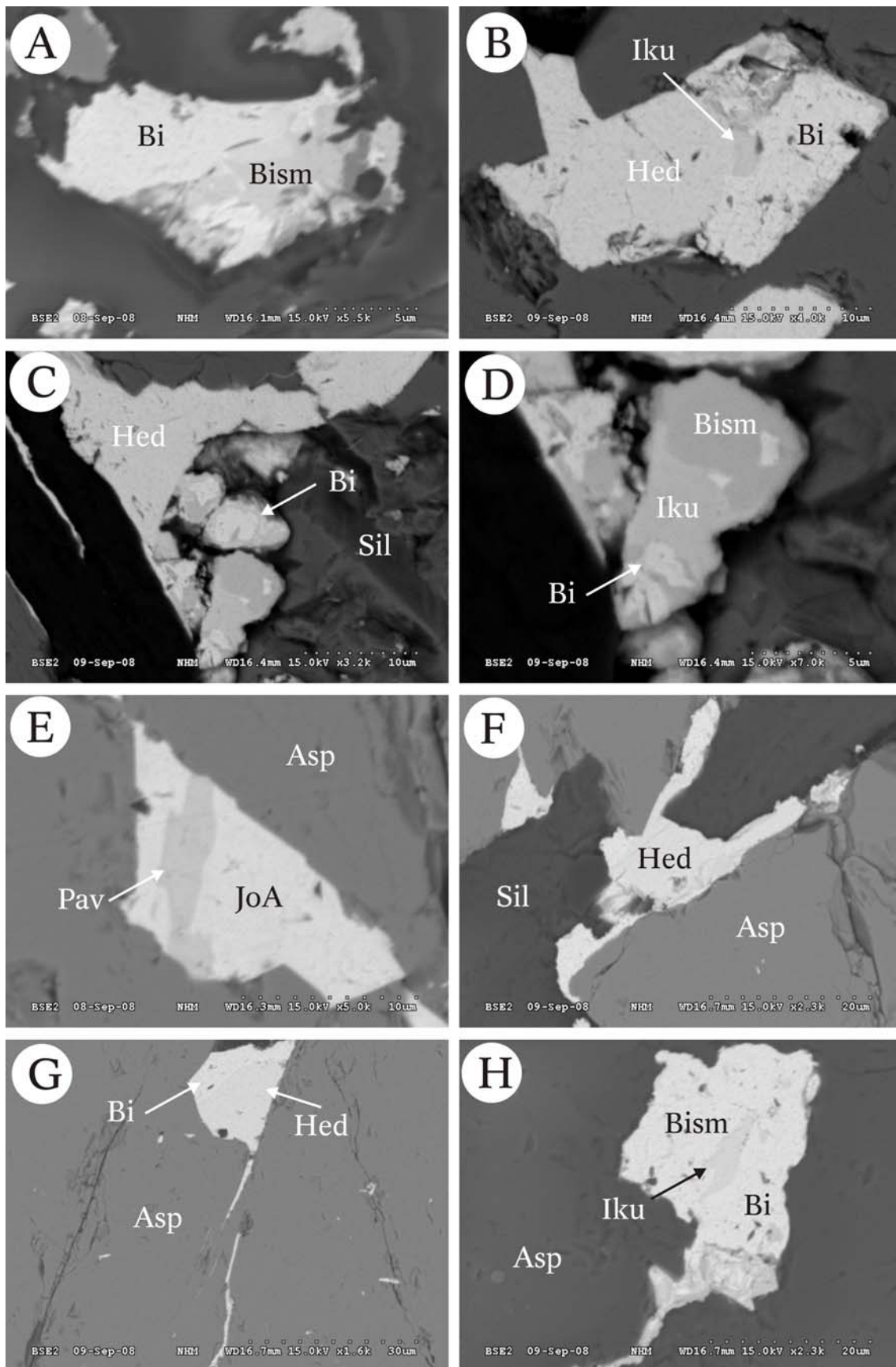
Sample L-04QVXtry consists of quartz and an **undetermined Mg-Fe-Al-silicate** (electron probe data required for identification) with variable amounts of sulphide. Accessory **monazite** is reasonably widespread (Fig. 1A). The polished section was prepared from the part of the sample with ca. 10% sulphide by volume.

Reflected light microscopy reveals that the sulphide is **arsenopyrite**; only **very minor pyrite** was observed in the sample (< 1% of total sulphide). The arsenopyrite is generally rather fine-grained, typically 0.5 - 1.0 mm diameter grains. It contains abundant microscopic inclusions of bismuth minerals typically as one- or two-phase blebs (Figs. 1 and 2).

The bismuth minerals are micron-sized bismuth telluride grains, typically < 50 μ m, with composition **unnamed Bi₂Te** (named hedleyite in the images, see formulae in table below), a **bismuthinite derivative mineral in the bismuthinite-aikinite solid-solution series Bi₂S₃ – CuPbBiS₃** (Topa et al. 2002), **native bismuth**, **joséite-A Bi₄S₂Te**, **ikunolite Bi₄S₃** with high Pb, no measured Se but significant Cu & Te. The rare Ag-Bi-sulphosalt mineral **pavonite (Ag,Cu)(Bi,Pb)₃S₅** occurs inside a joséite-A grain (Fig. 2A). Minor **molybdenite** occurs. No gold minerals were observed.



Figs. 1A & 1B. SEM back-scattered electron images of L-04QVXtry polished section showing Fig. 1A clustered coarse grains of arsenopyrite (Asp) containing finely distributed grains of bismuth minerals (circled area). Fig. 1B detail of circled area. Mnz – monazite. Field of view about 1.2 cm (1,200 microns).



Figs. 2A-2H Back-scattered electron images of L-04QVXtry showing bismuth mineral grains enclosed in arsenopyrite. The association in 2B is curious: ikunolite (without Se) has formed, not bismuthinite, adjacent to earlier? co-existing native bismuth and unnamed Bi_2Te [Hed].

Ikunolite may have crystallized after the other minerals, in a very local chemical environment with just the right amount of Bi and S to form this rarer bismuth sulphide. Figs. 2D and H are more difficult to interpret. After early (?) native bismuth both ikunolite and bismuthinite may have formed in a very localised closed system, with approximately equal amounts of Bi and S. These two minerals are stable with one another as bismuthinite is not a member of the tetradyomite group. In Fig. 2E the sulphosalt pavonite may have crystallised out of the josite-A (which cannot contain silver). Occurrence of Bi-tellurides and sulphosalts together like this one is uncommon. There is insufficient understanding of their co-stabilities, however pavonite seems to be more abundant in higher temperature (>300 °C) deposits, such as skarns. As it is a trace mineral in this one section it's unlikely to be very significant in the overall economic dimensions of the deposit. Abbreviations: Asp – arsenopyrite; Bi – native bismuth; Bism – bismuthinite; Hed – hedleyite actually unnamed Bi₂Te; Iku – ikunolite; JoA – josite-A; Pav – pavonite; Sil – Mg.Fe-Al-silicate

Semi-quantitative Energy-Dispersive Spectroscopic (EDS) analyses of phases in L-04QVXtry (elements in wt. %):

Analysis	Cu	Ag	Bi	Pb	Sb	Te	Se	S	Total
Bi ₂ Te 1	1.14	0.76	71.83	-	1.83	22.81	-	0.35	98.72
Bi ₂ Te 2	-	-	71.75	-	2.46	23.75	0.37	-	98.33
Bi ₂ Te 3	-	-	75.27	0.20	1.44	22.37	0.03	-	99.31
Bi ₂ Te 4	-	-	78.01	-	-	21.53	0.46	-	100.00
Bi ₂ Te 5	-	-	76.45	0.19	0.44	22.63	0.29	-	100.00
Bismuthinite derivative	2.50	-	73.19	10.64	-	-	0.24	15.43	102.00
Ikunolite 1	1.65	-	79.03	10.33	-	0.78	-	9.20	100.99
Ikunolite 2	1.04	-	86.97	-	0.03	3.09	-	8.89	100.02
+Josite-A 1	-	-	79.85	-	-	9.15	0.13	8.83	97.96
Josite-A 2	0.73	-	73.57	3.34	1.07	12.63	0.22	6.31	97.87
Josite-A 3	-	-	79.95	-	-	13.02	0.06	6.74	99.77
^Pavonite 1	1.09	11.89	54.43	13.80	0.34	-	0.25	13.89	95.69^
Pavonite 2	-	13.75	62.20	3.22	-	0.47	0.03	17.33	97.00

^low analysis total – possibly other unanalyzed elements present

+ non-stoichiometric: analysis low in metal, hi in chalcogens, possibly not josite-A

Hedleyite - actually near-stoichiometric unnamed Bi₂Te, formulae with sums

Mineral	Cu	Ag	Bi	Pb	Sb	Metal Sum	Te	Se	S	Chalcogen Sum
Bi ₂ Te 1	0.09	0.04	1.80	-	0.08	2.01	0.94	-	0.06	0.99
Bi ₂ Te 2	-	-	1.86	-	0.11	1.97	1.01	0.03	-	1.03
Bi ₂ Te 3	-	-	1.97	0.01	0.06	2.04	0.96	-	-	0.96
Bi ₂ Te 4	-	-	2.04	-	-	2.04	0.92	0.03	-	0.96
Bi ₂ Te 5	-	-	1.99	-	0.02	2.02	0.96	0.02	-	0.98
average L-04QVXtry unnamed Bi ₂ Te	0.018	0.008	1.932	-	0.054	2.012	0.958	0.016	0.012	0.984

Bismuthinite derivative mineral in bismuthinite-aikinite solid-solution series, Cu_xPb_xBi_{2-x}S₃ (0 ≤ x ≤ 1), formula with sums

Mineral	Cu	Cu + Ag Sum	Pb	Bi	Metal Sum	S	Se	S + Se Sum
?	0.21	0.21	0.28	1.89	2.38	2.60	0.02	2.62

No Ag or Sb present.

Ikunolite ideally Bi_4S_3 , formulae with sums

Mineral	Cu	Ag	Bi	Pb	Sb	Metal Sum	Te	Se	S	Chalcogen Sum
Ikunolite 1	0.24	-	3.54	0.47	-	4.25	0.06	-	2.69	2.75
Ikunolite 2	0.16	-	3.97	-	-	4.12	0.23	-	2.64	2.87
Average L-04QVXtry ikunolite	0.20	-	3.755	0.235	-	4.185	0.145	-	2.665	2.81

Joséite-A ideally $\text{Bi}_4\text{S}_2\text{Te}$, formulae with sums

Mineral	Cu	Ag	Bi	Pb	Sb	Metal Sum	Te	S	Se	S + Se Sum
+Joséite-A 1	-	-	3.66	-	-	3.66	0.69	2.64	0.02	2.66
Joséite-A 2	0.12	-	3.59	0.16	0.09	3.96	1.01	2.01	0.03	2.04
Joséite-A 3	-	-	3.85	-	-	3.85	1.03	2.12	0.01	2.13
Average L-04QVXtry Joséite-A	0.06	-	3.72	0.08	0.045	3.905	1.02	2.065	0.02	2.085

+non-stoichiometric: low in metal, hi in chalcogens, possibly not Joséite-A; not included in the average

Pavonite ideally $(\text{Ag,Cu})_1(\text{Bi,Pb})_3\text{S}_5$, formula with sums

Mineral	Ag	Cu	Cu + Ag Sum	Bi	Pb	Bi + Pb Sum	S	Se	Te	Chalcogen Sum
Pavonite 2	1.16	-	1.16	2.72	0.14	2.86	4.94	-	0.03	4.97



Fig. 3 Back-scattered electron image of elongate molybdenite grains (grey) in quartz + silicate matrix.

Conclusions re mineralogy of L-04QVXtry quartz + arsenopyrite vein

Mineralogical study of L-04QVXtry quartz plus arsenopyrite vein reveals a bismuth mineral assemblage- early-formed (?) native bismuth + ikunolite + bismuthinite - in the arsenopyrite matrix different from that in the Bunker Hill veins and Eloise Vein.

Ikunolite 1 has very high Pb and significant Cu, ikunolite 2 significant Cu and Te. Pb is extraordinarily abundant in ikunolite 1 at 10.33 wt. % or 0.47 apfu, possibly as Pb-for-Bi substitution. Average Cu is ~0.2 apfu; significance of this minor amount is unknown.

Ikunolite 2 has high 3.09 wt. % Te, 0.23 apfu. “Compositional data for ikunolite indicate very limited Te-for-(Se,S) substitution in most natural specimens (Cook et al. 2007)”.

Hedleyite does not occur like in Eloise vein, in both occurrences it is near-stoichiometric unnamed Bi₂Te. The average L-04QVXtry joséite-A is near-stoichiometric with only trace Pb.

A **bismuthinite–aikinite series mineral and pavonite, a rare Cu-Ag-Bi-Pb sulphosalt**, are first reported herein from the CLY locality. Occurrences of ikunolite in L-04QVXtry and those in the Blue Quartz vein (Cook & Ciobanu 2006a) are first finds in Canada.

Table of minerals identified in two polished sections of Lefevre mineralization, one quartz vein & one skarn, listed in decreasing order of metal: chalcogen ratio

	metal: chalcogen ratio	L-04QVXtry quartz + arsenopyrite vein from Lefevre tungsten + gold skarn / hornfels this report	L-11 skn from Lefevre tungsten + gold skarn / hornfels this report
native bismuth	very high	✓	✓
hedleyite	7:3 = 2.33		✓
unnamed Bi ₂ Te	2:1 = 2.00	✓	✓
joséite–A	4:3 = 1.33	✓	
joséite–B	4:3 = 1.33		✓
ikunolite	4:3 = 1.33	✓	
bismuthinite– aikinite series mineral	2:3 = 0.66	✓	
arsenopyrite	-	✓	
very minor pyrite	-	✓	✓
trace pavonite	-	✓	
sphalerite	-		✓
galena	-		✓
chalcopyrite	-		✓
minor molybdenite	-	✓	
scheelite	-		✓

Sample L-07 skn

Background

Sample L-07 skn is from the Lefevre workings trench #4 at UTM 471,610 mE 5,434,137 m N \pm 5 m. The field label was L-07. New sample 0548 was also collected here. H. Little (1959) noted “In trench # 4 and in the pits at either end, finely disseminated scheelite is distributed evenly. A chip sample from this trench taken across 35’ assayed 0.33% WO₃ with no detectable MoS₂. This represented the best scheelite-bearing material observed, except over narrow widths.” LS-04 skarn collected close-by ran 0.190 g/t Au & 0.126 g/t Ag by ICP MS, 21.1 Bi / 0.44 Te / 0.4 Se / 5,056 Mn / 4.0% Fe and >100 W, all ppm (Howard 2005). This was a re-analysis of LS-4, a composite of skarn from an old pit with pyrrhotite & pyrite (Kennedy 2003).

Polished section description

Sulfides account for ca. 10% of the sample. Most of the sulfide is pyrite, with lesser pyrrhotite. The sample appears rather altered, although the primary ‘colloform’ character of the pyrite is largely preserved (Fig. 1, left). Gangue minerals include coarse, partially replaced Mn-bearing garnet, as well as biotite, some quartz and calcite, and relict K-feldspar (mostly altered to kaolinite). The sample contains several grains of **scheelite**, 100-200 μ m in size, but no gold or bismuth phases were seen.

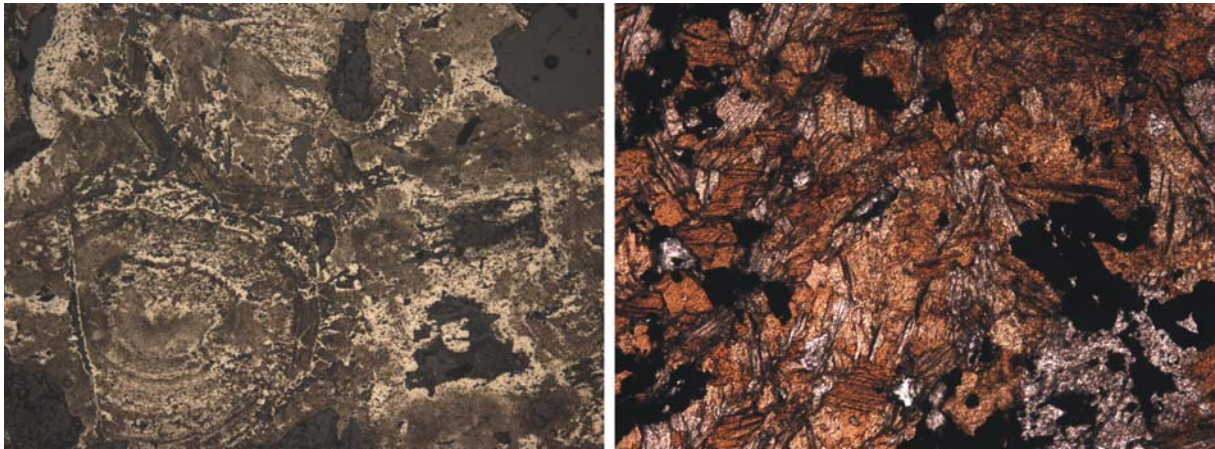


Fig. 1. Photomicrographs in reflected light (left) and transmitted light (right) showing typical textures in sample L-07 skn. Left picture shows highly-altered pyrite. Right picture shows silicate matrix dominated by biotite (pale brown, pleochroic). Horizontal axis: 450 μ m for both pictures.

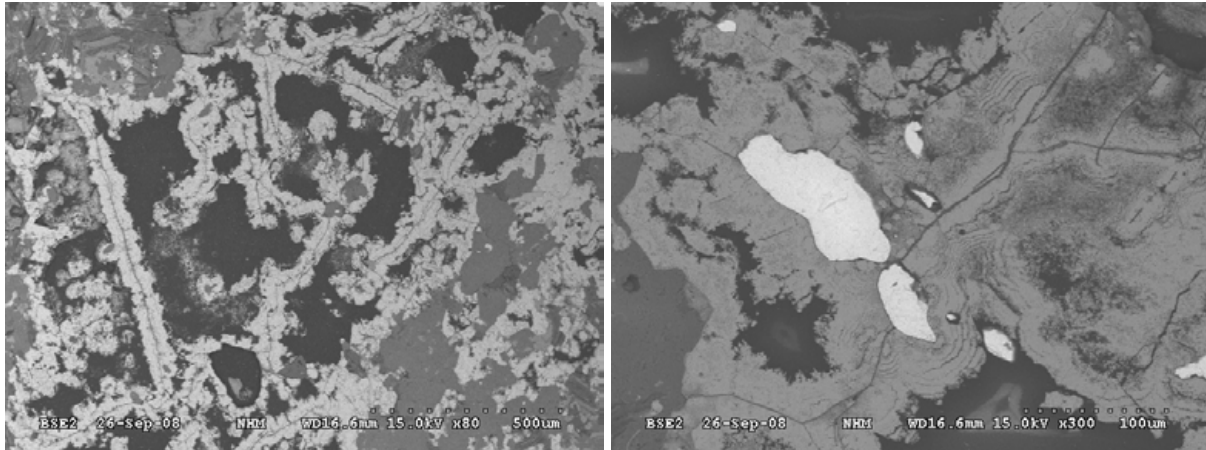


Fig. 2. Back-scattered electron microscope images. The left image shows pyrite along the margin of, and growing into a void in the sample. Darker areas adjacent to the pyrite are Fe-oxides/hydroxides. Right image shows moderately coarse grains of scheelite in a matrix of oxidized sulfides (probably mostly pyrrhotite in this case).

The Mn-bearing garnet is quite abundant throughout the sample (Fig. 3, left). It appears homogeneous with ca. 16 wt. % MnO. It has been extensively replaced by a fine-grained matrix of quartz, calcite, various fine-grained clay minerals and a dark Fe-rich biotite. The biotite is closely associated with the sulfides.

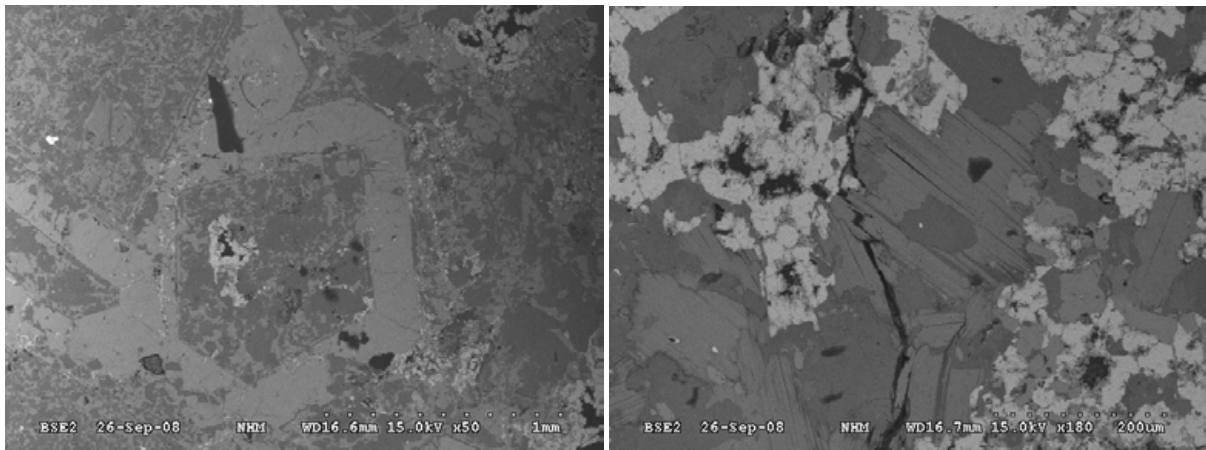


Fig. 3. Back-scattered electron microscope images. Left image shows coarse garnet (medium grey homogeneous areas) partially replaced by mixture of other silicates including calcic amphibole, calcite and quartz (products of retrograde skarnification?). Right picture shows coarse plates of biotite (centre of image) in the matrix between the relictic sulfides.

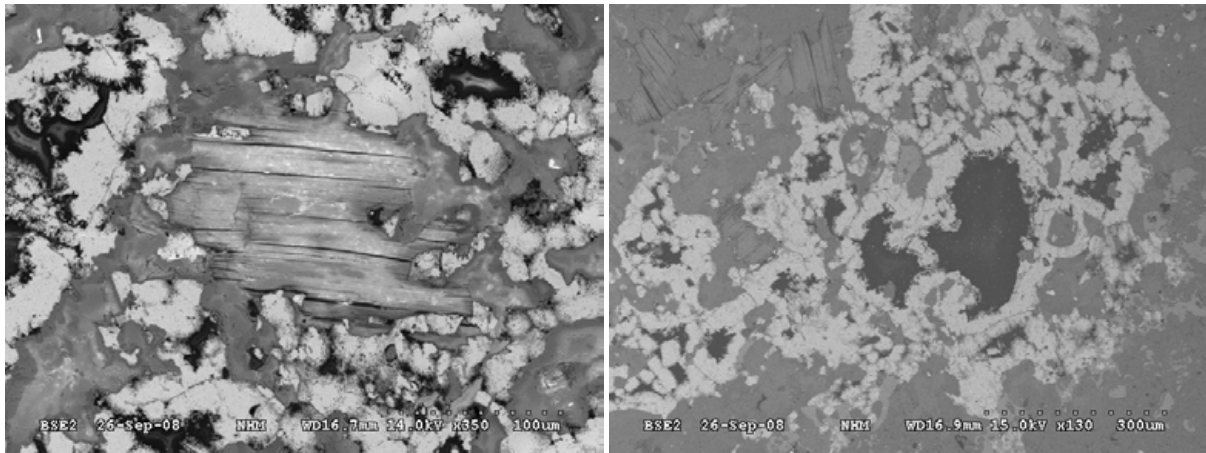


Fig. 4. Back-scattered electron microscope images. Left image shows higher contrast image of similar assemblage as in Fig. 3 (right). Right image shows similar association of pyrite as in Fig. 2 (right).

Sample L-09 skn

Background

L-09 skn is from trench #7 collected at UTM 471,612 mE 5,434,135 mN \pm 5m. The field label was L-09. BH-115 from the N side of Trench # 7 a composite chip sample over 1 m of very hard actinolite - garnet skarn ran 200 ppb Au / 13 ppm Bi and 5 ppm Te; only these elements were analyzed (Howard 2000). There is also a Bi-Te mineralized vein in trench #7, not examined.

Polished section description

Sulfides account for 25% of the sample – pyrrhotite is dominant, minor chalcopyrite is also present (Fig. 1, left). Although altered to some extent, the sample is considerably fresher than many others collected from the Lefevre trenches. Gangue minerals include Mn-bearing garnet, biotite, quartz, calcite, minor calcic amphibole, plagioclase feldspar and clay minerals (kaolinite etc.). Ilmenite is noted. The sample contains several small (sub-5 μ m) grains of **native bismuth**. No other trace minerals were observed in the sample.

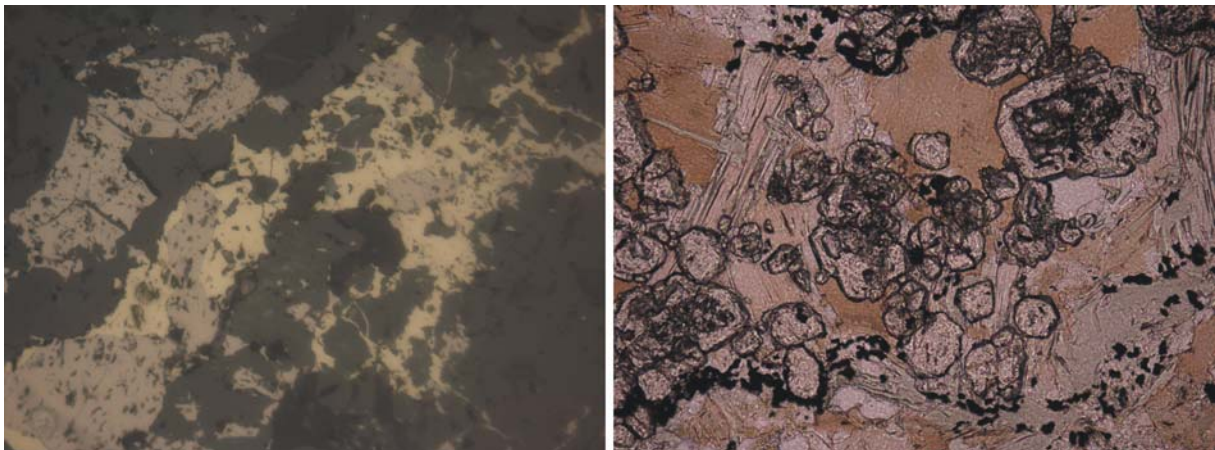


Fig. 1. Photomicrographs in reflected light (left) and transmitted light (right) showing typical textures in sample L-09 skn. Left picture shows intergrowths of pyrrhotite (pink) and chalcopyrite (yellow) in silicate matrix (dark). Right picture shows rounded crystals of Mn-garnet (pink, high relief) in matrix of quartz, calcite and biotite. Horizontal axis: 450 μ m for both pictures.

The Mn-bearing garnet is abundant and probably the most common mineral in this section (Fig. 1, right). MnO contents are in the range 12-16 wt. %. The mineral also shows a strong association with the sulfides and is most abundant in sulfide-rich portions of the sample. Sulfides may either form a matrix to fragmented and rounded garnet grains (Fig. 2) or fill fractures in brittle-deformed garnet (Fig. 3, left).

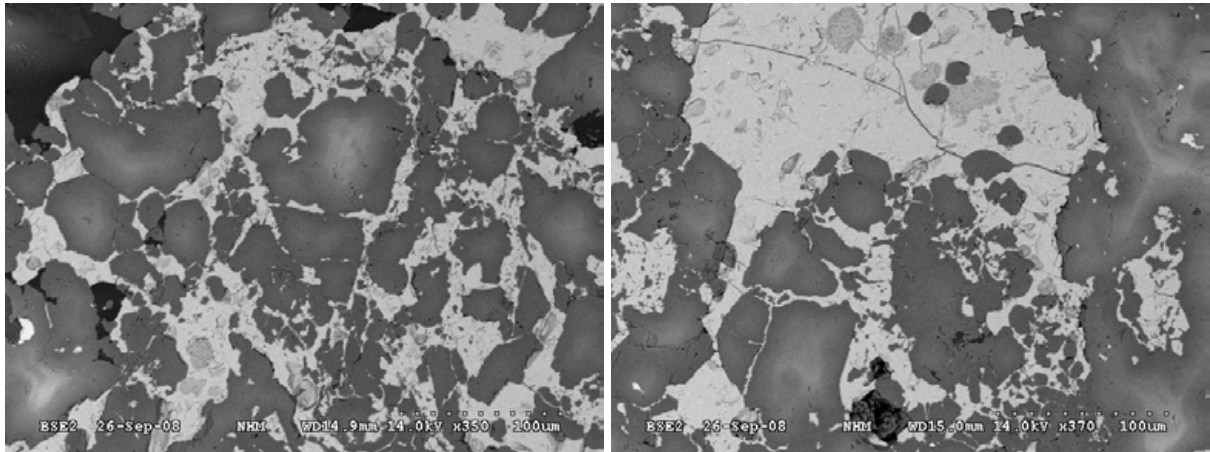


Fig. 2. Back-scattered electron microscope images. Both images show sulfide (bright – darker patches within sulfides are alteration products) forming the matrix between rounded and fragmented crystals of Mn-bearing garnet.

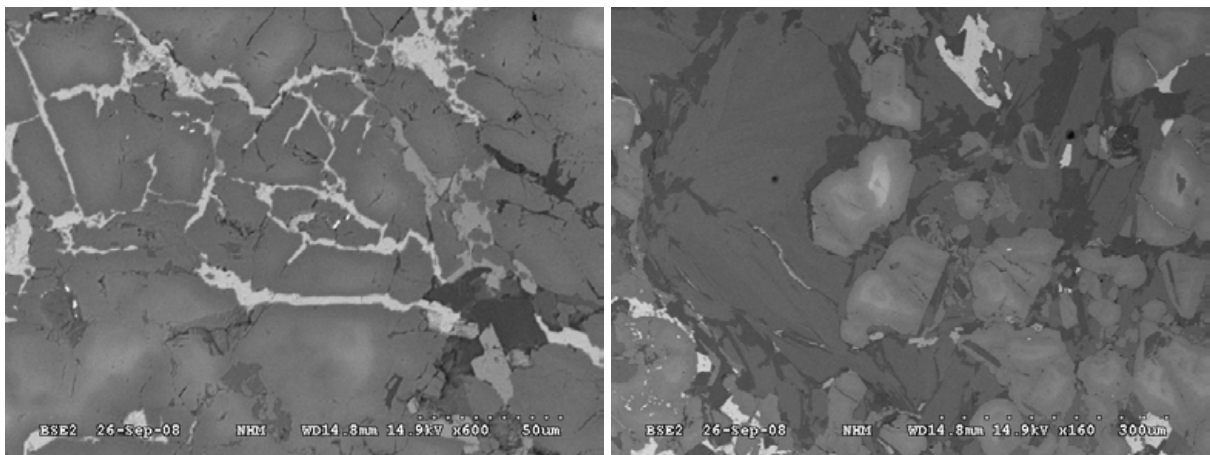


Fig. 3. Back-scattered electron microscope images. Left image shows sulfides (bright) filling fractures within a larger porphyroblast of Mn-bearing garnet. Medium grey mineral in right of picture is ilmenite. Right picture shows rounded garnet grains and coarse biotite (left of image).

Sample L-10a skn

Background

Sample L-10a skn is from the Lefevre workings in trench #10 at UTM 471,584 mE 5,434,168 mN. Field notes described the sample as sulfide skarn; the field label was L-10. Grab rock BH-314 collected close to here, a selected piece of garnet + actinolite (?) pyroxene + pyrrhotite + arsenopyrite + scheelite skarn, ran 1.225 g/t & Au 0.6 g/t Ag, 100 Bi / 31 Te / < 1 As / 17 Pb / 145 Cu / 130 Co / 235 Ni / 9,317 Mn and 435 W (all ppm) and 9.57% Fe (Howard 2000).

Polished section description

In contrast to most other samples from the Lefevre trenches, L-10a skn is dominated by pyrrhotite. The section contains ca. 10% total sulfides in a matrix essentially consisting of quartz, calcite and a small proportion (ca. 3-5 vol. %) of calc-silicate minerals. The sample is extensively altered (surface alteration?).

The sulfide mineralogy consists of massive pyrrhotite that is partially decomposed to a mixture of marcasite and various Fe-oxides/hydroxides. Marcasite forms characteristic lozenge-shaped domains within the pyrrhotite (Fig. 1). Neither gold minerals nor tellurides were observed. A single (5 μ m) grain of galena was noted.

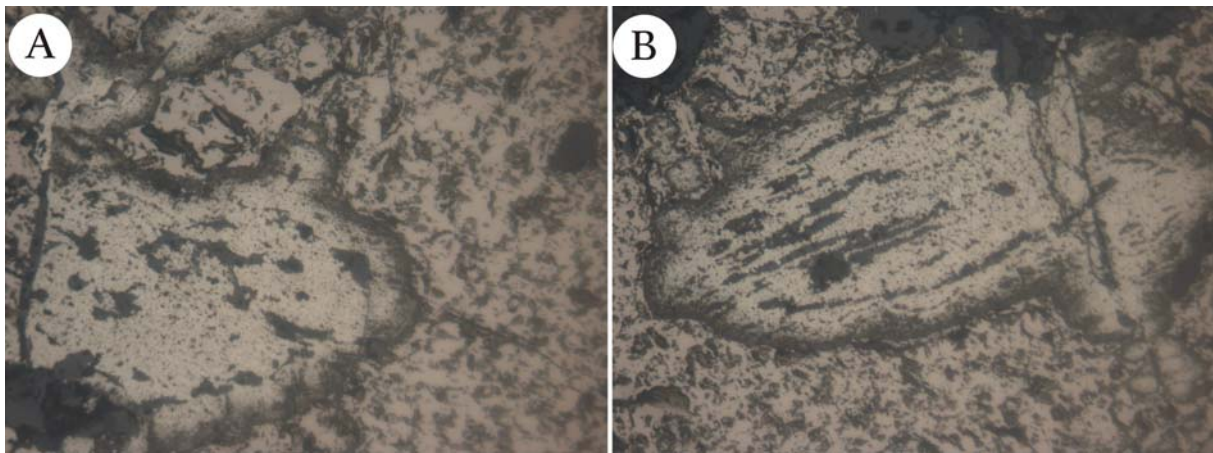


Fig. 1. Photomicrographs in reflected light showing typical textures in sample L-10a skn. Lozenge-shaped marcasite domains are present within the pyrrhotite. The dark areas within marcasite are Fe-oxides/hydroxides. Horizontal axis: 450 μ m for both pictures.

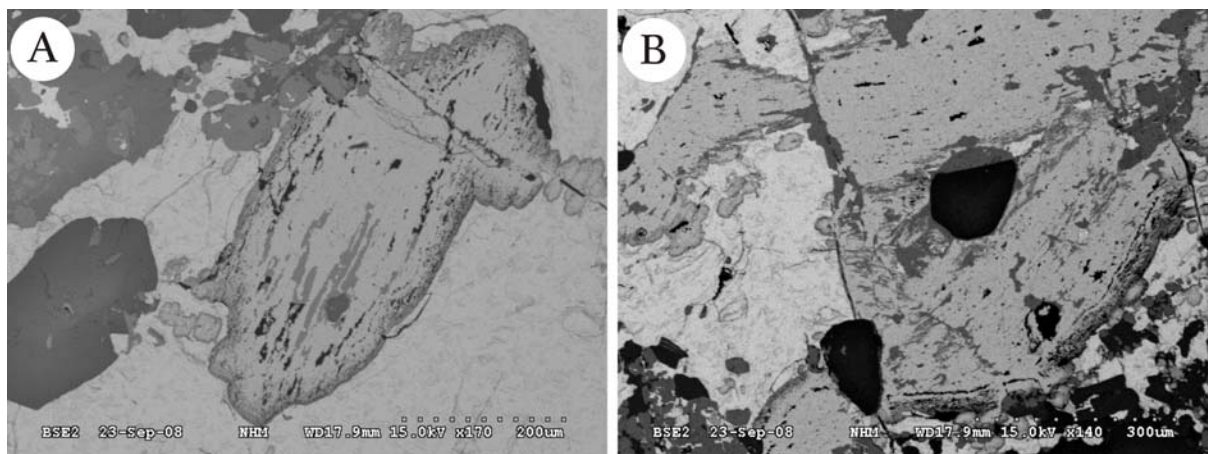


Fig. 2. Back-scattered SEM images showing alteration of pyrrhotite in L-10a skn. (A) shows the same area as in Fig. 1b. Marcasite occurs within pyrrhotite matrix and contains patches of Fe-oxides/hydroxides along the rim margin and cleavage planes. Gangue minerals include quartz (large grain on left of image) and calc-silicates (darker grey, top left). In (B), set at a different image contrast, marcasite is brighter white and relict pyrrhotite in gray colors. Both minerals are altering to Fe-oxides/hydroxides.

The single remarkable feature of L-10a skn is the abundance of **scheelite** throughout the sample. The mineral occurs as moderately coarse (100-200 μm) grains scattered throughout the sulfide matrix (Fig. 3).

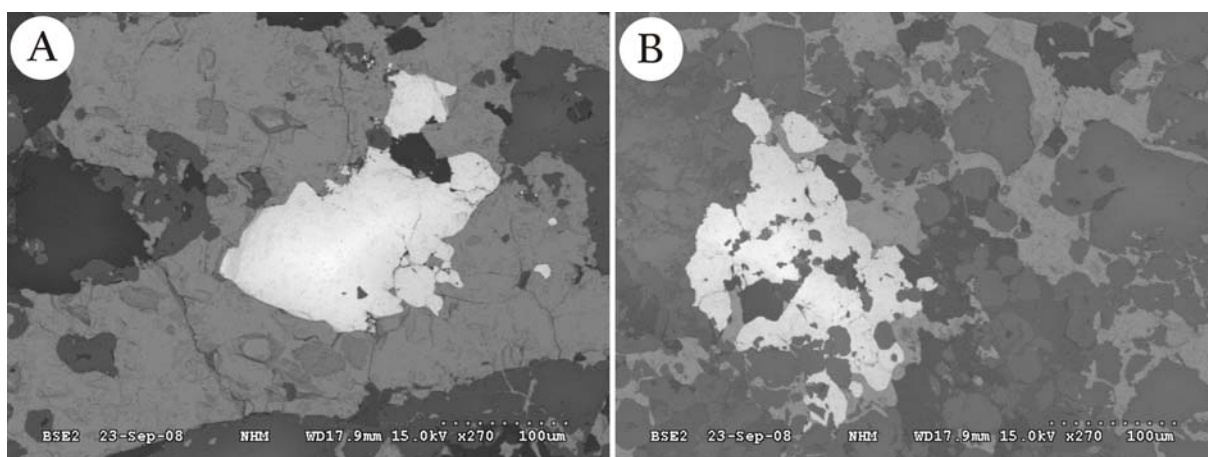


Fig. 3. Back-scattered SEM images showing grains of scheelite (bright white) in matrix of pyrrhotite (medium grey) and quartz (dark) in L-10a skn.

Sample L-12 Sp skarn

Background

Sample L-12 Sp skarn was collected from the S wall of trench #1, the southernmost trench of the Lefevre workings. Field label was L-12. A grab sample 0421 collected here at UTM 5,434,078 m N 471,615 m E is “abundant massive very coarse grained (2-3 mm sized) disseminated very dark brown sphalerite with recrystallized quartz and medium brown plagioclase (or partly scheelite?). Outer weathered surfaces are coloured medium red brown by limonite (Howard 2005).” 0421 ran 0.007 ppb (nil) Au / 272 Cd / > 10,000 Zn / 0.22 Ag / 1.14% Fe / 58.7 W (anomalous) (all ppm).” Additionally Bi is 1299 / Te 40.2 / Cu 240.8 and Pb 6.8 ppm.

Polished section description

L-12 Sp skarn is a semi-massive sulfide sample comprising dark-colored sphalerite (ca. 15 vol. %) and minor other sulfides in a matrix of skarn minerals. The polished block was prepared from an area of the sample in which the sulfide minerals account for about 20% of the sample by volume.

Reflected light microscopy reveals that sphalerite dominates the sulfide mineralogy of the sample. Small amounts of pyrite were noted, closely intergrown with sphalerite, as were trace amounts of chalcopyrite and galena. No gold or bismuth minerals have been observed in the polished section.

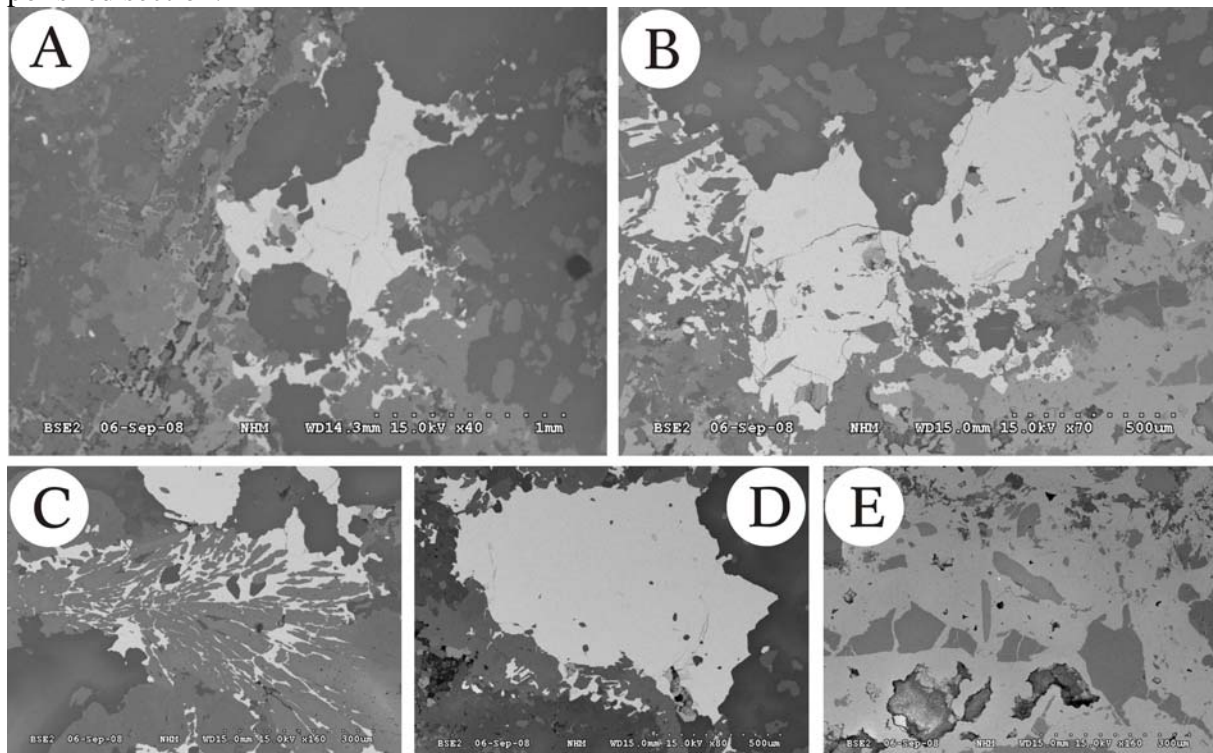


Fig. 1. Back-scattered scanning electron microscope images showing typical textures in sample L-12 Sp skarn. (A) and (B): Sphalerite (light grey) in a matrix of quartz (black), ankerite (darkest grey) and Ca-Mg-pyroxene (medium grey). (C) Sphalerite crystallized along cleavage planes in pyroxene, giving the appearance of splays. (D): Sphalerite in matrix of quartz and pyroxene. Note rounded grain boundaries between sulfide and silicate. (E): Brecciated (?) remnants of pyroxene within sphalerite.

The skarn gangue consists largely of quartz (ca. 25%), a Ca-Mg-Al pyroxene (ca. 35%) and Ca-Fe-carbonate (ca. 15%). Minor amounts of an **unidentified Na-Zn-bearing sulfate phase** were also noted.

Semi-quantitative SEM-EDS analyses of sphalerite in sample L-12 Sp skarn confirmed the high Fe content suggested by its black color. Spot analyses of three sphalerite grains gave 12.07, 11.30 and 10.91 wt. %, respectively. Sphalerite is commonly also a mineralogical host for elements such as Cd, In [Indium] and Mn. Analyzed Cd contents in sphalerite were 1.12, 0.46 and 0.32 wt. %. Contents of In were 0.45, 0.18 and 0.22 wt. % [these values are high! – The laser ablation study (below) gives lesser values with a mean 180 ppm or 0.018%]; Mn contents were below minimum detection limit (ca. 0.05 wt. %) in all cases. Trace levels of Se and Ag were also noted in the analyses.

The relatively high Cd content is also suggested by the presence of small (< 50 μm) grains of **greenockite** (CdS) in the sample. These (Fig. 2a) are compositionally zoned, suggesting reaction during overprinting.

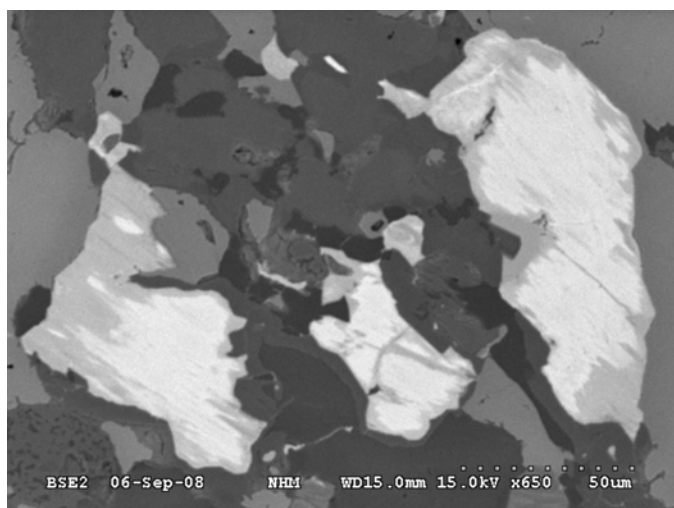


Fig. 2 Back-scattered SEM image of compositionally-zoned greenockite grains. The white areas are close to end-member CdS (< 1 wt. % Zn) in composition. The darker areas around the edge of the grains are intermediate within CdS-ZnS solid solution (ca. 50 atom. % CdS).

Laser ablation analysis of sphalerite in sample L-12 Sp skarn

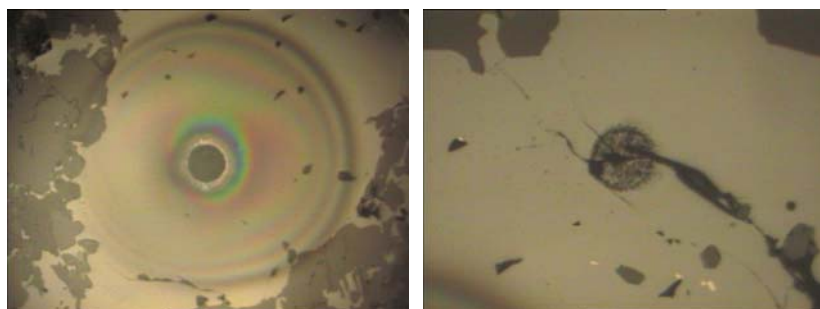
In situ laser ablation analysis is an efficient method to determine the trace element concentrations in a range of minerals. Sphalerite can, in some deposits, be an important host mineral for a wide range of minor and trace elements, including some of by-product interest. Here, the LA-ICP-MS technique investigates the distribution of Ag, As, Bi, Cd, Co, Cu, Fe, Ga, Ge, In, Mn, Mo, Ni, Pb, Sb, Se, Sn and Tl in sample L-12 Sp skarn

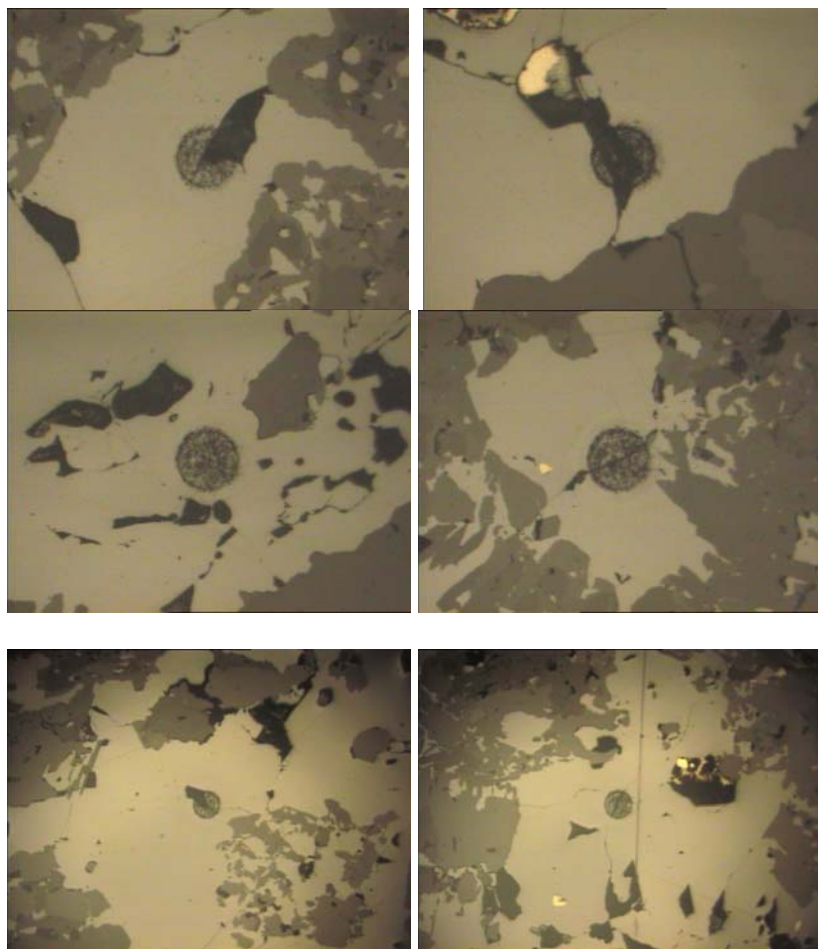
Analytical

LA-ICPMS analysis of sphalerite was made using the Agilent HP4500 Quadripole ICP-MS instrument at CODES (University of Tasmania, Hobart, Australia). This instrument is equipped with a high-performance New Wave UP-213 Nd:YAG Q-switched laser ablation system equipped with MeoLaser 213 software. The laser system was operated at constant 5 or 10 Hz pulse rate; laser energy was typically $5\text{--}6\text{ Jcm}^{-2}$. Pre-defined areas of the polished blocks were ablated; spot sizes of the 186 analyses varied from 25 to 80 μm in diameter. The following isotopes were monitored: ^{55}Mn , ^{57}Fe , ^{59}Co , ^{60}Ni , ^{65}Cu , ^{66}Zn , ^{69}Ga , ^{72}Ge , ^{75}As , ^{77}Se , ^{95}Mo , ^{107}Ag , ^{111}Cd , ^{115}In , ^{118}Sn , ^{121}Sb , ^{125}Te , ^{197}Au , ^{202}Hg , ^{205}Tl , ^{208}Pb and ^{209}Bi . Total analysis time (30 s pre-ablation and 60 s ablation time) was 90 s.

Calibration was performed using an in-house standard (STDGL2b-2), comprising powdered sulfides doped with certified element solutions and fused to a lithium borate glass disc. This standard is suitable for quantitative analyses in different sulfide matrixes. An integration time of 0.02 seconds was used for each of the elements measured. The raw analytical data for each spot analysis was plotted as a line graph and the integration times for background and sample signal selected. The counts are then corrected for instrument drift (standards were run each two hours) and converted to concentration values using known values of a major element in the analyzed minerals as an internal standard. Knowing the sphalerite composition, Zn was set in 'analogue' mode and this element served as an internal standard (IS) to quantify the analyses. The average cps of four STDGL2b-2 standard analyses run each two hours are used to calculate the concentration of each measured element in ppm where the relationships between the standard and unknown is given by the formula: $(\text{cps/ppm})^{\text{IS}}_{\text{Std}}/(\text{cps/ppm})^{\text{El}}_{\text{Std}} = (\text{cps/ppm})^{\text{IS}}_{\text{Smp}}/(\text{cps/ppm})^{\text{El}}_{\text{Smp}}$. In this formula cps=counts per second; ppm=concentration; Std=standard (STDGL2b-2); Smp=unknown sample; IS=internal standard element; El=element analyzed.

The eight laser ablation holes in sphalerite grains in sample L-12 Sp skarn are shown in the following microphotographs:





Results

The following table summarizes the data for the 8 spots (mean, standard deviation, maximum and minimum, all in ppm). <mdl is less than the analytical minimum detection limit.

	Mean	S.D.	Max	Min
Mn	3050	889	5186	2396
Fe	103995	8228	119230	92428
Co	328	17	355	300
Ni	4.6	7.2	19.2	0.3
Cu	306	401	1268	107
Ga	0.8	0.6	2.1	0.3
Ge	2,3	0.6	3,7	1.8
As	0.3	0.3	0.9	<mdl
Se	16,2	2.1	19,2	12.9
Mo	0.2	0.2	0.8	0.1
Ag	3.4	1.3	5.2	2.5
Cd	10804	595	11945	10071
In	180	22	203	140
Sn	0.1	0.1	0,2	<mdl
Sb	0.1	0.1	0.4	<mdl
Te	0.1	0.1	0.4	<mdl
Au	<mdl	-	0.01	<mdl
Tl	0.1	0.1	0,4	<mdl
Pb	3.8	3.3	8.6	1.6
Bi	2.4	1.9	5.4	1.6

Interpretation and comments

The analyzed sphalerite in L-12 Sp skarn is fairly rich in Fe (mean 10.4% by wt.) and also contains minor contents of Mn (mean 0.3%) and Cd (ca. 1.0 %). Most trace elements that can be accommodated in sphalerite are low to very low – there is, for example, no apparent enrichment in the potentially economic elements Ga or Ge. Co content is relatively high though this is typical for skarn deposits. The single noteworthy exception is indium – the contents are very high with a mean of 180 ppm or 0.018% in a sphalerite-rich sample of the Lefevre skarn. If sufficient Zn resources as sphalerite were located, this could be of significant economic interest.

Sample L-15 skn

Background

Sample L-15 skn was collected from trench #13 of the Lefevre skarn workings at UTM 471,605 mE 5,434,182 mN \pm 10 m. The field label was L-15. 0483 was a 2.38 m chip sample collected May 24 2006 at UTM 471,614 mE / 5,434,179 mN is also from this northernmost trench. It is well fractured, very rusty hard skarn collected from the north wall of trench #13 ~1.5 m high. Sample 0483 ran 0.627 g/t Au and 0.225 g/t Ag, 54.4 Bi / 0.82 Te / 1.4 As / 0.3 Sb / 2.5 Pb / 47.3 Cu / 43.8 Zn / >100 W (all ppm) and 5.67% Fe (Howard 2006a). The sample was taken as a check of an estimate of the (trimmed) mean gold grade of the Lefevre skarn 1.4 g/t Au, so the gold value is reasonable. A duplicate sample near 0483, a “Chip sample over ~ 2 meters, from the wall of trench [#13], siliceous hornfels + pale green pyroxene-garnet skarn with pyrite and arsenopyrite, very rusty” ran 1.783 g/t Au (gold only analyzed, Caron 2006). This further confirms the mean gold estimate. Sample 0561 (unanalyzed) was collected here in 2008.

Polished section description

Field notes describe L-15 skn as “quartzitic hornfels, with sulfides”. The sample contains about 25% sulfides, chiefly pyrite.

Reflected light microscopy shows the sulfides have a very interesting texture. **Pyrite** forms a brecciated collomorphic texture (Fig. 1a-d), partially replaced by **marcasite**. Other sulfides include **chalcopyrite** (ca. 5% of total sulphides), **sphalerite** (1 % of total sulphides) and minor **pyrrhotite** (< 1 % of total sulphides). The gangue matrix is mostly quartz, with small amounts of Fe-Mg-Al-silicates. A slight tarnish on the chalcopyrite reveals internal (growth?) zoning. The sulphide matrix contains **very minor quantities of native bismuth and bismuthinite** (five grains, each < 10 μ m), but no gold minerals or tellurides were observed. **Scheelite** (CaWO₃), occurring as relative coarse grains exceeding 500 μ m in diameter, is a prominent accessory phase.

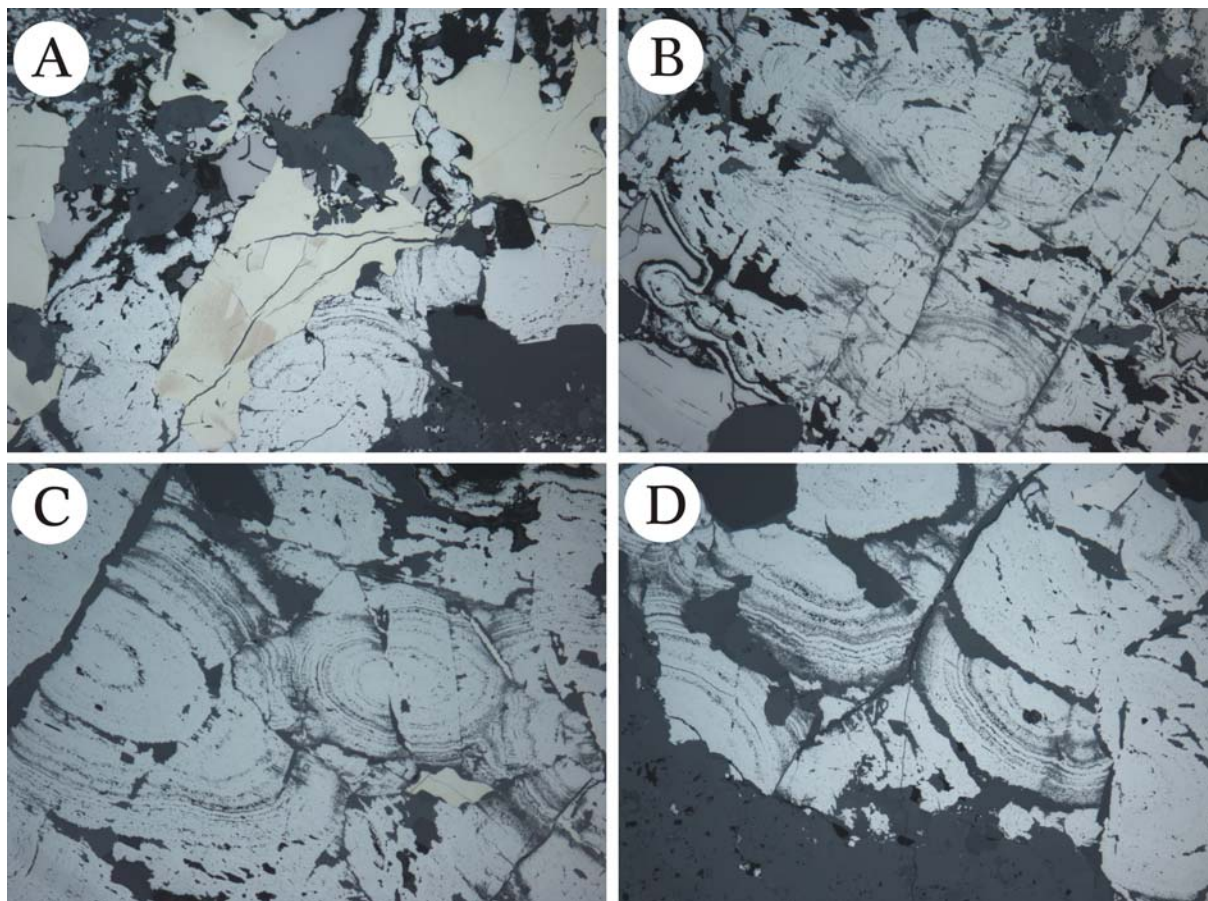


Fig. 1. Photomicrograph in reflected light showing typical textures. (A) Pyrite replaced by marcasite (grey-white), chalcopyrite (yellow) and sphalerite (medium grey). (B)-(D) collomorphic textures in pyrite – note these patterns have been brecciated and fractures and commonly overgrown – presumably during a post-formational event. Horizontal axis: 600 μm for all pictures.

Scanning electron microscopy did not reveal any compositional variation within pyrite or chalcopyrite.

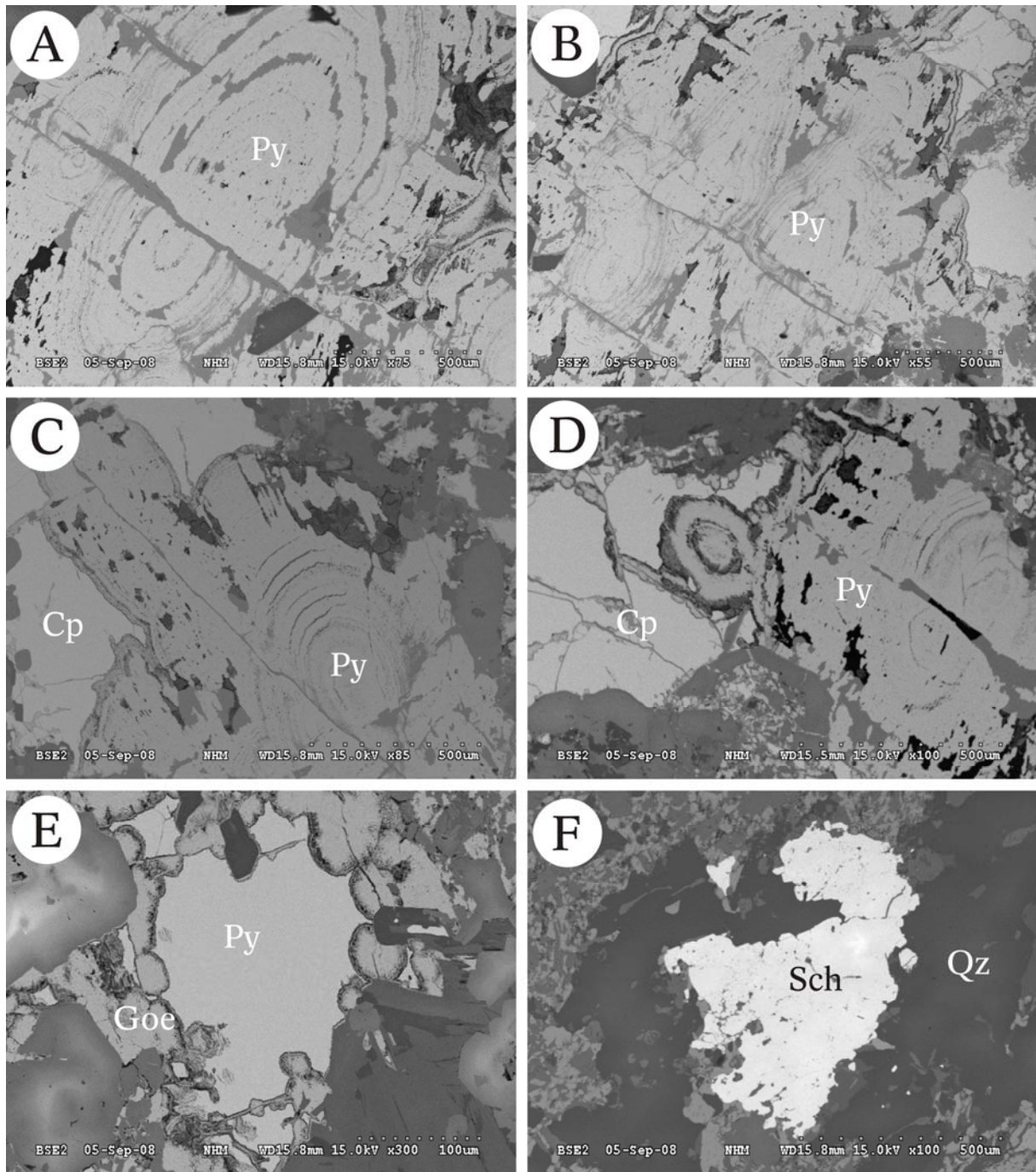


Fig. 2. Back-scattered electron microscope images showing aspects of sample L-15 skn. (A) and (B) show collomorph character of pyrite (Py). (C) and (D) Pyrite, undergoing alteration in association with chalcopyrite (Cp). (E) Breakdown of pyrite to goethite (Goe). (F) Scheelite grain in quartz matrix.

L-15 skn has moderately advanced secondary alteration. The collomorph textures are, however, primary and commonly observed in skarn deposits. This is probably the most Cu-rich sample viewed to date.

Polished sections from Bunker Hill mine veins

In 2006 the author investigated the mineralogy of a single sample from the Adit 2 Underhand Stope Vein at the former Bunker Hill mine in British Columbia MINFILE082FSW002 (Cook & Ciobanu). Four more samples are the subject of this present study: two additional samples of dump material documented to be from the Underhand Stope Vein mined in Adit 2, a sample from the Adit 1 Crush Vein and a sample from a trenched vein possibly north and slightly uphill of Adit 1. The objectives are to verify the mineralogy of the veins, particularly with respect to the association of gold with bismuth and bismuth telluride minerals and sulphides, and to compare the findings with other veins on the CLY – Nox Fort property, particularly the gold-associated mineralogy of Eloise Vein and the Blue Quartz Vein on BiTel Knoll and a vein crosscutting hornfels of the Lefevre skarn L-04QVXtry (which see).

The samples were studied using conventional reflected light ore microscopy and scanning electron microscopy [SEM] at the Natural History Museum, University of Oslo. Many of the SEM Energy Dispersive Spectroscopic analyses (SEM-EDS) were in back-scattered mode. This allows the SEM images to express mineral brightness as a function of the average atomic weight, i.e. pyrite appears brighter than low atomic-weight quartz but less bright than ‘heavy’ gold.

Sample BH UHS 1 from Adit 2 Underhand Stope Vein, Bunker Hill mine

Background

BH UHS 1 is a piece from the lower roadside dump in front of Adit 2 of the Bunker Hill mine. It is part of the unshipped ~91 ton portion, half of what was mined from the Underhand Stope Vein [UHS Vein] in 1934 (Annual Report Minister of Mines 1934, 1936). Simple calculation shows the entire lot mined runs a *minimum* 10.73 g/t Au and 7.54 g/t Ag (Annual Report Minister of Mines 1936 p. E20). Field label was UHS-1, site is at UTM 471,428 mE 5,434,282 mN ± 10 m.

G. Ray (2003 p. 23) described the Adit 2 vein material as “gold-bearing quartz + pyrite ± pyrrhotite ± arsenopyrite ± sphalerite ± galena ... sporadically enhanced in Ag, Bi, As, Te and possibly Se.” Presence of the latter three minerals is not supported by an earlier geochem analysis of BH-306 with 29.76 g/t Au by FA, 2.9 Ag / 1,150 Bi / 92 Te / 141 Cu / 60 Pb / 8 Zn / 13 As / (all ppm) in Howard (2000). Rock #362645 a selected grab sample of the dump ran 3.87 g/t Au (Caron 2006). Only gold was analyzed in that sample. Howard (2006a p. 42-45) describes the locale, hand specimens, geochemistry and genesis.

The former examination of similar UHS Vein sample (Cook & Ciobanu 2006) found small inclusions of galena in pyrite grains – in turn galena contains sub-10 µm inclusions of **cosalite**, Bi₂Pb₂S₅ a Bi-sulphosalt. This is evidently the “unidentified Bi-Pb mineral, probably galenobismutite PbBi₂S₄” identified in the early ore petrography study by H.V. Warren & J.C. Cummings (1937). They observed “Gold is present as a telluride which, in close association with an unidentified bismuth mineral, veins pyrite. Gold - bearing telluride has been introduced during a late period of mineralization ... in fractured portions of an old period of mineralization”. Warren likely collected that mineralized piece, much like BH UHS 1, from Underhand Stope Vein production while mapping Adit 2 in 1934 with A.G. Langley for Waneta Gold Mines, Limited (Annual Report Minister of Mines 1934).

Polished section description BH UHS 1

Sample BH UHS 1 consists of milky quartz with a small proportion (circa 1 volume %) of pyrite and trace amounts of pyrrhotite, bismuth minerals, galena and the Ag-telluride **hessite** (Ag_2Te).

Reflected light microscopy reveals a number of patches, typically 50-100 μm in size, of bismuth minerals either associated with the pyrite or enclosed within quartz. Smaller patches occupy grain boundaries within the quartz matrix. One larger patch, ca. 300 μm across is investigated in detail (Figs. 1 and Fig. 2). The other smaller patches observed consist of native bismuth and bismuthinite only. Some of the bismuth minerals have been altered to various undetermined oxides and/or hydroxides. No gold minerals are observed in this polished section.

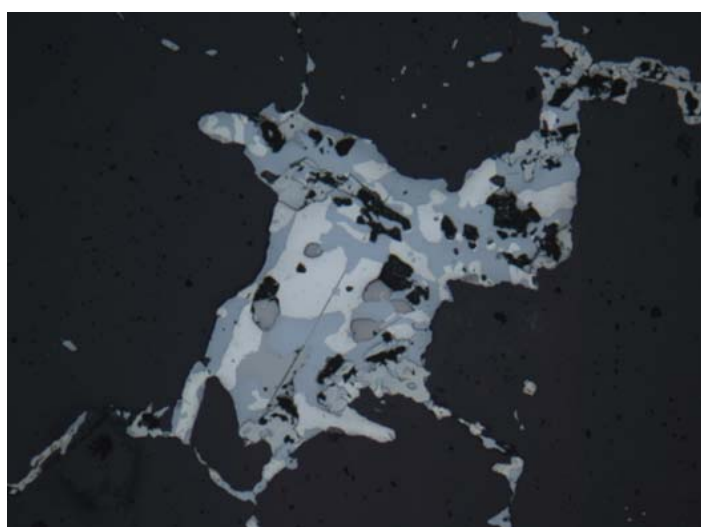


Fig. 1. Reflected light colour photomicrograph of the ca. 300 μm bismuth mineral patch in BH UHS 1. The main mineral in the patch (medium grey) is bismuthinite; native bismuth appears very light grey. Hedleyite, pyrite and pyrrhotite all appear slightly brownish next to very light grey native bismuth. The ‘higher relief’ darkest brown mineral is magnetite. The lighter pink-brown mineral, for one the elongate grain toward the upper right side, is pyrrhotite. Black matrix is quartz, horizontal axis is 450 μm .

The ca. 300 μm (0.3 mm) patch consists of **magnetite** and **native bismuth** (Bi) in a matrix of **bismuthinite** (Bi_2S_3), **hessite** (Ag_2Te) and minor **hedleyite** (Bi_7Te_3) and trace **joséite-B** ($\text{Bi}_4\text{Te}_2\text{S}$); Fig. 2 has back-scattered SEM images. **Hessite** is new for this locality and first described in this report. Magnetite, native bismuth, bismuthinite, hedleyite and joséite-B are first described in the Adit 2 Underhand Stope Vein herein.

Interestingly, both pyrite and pyrrhotite form part of the patches in BH UHS 1. Both these iron sulfides and hedleyite look uncharacteristically slightly brown and grey against the native bismuth and/or bismuthinite grains. The presence of pyrite and pyrrhotite, never in texturally-stable grain contact with one another but displaying textures of resorption and partial replacement, suggest a later overprinting event modified the assemblage, at least locally.

In a similar UHS vein sample Cook & Ciobanu (2006) found pyrite the dominant ore mineral; “marcasite is also present – the latter appears to have been formed from pyrrhotite. In addition there are some relicts of pyrrhotite within pyrite. Scarce chalcopyrite and bornite are noted...” In that sample “Gold is abundant as fine- to very-finely dispersed inclusions within pyrite (never marcasite). Many of these are sub-microscopic. Larger grains (though still only 10-20 μm in size) are noted along pyrite grain boundaries or at triple points between pyrite grains. The gold (electrum) is relatively Ag-rich ($\sim\text{Au}_{55}\text{Ag}_{45}$). Some gold is also seen outside of the pyrite domains or at the boundaries of pyrite with gangue.”

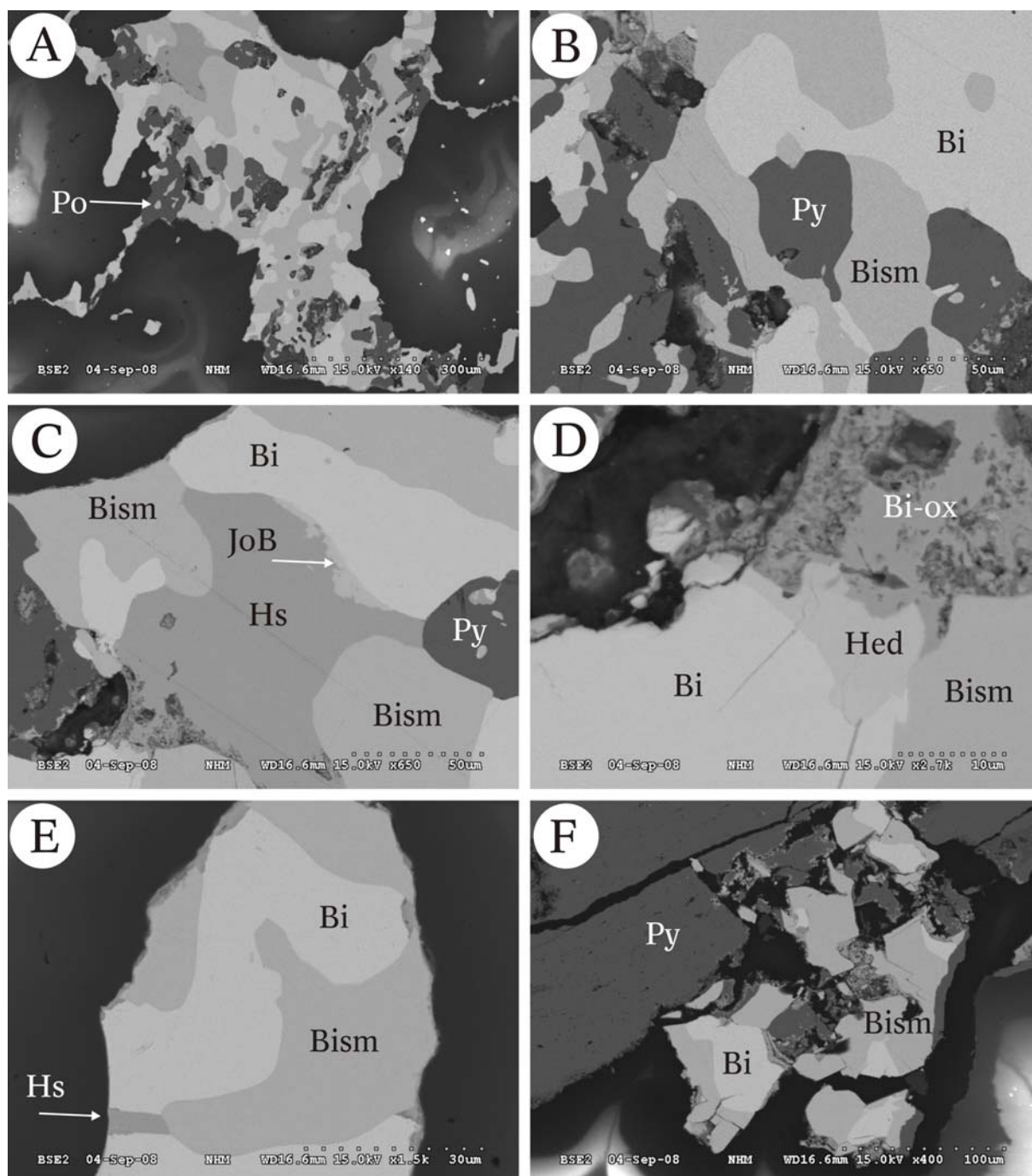


Fig. 2 Back-scattered SEM images of Bi-mineral assemblages in the ca. 300 μm patch of sample BH UHS 1. (A) Overview, dark grains within the patch are pyrite and pyrrhotite. Note pyrite surrounds small grains of relict pyrrhotite (lighter). (B), (C) and (D) show detail of (A). These left-over small inclusions of Po in many of the Py

grains show replacement was only partial. Minerals were deposited (or modified) at conditions fairly close to the py/po stability boundary. Figure shows highly localised oxidized and/or reduced domains. Dominantly, the assemblage must have been formed in a reducing pyrrhotite-stable environment, with a more oxidising overprint. Much, if not all, of the pyrite must have formed after pyrrhotite. (A) Lightest grey is native bismuth; medium grey bismuthinite envelops & replaces native bismuth grains. This is analogous to pyrite formation after pyrrhotite. Both reactions are expressions of sulfidation. (B) Find fish-shaped relict Po grain, colour like Bism, in Py at SW corner of image. (C) clearly displays Jo-B exsolved out of hessite, possibly during cooling. Hessite cannot incorporate even small amounts of S or Bi, so these elements are expelled, together with some Te to form the discrete mineral Jo-B, which has nucleated at the margin of the grain. This is not a replacement texture. (D) is highly magnified, the location is in the top left hand corner of the grain above the arrow to 'Po' in (A). Hed + Bi + Bism appear in textural equilibrium. (E) is a typical smaller patch consisting of native bismuth bismuthinite and hessite. Bi + Bism are in equilibrium (there is no replacement). Evidently this 'bleb' didn't contain enough S to form only Bis, so Bi + Bism formed together with nice curvilinear boundaries. In (E) hessite looks to exsolved out of the Bi-minerals - the opposite of the case in C - as only very low amounts of silver can enter Bism. All Fig. 2 images show effectively closed systems, each with a distinct chemistry, expressed by the observed mineralogy. (A) and (F) show deformed and partially replaced assemblages of pre-existing bismuth and bismuthinite. Note the grains have been fractured, presumably during overprinting. Both minerals are subsequently attacked (altered) to form a rather messy assemblage. It is unsure how much of the 'alteration' seen in this polished section and others is supergene and how much resulted from the action of the 'latest' fluids during the overprint. Mineral abbreviations: Bi - native bismuth; Bism - bismuthinite; Bi-ox – unidentified bismuth oxides/hydroxides; JoB – joséite-B; Hs - hessite; Hed – hedleyite; Po – pyrrhotite; Py – pyrite. The matrix mineral (black) is quartz.

Table of semi-quantitative SEM-EDS analyses of phases in sample BH UHS 1, elements in wt. %:

Phase Analyzed	Cu	Ag	Bi	Pb	Sb	Te	Se	S	Total
Hessite 1	-	58.31	-	-	1.44	39.58	0.68	-	100.01
Hessite 2	-	61.22	-	-	0.55	38.16	0.14	-	100.07
Bismuthinite 1	-	-	79.76	-	0.22	-	0.12	18.03	98.13
Bismuthinite 2	-	-	80.88	0.08	0.25	-	0.13	17.77	99.11
Native bismuth 1	-	-	96.62	0.71	2.27	-	0.75	-	100.35
Native bismuth 2	-	-	97.29	0.11	1.05	-	0.11	-	98.56
Hedleyite 1	-	-	79.87	-	0.14	19.54	-	-	99.55
Hedleyite 2	-	-	79.77	-	0.22	19.22	-	-	99.21

The analyzed phases are near-stoichiometric excepting the two hedleyite analyses:

Hessite ideally Ag_2Te , formulae with sums

Phase Analyzed	Cu	Ag	Bi	Pb	Sb	Metal Sum	Te	Se	S	Chalcogen Sum
Hessite 1	-	1.86	-	-	0.04	1.90	1.07	0.03	-	1.01
Hessite 2	-	1.95	-	-	0.02	1.97	1.03	0.01	-	1.03

Bismuthinite ideally Bi_2S_3 , formulae with sums

Phase Analyzed	Cu	Ag	Bi	Pb	Sb	Metal Sum	Te	Se	S	Chalcogen Sum
Bismuthinite 1	-	-	2.01	-	-	2.02	-	0.01	2.97	2.98
Bismuthinite 2	-	-	2.05	-	0.01	2.06	-	0.01	2.93	2.94

Native bismuth ideally Bi, formulae with sums

Phase Analyzed	Cu	Ag	Bi	Pb	Sb	Metal Sum	Te	Se	S	Total Sum
Native bismuth 1	-	-	0.94	0.01	0.04	0.98	-	0.02	-	1.00
Native bismuth 2	-	-	0.98	-	0.02	1.00	-	-	-	1.00

Hedleyite ideally Bi_7Te_3 , formulae is in the range of $\text{Bi}_{2+x}\text{Te}_{1-x}$ ($x = 0.13$ to 0.19)

Phase Analyzed	Cu	Ag	Bi	Pb	Sb	Metal Sum	Te	Se	S	Chalcogen Sum
Hedleyite 1	-	-	7.12	-	0.02	7.15	2.85	-	-	2.85
Hedleyite 2	-	-	7.15	-	0.03	7.18	2.82	-	-	2.82

Although no gold minerals are observed in sample BH UHS 1, the occurrence of bismuth minerals, similar to those seen elsewhere in the other veins on CLY, is a good indication that the vein systems on CLY are directly comparable in terms of overall metal signature: Au(Ag)-Bi-Te.

Observations on BH UHS 1 suggest the Bi-Te mineral assemblages initially formed in the pyrrhotite stability field. Thereafter there was a sulphidising overprint at more oxidizing conditions, forming pyrite at the expense of pyrrhotite and bismuthinite at the expense of native bismuth. This also modified some tellurides, resulting in some cases with the metal:chalcogen ratio $\text{Bi}/\text{X} < 1$ which is otherwise atypical for reduced systems, namely most gold skarns.

Sample BH UHS-4 from Adit 2 Underhand Stope Vein, Bunker Hill mine–

Background

The sample was collected from the upper dump of the ‘Underhand Stope Vein’ in front of Adit 2 of the Bunker Hill mine. It was selected as the former study found gold grains amongst pyrites (Cook & Ciobanu 2006). Field label was UHS-4, site at UTM 471,428 mE 5,434,282 mN \pm 10 m.

Polished section description

The sample is essentially vein quartz with variable quantities of pyrite. The polished section was prepared from a portion of the sample containing ca. 15% pyrite by volume. Reflected light microscopy reveals that the sulphide is mostly all **pyrite**; individual grains attain dimensions to 1 mm. Pyrite contains abundant inclusions of bismuth minerals: mostly **bismuthinite**, some **native bismuth**. The majority are partially altered to bismuth oxides and/or hydroxides. The pyrite also includes **electrum grains**, all restricted to pyrite-bearing parts of the sample and not in the quartz. (Definition: electrum is native gold with 20-80% silver by weight.) Two grains of **scheelite** were also noted – this report first identifies this calcium tungstate mineral in the Bunker Hill mine veins. No tellurides were observed.

More than 20 individual grains of electrum were counted (Figs. 1 and 2). The majority of these are less than 10 μ m in diameter. Many are elongate to 30 μ m long. Some (10%) are in paragenetic association with bismuthinite; there is no discrimination in size between gold grains by themselves or those together with bismuthinite, a single population is evident. Otherwise electrum occurs as monophase inclusions in the pyrite grains. Some are clustered within, seemingly aligned along pyrite grain cleavage planes (Fig. 1).

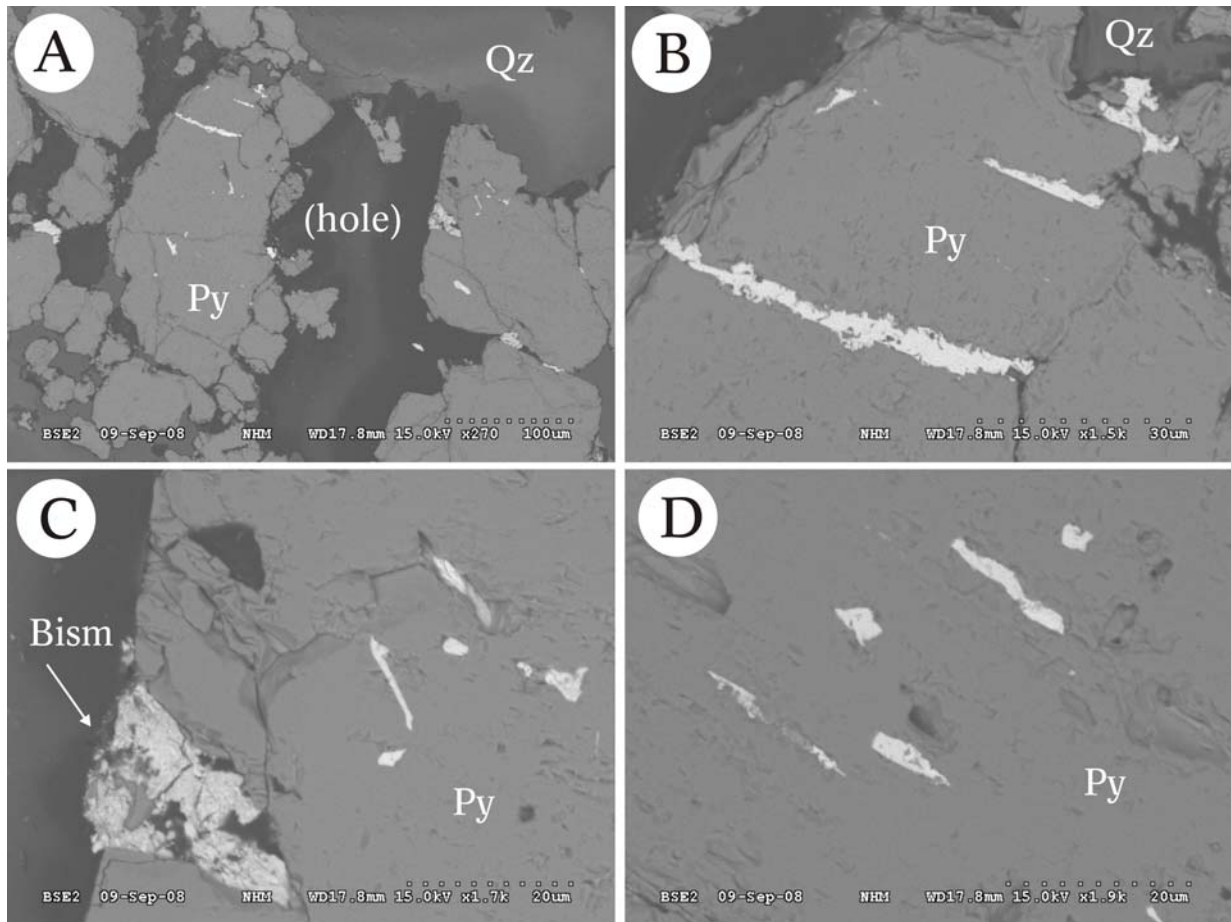


Fig. 1. Back-scattered SEM images showing clustered grains of electrum (bright white) in matrices of pyrite grains (Py, grey). Bism – bismuthinite; Qz - quartz. Note many are elongate with aspect ratios 5:1 or more.

Semi-quantitative Energy-Dispersive Spectroscopic (EDS) analyses of the electrum grains show most are silver-rich, occupying a central position in the Au-Ag solid solution series. Individual ‘atomic’ fineness values¹ of eight grains are close together, 0.517, 0.498, 0.561, 0.566, 0.558, 0.528, 0.522 and 0.416. The average is 0.521. No minor admixtures were noted.

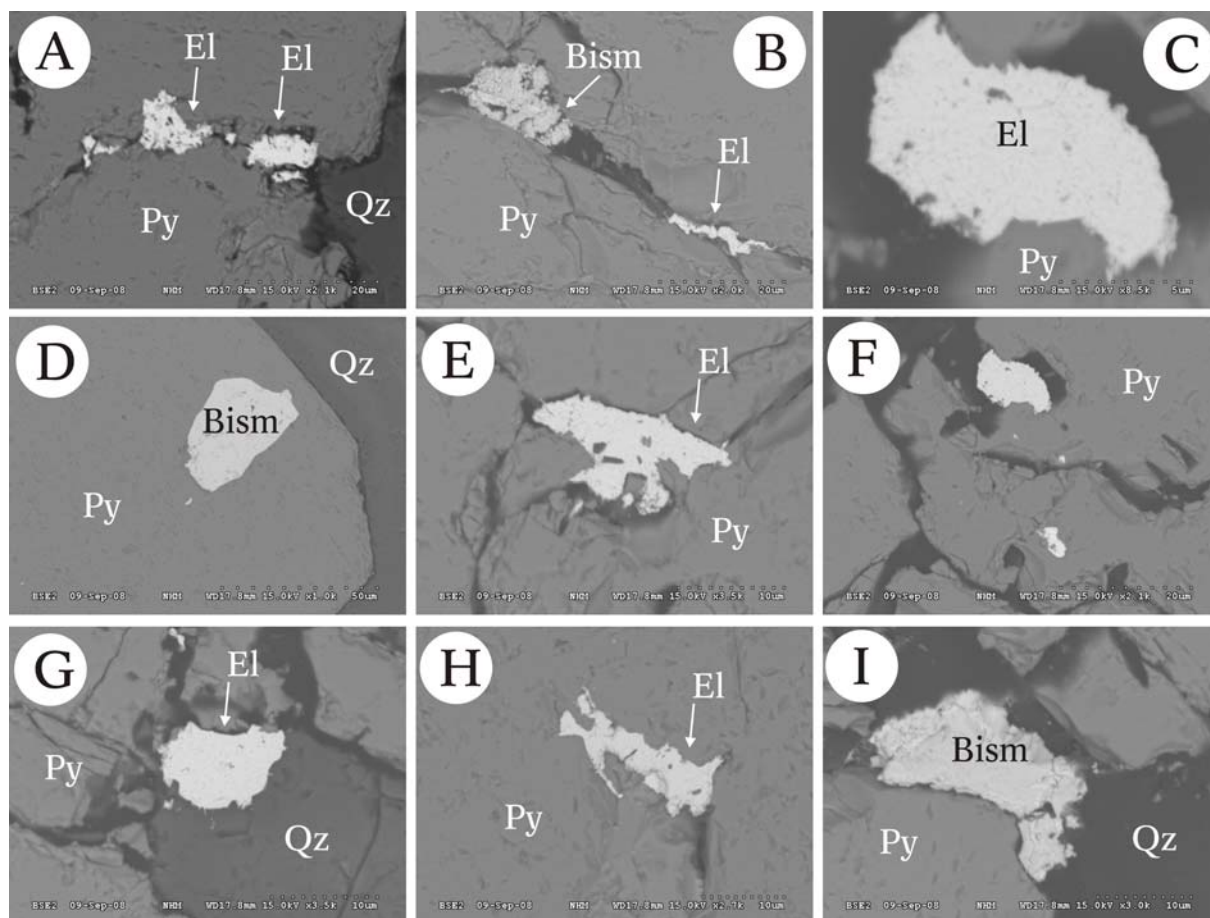


Fig. 2. (A) to (H). Back-scattered SEM images showing grains of electrum (El) and (I) bismuthinite (Bism) in pyrite matrix (Py, grey); Qz - quartz.

Mineralogical study of this sample gives two important pieces of information. Firstly, these veins do carry significant amounts of gold, as fine-sized grains not necessarily tied to Bi-minerals. Secondly, **gold grains are closely associated with pyrite** and not finely distributed throughout the quartz. This was known previously: “The operation of the old 10-stamp mill erected in 1900 is reported to have been of very short duration as the ore was not amenable to straight amalgamation, the gold values being chiefly associated with pyrite (AR 1934 p. E24)”.

Concluding, pyrite content of the Bunker Hill mine veins may be a reliable indicator of gold content.

¹ Atomic fineness, not fineness by wt. %

Sample BHA-1-8 Adit 1 Crush Vein of Bunker Hill mine

Background

BHA-1-8 was collected from the dump of Bunker Hill mine Adit 1, very likely from the 'Adit 1 Crush Vein' mined in 1900 (1901 Annual Report of the Minister of Mines p. 846). Early production is unrecorded (1933 Annual Report of the Minister of Mines p. A238). The Adit 1 Crush Vein was mined for a length of 135' (41 m) before fault offset. A columnar ore shoot of this was stoped-to-surface in 1934 (1934 Annual Report of the Minister of Mines). Sample site is UTM 471,463 mE 5,434,276 mN \pm 10 m, field label UHS 8 but it is not from the Adit 2 Underhand Stope Vein. A select grab sample #BH-059 collected by L. Caron near the BH-059 sample flag of the Adit 1 Gallery Quartz Vein (not examined), is "massive white to bluey-grey vitreous quartz with 5% very fine sulfides [and bismuth tellurides] which give quartz a bluish colour, and patchy coarse frothy pyrite. With minor vugs (Caron, 2006)." This ran 0.122 oz. / ton gold (4.18 g/t), gold only analyzed.

Polished section description

The sample consists of clear quartz with variable proportions (generally 1-10 vol. %) of **pyrite**. The pyrite tends to occur in clusters; individual pyrite cubes are up to a couple of mm in size. The polished block was prepared from an area of the sample in which pyrite was about 15 vol. %.

Reflected light microscopy of a polished block reveals that small quantities of bismuth minerals are contained within the pyrite. Typically, the bismuth minerals occur as inclusions in pyrite and are particularly concentrated towards the pyrite margins. These also however occur outside pyrite grains within quartz. They seldom exceed 50 μ m in diameter but are abundant. Small amounts of native gold occur associated with the bismuth mineral patches.

Native bismuth and bismuthinite are the most abundant bismuth phases observed in the inclusions. Bismuthinite grains are commonly partially decomposed to unidentified bismuth oxides and/or hydroxides. Several telluride species are, however, noted in the sample: most abundant is **joséite-B** ($\text{Bi}_4\text{Te}_2\text{S}$), **hedleyite** (Bi_7Te_3), **pilsenite** (Bi_4Te_3) and **ikunolite** (Bi_4S_3). **Pilsenite has not been previously reported from the CLY property.**

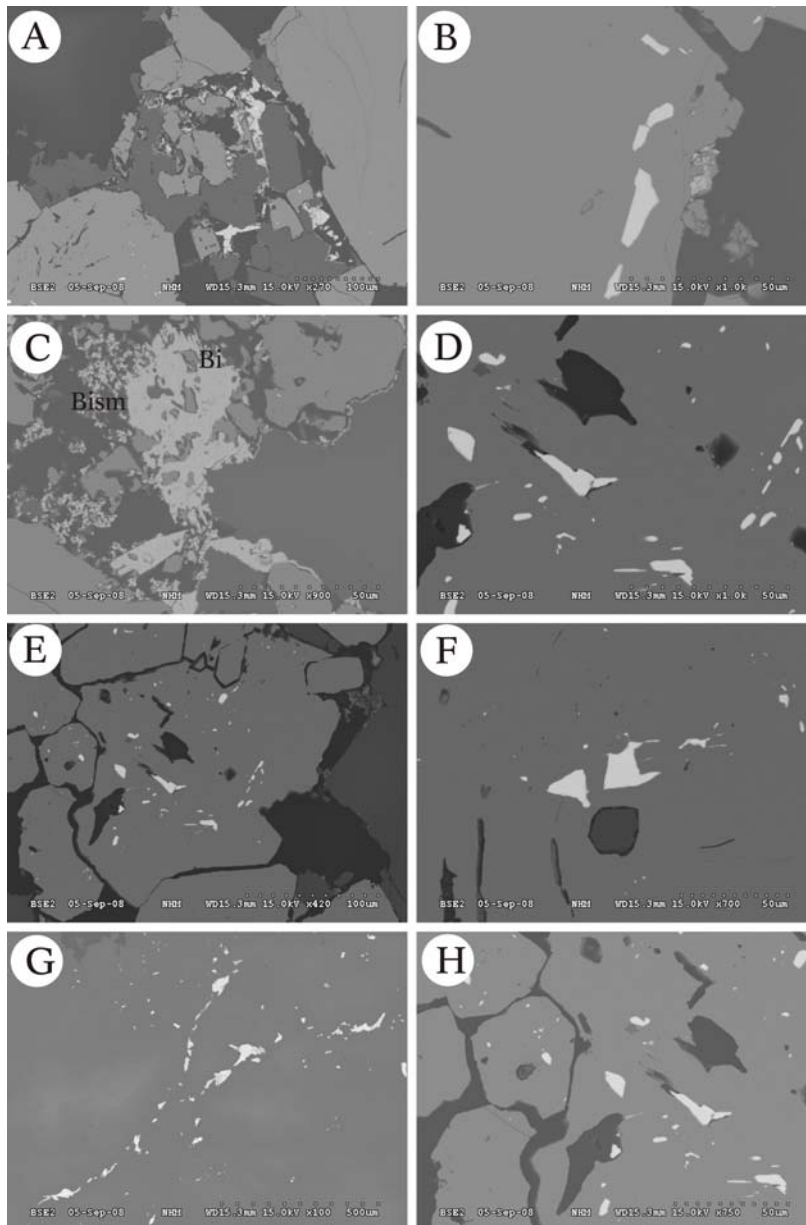


Fig. 1. Back-scattered scanning electron microscope images of BHA-1-8 showing small inclusions of bismuth minerals (bright white) associated with pyrite (medium grey matrix); black is quartz. Note in particular bismuth inclusions may align within pyrite grains - parallel to cleavage planes - and are often concentrated towards pyrite grain margins (e.g. image 1B). In Fig. 1A & 1C darkest mineral is quartz, third darkest is pyrite, obvious from its crystal morphology. Both native bismuth and bismuthinite occur but are not easy to distinguish in the low contrast image of Fig. 1C. Most of the messy looking grains are bismuthinite, whereas 'cleaner looking' parts are native bismuth. The second darkest grey minerals (immediately around the Bi-minerals) are Fe-oxides / hydroxides, most probably goethite, but the BSE method does not allow for their identification. Fig. 1F is of two tetradymite ($\text{Bi}_2\text{Te}_2\text{S}$) grains in pyrite and a ringed hole.

Also noted for the first time from the locality is **tetradymite** ($\text{Bi}_2\text{Te}_2\text{S}$), the two grains in Fig. 1F and the grain in Fig. 2B coexisting with electrum. Tetradymite is not associated with other Bi-tellurides, but occurs as a monophase inclusion within pyrite. It is not normally chemically stable with joséite-B, hedleyite etc., but evidently it is stable here as it is buffered by an enclosing pyrite grain. Tetradymite $\text{Bi}_2\text{Te}_2\text{S}$ has a metal:chalcogen ratio "2:3", thus $(\text{Bi} + \text{Pb} + \text{Sb}) / (\text{Te} + \text{Se} + \text{S}) < 1$ in contrast with the other bismuth tellurides present. Other minor opaque minerals noted include **galena** and **chalcopyrite**.

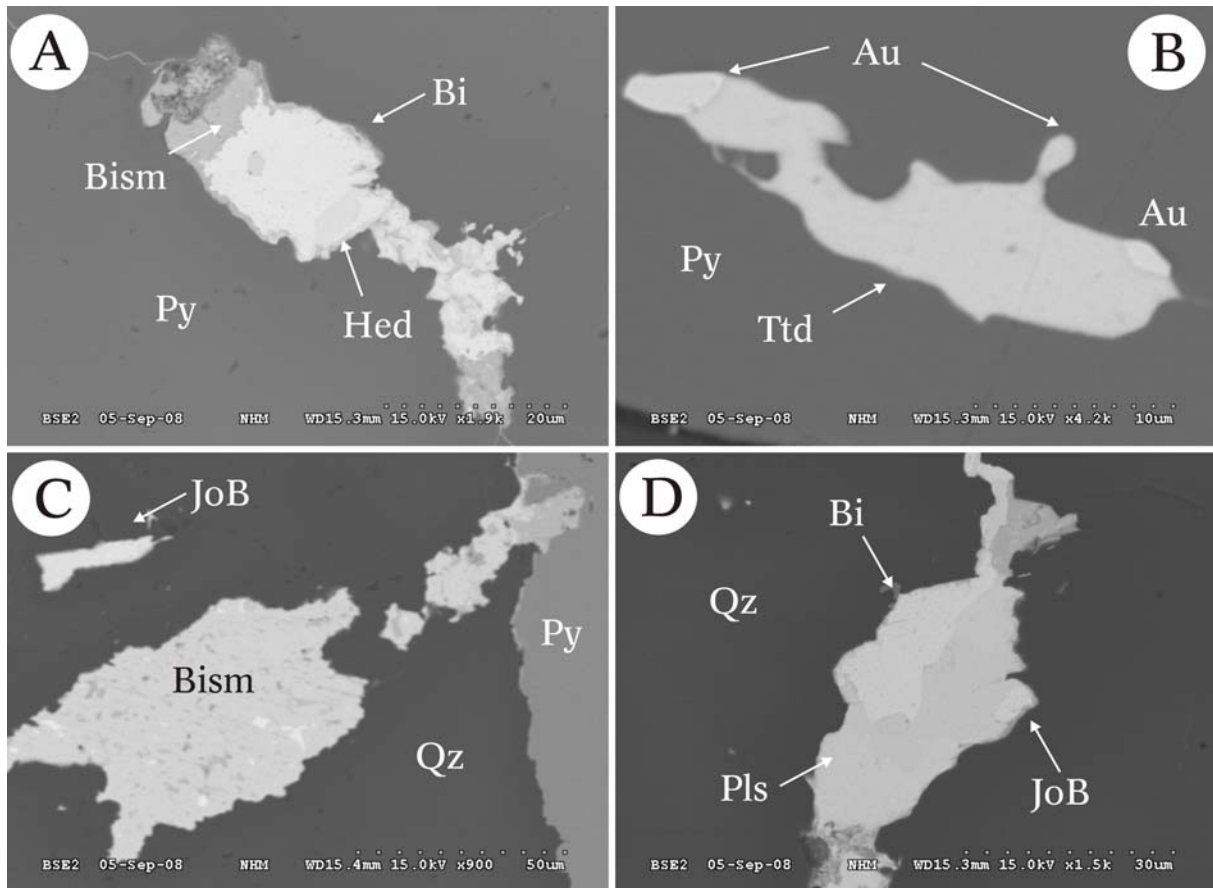


Fig. 2. Back-scattered scanning electron microscope images showing details of bismuth mineral inclusions in sample BHA-1-8. Abbreviations: Au – electrum; Bi – native bismuth; Bism – bismuthinite; Hed – hedleyite; JoB – joséite-B; Pls – pilsenite; Py – pyrite; Qz – quartz; Ttd - tetradymite

Electrum was observed together with tetradymite (Fig. 2B) and in a smaller inclusion together with joséite-B. The electrum grains in Fig. 2B have approx. compositions $\text{Au}_{70}\text{Ag}_{30}$.

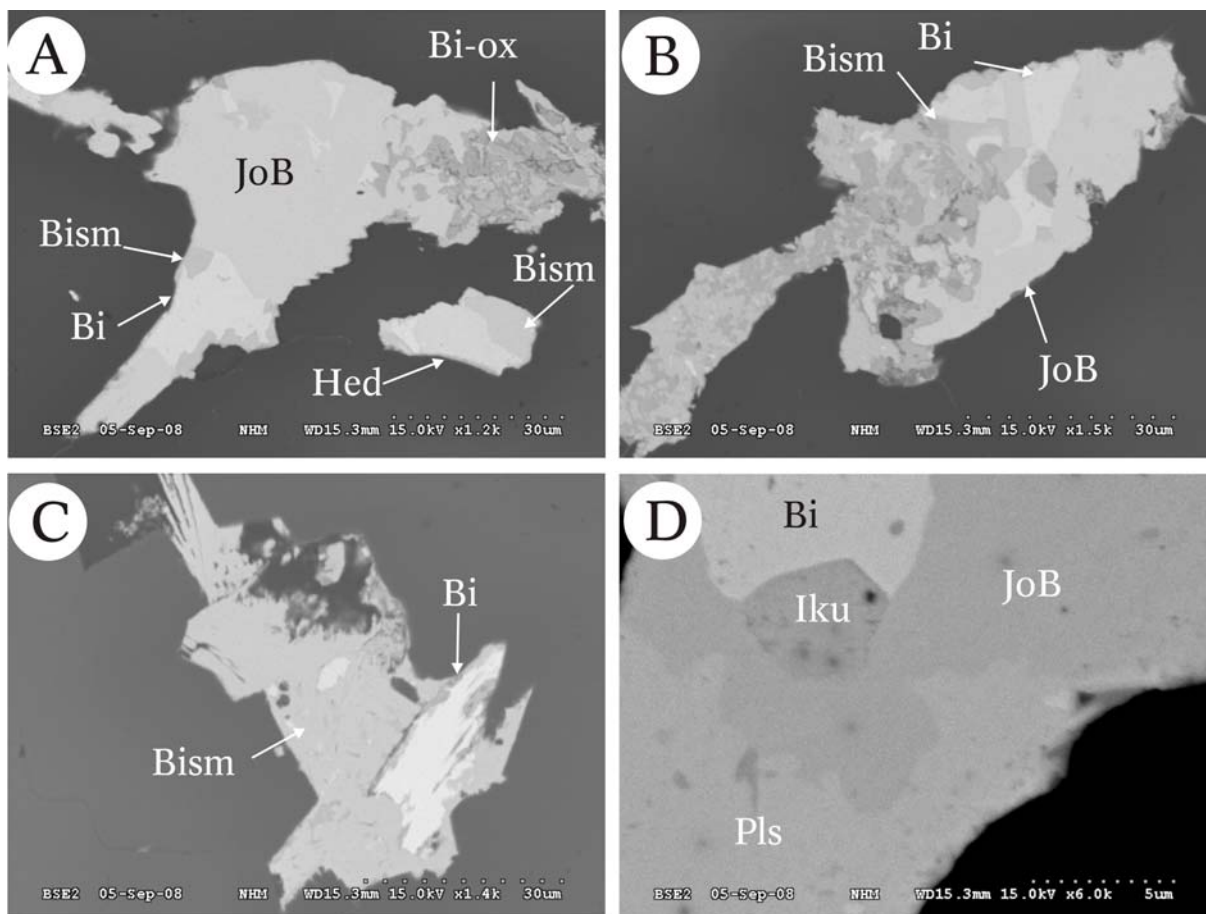


Fig. 3. Additional back-scattered scanning electron microscope images showing details of bismuth mineral inclusions in sample BHA-1-8. In (3A) Bi and JoB appear to be in textural equilibrium with one another in the larger patch. Hed is clearly in equilibrium with Bism in the smaller patch; presumably excess sulphur enabled JoB rather than Hed to form in the larger path. In (3B) Bi and JoB again appear to be in textural equilibrium; Bism may be later. Image (3C) shows native bismuth within bismuthinite. Texture suggests Bism replaces Bi. Image (3D) is from an area beyond the top of the area shown at lower magnification in (B). A small grain of ikunolite is positioned between JoB and Bi. This looks like a stable assemblage. Indented ‘dental caries’ texture infers pilsenite replaces JoB; possibly the released sulphur formed ikunolite. The association is unusual and atypical as ikunolite and pilsenite are unlikely to be stable together; this cannot be a ‘primary’ assemblage. Small-scale mobilization / diffusion of elements may have influenced formation of this micro-assemblage. If, however, pilsenite replaces JoB the assemblage is contrary to the more widely identified, later-stage superimposed sulfidation trend. Abbreviations: Bi – native bismuth; Bi-ox – unspecified bismuth oxides/hydroxides; Bism – bismuthinite; Hed – hedleyite; Iku – ikunolite; JoB – joséite-B; Pls – pilsenite.

Semi-quantitative SEM-EDS analyses give compositions of bismuth minerals in BHA-1-8. Analyses are referenced to the labeled photomicrographs:

Analyzed grain in:	Cu	Ag	Bi	Pb	Sb	Te	Se	S	Total
Fig. 1F									
*Tetradymite	-	-	57.55	4.98	-	27.99	-	4.12	94.75
Fig. 2A									
Hedleyite	-	-	81.46	1.35	0.60	19.11	-	-	102.52
Fig. 2B									
*Tetradymite	-	-	57.75	2.93	0.26	30.67	0.23	5.46	96.30
Fig. 3A									
Bismuthinite	0.30	-	72.48	10.02	-	-	0.22	16.31	99.33
Bismuthinite	0.78	-	70.68	15.38	0.14	-	-	15.01	101.99
*Joséite-B 1	-	-	68.43	2.03	-	22.77	0.75	1.96	95.94
*Joséite-B 2	0.51	0.08	68.68	-	0.08	23.42	1.23	2.51	96.51
Fig. 3B									

*Joséite-B 1	-	-	69.03	2.08	-	22.54	0.93	2.07	96.65
Joséite-B 2	-	-	73.61	-	-	22.67	1.14	2.58	100.00
Fig. 3D									
Joséite-B 1	-	0.16	70.75	0.94	0.92	21.88	1.51	2.06	98.22
*Joséite-B 2	-	-	70.13	-	-	21.39	1.87	2.44	95.83
Pilsenite	-	0.02	74.04	-	-	24.31	0.48	0.59	99.44
Ikunolite 1	-	-	80.07	5.55	-	5.25	0.15	8.46	99.48
Ikunolite 2	-	0.64	81.67	4.38	-	4.40	0.05	8.90	100.04

* low wt % total < 97%

Tetradymite ideally $\text{Bi}_2\text{Te}_2\text{S}$, formulae with sums

Mineral	Bi	Pb	Sb	Metal Sum	S	Se	Te	Chalcogen Sum
*Tetradymite Fig. 1F	2.13	0.19	-	2.31	0.99	-	1.69	2.69
*Tetradymite Fig. 2B	1.96	0.01	0.02	2.07	1.21	0.02	1.70	2.93

Second analysis is preferred but still suspect.

Hedleyite ideally Bi_7Te_3 , but formula is non-stoichiometric, outside of the range $\text{Bi}_{2+x}\text{Te}_{1-x}$ ($x = 0.13$ to 0.19)

Mineral	Bi	Pb	Sb	Metal Sum	Te	Se	S	Chalcogen Sum
Hedleyite Fig. 2A	7.07	0.12	0.09	7.28	2.72	-	-	2.72

Bismuthinite–aikinite ideally $\text{Bi}_2\text{S}_3 - \text{CuPbBiS}_3$, formulae with sums

Mineral	Bi	Pb	Cu	Sb	Metal Sum	S	Se	Chalcogen Sum
Bismuthinite–aikinite 1 Fig. 3A	1.90	0.27	0.03	-	2.19	2.79	0.02	2.81
Bismuthinite–aikinite 2 Fig. 3A	1.86	0.42	0.07	0.01	2.38	2.62	-	2.62

Joséite–B ideally Bi_4STe_2 , formulae with sums

Mineral	Ag	Cu	Bi	Pb	Sb	Metal Sum	S	Se	S + Se Sum	Te
*Joséite–B 1 Fig. 3A	-	-	3.91	0.12	-	4.03	0.73	0.11	0.84	2.13
*Joséite–B 2 Fig. 3A	0.01	0.09	3.74	-	0.01	3.85	0.89	0.18	1.07	2.09
*Joséite–B 1 Fig. 3B	-	-	3.90	0.12	-	4.02	0.76	0.14	0.90	2.08
Joséite–B 2 Fig. 3B	-	-	3.95	-	-	3.95	0.90	0.16	1.06	1.99
Joséite–B 1 Fig. 3D	0.02	-	3.90	0.05	-	4.06	0.74	0.22	0.96	1.98
*Joséite–B 2 Fig. 3D	-	-	3.90	-	-	3.90	0.88	0.27	1.16	1.95
BHA-1-8 average	0.01	-	3.925	0.025	-	4.005	0.82	0.19	1.01	1.985
Joséite–B n=2										

* low wt % total < 97%

Pilsenite ideally Bi_4Te_3 , formula with sums

Mineral	Bi	Pb	Sb	Metal Sum	Te	Se	S	Chalcogen Sum
Pilsenite Fig 3D	4.35	-	-	4.36	2.34	0.07	0.23	2.64

Ikunolite ideally Bi_4S_3 , formulae with sums

Mineral	Cu	Ag	Bi	Pb	Sb	Metal Sum	Te	Se	S	Chalcogen Sum
Ikunolite 1 Fig 3D	-	-	3.74	0.26	-	4.00	0.40	0.02	2.58	3.00
Ikunolite 2 Fig 3D	-	0.06	3.74	0.20	-	3.95	0.33	0.01	2.66	3.00
BHA-1-8 average Ikunolite	-	0.03	3.74	0.23	-	4.00	0.365	0.015	2.62	3.00
Blue Qtz Vein 0414	Cd	-	3.71	0.19	-	3.92	0.07	0.02	2.99	3.08
average Ikunolite by microprobe (Cook et al. 2007)	0.02									

BHA-1-8 ikunolite in Fig 3D is tellurian with 0.365 apfu; this corresponds to its occurrence with pilsenite, a telluride possibly a late-stage.

The presence of electrum in intimate association with Bi-tellurides in this polished section provides evidence that the Bunker Hill vein system is directly comparable with that of Eloise Vein at BiTel Knoll. Two Bi-telluride species new for the CLY locality pilsenite and tetradymite are first described herein. Ikunolite was formerly described only in sample 0414 of the Blue Quartz Vein (Cook & Ciobanu 2006).

Ikunolite Bi_4S_3 is less sulphurated than bismuthinite Bi_2S_3 , so it is logical its formation would require a lower $f\text{S}_2$ or a higher activity of Bi. It may be an early phase in BHA-1-8, but its occurrence may be possible only because of closed chemical systems localised at the present microscopic scale of thick section examination. Globally, ikunolite is much rarer than bismuthinite although it may be more common in nature but under-recognized.

Pilsenite Bi_4Te_3 and joséite-B Bi_4STe_2 both have “4:3” metal: chalcogen ratio stoichiometry, i.e. $(\text{Bi} + \text{Pb} + \text{Sb}) / (\text{Te} + \text{S} + \text{Se}) = 4/3$ in their formulae. Thus they are presumed to be stable over the same unknown range of conditions so their occurrence together as in Fig. 2B is not so unusual. In Fig. 3D of a different grain the replacement texture suggests joséite-B formed first and ‘corroding’ pilsenite later, possibly via a de-sulphidation reaction.

Sample BH-0567 from dump close to Adit 1 of Bunker Hill mine, uncertain vein

Background

The sample was collected from a dump pile ~10 m N (to left) of the main dump in front of Adit 1 of the Bunker Hill mine; this placement suggests it might be a sample of a different vein, possibly one formerly trenched up-hill but now buried. Alternately it could be from a vein in Adit 1. The site is UTM 471,465 mE 5,434,293 mN \pm 10 m. No assay of similar material is available. The field label was UHS7 but the sample *is not* pieces of the Underhand Stope Vein in front of Adit 2. Hand specimens are very vuggy coxscumb quartz with minor blue-grey bismuth tellurides; weathering products of both these and the minor associated arsenopyrite {the secondary mineral scorodite, $\text{Fe}^{3+}(\text{AsO}_4) \cdot 2(\text{H}_2\text{O})$ } are a characteristic lemon-yellow colour:



Photo of vuggy quartz specimen BH-0567 collected Oct. 10 2007 from the small dump near a tree, about 10 m N of Adit 1. Terminations of the very coarse, cm-sized, euhedral quartz crystals show growth under extensional conditions was to bottom left or upper right of photo. At left of the cm scale find several 'coating' laminae of very fine grained blueish-grey admixed bismuth tellurides with slight metallic lustre. Uncommon spots of brown limonite are from weathered pyrites.

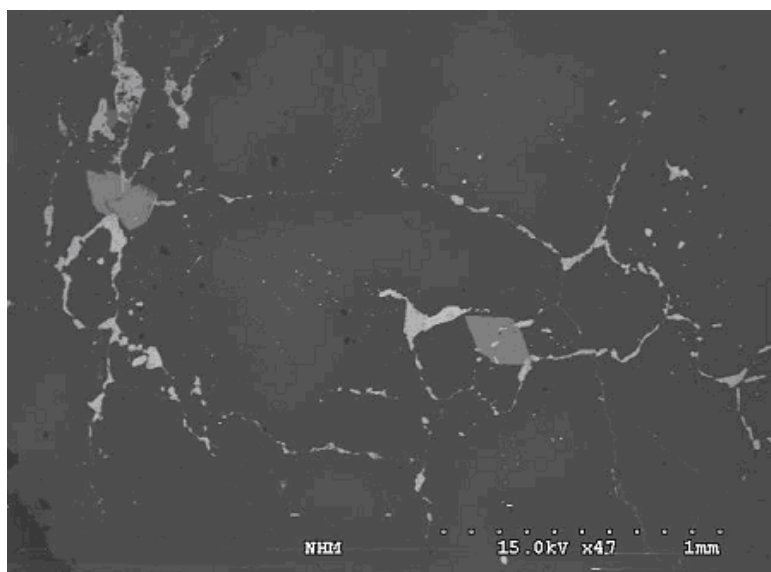
Polished section description

The BH-0567 polished section is slightly grey quartz; trace amounts ($\ll 1$ vol. %) of pyrite are present – two grains each ca. 1 mm in diameter are noted. Away from these pyrite grains there are several fine swarms of Bi-Te minerals and native gold grains (Fig. 1).

These swarms consist of individual composite grains up to ca. 50 μm (rarely 100 μm) in size within the quartz. They are commonly interconnected with one another via fractures in the quartz. Eleven grains of gold (actually electrum, and in one case, native silver) were noted – six are intimately associated with Bi-Te minerals and in grain contact, five occur as discrete grains enclosed within the quartz, but always close to (i.e., within 500 μm) Bi-Te minerals. No gold grains were observed in parts of the section away from clusters of Bi-Te minerals. Interestingly in BH-0567 small amounts of prismatic crystals of arsenopyrite are associated with these clusters (Figs. 1b & 2). Trace galena also occurs (Fig. 2 middle left image).



Fig. 1 a and b. Reflected light photomicrograph (a) and back-scattered electron image (b) of Bi-Te mineral assemblages in quartz matrix of polished section BH-0567. The Bi-Te minerals are associated with arsenopyrite (medium grey, prismatic diagonal shaped grains in b). Generally the Bi-Te minerals are partly interconnected via fractures within the quartz matrix.



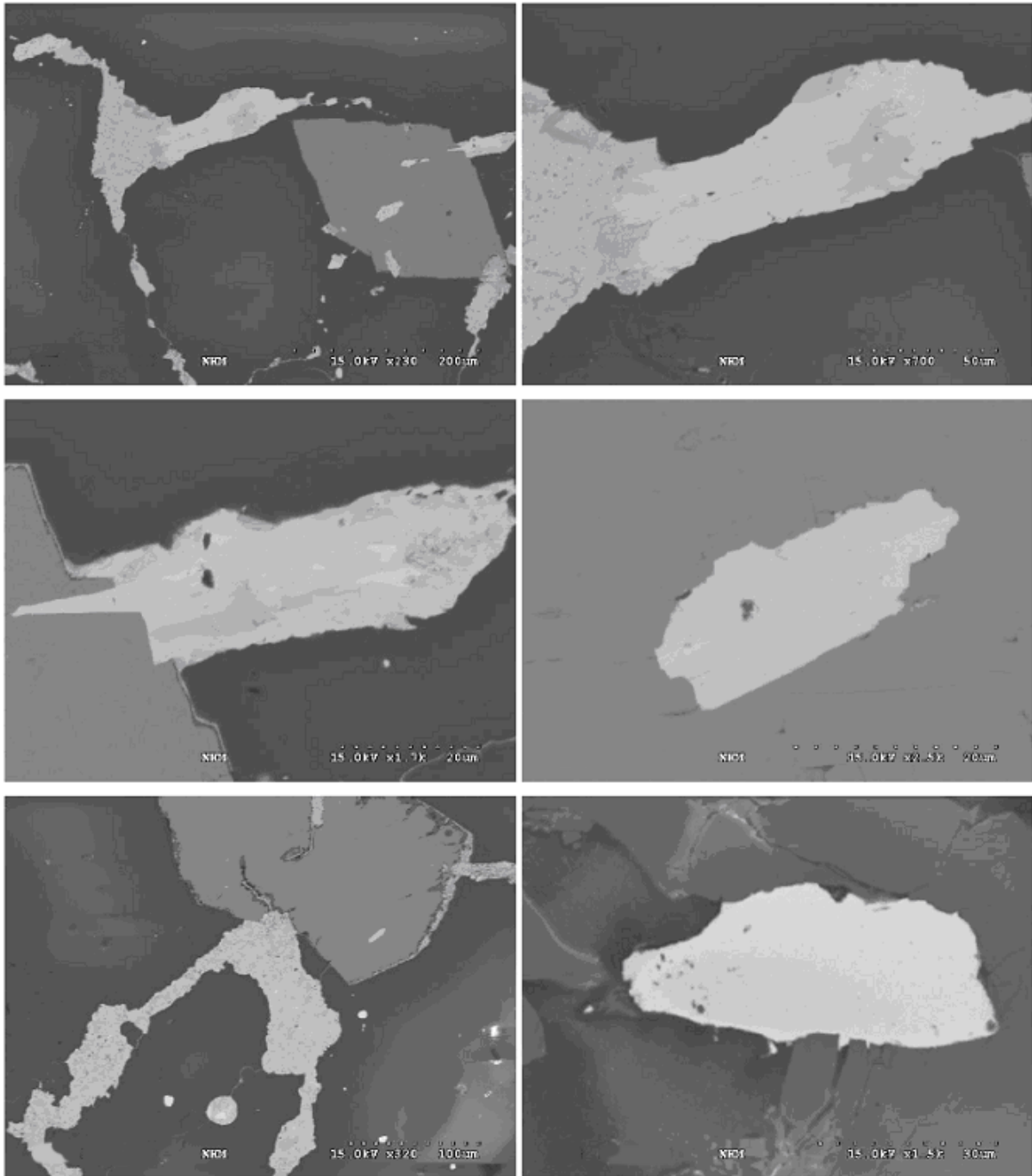


Fig. 2. Electron back-scattered electron image showing a number of Bi-Te mineral grains in polished section BH 0567 associated with arsenopyrite. (Top left) Assemblage of arsenopyrite, the prismatic dark grey grain, and bismuth telluride minerals within quartz. (Top right) Close-up of Bi-Te mineral assemblage above top left corner of the arsenopyrite grain. Brighter area is hedleyite; bismuthinite is slightly darker and altered to Bi-oxides/hydroxides (darker shades of grey). (Middle left) Close-up of composite grain attached to the top right of the arsenopyrite grain in the first image, consisting of hedleyite (homogeneous, brighter area), bismuthinite (lower and right hand margins) and galena (darker grey between the two). Large dark grey on left is an arsenopyrite crystal. (Middle right) Homogeneous grain of hedleyite in the centre of the arsenopyrite grain in first image. (Lower left) Relatively large, totally decomposed grain of bismuthinite (brighter shades) associated with arsenopyrite (darker grey, top of image). A number of micron-sized bleb-shaped gold grains (likely electrum) can be seen (brightest white). (Lower right) Homogeneous grain of hedleyite (white) at the grain margin of arsenopyrite (dark grey).

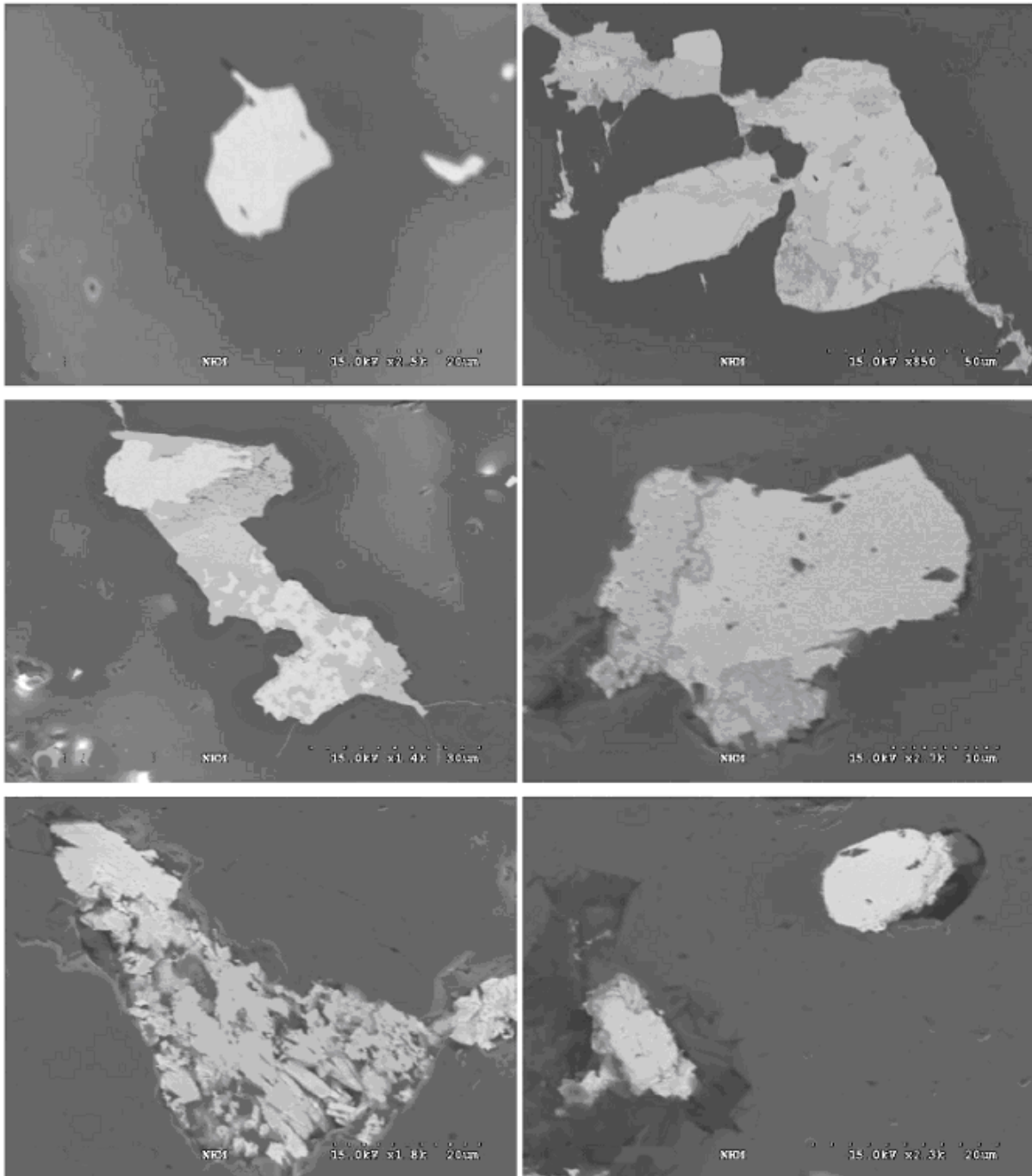


Fig. 3. Electron back-scattered electron image showing a number of gold and Bi-mineral grains in polished section BH 0567. (Top left) One of the larger gold grains in the section, 10 μm in diameter, within quartz. (Top right) Composite grain of joséite-B, bismuthinite and galena, in quartz. Larger grey patch at top is the galena, brighter patches at the bottom are the JoB, all the darker grey is the bismuthinite. (Middle left) Composite grain consisting of electrum (the upper part of the grain, extremely Ag-rich, hence a darker shade than high atomic-weight native gold), surrounded by bismuthinite. White parts towards bottom of the image are native bismuth grains. (Middle right) Large composite grain of joséite-B surrounded by secondary Bi-minerals after bismuthinite, mostly bismite; subhedral crystal habit starting to develop. (Lower left) Similar composite grain to previous image. (Lower right) Rounded grain of electrum (white, top right of image) and prismatic grain of partially-decomposed bismuthinite at bottom left.

The Bi-Te mineral assemblages in BH 0567 consist of **joséite-B**, **hedleyite**, and **bismuthinite** with minor amounts of **native bismuth**; **arsenopyrite** and **galena** are associates. Bi-Te minerals may originally have been in textural equilibrium with bismuthinite, but this relationship is somewhat obliterated by later alteration of bismuthinite to, for example, **bismite** (Fig. 3 Middle right). Joséite-B is by far the most abundant bismuth telluride. As in other samples, bismuthinite is extensively replaced by secondary alteration.

One grain gave a composition that deviated somewhat from ideal joséite-B stoichiometry – it is closer to the $\text{Bi}_4\text{Te}_3\text{S}_2$ stoichiometry recorded from grains in Eloise Vein sections. However the small size of that grain and the fact that it is intergrown with native bismuth and bismuthinite urges extreme caution before relying on the compositional data in this case.

In contrast to other polished sections, the composition of the ‘native gold’ grains seems to vary extremely widely across the entire field of **electrum** (20-80 wt. % Ag, the rest gold). Spot analyses of seven electrum grains gave contents of 22.8, 26.3, 39.4, 47.4, 50.0, 50.8 and 62.8 wt. % Ag. One grain (82.8 wt. % Ag) even falls within the compositional field of **native silver**.

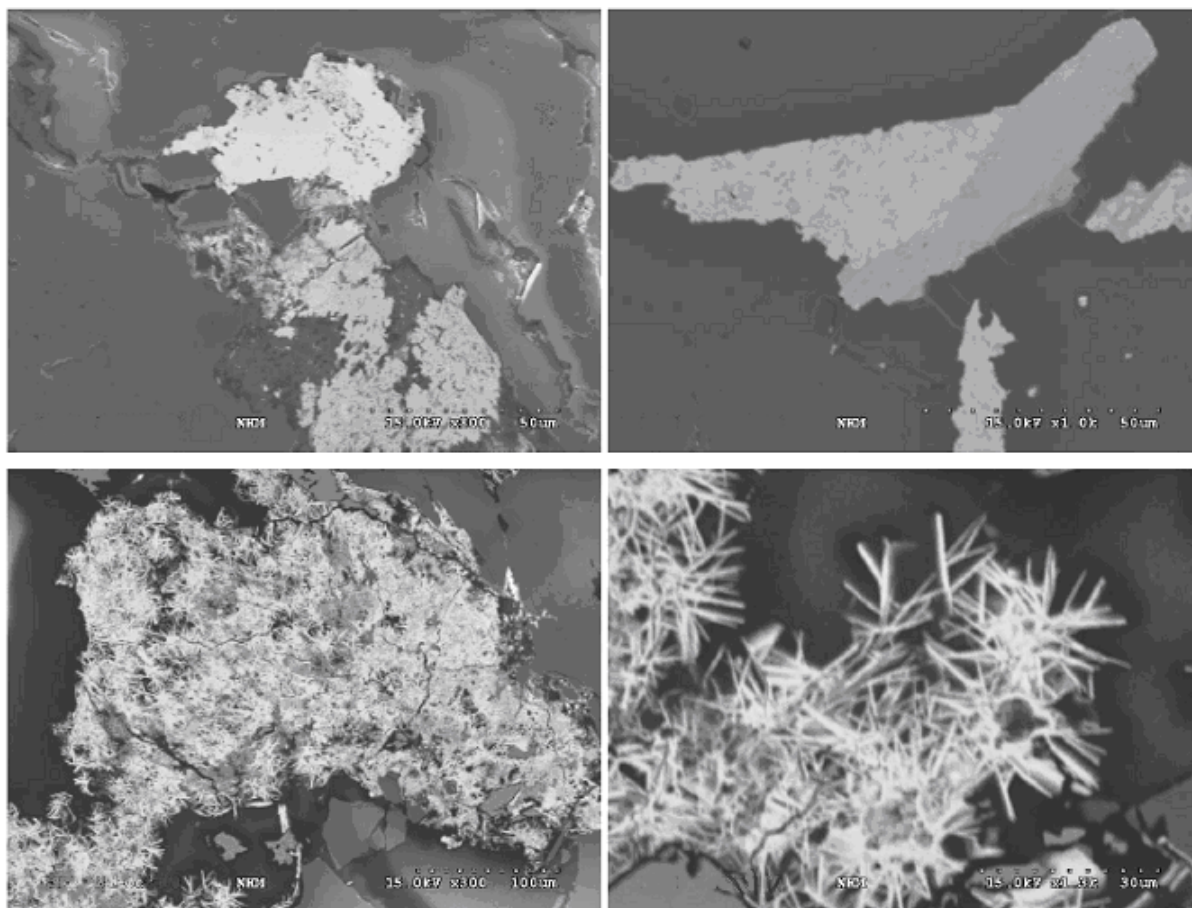


Fig. 4. Electron back-scattered electron image showing a number of Bi-mineral grains in polished section BH 0567. (Top left) Relict bismuthinite at top of image and abundant secondary bismite. (Top right) Composite grain of native bismuth (patchy area on left of image) and galena (medium gray, right of grain). (Lower left and Lower right) Images showing a cavity in the quartz matrix filled with fine acicular needles of a secondary undetermined bismuth oxide (or possibly a hydroxide?). Image on right is a close-up of part of the image on the left, at bottom of the picture, two thirds of the way to the left edge.

Energy-dispersive spectroscopic (SEM-EDS) analyses of Bi-tellurides are given in the following table (elements in wt. %).

Analysis	Ag	As	Bi	Pb	Sb	Te	Se	S	Total
joséite-B I	-	-	69.48	4.95	-	22.83	0.68	1.98	99.92
joséite-B II	-	-	68.64	4.67	-	23.25	1.12	2.03	99.71
joséite-B III	-	-	68.12	5.82	-	22.38	1.47	1.62	99.41
joséite-B IV	-	-	72.07	3.04	0.06	21.82	0.22	2.67	99.88
joséite-B V	-	-	68.21	6.30	-	21.19	1.19	2.23	99.12
*hedleyite	-	-	76.83	0.43	0.11	20.11	0.13	-	97.61
Bi ₄ Te ₃ S ₂ (??)	-	-	63.91	2.48	1.44	26.35	0.32	5.27	99.87

* low wt % total 97.61%

Joséite-B ideally Bi₄STe₂, formulae with sums

Phase	Bi	Pb	Sb	Metal Sum	Te	Se	S	Se + S Sum
joséite-B I	3.84	0.28	-	4.12	2.07	0.10	0.71	0.81
joséite-B II	3.76	0.26	-	4.02	2.09	0.16	0.73	0.89
joséite-B III	3.81	0.33	-	4.14	2.05	0.22	0.59	0.81
joséite-B IV	3.84	0.28	0.01	4.08	1.94	0.03	0.94	0.97
joséite-B V	3.76	0.35	-	4.11	1.91	0.03	0.80	0.83
Ave. BH 0567 joséite-B	3.802	0.30	-	4.094	2.012	0.108	0.754	0.862

Hedleyite near ideal Bi₇Te₃ but analysis has a low wt % total - 97.61%

Phase	Bi	Pb	Sb	Metal Sum	Te	Se	S	Chalcogen Sum
*hedleyite	6.94	0.04	0.02	6.99	2.97	0.03	-	3.00

Unnamed phase, non-stoichiometric

Phase	Bi	Pb	Sb	Metal Sum	Te	Se	S	Se + S Sum
Bi ₄ Te ₃ S ₂ (??)	3.91	0.15	0.15	4.21	2.64	0.05	2.10	2.15

With the exception of the last non-stoichiometric analysis, bismuth telluride phases are within the Bi-rich hedleyite or joséite-B range of compositions, meaning the metal:chalcogen ratio = (Bi + Pb) / (Te + Se + S) > 1, like many of the other SEM-EDS analyses of minerals from the other investigated CLY occurrences.

BH 0567 is of special mineralogical interest because of the large number of electrum grains, their close association with the Bi-Te minerals and their unusually large range of composition grading from almost native gold to grains correctly named native silver.

The association of arsenopyrite with bismuth telluride minerals is also noteworthy; formerly arsenopyrite had been identified only in the Lefevre skarn and in Lefevre vein sample L04 QVXTRY where it is abundant. Arsenopyrite has not been observed in Eloise Vein or others on BiTel Knoll. BH 0567 arsenopyrite formed in a chemical environment of higher As activity, possibly at higher temperatures than the other Bunker Hill veins or Eloise. The Bi-Te mineral association in BH 0567 may be early-stage: joséite-B, hedleyite and bismuthinite with minor amounts of native bismuth; arsenopyrite and galena are associates.

Conclusions re mineralogy of Bunker Hill mine veins

Table of minerals identified in 5 polished sections of Bunker Hill mine veins, listed in decreasing order of metal: chalcogen ratio

	metal: chalcogen ratio	Vein piece from Adit 2 Underhand Stope Vein (Cook & Ciobanu 2006)	BH UHS 1 from Adit 2 Underhand Stope Vein this report	BH UHS-4 from Adit 2 Underhand Stope Vein this report	BHA-1-8 Adit 1 Crush Vein this report	BH-0567 uncertain vein from dump close to Adit 1 this report
native gold	-	✓ (electrum)		✓ (electrum)	✓ (electrum)	✓ (electrum)
native silver	-					✓
native bismuth	very high		✓	✓	✓	✓
hedleyite	7:3 = 2.33		✓		✓	✓
trace hessite Ag ₂ Te	2:1 = 2.0		✓			
joséite-B Bi ₄ STe ₂	4:3 = 1.33		✓		✓	✓
ikunolite	4:3 = 1.33				✓	
trace pilsenite	4:3 = 1.33				✓	
unnamed Bi ₄ Te ₃ S ₂	4:5 = 0.80					?
bismuthinite	2:3 = 0.66		✓	✓	✓	✓
trace tetradyomite Bi ₂ Te ₂ S	2:3 = 0.66				✓	
magnetite	-		✓			
pyrrhotite	-	✓	✓			
arsenopyrite	-					✓
marcasite	-	✓				
pyrite	-	✓	✓	✓	✓	✓
trace scheelite	-			✓		
trace cosalite	-	✓				
trace galena	-		✓		✓	✓
trace chalcopyrite	-	✓			✓	
trace bornite	-	✓				

In each polished section different mineral assemblages are observed; the most common minerals are pyrite, bismuthinite, native bismuth, joséite-B, hedleyite, trace galena and gold. Gold are actually silver-rich and correctly named electrum. Arsenopyrite is common in BH-0567. Pyrrhotite relicts in common pyrite grains in BH UHS 1 from Adit 2 Underhand Stope Vein and magnetite suggest a 'reduced' chemical environment of formation in that single vein. Minerals in BH UHS 1 were deposited (or modified) at conditions fairly close to the pyrite + pyrrhotite stability boundary.

Ingodite, joséite-A, unnamed Bi₂Te and the two uncharacterized 'new' phases found in Eloise Vein do not occur in the Bunker Hill veins. Perhaps the Bunker Hill veins in general formed from hydrothermal fluids with a more homogeneous chemistry than in Eloise vein. In the latter the chemical systems were possibly very localized and closed, allowing for a greater diversity of minerals including phases with the metal:chalcogen ration < 1. In this scenario stronger alteration (latter-stage sulfidation) of Eloise vein would not be responsible for its observed mineralogical diversity.

M-01 Moly Quartz Vein

Background

Sample M-01 was collected in the trench along the Moly Quartz Vein, just south of BiTel Knoll, at UTM 471,665mE 5,434,356 mN \pm 10m. The field label is Mo-01.

Repeated recent analyses of rock samples from several surveys show little gold content; of five 1999 rock samples BH-308 ran highest in gold at 0.15 g/t; others are background (Howard 2000). Nevertheless old reports confirm gold values somewhere along the vein:

The Moly “Quartz Vein is 40 inches wide striking about N 85° W [095° azimuth] dipping 35° N. The footwall country rock is granite ... Samples across 27 and 39 inches both assayed 0.40 oz. gold per ton (Minister of Mines 1933)”. “In the granite there is from 1 to 3 1/2 feet of quartz irregularly mineralized with molybdenite, pyrite and some fine black sulphide [sulphosalts?]. This quartz is reported to carry spotty gold values. Some 30 tons of rather low-grade material shipped in 1933 was reported to come principally from cut (Minister of Mines 1936).” 1933 production was 8 oz. Au and 150 oz. Ag; calculated bulk gold fineness is 50, very low.

Evidently these two auriferous vein intersections with 0.40 oz. / ton, 27 and 39 inches wide, have not been re-sampled. G. Ray (2004 Map 2) notes the vein “contains gold, pyrite plus galena” but native gold has not since been observed. A grab rock sample 0540 “is quartz with about 5% **galena** (fig. 6). Bands, 2.5 and 2.0 cm wide, of light blue-grey quartz enclose a central 3 cm thick layer of dark bluish grey quartz and cryptocrystalline limonite-strained quartz. On one side are clusters of coarse-sized (1 mm) galena crystals. Another piece has common limonite-coated vugs to 7 mm sized, and very coarse galena as 5x7x10 mm sized crystals. Very fine-grained **molybdenite** likely occurs; admixed with galena it could be visually mistaken for Bi minerals (Howard, 2005).” This rock 0540 ran

Au g/t by FA	Bi	Te	Ag	Mo	Pb	W	As	Sb (all ppm)
0.28	23	1.8	80.39	1,062	> 10,000	12.9	14	31

Polished section description

M-01 is from the margin of the vein and is mostly vein selvage with a variety of silicate minerals present alongside quartz. Sulfides are about 2 vol. % of the sample, dominantly **pyrite** and minor (sub-100 μ m sized) **molybdenite**. No gold or bismuth minerals were seen.

Notable features of M-01 include the following:

- Pyrite grains are characterized by pronounced cores and rims – the rim representing a second generation overgrowth on a primary core (Fig. 1). This substantiates previously expressed evidence for an overprinting event in the CLY area and remobilization of sulfide components in the veins (Cook et al., 2007b).
- Parts of the vein selvage are characterized by fragments displaying breccia textures (Fig. 2, left). This is additional evidence for some type of secondary event.

- The silicate mineral assemblage in the sample is quite diverse (Fig. 2, right). Dark (Fe-rich) chlorite is relatively abundant; muscovite (some of which lacks a preferred orientation suggesting post-stress crystallization) and ‘epidote’ (compositionally probably closer to clinozoisite) are both widespread (Fig. 3).
- The minor molybdenite present is always closely associated with muscovite (Fig. 4).

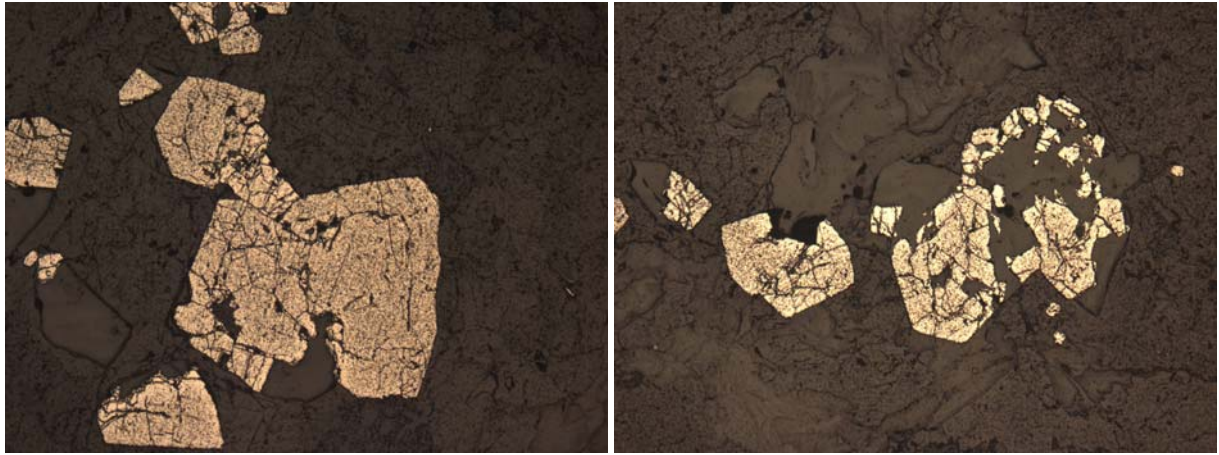


Fig. 1. Reflected light photomicrographs of pyrite grains within the silicate matrix of the Moly Quartz Vein. All the pyrite grains in the sample, irrespective of their size, have cores and overgrowing rims. This suggests growth during an overprinting event. Horizontal axis is 450 μm for both.

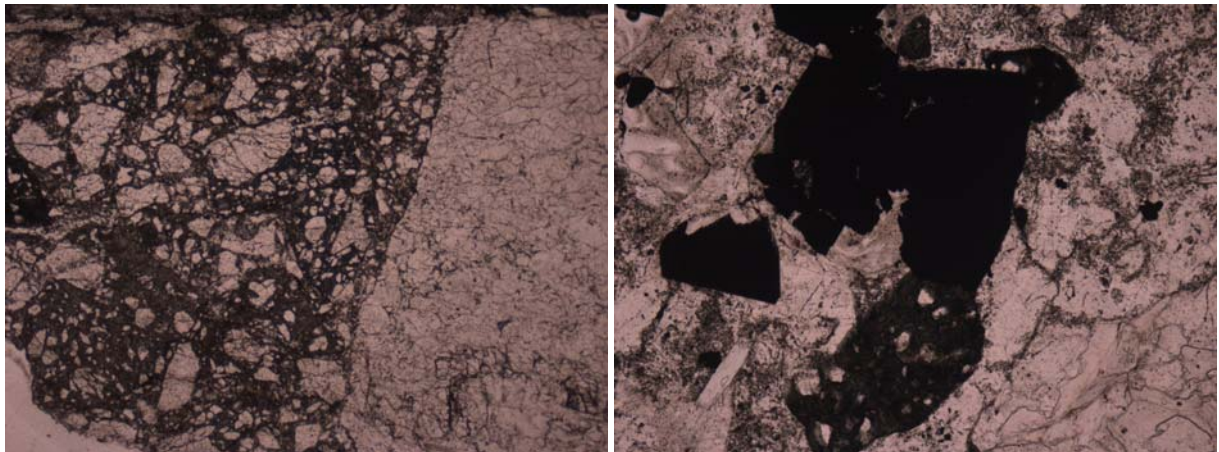


Fig. 2. Transmitted light photomicrographs. The left image shows a fragment consisting of crushed wallrock within a vein selvage. Fine-grained quartz aggregates appear on the right of the image. The right image shows the same pyrite grain as in Fig. 1 (left). Coarse chlorite appears underneath this. Other minerals in the assemblage include quartz, calcite, epidote and muscovite. Horizontal axis is 450 μm for both pictures.

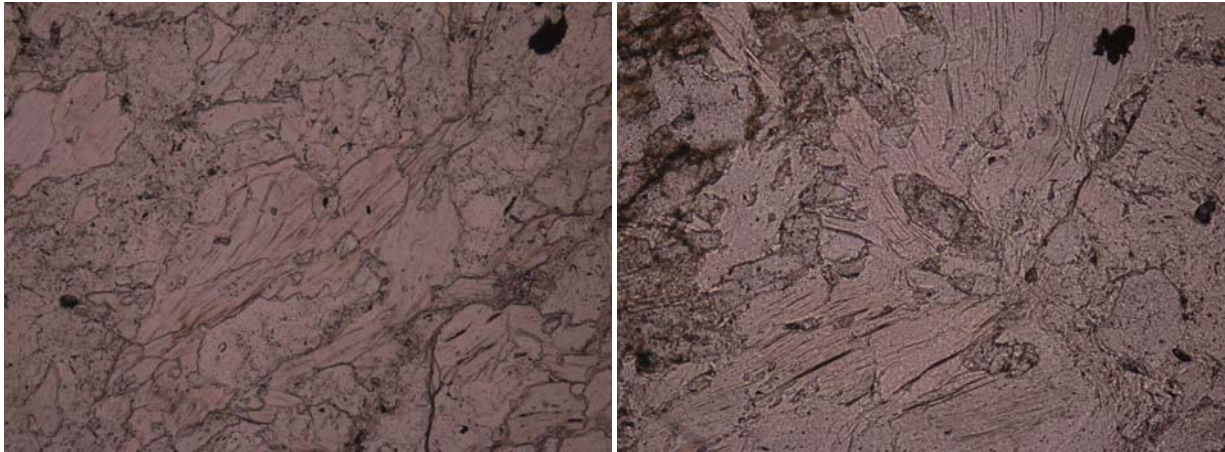


Fig. 3. Transmitted light photomicrographs. The left image is fine-grained foliated muscovite. The right image shows platy muscovite, without notable foliation, and higher-relief slightly bluish epidote grains. Horizontal axis is 225 µm for left image and 450 µm for right.

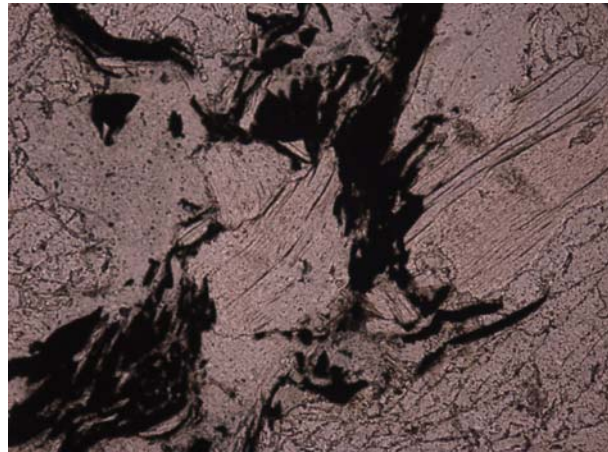


Fig. 4. Transmitted light photomicrograph. Fine-grained molybdenite (opaque) is associated with muscovite. Horizontal axis is 225 µm.

Blue Quartz Vein Mineralogical study

Two samples from the Blue Quartz vein were investigated BQ-01 and BQ-02. The objectives were to verify the mineralogy of the vein, particularly with respect to the association of gold with bismuth minerals and sulphides, and to compare it with other veins in the immediate vicinity. The samples were studied using conventional reflected light ore microscopy and a Scanning Electron Microscope at the Natural History Museum, University of Oslo. Much of the SEM work was carried out in back-scattered mode, whereby the brightness of the mineral in the image is an expression of its average atomic weight, i.e. pyrite appears brighter than quartz but less bright than ‘very heavy’ gold.

Sample BQ-01 - Background

BQ-01 was collected from the Blue Quartz Vein trench, just downhill of the BiTel Knoll veins at UTM 471,600 mE 5,434,386 mN \pm 10 m. The field label was BQ-1 0543; no assay is available but some very high grade grab samples have been collected from the trench (see 0414 discussed under BQ-02 below). The vein is largely quartz.

Sample BQ-01 –Polished section description

BQ-01 consists of clear quartz with a small proportion (ca. 1 vol. %) of opaque minerals. Individual patches attain sizes to 8-10 mm (i.e., macroscopic). The polished section block was prepared from an area of the sample in which opaque minerals account for ~ 10 vol. %.

Reflected light microscopy reveals the patches to essentially consist of **galena**. Very minor amounts of **native bismuth** and **trace quantities of bismuthinite** also occur. Parts of the bismuth mineral inclusions in the galena patches have altered to various bismuth oxides/hydroxides. No gold minerals or tellurides were observed.

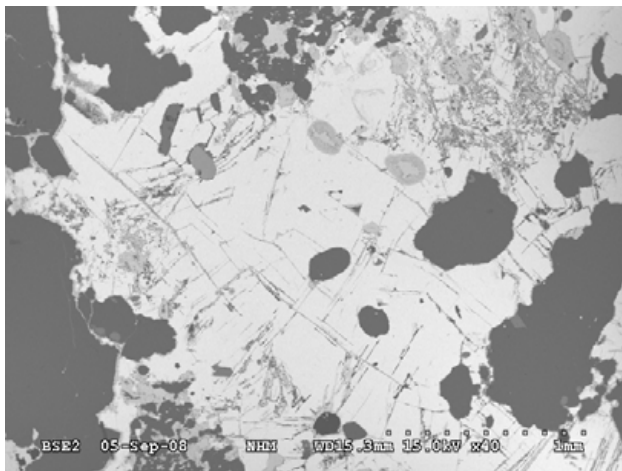


Fig. 1A: Galena (bright white and with characteristic triangular cleavage marks) forms the main part of the largest patch (ca. 3 mm in diameter). Black areas within the galena and in the matrix are quartz. Note that galena is undergoing intense alteration with parts of the grain decomposed to lead oxides and/or hydroxides (patchy grey areas through the galena). Back-scattered SEM images

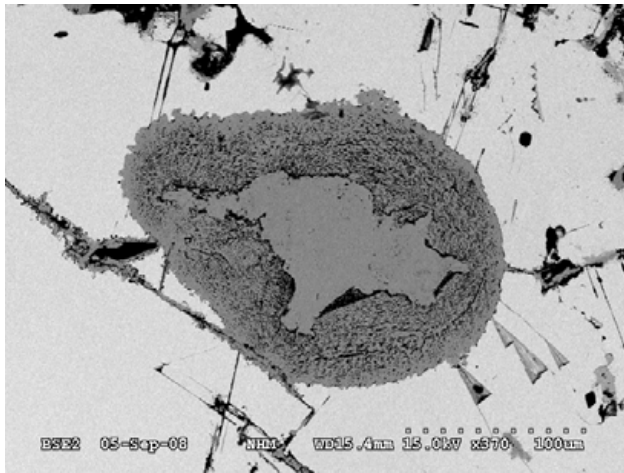


Fig. 1B: Detail of halo-like alteration within galena. A central area of oxide (middle grey) is surrounded by a halo of porous hydroxide (darker grey).

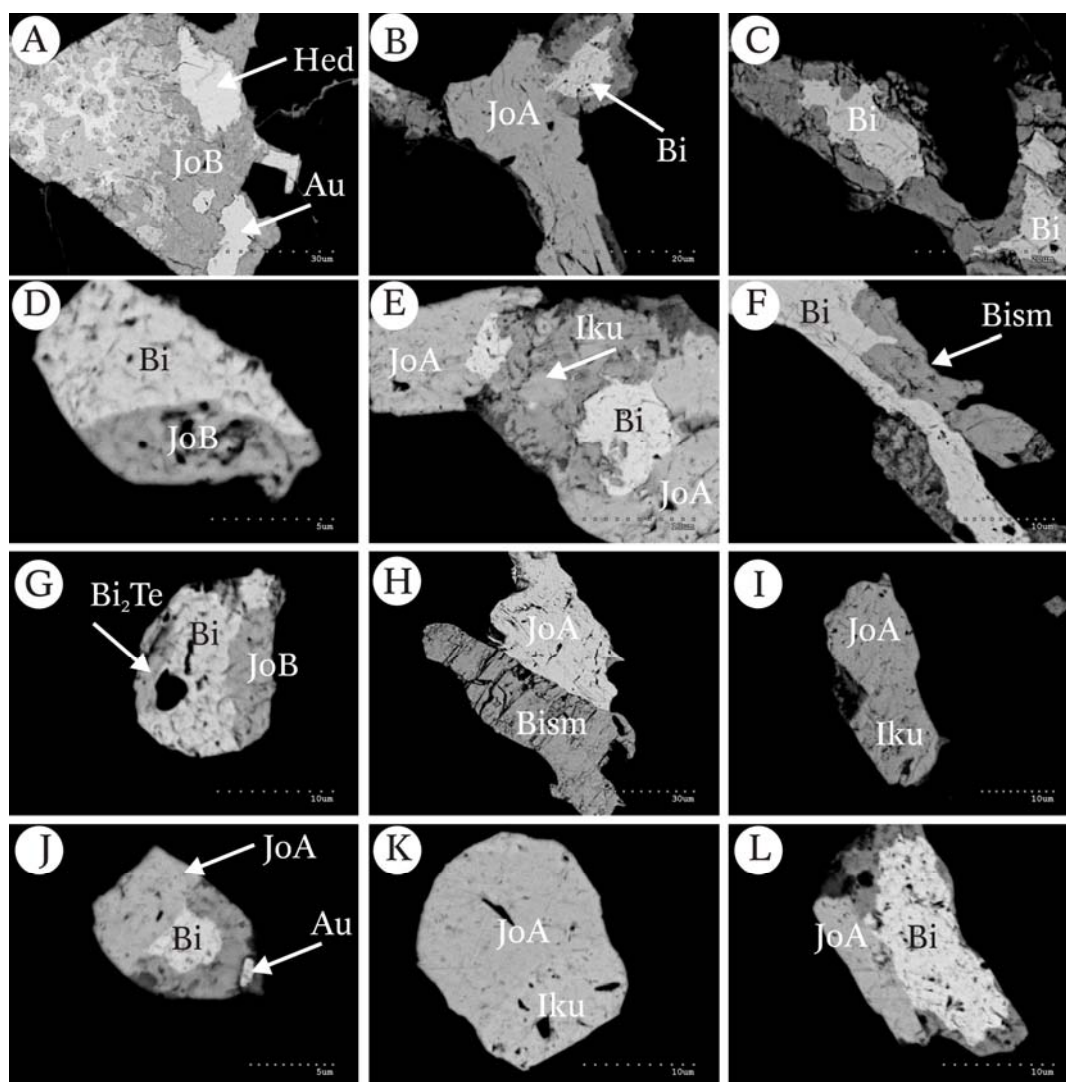
Semi-quantitative analyses (SEM-EDS) of the galena did not reveal the presence of any minor elements.

Although no gold minerals or tellurides have been observed in BQ-01, the occurrence of bismuth minerals in the vein, even if in only minor amounts - similar to those seen elsewhere in other polished sections from CLY - suggests that the Blue Quartz vein is directly comparable to those vein systems. Bismuth tellurides and native gold might be observed if additional polished sections were prepared from the sample material.

Sample BQ-02 – Background

BQ-02 was collected from the Blue Quartz vein trench at the 0414 site just below BiTel Knoll at UTM 471,607 mE 5,434,383 mN \pm 10 m. The field label was ‘BQ-2 Hi-grade’. Analysis of 0414 (in Howard, 2006b) ran 8.65 g/t Au and 1.18 g/t Ag by metallic screen FA procedure on 490 g, and 478 Bi / 23 Te / 23 Mo / 13 Pb / background 2.1 As / 0.7 Sb / 0.5 W / 0.5 Se (all ppm by ICP-MS). ‘Bulk’ gold fineness is 880. B. Doyle of Nelson in Sept. 2005 first identified native gold here with a 14 x power hand lens. Gold is primarily associated with weathered, bluish-grey indeterminate “bismuth minerals” in the fault-hosted quartz vein (photo Fig. 7 in Howard, 2006b).

Two polished sections of 0414 previously examined by the writer (Cook & Ciobanu, 2006) have “Bi-minerals and gold present as small swarms of fine-grained inclusions within the vein. There is also some native gold outside of these swarms, i.e., within the vein matrix (photographs therein). The composition of the native gold is relatively constant (\sim Au₇₅Ag₂₅ atomic proportions) [thus it is actually electrum]. The Bi-mineral assemblage is dominated by joseite–A (Bi₄S₂Te), together with bismuthinite and native bismuth as major components of the swarms. Lesser amounts of joseite–B (Bi₄Te₂S), hedleyite (Bi₇Te₃) {rather this is now determined by microprobe analyses to be near stoichiometric unnamed Bi₂Te} and close-to-end-member ikunolite (Bi₄S₃) complete the assemblage. The sample is rather altered (surface alteration), with the Bi-assemblage partially decomposed to a range of unidentified secondary minerals.”



Some of the back-scattered SEM images in Fig. 2 of Cook & Ciobanu (2006) illustrate “apparent eutectic crystallisation between [some] phases” in 0414. Fig 2A has hedleyite {now considered unnamed Bi_2Te } surrounding joséite–B and native gold grains. Grain boundaries are not smooth so it is inferred that the mineral assemblage did not form in equilibrium. The texture may record a sulphidation event. Fig. 2D has joséite–B + native bismuth with curvilinear contact, Fig. 2G same pair also with unnamed Bi_2Te . Fig. 2J & 2L have joséite–A + native bismuth in textural equilibrium and ‘stable’; in Fig. 2L the pair also co-exists with native gold. Figs. 2I & 2K have joséite–A + ikunolite stably coexisting as interstitial blebs with curvilinear boundaries. Fig. 2H has the stable pair joséite–A + bismuthinite. Fig. 2E shows two native bismuth cores surrounded by the pair joséite–A + ikunolite on each of their sides. This replacing texture shows joséite–A + ikunolite is younger than native bismuth [?]. Fig. 2F illustrates bismuthinite corroding native bismuth, same as in Fig. 2C though the surrounding bismuthinite is not labeled. This may indicate a sulphur bearing event with later-formed bismuthinite. Fig. 2B has joséite–A + native bismuth, again the latter partially replaced by bismuthinite.

In 0414 “Most abundant are blebs containing an association of native Bi + bismuthinite. ... Joséite–B is found especially in blebs that contain native bismuth (Figs. 2D) and also Bi_2Te and/or hedleyite (Fig. 2A) or the pair with native gold (Fig. 2G).

Sulphur-rich blebs dominated by joséite–A may occasionally also contain ikunolite (Fig. 2E). These Bi-rich associations are similar to those typically reported from gold skarns (after Cook et al., 2007)”.

In 0414 paired Bi–telluride associations have the metal:chalcogen ratio $\text{Bi (+ minor Pb + trace Sb) / (Te + S + trace Se)} > 1$, e.g. the stable mineral assemblages are

[1] joséite–B + unnamed $\text{Bi}_2\text{Te} \pm$ native gold

[2] joséite–B + native bismuth \pm native gold

[3] joséite–A + ikunolite

[4] joséite–A + native bismuth

[5] ikunolite + native bismuth

These may represent binary eutectics in the Bi–Te–(S) system.

Texturally, native bismuth is an early phase of the Au–Bi–Te association as in

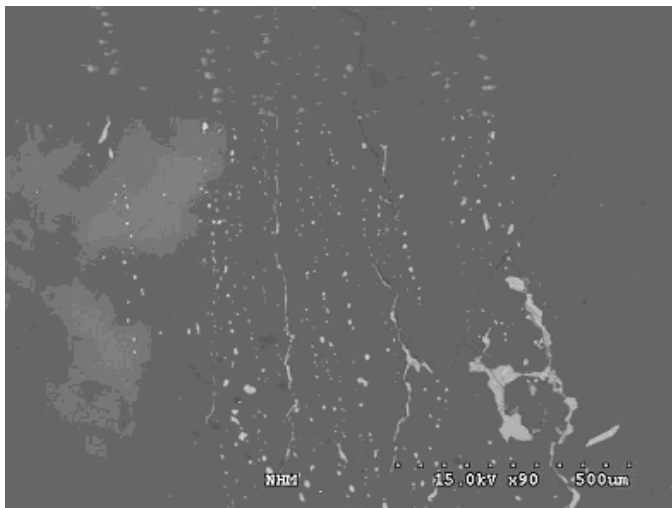
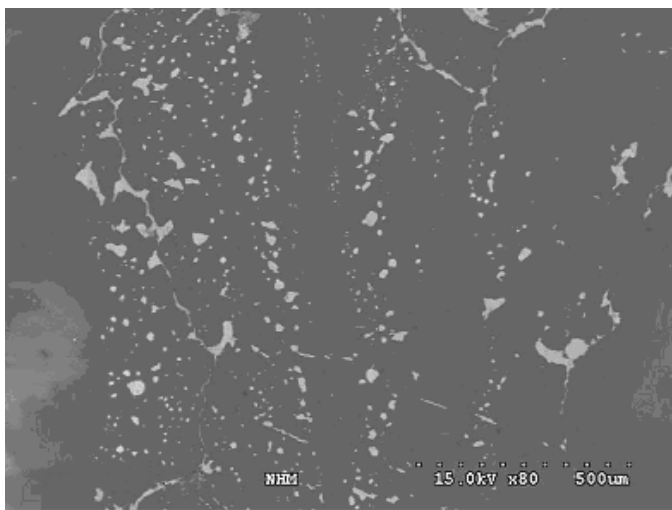
- Fort Knox (McCoy, 2000; McCoy et al., 2002)
- Petrůvka in the Czech Republic (Zachariáš et al., 2001)
- Maiskoe in the Ukraine

and other deposits. The inference regarding the origin of mineralization is that bismuth-rich Bi–Te–S–Se melt collected gold and thereafter under sulphidation conditions deposited native gold with bismuthinite and other rare bismuth telluride minerals in the Blue Qtz Vein.

Cook et al. 2007 give average microprobe analysis of minerals and a laser ablation study of Bi–Te in 0414.

Sample BQ-02 –Polished section description

The sample consists of cloudy, slightly grey quartz. There are no visible macroscopic ore minerals. Microscopy reveals an abundance of fine swarms of bismuth minerals (and omnipresent **galena**) throughout parts of the section (Fig. 1A & 1B). These swarms consist of numerous blebs, from $<5\ \mu\text{m}$ up to a maximum of ca. $100\ \mu\text{m}$ in size, commonly interconnected with one another as well as other bodies of Bi-minerals infilling fractures in the quartz. The blebs follow trails or arrays within the quartz matrix. Figs. 2-5 illustrate some of the larger grains. The bismuth minerals are fairly extensively replaced by alteration phases. **Bismuthinite** is by far the most abundant Bi-mineral and has undergone the most extensive replacement. **Native bismuth** is a maximum 10% of all the Bi-minerals. **Joséite-A** is the only Bi-telluride identified; it is, however, a conspicuous component of many of the larger blebs. No gold minerals were, however, seen in the polished section.



Figs. 1A & 1B Back-scattered electron images showing arrays of oriented blebs of various bismuth minerals (bismuthinite, joséite-A and native bismuth) plus galena within quartz. Note many of the individual blebs interconnect with one another along fine fractures, infilling the quartz matrix.

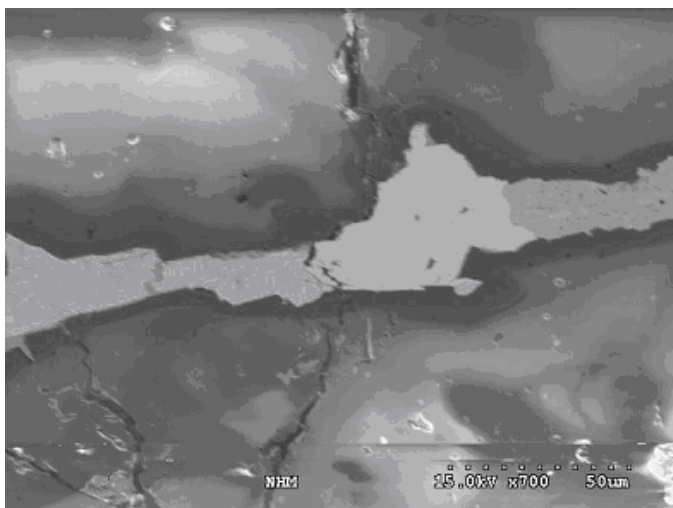


Fig. 2A-2F. SEM back-scattered image showing Bi-mineral grains in sample BQ-02. **Fig. 2A** fracture in quartz filled with Bi-minerals, brighter portion in centre of image corresponds to joséite-A; most Bi-minerals replaced by secondary phases

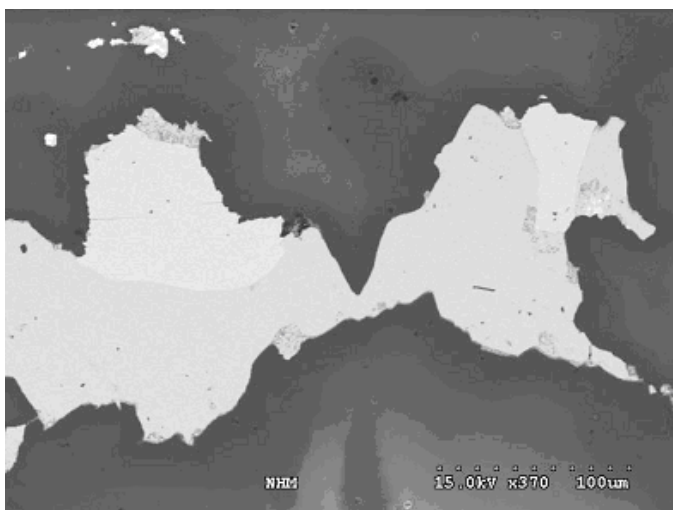


Fig. 2B Composite grain consisting of bismuthinite (slightly darker grey, major part of the grain) and joséite-A. Smooth curvilinear boundaries suggest the minerals are in textural equilibrium.

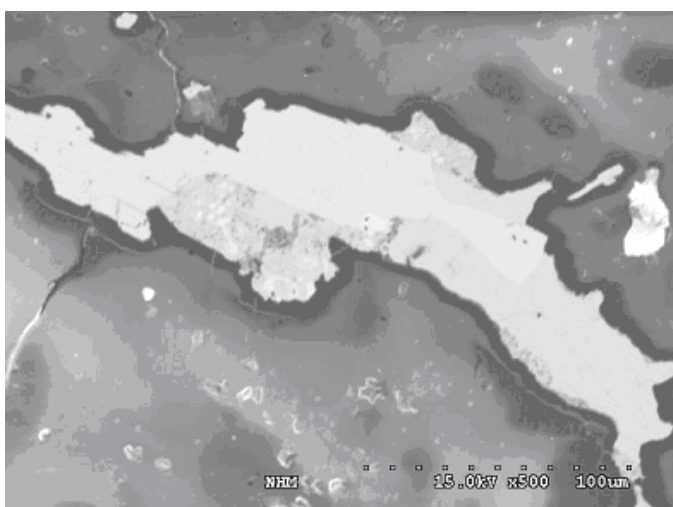


Fig. 2C Grain of joséite-A with tabular prismatic habit stably co-existing with partially-replaced bismuthinite. Joséite-A more typically has a platy appearance.



Fig. 2D Similar to previous, the brighter white is joséite-A.

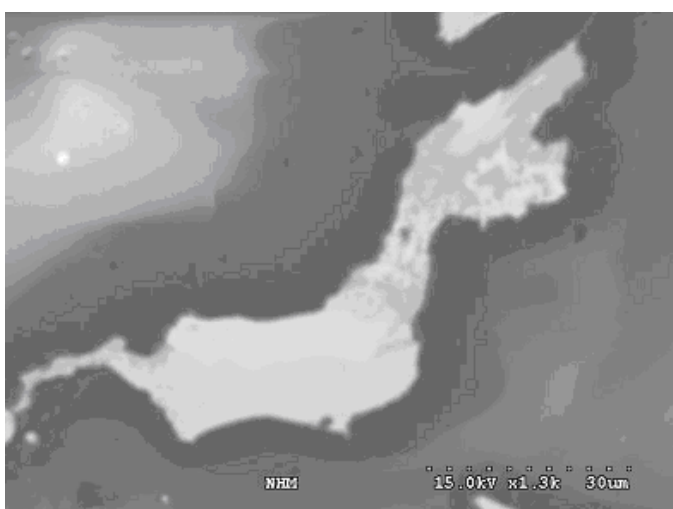


Fig. 2E Similar to previous, the brighter white is joséite-A. White spots in altered bismuthinite at top right of composite grain are native bismuth.

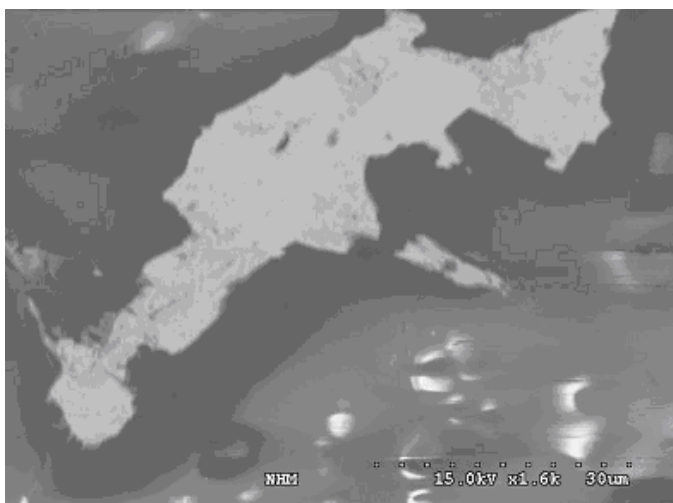


Fig. 2F Similar to other images; brightest portions are prismatic joséite-A grains.



Fig. 3A

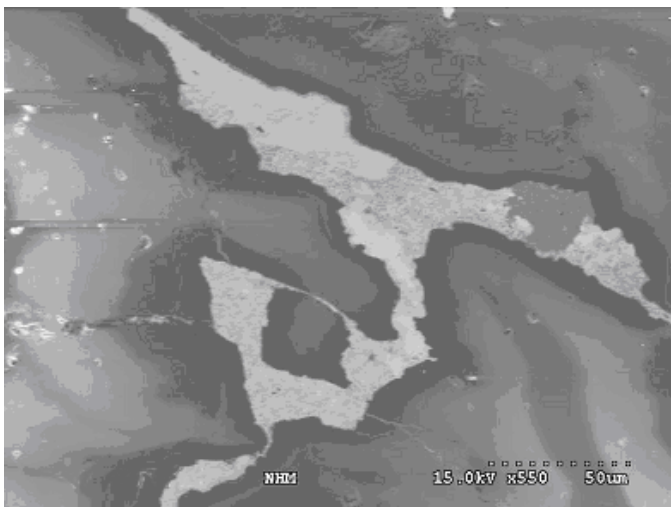


Fig. 3B

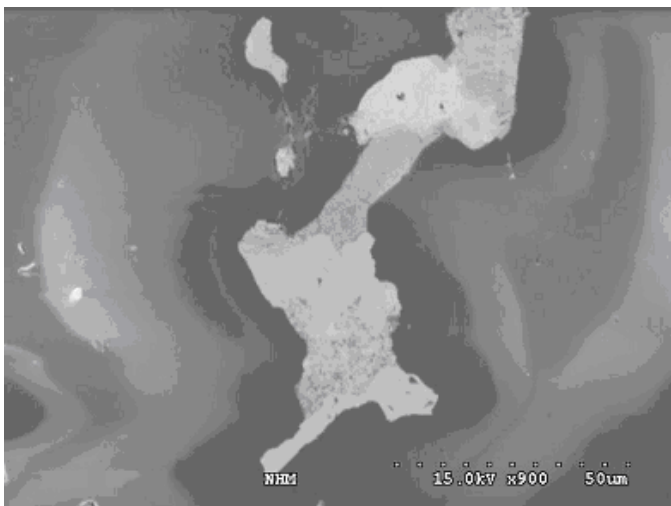


Fig. 3C

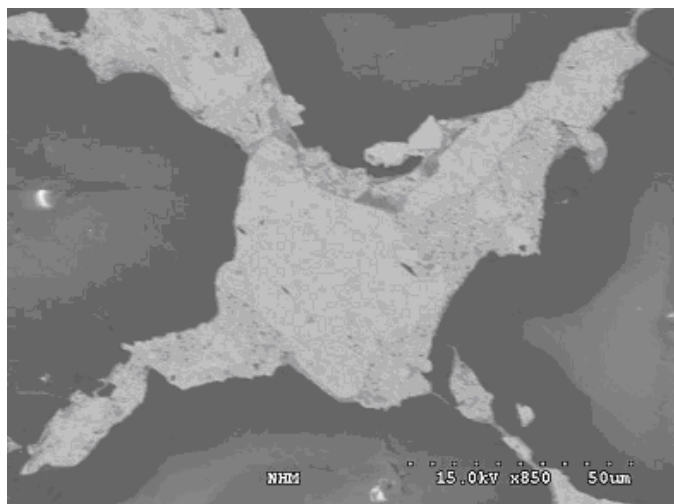


Fig. 3D

Figs. 3A-D. Electron back-scattered electron images showing additional composite grains of Bi-mineral grains in sample BQ-02. In each image brighter area in central part is joséite-A, darker areas are bismuthinite and its alteration products. In Fig. 3C in addition to joséite-A and bismuthinite, native bismuth and galena occur. Joséite-A is the main light grey mineral in the centre of the image. Bismuthinite is much darker grey and messy looking. Native bismuth in upper part of image is the brightest phase. In the middle joséite-A is slightly brighter than adjacent galena. Textures suggest joséite-A and galena formed in equilibrium.

Energy-dispersive spectroscopic (SEM-EDS) analyses of joséite-A is given in the following table (elements in wt. %)

Analysis	Ag	As	Bi	Pb	Sb	Te	Se	S	Total
joséite-A	-	-	66.93	9.51	-	12.53	3.78	4.19	96.94
joséite-A	-	-	69.25	9.46	-	15.04	0.28	5.97	100.00

Joséite-A, ideally Bi_4TeS_2 , formulae:

Analysis	Ag	As	Bi	Pb	Sb	Metal total	Te	Se	S	Se + S Total
joséite-A	-	-	3.99	0.05	-	3.99	1.07	0.52	1.42	1.94
joséite-A	-	-	3.39	0.47	-	3.85	1.21	0.04	1.90	1.94
joséite-A BQ-02 average	-	-	3.69	0.26	-	3.92	1.14	0.28	1.66	1.94
joséite-A Eloise Vein South 0441 average n=9 by microprobe	-	-	3.68	0.15	0.01	3.84	1.15	0.01	2.00	2.01
joséite-A Eloise Vein North 0412 average n=9 by microprobe	-	-	3.70	0.14	0.01	3.85	1.12	0.01	2.01	2.02

Joséite-A has 0.28 apfu Se in the Blue Quartz Vein, considerably more than in joséite-A from Eloise Vein.

Table of minerals identified in three Blue Quartz Vein polished sections, listed in decreasing order of metal: chalcogen ratio

	metal: chalcogen ratio	*Blue Quartz Vein 0414 (Cook & Ciobanu 2006)	BQ-01 this report	BQ-02 this report this report
native gold	-	√(electrum)		
native bismuth	very high	√	√	√
unnamed Bi ₂ Te	2	√		
joséite-A	4:3 = 1.33	√		√
joséite-B	4:3 = 1.33	√		
ikunolite	4:3 = 1.33	√		
bismuthinite	2:3 = 0.66	√	√	√
molybdenite	-	√		
galena	-		√	√
scheelite	-			

*0414 also has rutile, ilmenite, magnetite and various REE-phosphates

Concluding comments on ore genesis

That no grains of gold are seen in either Blue Quartz Vein 2008 sample despite known high gold grades (8.65 g/t) can be attributed to inhomogeneous distribution of gold in the vein - a 'nugget effect'. Considering this, it is difficult to achieve representative sampling of the Blue Quartz vein by investigating only a few cm-scale polished sections. Results of a former microscopic study (Cook & Ciobanu, 2006) that did observe gold grains and many Bi-Te mineral assemblages combined with the present one assist in interpreting the nature of this gold occurrence. The bismuth telluride minerals observed in BQ-02 substantiate the analysis of 478 ppm Bi & 23 ppm Te in sample 0414. The abundant oriented arrays of blebs in the BQ-02 quartz matrix or 'fracture-trails' are visually spectacular (Fig. 1) These characteristic trails of Bi-minerals as blebs in quartz are, in the author's experience, very typical of intrusion-related gold deposits (Hart, 2007). Formation of the Blue Quartz vein may have taken place under high-volatile, CO₂-rich conditions with sudden catastrophic and erratic release of volatiles from hydrothermal fluids.

Similar trails of Bi-Te mineral-bearing fluid inclusions are observed in the quartz-sulphide vein system of the Batman orebody (Mt Todd mine) in Australia by Hein et al. (2006): "Detailed paragenetic and textural studies ... establish a sequence in sulphide and silicate precipitation (detailed in their Fig. 2): formation of sulphides; replacement of pyrrhotite by pyrite and marcasite; Bi-Te ± Pb ± Ag mineralisation; and finally Bi-Au mineralisation." This is discussed elsewhere in the accompanying Assessment Report.

High fluid circulation and/or percolation rates would assist hydraulic brecciation, represented by late-stage crushing and fracturing of the vein. This is also observed in Eloise Vein with its multiple fracture sets. Such conditions are some of the features enabling formation of reduced intrusion-related gold systems: deep fluid sources and CO₂-rich hydrothermal fluids that deposit gold and intimately associated bismuth telluride minerals (Hart, 2007).

Microscopic study of other CLY samples indicates that most gold is finer-grained and generally not coarser than the Bi-minerals with which it associates. The occurrence of bismuth minerals in the Blue Quartz vein, even in only minor amounts - similar to those in

other polished sections from the other occurrences - suggests that this vein is directly comparable to those. The Bi-telluride mineral assemblages are characteristic: they are limited to a narrow range of metal:chalcogen ratio, that is $(\text{Bi} + \text{minor Pb} + \text{trace Sb}) / (\text{Te} + \text{S} + \text{trace Se})$, generally > 1 , with high sulphide content. Joséite-A is dominant as the main Bi-telluride in sample BQ-02. In the Blue Quartz vein there is a tendency for more S-rich species to envelop low-S or S-free minerals .

Stably coexisting pairs of Bi-tellurides in sample 0414 of the Blue Quartz vein (Cook & Ciobanu, 2006) are

[1] joséite-B + unnamed $\text{Bi}_2\text{Te} \pm$ native gold

[2] joséite-B + native bismuth \pm native gold

[3] joséite-A + ikunolite

[4] joséite-A + native bismuth

[5] ikunolite + native bismuth

and [6] joséite-A + bismuthinite in BQ-02. Joséite-A + galena also stably co-exist in BQ-02.

Additional Refs.

Hein, K.A.A., et al., (2006) Linking mineral and fluid inclusion paragenetic studies: The Batman deposit, Mt. Todd (Yimuyun Manjerr) goldfield, Australia. *Ore Geology Reviews* 28 p. 180–200.

Hart, C.J.R., (2007) Reduced intrusion-related gold systems. p. 95-112 in *Mineral deposits of Canada: A Synthesis of Major Deposit Types, District Metallogeny, the Evolution of Geological Provinces, and Exploration Methods*. Ed. Goodfellow, W.D., Geological Association of Canada, Mineral Deposits Division, Special Publication No. 5

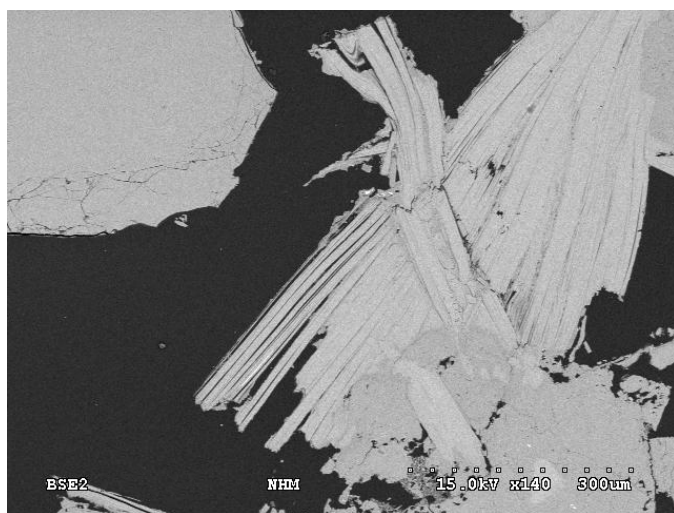
Sample Clease 0446 shear, vein

Background

Sample Clease 0446 shear is from a showing named 'Clease 0446-BHCK-13 Shear' in granitoid located downhill and south of the Lefevre workings (Howard, 2006a). Site is at UTM 471,636 mE 5,433,947 mN \pm 25 m. 0446 resamples BHCK-13 of Kennedy (2003). Clease 0446 shear is a 1.52 m chip sample from a hand dug trench in limonitic, clayey (sericite?) intensely altered Bunker Hill Sill granitoid. The shear trends 128° and subcrops for several meters. "Shining Bi minerals and sericite are common in mm-sized vugs; patches of lemon-yellow secondary Bi minerals occur in limonitic rusty parts (Howard, 2006a)". See photos figs. 12 & 13 in that report. 0446 ran 6.411 g/t Au by FA, 6.796 g/t by ICP-MS, 1.921 g/t Ag / 462 Bi / 16.7 Te / 48.5 Pb / Mo 48.5 / 83.8 Cu / 123.4 As (all ppm). This analysis confirms auriferous bismuth tellurides do occur. 0.8 Se / 1.8 Sb / Nb 2.2 / Zr 1.8 / Th 10.2 (ppm) are not anomalous.

Polished section description

Clease 0446 shear consists of a dark grey quartz-rich matrix. There are no visible macroscopic ore minerals, and none were found during optical and scanning electron microscopy. Quartz, accounting for >80% of the polished section despite the colour, contains abundant fine-grained, bladed phengitic white mica (Fig. 1) and lesser amounts of biotite, plagioclase and epidote. Accessory minerals are dominated by abundant zoned grains of zircon and ilmenite, rutile, hematite, apatite, and a number of different REE- and Nb-bearing phases, including monazite and possibly other phosphates (Figs. 1 and 2).



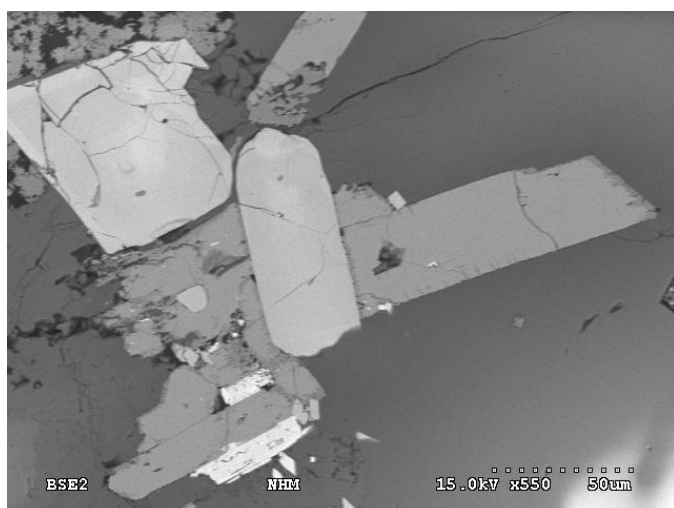
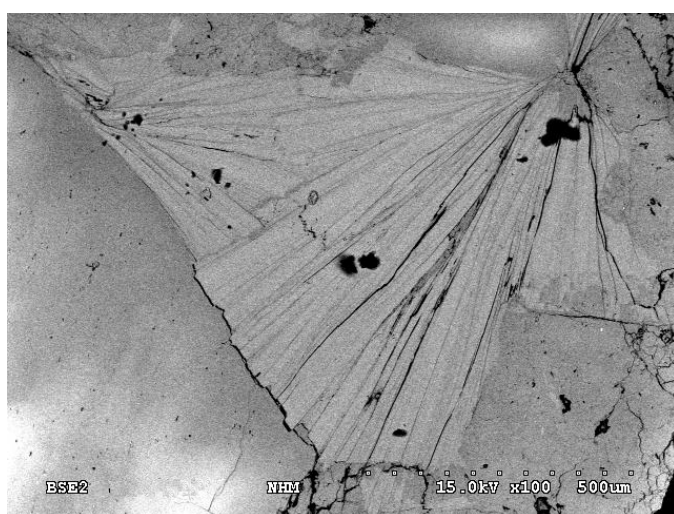
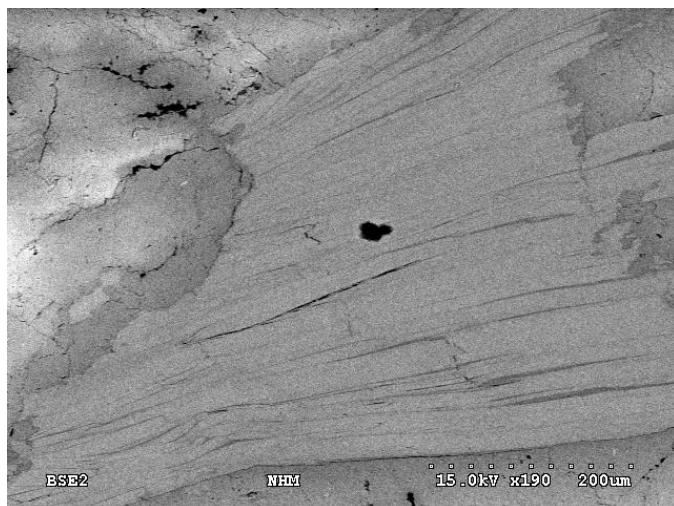


Fig. 1. Back-scattered electron images of mineralogical aspects of CLS 0446. (First three) Blades of phengitic white mica within quartz. (Last image just above) Assemblage of accessory minerals: zoned grains of zircon (prominent light grey grains) and tabular ilmenite (medium grey) onto which the zircon is growing. The brightest grain (lower part of image) is a REE-phosphate. Matrix is quartz.

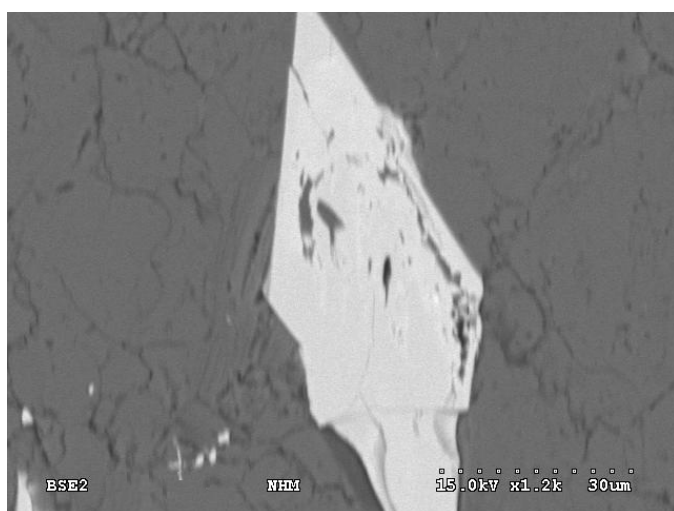
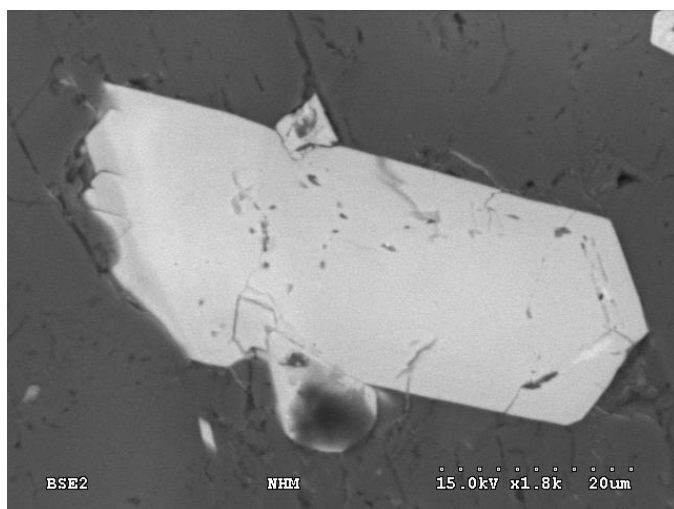
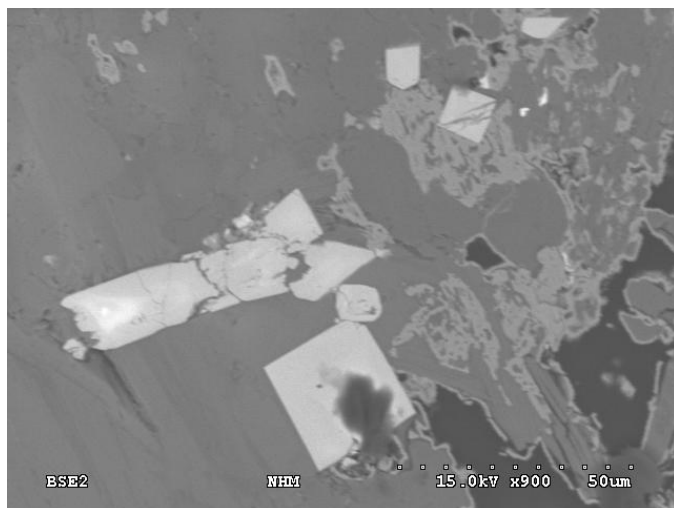




Fig. 2. Back-scattered electron images showing further mineralogical aspects of sample CLS 0446. First shows a cluster of prismatic zircon grains (bright on the image) within quartz. The irregular, darker grey mineral to the right of the zircon cluster is rutile. Second & third show compositionally-zoned grains of zircon within a quartz matrix. Fourth image just above is an elongate lath of ilmenite (the main part of the grain, light grey), with some rutile contained within it (medium grey). The small, bright white grain at the bottom and in the ilmenite lath is monazite.

Laser ablation analysis of Fe sulphides for ‘invisible gold’ in samples L-11 from the Lefevre workings and BHUS-01 from Adit 1 of the Bunker Hill mine

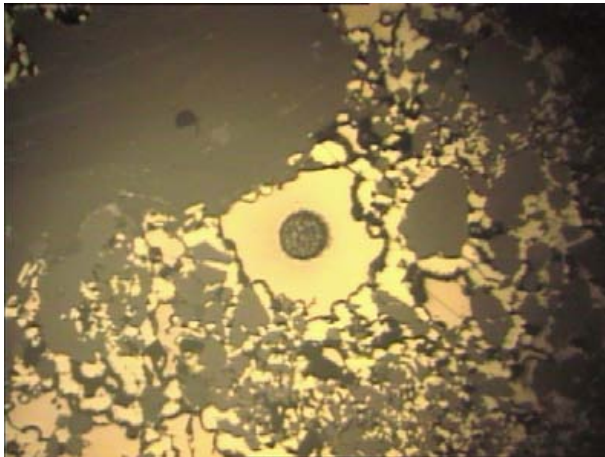
In situ laser ablation analysis is an efficient method to determine the trace element concentrations in a range of minerals. Pyrite can, in some deposits (epithermal, Carlin-type...), be an important host mineral for so-called ‘invisible gold’ (a term for both gold in the pyrite lattice itself and as sub-microscopic inclusions). Here, the LA-ICP-MS technique investigates the distribution of Mn, Co, Ni, Cu, Zn, Ga, Ge, As, Se, Mo, Ag, Cd, In, Sn, Sb, Te, Au, Tl, Pb and Bi within iron-sulfides (pyrite, marcasite and pyrrhotite) in sample L-11 and two pyrite grains in sample BHUS-01.

Analytical

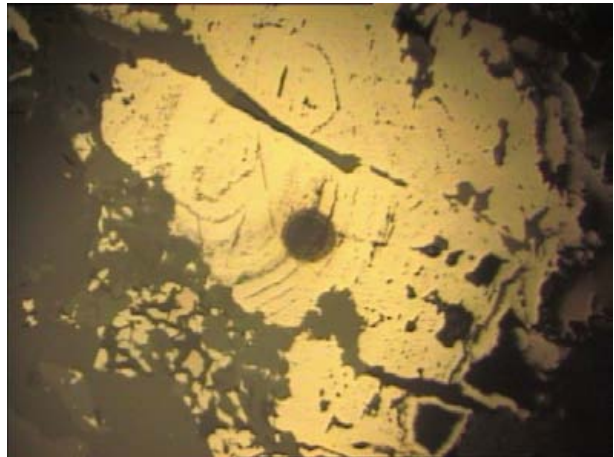
See the analytical technique for sphalerite in the sample L-12 report. Iron is used as the internal standard for these analyses.

BHUS-01 is from the Underhand Stope Vein in Adit 1. The nine laser ablation holes in the Fe sulphides (seven in L-11, two in BHUS-01) are in the following microphotographs:

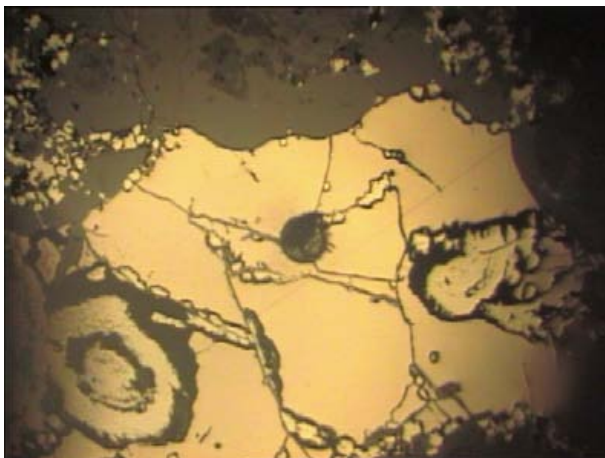
L-11 (pyrite – grain 1)



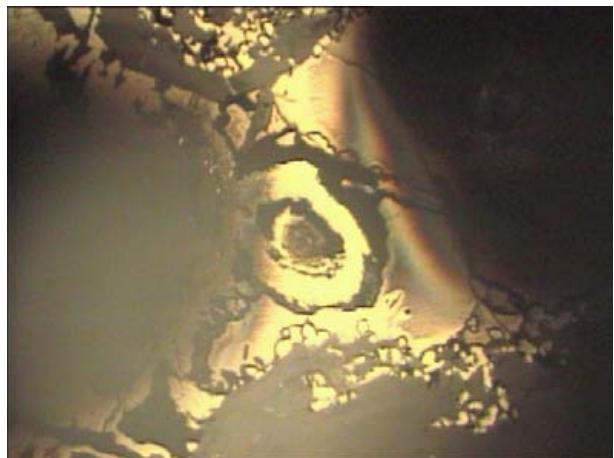
L-11 (marcasite-grain 2)



L-11 (pyrrhotite/marcasite – grain 3)

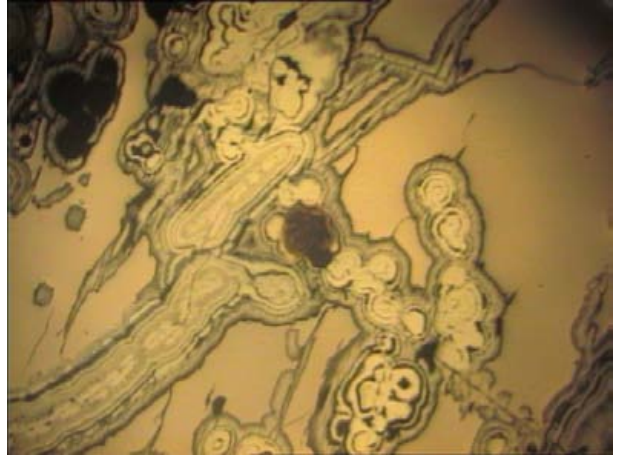
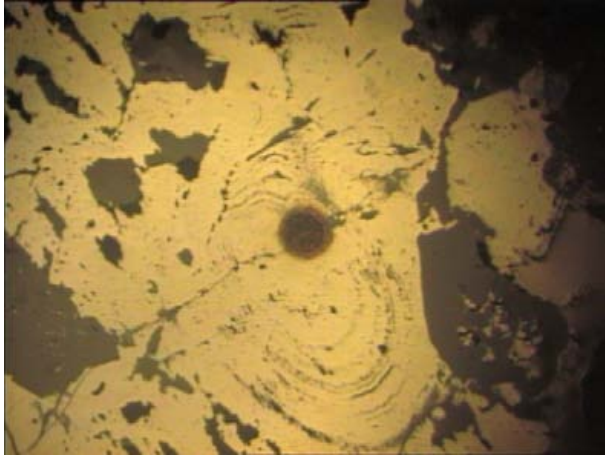


L-11 (marcasite-grain 4)

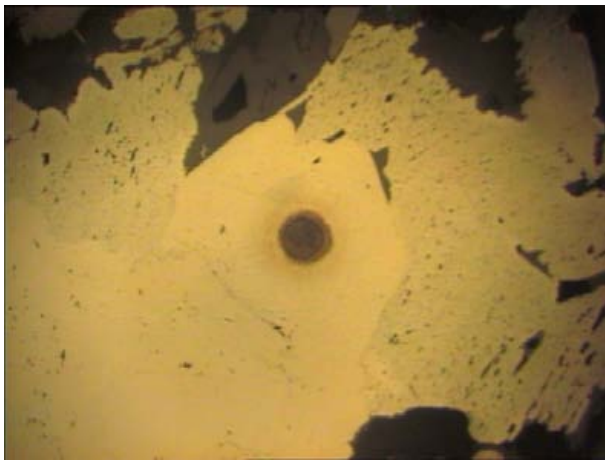


L-11 (marcasite – grain 5)

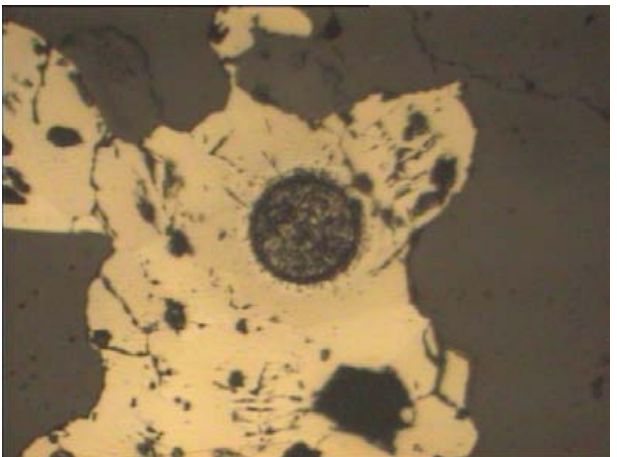
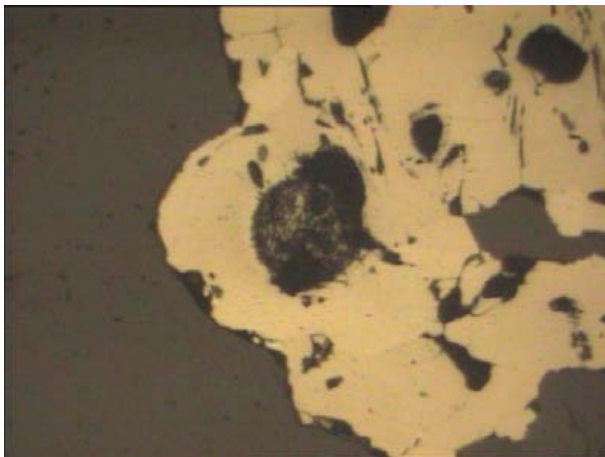
L-11 (marcasite-grain 6)



L-11 (pyrite – grain 7)



BHUS-01(pyrite)



Results

The following table summarizes the data for the nine spots (mean, standard deviation, maximum and minimum for L-11, two individual spot analyses for BHUS-01, all in ppm). <mdl is less than the analytical minimum detection limit.

	Mean (L-11)	S.D. (L-11)	Max (L-11)	Min (L-11)	BHUS-01 (1)	BHUS-01 (2)
Mn	180	219	452	3	72	1419
Co	156	27	187	118	29	35
Ni	288	106	408	149	145	181
Cu	0.7	1.4	3.7	<mdl	16.0	26
Zn	4.1	4.3	13.4	0.8	4.6	14.4
Ga	<mdl	<mdl	<mdl	<mdl	0.3	<mdl
Ge	6.5	0.2	6.7	6.2	6.5	6.7
As	0.4	0.7	1.7	<mdl	7.2	30.5
Se	12.1	4.6	19.0	8.0	5.1	4.9
Mo	2.4	2.6	5.7	0.1	1.6	1.2
Ag	0.4	0.2	0.6	0.2	10.6	4.8
Cd	<mdl	<mdl	<mdl	<mdl	8.6	10.1
In	<mdl	<mdl	<mdl	<mdl	<mdl	<mdl
Sn	0.09	0.09	0.20	<mdl	0.12	1.42
Sb	0.34	0.44	1.08	0.03	0.84	0.43
Te	0.07	0.04	0.12	<mdl	0.77	0.72
Au	0.11	0.12	0.33	<mdl	0.01	0.01
Tl	0.21	0.34	0.88	<mdl	0.04	0.04
Pb	2.83	2.27	6.17	0.22	687	44.7
Bi	2.13	2.27	7.10	0.13	462	10.3

Interpretation and comments

The analyzed sulfides do not contain any significant invisible gold (as might be expected given their geological history). The contents of As are negligible. The only minor components at levels in the hundreds of ppm range are cobalt and nickel. Concentrations of other elements commonly occurring in Fe-sulfides (Cu, Se) are very low, excepting Bi at 462 ppm and Pb at 687 ppm in BHUS-01 (spot 1). Te is also enhanced at 0.77 ppm.

Eloise Vein

The writers (Cook & Ciobanu 2006, Part II in Howard 2006a) reported on the mineralogy of one sample from Eloise Vein South in ‘Mineralogical investigation of polished sections from CLY Group, Southeastern B.C., Canada Preliminary report Aug. 10 2006’ Details have also appeared in a research paper and an abstract (Cook et al., 2007b; Howard et al., 2007).

The objectives of this study are to verify if the mineralogy is consistent along Eloise Vein and to further constrain the mineral associates of gold.

Three samples EL-02 EL-05 and EL-07 were studied using conventional reflected light ore microscopy and scanning electron microscopy [SEM] at the Natural History Museum, University of Oslo. EL-02 is from Eloise Vein South; EL-05 & EL-07 are about 4 m apart, EL-05 to the N, both from Eloise Vein North (Map 1).

Many of the SEM Energy Dispersive Spectroscopic analyses (SEM-EDS) were performed in back-scattered mode. This allows the SEM images to have mineral brightness as an expression of the average atomic weight, i.e. pyrite appears brighter than low atomic-weight quartz but less bright than ‘heavy’ gold.

Sample EL-02

Background

Sample EL-02 was collected from Eloise Vein South at UTM 471,648 mE 5,434,396 mN \pm 4 m. It is from the site of rock 0441 a 0.3 m chip sample of limonite-stained quartz with about 0.5% Bi minerals (Howard 2005), the same site as BHCK-24 (see Map 1). Acme Analytical Labs reported Au 8.17 g/t by Fire Assay [FA], 7.97 g/t by ICP-MS, 1.43 Ag / 564 Bi / 33 Te / 4.8 Pb / 2.9 Cu / 15.2 Zn / 30.1 Mo / 37.1 W / 0.8 As and 0.2 Se, all in ppm. Bulk fineness is 851.

A former polished section examination of 0441 in 2006 found “relatively coarse (50-100 μ m) patches of Bi-Te¹ minerals within the quartz vein (Cook & Ciobanu Part II in Howard 2006a)”. Ingodite, hedleyite (or more correctly near-stoichiometric unnamed Bi₂Te) are equally abundant. Minor joséite-B occurs as fine-grained exsolutions within unnamed Bi₂Te grains (their fig. 4F). Their Figs. 8A & 8B image a well developed corona texture about cores of ingodite grains. These are surrounded by unnamed Bi₂Te with native gold deposited at grain interfaces and also within evidently later-formed Bi₂Te. “Coarser native gold grains also occur towards the margins of the Bi-Te minerals. Coarse symplectites of joséite-A and joséite-B and, tentatively, minor bismuthinite were observed (Cook et al., 2007b)”. Symplectites are equilibrium intergrowths of two mineral phases in approximately equal proportions that formed from a higher temperature mineral. Rounded boundaries characterize the texture. Symplectites are common in metamorphic rocks/ores; myrmekites are feldspar symplectites.

¹ Bismuth and bismuth telluride minerals

In that 2007b research paper formulae for these 5 minerals in two polished sections 0441a & 0441b were reported from microprobe analysis with a CAMECA SX-51 instrument at Adelaide Microscopy, Adelaide, South Australia. The 0441 sample site is referred to as 'Eloise' or the 'first location' in that paper.

Average formulae and the number n of determinations are:

ingodite ideally $\text{Bi}_2(\text{Te},\text{S})$ n= 10
($\text{Bi}1.88\text{Pb}0.04$)SUM1.94($\text{Te}1.06\text{Se}0.02\text{S}1.00$)SUM2.08

hedleyite-like phase – actually near-stoichiometric unnamed Bi_2Te n=12
($\text{Bi}1.97\text{Pb}0.02\text{Sb}0.01$)SUM2.00($\text{Te}0.93\text{S}0.06\text{Se}0.01$)SUM1.00. Pb Sb S & Se are near absent.

joséite–A ideally $\text{Bi}_4\text{S}_2\text{Te}$ n=8
($\text{Bi}3.68\text{Pb}0.15\text{Sb}0.01$)SUM3.84 $\text{Te}1.15(\text{S}2.00\text{Se}0.01)$ SUM2.01

joséite–B ideally $\text{Bi}_4\text{Te}_2\text{S}$ n=6
($\text{Bi}4.03\text{Pb}0.04\text{Sb}0.02$)SUM4.08 $\text{Te}1.89(\text{S}1.01\text{Se}0.02)$ SUM1.03

bismuthinite ideally Bi_2S_3 representative
($\text{Bi}1.96\text{Pb}0.03\text{Cu}0.02\text{Sb}0.02$)SUM2.03($\text{S}2.98\text{Se}0.01$)SUM2.99

On these same polished sections isotopes of 11 elements were monitored in symplectites of joséite–B & –A, ingodite and unnamed Bi_2Te by LA-ICP-MS microanalysis using the Agilent HP4500 Quadrupole ICP-MS instrument at CODES, University of Tasmania in Australia. Results are also reported in Cook et al. (2007b). Investigating the 'gold corona texture', three spots ablated in unnamed Bi_2Te surrounding ingodite ran 57 ± 8 ppm, 6.8 ± 1 ppm and 3.6 ± 0.7 Au (their Fig. 3). "The mantling of ingodite by Bi_2Te and the rim of native gold formed at the boundary between the two (their Fig. 2c, d) can be interpreted as replacement of ingodite that also may have released gold (op. cit.)".

Polished section description

EL-02 is white, slightly milky quartz, similar in appearance to EL-05 and EL-07. There are no visible opaque minerals on the surface of the polished section when viewed with the naked eye, but reflected light microscopy reveals a number of very small particles, each up to a maximum of ca. 60 μm in diameter along fractures in the quartz and along boundaries of quartz grains. These tend to be arranged in patches; the section contains three of these (Fig. 1). The ore minerals consist of bismuthinite, native bismuth, alteration minerals replacing bismuthinite and very minor quantities of Bi-tellurides. Two grains of native gold are noted. The section also contains a single, rather coarse grain of scheelite (Fig. 2).

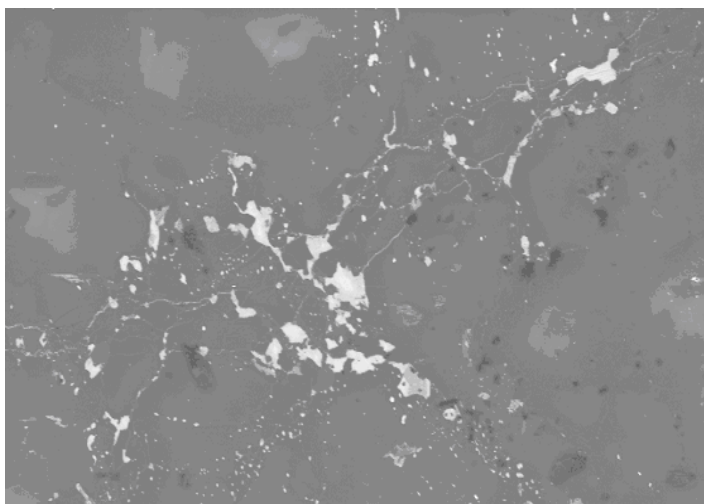
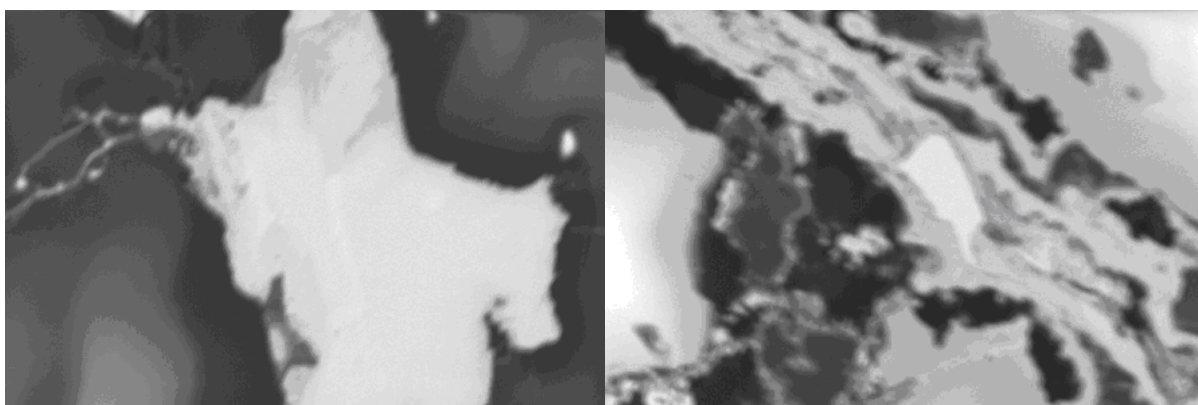


Fig. 1. Electron back-scattered electron image showing a relatively large patch of Bi-minerals located along grain boundaries and in fractures within the quartz matrix. The “shades” within the quartz are due to electronic effects or instrument charging. Horizontal field of view: ~1500 μm or ~1.5 mm.



Fig. 2. Photomicrograph in reflected light of a coarse grain of scheelite (medium grey), partially replaced by a secondary tungstate mineral (?) appearing almost as dark as the matrix quartz in the far right and left of the image. A small grain of gold can be seen in the centre of the grain, within a fracture in the scheelite. This is also filled by replaced Bi-Te minerals. Horizontal field of view: 650 μm.

Scanning electron microscope study shows that the Bi-tellurides are joséite-B and phases with high Bi / (Te + Se +S) in the range Bi_2Te – Bi_7Te_3 .



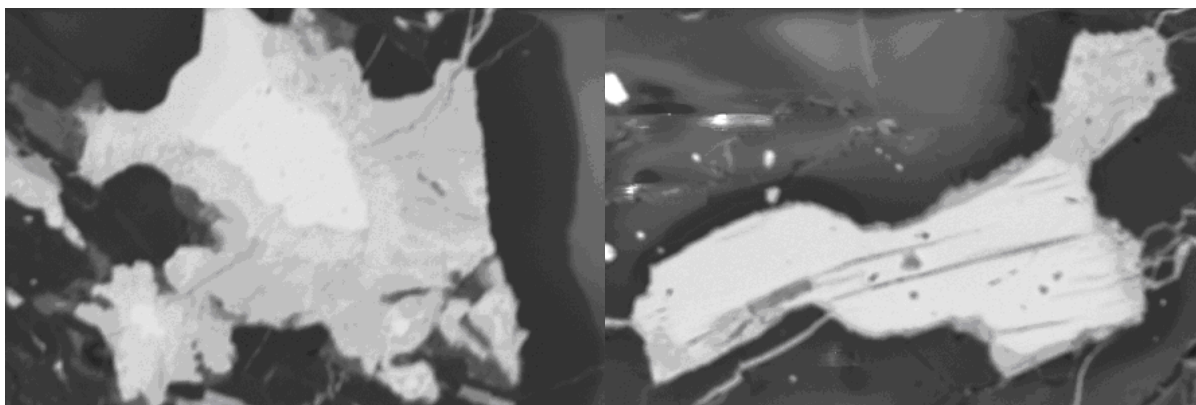


Fig. 3 Back-scattered electron images of Bi-minerals in sample EL-02. (Top left) The largest grain of Bi-minerals, with a composition near stoichiometric Bi_2Te (very light grey, the major part of the grain), native bismuth (white, small elongate grains) lying within the Bi_2Te , and alteration minerals after bismuthinite (top right of the image). Horizontal field of view 100 μm . (Top right) Small grain of native gold (bright white, middle of image) containing 21.1 wt. % Ag, within a narrow fracture in scheelite (seen in Fig. 2) partially filled with replaced Bi-minerals. Horizontal field of view 60 μm . (Lower left) Composite grain composed of native bismuth (white, in centre), bismuthinite (light grey, immediately surrounding the native bismuth), joséite-B (lighter grey immediately 'above' the native bismuth) and galena (above the joséite-B, on the upper left-side rim of the grain). Horizontal field of view 100 μm . (Lower right) Grain of joséite-B with alteration rim within quartz. Horizontal field of view 120 μm .

Two grains of native gold were seen in the sample: the one in the fracture within scheelite (Fig. 1, Fig. 3, upper right) and another grain (ca. 10 μm in diameter, 23.2 wt. % Ag) within one of the Bi-mineral patches. At 21.2 and 2.3.2 % silver these gold grains are more correctly named **electrum**.

Energy-dispersive spectroscopic (SEM-EDS) analyses of Bi-minerals are given in the following table (elements in wt. %).

Analysis	Ag	As	Bi	Pb	Sb	Te	Se	S	Total
Bi-telluride I	-	-	71.30	4.08	-	23.65	0.10	-	99.13
Bi-telluride II	-	-	72.68	4.05	-	22.36	0.27	-	99.36
*Bi-telluride III	-	-	74.75	0.36	-	22.16	0.07	-	97.34
Bi-telluride IV joséite-B	-	-	71.64	0.41	-	23.44	0.63	3.57	99.69

*Analysis III has little Pb and a low analysis total; it is considered suspect and not included in the average

Phase	Ag	As	Bi	Pb	Sb	Metal Sum	Te	Se	S	Chalcogen Sum
Bi-telluride I	-	-	1.87	0.11	-	1.99	1.02	0.01	-	1.02
Bi-telluride II	-	-	1.91	0.11	-	2.02	0.96	0.02	-	0.98
*Bi-telluride III	-	-	2.01	0.01	-	2.02	0.98	-	-	0.98
unnamed Bi_2Te average of 2	-	-	1.89	0.11	-	2.005	0.99	0.015	-	1.00

Analyses I-III on the largest grain in the section (Fig. 2, top left) and are near-stoichiometric unnamed Bi_2Te . This may indicate little lattice-scale disordering and a homogeneous phase; the composition is not hedleyite Bi_7Te_3 or $\text{Bi}_{2+x}\text{Te}_{1-x}$ ($x = 0.13$ to 0.19) but rather unnamed Bi_2Te . Presence of unnamed Bi_2Te in EL-02 from Eloise Vein South contrasts with hedleyite identified in polished sections of Bunker Hill mine veins: BH UHS 01 from Adit 2 and BH 0567 & BHA-1-8 from Adit 1 (which see).

Phase	Ag	As	Bi	Pb	Sb	Metal	Te	Se	S	Chalcogen
-------	----	----	----	----	----	-------	----	----	---	-----------

						Sum				Sum
Bi-telluride IV joséite-B	-	-	3.70	0.02	-	3.73	1.99	0.09	1.20	2.07

Analysis IV was made on the grain of joséite-B in Fig. 2 (lower right); it has trace Pb & Se.

Sample EL-05

Background

EL-05 was collected from Eloise Vein North near 0424, precisely at UTM 471,652 mE 5,434,412 mN \pm 4 m (Map 1). Here Clarissa Vein joins Eloise Vein North on the latter's E side and ends. 0424 was a grab sample of "rusty, well fractured quartz taken 0.2 m downslope of rock 0412 [also from Eloise Vein North]. White and rusty quartz has very common limonite-coated fractures; the dominant set is spaced 5–10 mm apart. Minor vugs are 1–3 mm in size. Uncommon clots of dark grey blue bismuthoid minerals colour the quartz. Very fine sized grains of visible gold are set amongst weathered Bi minerals and rare traces of a straw yellow-green mineral (Howard 2005)." EL-05 is about 4 meter N of EL-07 (discussed below, see Map 1).

Grab rock sample 0424 ran 9.94 g/t Au by metallics double FA on 485 g, 10.29 g/t Au & 1.52 g/t Ag by ICP-MS, and 476 Bi / 55.8 Te / 15.4 Pb / 6.5 Cu / 8.6 Mo / 0.8 W / 2.4 As / 0.2 Sb / 0.2 Se (bkgd), all in ppm. Calculated 'bulk' fineness is 868 (op. cit.). Total Pb is low, 15.4 ppm.

Polished section description

EL-05 consists of white, slightly milky quartz, like EL-07 described below. Minor quantities of ore minerals occur along as patches, up to ca. 500 μ m in size and in fractures along grain boundaries within the quartz (comprising <1 vol.% of the polished section). The ore minerals consist of bismuthinite, minor native bismuth and alteration minerals replacing bismuth, as well as a number of different Bi-tellurides. Native gold and scheelite are also noted. A total of 29 gold grains have been observed; most are < 10 μ m in size (see below).

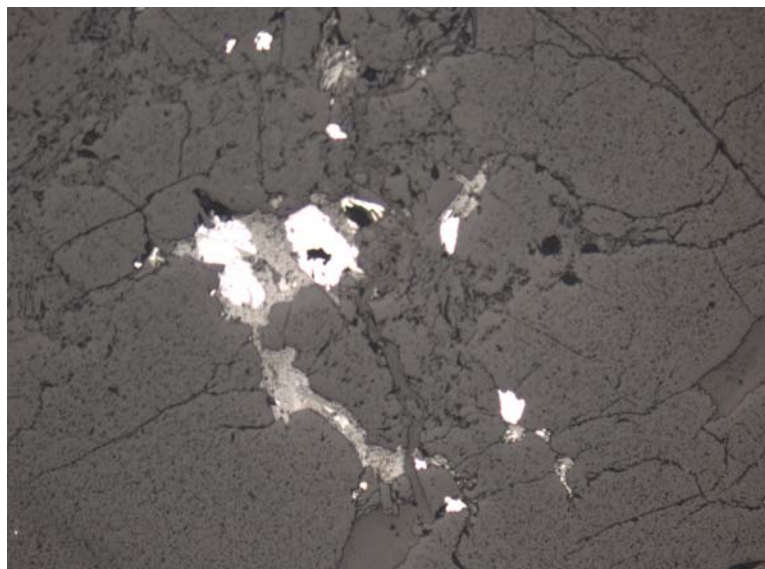


Fig. 1. Photomicrograph in reflected light of a typical patch of bismuth minerals in quartz (dark grey) matrix. Bismuthinite and Bi-tellurides stand out as bright, white grains; associated replacing alteration minerals are medium grey. The Bi-mineral assemblages occur along fractures in quartz grains and around their grain boundaries. Horizontal axis: 1.3 mm.



Fig. 2. Photomicrograph in reflected light of a patch of bismuthinite (grey-white, right of image) and an altered, near-broken scheelite crystal displaying cleavage (?) (medium grey, left of image) within a mass of unidentified, oxidized, Fe-Bi-bearing minerals (darker grey), within (black) quartz matrix. Horizontal axis: 650 μm .

Scanning electron microscope study shows that there are several Bi-telluride phases present in the sample. Both joséite-B and -A are noted, as well as the $\text{Bi}_4\text{Te}_3\text{S}_2$ phase (*cf* sample EL-07 described below) and several phases in the $\text{Bi}(\text{Te},\text{S}) - \text{Bi}_8(\text{Te},\text{S})_9$ compositional range. Joséite-B appears to be the most common Bi-telluride. Unlike bismuthinite, which is commonly completely replaced, the Bi-tellurides show only moderate degrees of replacement by secondary minerals. Figs. 3-6 are a series of back-scattered images that illustrate textures and associations in a number of grains in EL-05.

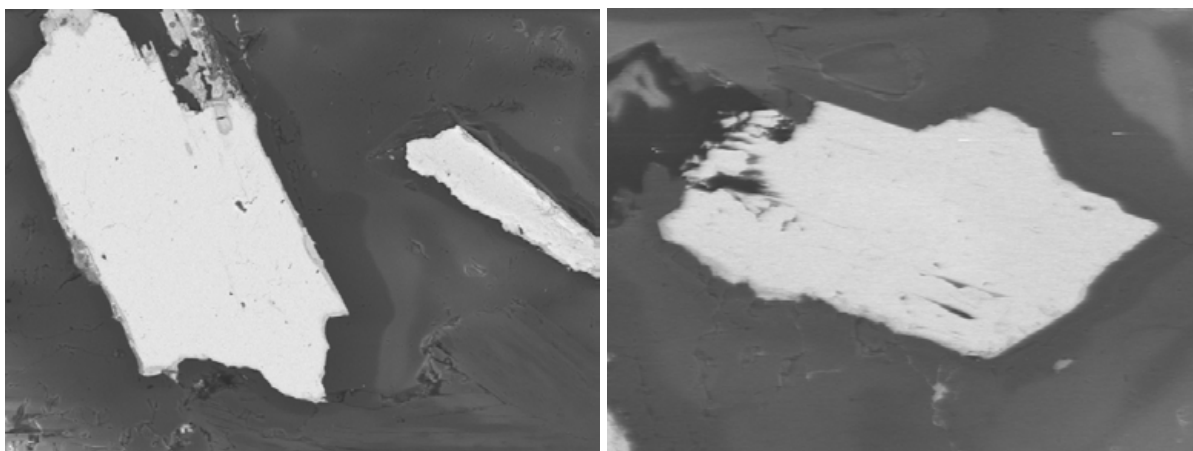


Fig. 3 Back-scattered electron images of Bi-minerals in sample EL-05. (Left) Grain of unnamed $\text{Bi}_4\text{Te}_3\text{S}_2$ in quartz matrix. Horizontal axis: 145 μm . (Right) Another grain of unnamed $\text{Bi}_4\text{Te}_3\text{S}_2$ in quartz matrix. Horizontal axis: 135 μm .

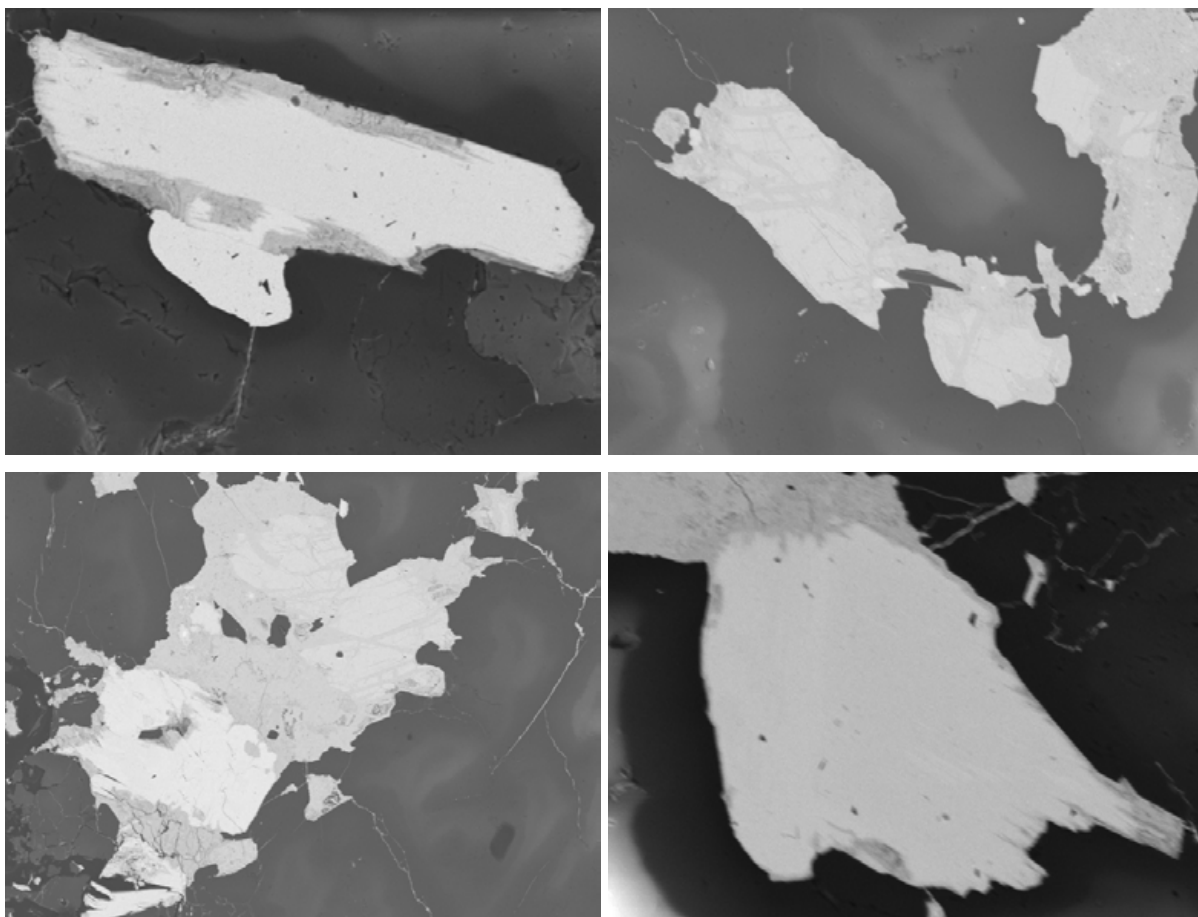


Fig. 4 Back-scattered electron images of Bi-minerals in sample EL-05. (Top left) acicular grain of $\text{Bi}_4\text{Te}_3\text{S}_2$ showing some modest alteration towards its margins and an adjacent grain of native gold, the rounded, brighter part underneath it. The native gold is 15.2 wt. % Ag. Horizontal axis: 80 μm . (Top right) Grains of altered, replaced bismuthinite. Note how the replacement follows crystallographic planes. Horizontal axis: 185 μm . (Lower left) Large, composite grain (the same grain is also pictured in Fig. 1). Bi-telluride (here, joséite-B) appears white, bismuthinite light grey; replacing alteration minerals are medium grey. Horizontal axis: 520 μm . (Lower right) Grain of Bi-telluride, mostly corresponding to ingodite $\text{Bi}(\text{Te},\text{S})$ – see table below, but with one spot corresponding to joséite-A. It is hard to discern in the microphoto, but minute compositional inhomogeneities are visible on the image. Horizontal axis: 95 μm .

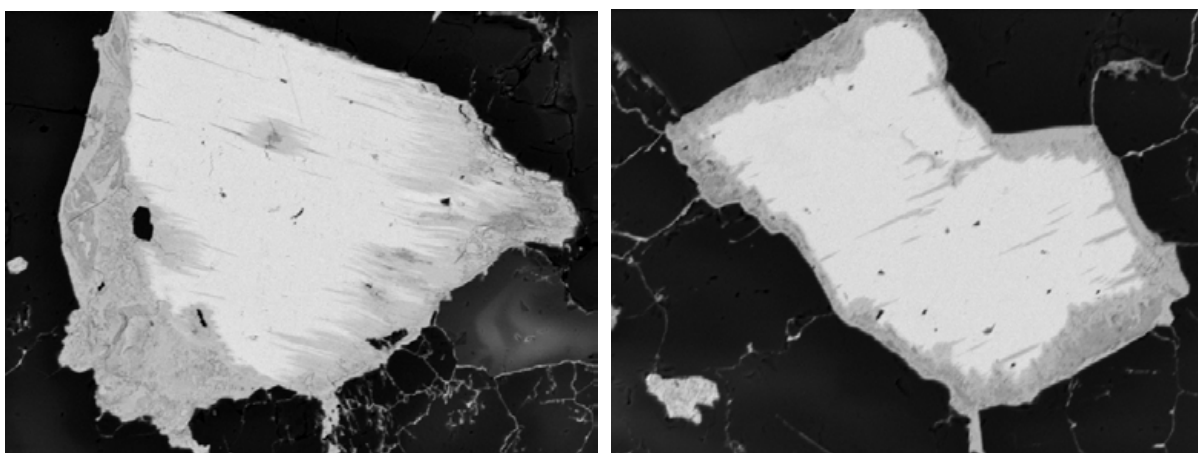


Fig. 5 Back-scattered electron images of Bi-telluride grains in sample EL-05. (Left) Grain of unnamed $\text{Bi}_4\text{Te}_3\text{S}_2$ in quartz matrix like those in fig. 3. Horizontal axis: 120 μm . (Right) Grain of joséite-B. Horizontal axis: 95 μm .

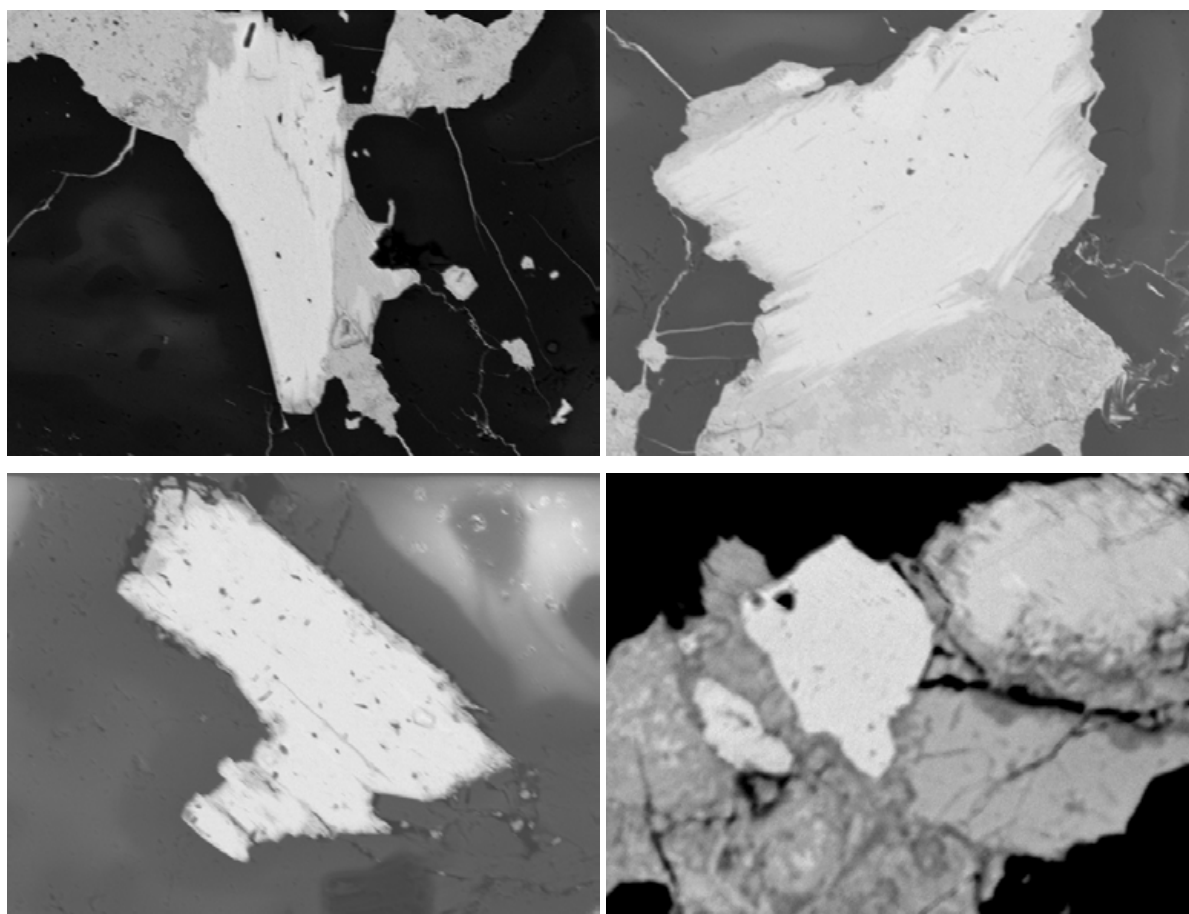


Fig. 6 Back-scattered electron images of Bi-telluride grains in sample EL-05. (Top left) Strongly replaced Bi-telluride grain. Unaltered parts of grain in centre give a composition between $\text{Bi}_4\text{Te}_3\text{S}_2$ and $\text{Bi}(\text{Te},\text{S})$, $\sim \text{Bi}_8\text{Te}_5\text{S}_4$. Horizontal axis: 85 μm . (Top right) Partially replaced Bi-telluride grain, with similar composition as previous image. Horizontal axis: 90 μm . (Lower left) Similar grain to previous, similarly altered, with comparable composition $\sim \text{Bi}_8\text{Te}_5\text{S}_4$. Horizontal axis: 90 μm . (Lower right) Grain of native gold (16.1 wt. % Ag), bright white, in matrix of replaced Bi-minerals. Relict bismuthinite is seen to the upper right. This image in particular illustrates the close association between gold and bismuth in EL-05.

Of 29 gold grains (!) observed in sample EL-05, most are isolated grains less than 10 μm in size within the quartz matrix. Two analyses 15.2 and 16.1 wt. % Au show the grains are native gold and not electrum as in EL-02. Grains in paragenetic association with Bi-Te minerals are the exception rather than the rule; these are however generally larger in size (up to 20-25 μm). The following table gives Energy-dispersive spectroscopic analyses (SEM-EDS) of the Bi-Te minerals, elements in wt. %:

Analysis	Ag	As	Bi	Pb	Sb	Te	Se	S	Total
Bi-telluride I	0.44	0.09	64.64	-	0.72	26.76	0.48	5.84	98.97
*Bi-telluride II	1.07	0.29	62.93	-	2.37	24.35	-	6.04	97.05
Bi-telluride III	-	-	59.87	8.12	1.20	25.54	-	5.28	100.01
**Bi-telluride IV	-	-	57.11	9.87	0.74	25.61	0.12	4.17	97.62
Bi-telluride V	-	-	63.15	7.28	0.04	23.54	-	4.78	98.79
Bi-telluride VI	-	-	64.37	5.41	0.45	24.71	-	4.82	99.76
Bi-telluride VII	-	-	73.33	6.10	0.18	12.69	-	6.19	98.49
Bi-telluride VIII	-	-	63.07	4.98	1.92	24.27	-	5.38	99.62
Bi-telluride IX	-	-	67.61	-	0.90	26.08	-	5.10	99.69
Bi-telluride X	-	-	62.40	5.99	-	24.87	-	5.37	98.63
Bi-telluride XI	-	-	61.66	5.44	1.14	26.53	0.12	4.80	99.69
Joséite-B I	-	-	64.52	7.15	0.67	24.15	0.07	2.15	98.71

Joséite-B II	-	-	68.40	5.52	1.39	22.27	-	2.26	99.84
--------------	---	---	-------	------	------	-------	---	------	-------

*low analysis total 97.05% ** low analysis total 97.62%

Mineral Formulae

Unnamed Bi₄Te₃S₂ mineral, formulae with sums

Phase	Ag	As	Bi	Pb	Sb	Metal Sum	Te	Se	S	Se + S Sum
Bi-telluride I	0.05	0.02	3.87	-	0.07	3.96	2.63	0.08	2.28	2.36
*Bi-telluride II	0.13	0.05	3.80	-	0.25	4.09	2.41	-	2.38	2.38
Bi-telluride III	-	-	3.68	0.50	0.13	4.31	2.57	-	2.12	2.12
average Bi ₄ Te ₃ S ₂ not including II	0.025	0.01	3.775	0.25	0.10	3.985	2.60	0.04	2.20	2.24

*low analysis total 97.05%

The first three analyses (I-III) correspond reasonably closely to the same unnamed Bi₄Te₃S₂ phase that was first documented in sample EL-07 (below). Analysis II has a low wt % total and is considered inaccurate; it is not included in the average. Analysis III has significant 8.12% Pb, 0.50 formula units. It is known that variable Pb content is a characteristic of Bi-chalcogenides belonging to the tetradymite group (*sensu latu*) which can be referred to (*cf* Ciobanu et al., 2009 in press) as structures with the general formula $S'(Bi_{2k}X_3)L'(Bi_{2(k+1)}X_3)$ (X=chalcogen element; S' , L' =number of short and long modules, respectively)². All three analyses have trace Sb. Average Bi₄Te₃S₂ in EL-05 is (Ag0.025As0.01Bi3.775Pb0.25Sb0.10)SUM3.985Te2.60Se0.04S2.20(Se+S)SUM 2.24

Ingodite ideally Bi₂(Te,S)₂, formulae with sums

Phase	Ag	As	Bi	Pb	Sb	Metal Sum	Te	Se	S	Chalcogen Sum
**Bi-telluride IV	-	-	1.66	0.29	0.04	1.98	1.22	0.01	0.79	2.02
Bi-telluride V	-	-	1.80	0.21	-	2.01	1.10	-	0.89	1.99
Bi-telluride VI	-	-	1.81	0.15	0.02	1.98	1.14	-	0.88	2.02

** low analysis total 97.62%

These three analyses IV-VI, all from the grain shown in Fig. 4, lower right, correspond to ingodite Bi(Te,S) with (Bi + Pb + Sb) / (Te + S + Se) ~ 1. The formula used in the table is Bi₂(Te,S)₂ emphasizing one apfu of Te and S. Minor Pb is present, as formerly found in 16 microprobe analyses of ingodites in sample 0412 of Eloise Vein North, only 20 cm away (Cook et al., 2007b). Discounting analyses IV, as its wt % adds only to 97.62%, and including analyses V & VI with VIII below, the average of these three EL-05 ingodites is near-stoichiometric ingodite: Bi1.78Pb0.17Sb0.04SUM1.99(Te1.11Se0.00S0.91)SUM2.02.

Significant 0.17 apfu³ Pb substitutes for Bi. This is irrespective of low 15.4 ppm Pb in rock sample 0424 and only slightly more Pb, 84.1 ppm, in nearby rock 0412. To compare, the average formula from 16 microprobe analyses of 0412 is Bi1.85Pb0.09Cd0.02SUM1.97(Te0.98S1.05)SUM2.03 (op. cit.). That both averages give near-equivalent formulae for EL-05 ingodite substantiates determination of the present Bi-Te mineral compositions by the SEM-EDS method.

² k is a number expressing the number of modules in the stacking sequence, using the formula nBi₂.mBi₂X₃ describing the configuration for Bi₂kX₃ modules by n/m=k-1.

³ atom per formula unit

Joséite–A ideally Bi_4TeS_2 , formula with sums

Phase	Ag	As	Bi	Pb	Sb	Metal Sum	Te	Se	S	Chalcogen Sum
Bi-telluride VII	-	-	3.64	0.31	0.02	3.96	1.03	-	2.0	3.03

Analysis VII, also within the same grain in Fig. 4, gives an excellent joséite–A (Bi_4TeS_2) stoichiometry.

Ingodite ideally $\text{Bi}_2(\text{Te,S})_2$, formula with sums

Phase	Ag	As	Bi	Pb	Sb	Metal Sum	Te	Se	S	Chalcogen Sum
Bi-telluride VIII	-	-	1.73	0.14	0.09	1.95	1.09	-	0.96	2.05

Analysis VIII (grain in Fig. 5, left) corresponds to $\text{Bi}(\text{Te,S})$, i.e., like the ingodite analyses IV–VI, again with minor Pb.

Phase	Ag	As	Bi	Pb	Sb	Metal Sum	Te	Se	S	Se + S Sum	Chalcogen Sum
Bi-telluride IX	-	-	7.92	-	0.18	8.10	5.00	-	3.89	3.89	8.89
Bi-telluride X	-	-	7.36	0.71	-	8.07	4.80	-	4.13	4.13	8.93
Bi-telluride XI	-	-	7.27	0.65	0.23	8.15	5.12	0.04	3.69	3.73	8.85
average $\text{Bi}_8\text{Te}_5\text{S}_4$	-	-	7.517	0.453	0.137	8.107	4.973	0.013	3.960	3.973	8.89

Analyses IX, X and XI (grains in Fig. 6, top left and right and lower left, respectively) give compositions that lie somewhere between $\text{Bi}_4\text{Te}_3\text{S}_2$ and $\text{Bi}(\text{Te,S})$, actually very close to stoichiometric $\text{Bi}_8\text{Te}_5\text{S}_4$.

Phase	Ag	As	Bi	Pb	Sb	Metal Sum	Te	Se	S	Chalcogen Sum
Joséite–B I	-	-	3.57	0.40	0.06	4.03	2.19	0.01	0.77	0.78
Joséite–B II	-	-	3.75	0.31	0.13	4.19	2.00	-	0.81	0.81

Joséite–B analyses are close to stoichiometric $\text{Bi}_4\text{Te}_2\text{S}$ with minor Pb content.

Sample EL-07

Background

EL-07 was collected from Eloise Vein North near 0412, precisely at UTM 471,656 mE 5,434, 420 mN \pm 4 m. 0412 was a “41 cm chip sample of moderately fractured quartz with minor Bi minerals. At least 3 crosscutting fracture sets are present. The closest-spaced is 3-5 mm apart. Another set for a 3 cm length has mm-thick seams of dark grey-blue very fine to coarse (one mm-sized) Bi minerals, about 0.3% to 0.5% of the sample. Accompanying are many grains of coarse-grained visible gold. Rare microvugs are infilled by metallic-luster Bi minerals with trace whitish green secondary Bi minerals. A metallics double-screened fire assay on 500 g of grab rock sample 0412 found 1.18 mg native gold, the weighted total for the sample 27.03 g/t Au (Howard 2005).” 0412 also ran 23.10 g/t Au & 4.15 g/t Ag by ICP-MS, and 1,601 Bi / 95.4 Te / 84.1 Pb / 4.6 Cu / 13.2 Mo / 0.3 W / 2.2 As / 3.2 Sb / 1.0 Se (high for the property), all in ppm. Calculated ‘bulk’ fineness is 867 (op. cit.).

EL-05 & EL-07 are about 4 m apart, EL-05 on the N side of Eloise Vein North.

A polished section examination of 0412 in 2007 found “mm-sized patches of bismuthinite (<50% remain non-weathered). Tellurides such as ingodite, joséite–A and joséite–B occur either as 10-20 μ m-sized inclusions, or as larger (100-500 μ m) masses at the margin of bismuthinite. The inclusions [in bismuthinite] can be euhedral or are slightly deformed. A comparable deformation is observed along the cleavage planes of host bismuthinite. Scarce native gold is present as <10 μ m-sized inclusions in bismuthinite, sometimes combined with tellurides (their Fig. 2f). The same coarse symplectites between joséite–A and –B as in polished sections from [Eloise Vein South 0441] are observed in the larger patches at the margins of bismuthinite (Cook et al., 2007b).”

In that 2007b research paper formulae for these 4 minerals in polished section 0412 were reported from microprobe analysis with a CAMECA SX-51 instrument at Adelaide Microscopy, Adelaide, South Australia. Average formulae and the number n of determinations are:

ingodite ideally $\text{Bi}_2(\text{Te},\text{S})$ n= 16
(Bi1.86Pb0.10)SUM1.96 (Te0.98S1.06)SUM2.04

joséite–A ideally $\text{Bi}_4\text{S}_2\text{Te}$ n=9
(Bi3.70Pb0.14Sb0.01)SUM3.85S2.01(Te1.12 Se0.01)SUM1.13

joséite–B ideally $\text{Bi}_4\text{Te}_2\text{S}$ n=7
(Bi3.97Pb0.02Sb0.01)SUM4.01(Te1.85Se0.01)SUM1.86S1.13

bismuthinite ideally Bi_2S_3 representative (corrected)
(Bi1.95Pb0.02Cu0.03Sb0.02)SUM2.02(S2.98Senil)SUM2.98

In this same polished section isotopes of 11 elements were monitored in symplectites of joséite–B & –A, ingodite and bismuthinite by LA-ICP-MS microanalysis using the Agilent HP4500 Quadripole ICP-MS instrument at CODES, University of Tasmania in Australia. Results are reported in Cook et al. (2007b): “...joséite–A and –B symplectites (their Fig. 7 and close-up Fig. 8) gave values of 0.13 and 0.65 ppm Au. Ingodite was analysed by four

spots of which two gave Au values below the detection limit (ca. 0.005 ppm) [two] 0.11 and 1.13 ppm. Six spot analyses of bismuthinite [had] gold values over two orders of magnitude from 0.02 to 2 ppm”.

Polished section description

EL-07 is from Eloise Vein North within about a meter of EL-05. It consists of white, slightly milky quartz. Reflected light microscopy reveals that very minor quantities of ore minerals, <<1 vol.% of the polished section, occur as patches, up to nearly 1 mm in size, along and in fractures within the quartz. These consist of bismuthinite and alteration minerals replacing bismuthinite, and minor amounts of a single undetermined Bi-telluride phase and gold (actually electrum). No other opaque minerals are seen; native bismuth, joséite-B and -A, ingodite and scheelite are not observed unlike in EL-05, and unnamed Bi₂Te present in EL-02. Bismuthinite and its alteration products are ca. 10 times more abundant than the single telluride. Very small grains of bismuthinite, the Bi-telluride and gold occur throughout portions of the sample that are fractured or brecciated. A total of 11 gold grains are seen (Fig. 5 below).



Fig. 1. Colour photomicrograph in reflected light of coarse patch of bismuth minerals in quartz (very dark grey) matrix. The lighter colored pink-brown mineral in the centre of the grain is the single undetermined Bi-telluride investigated. This is enclosed by bismuthinite (medium grey). See SEM analytical study (below) of this phase. Horizontal axis: 1.35 mm so grain size ~ 0.5 mm.

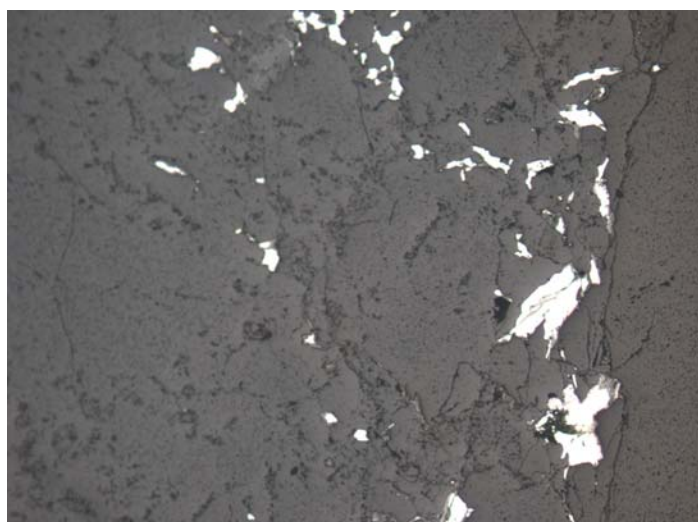


Fig. 2. Photomicrograph in reflected light of patch of bismuth minerals (white) in quartz (medium grey) matrix, showing arrangement within the matrix. Horizontal axis: 650 µm.

Scanning electron microscope study shows only a single stable Bi-telluride phase in the sample and that this is seemingly homogeneous (uniform) in composition. Unlike the bismuthinite it is little altered. Figs. 3 & 4 are a series of back-scattered images illustrating the textures and associations of grains of this Bi-telluride phase.

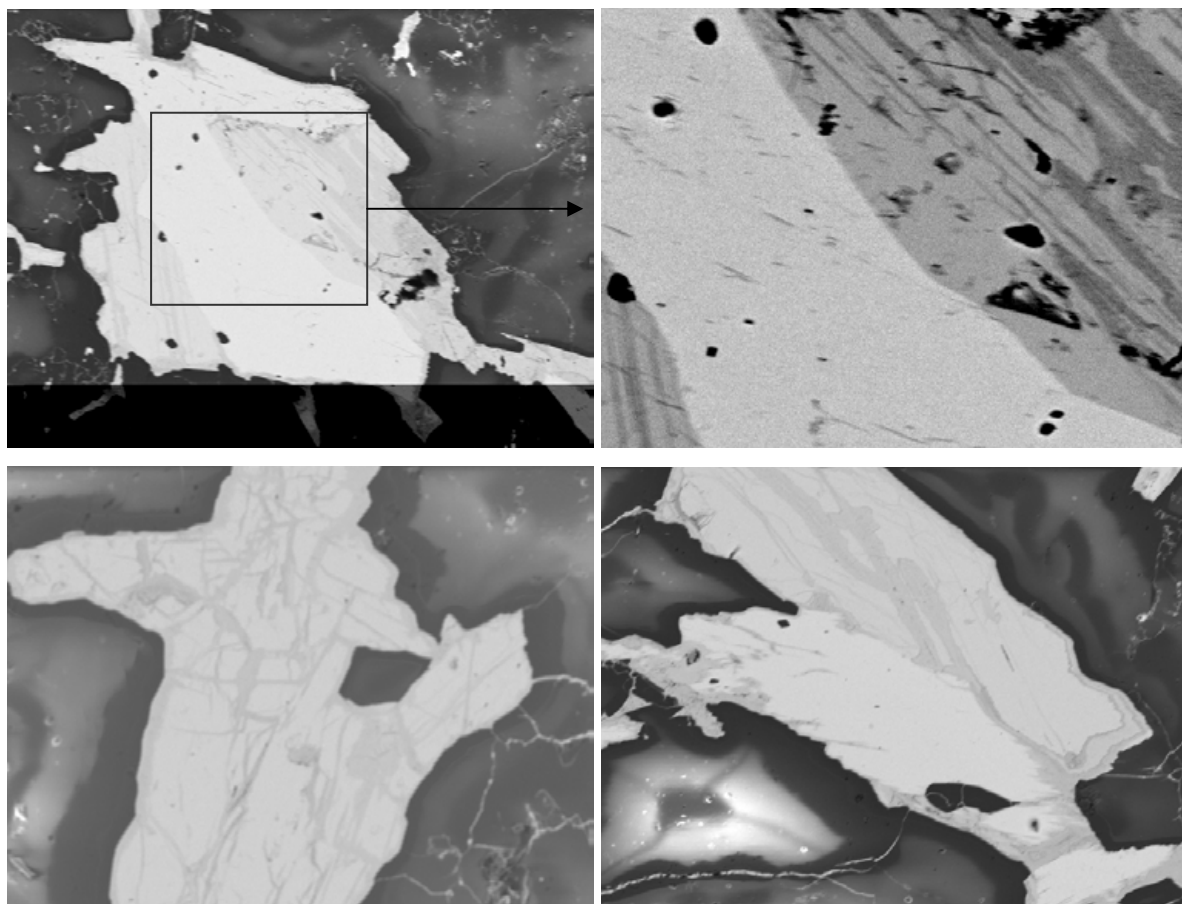


Fig. 3 Back-scattered electron images of Bi-mineral assemblages in sample EL-07. (Top left) Larger patch with the Bi-telluride phase in the centre surrounded by bismuthinite. Note the bismuthinite is altered – darker portions are Bi-oxide. Horizontal axis: 250 μm . (Top right) shows an enlargement of the central part of the previous image showing homogeneity of the Bi-telluride in contrast to inhomogeneous altered bismuthinite. Horizontal axis: 85 μm . (Lower left) Bismuthinite grain with domains of alteration. Horizontal axis: 110 μm . (Lower right) Composite grain composed of partially-replaced bismuthinite (top half of grain) and the Bi-telluride (lower part).

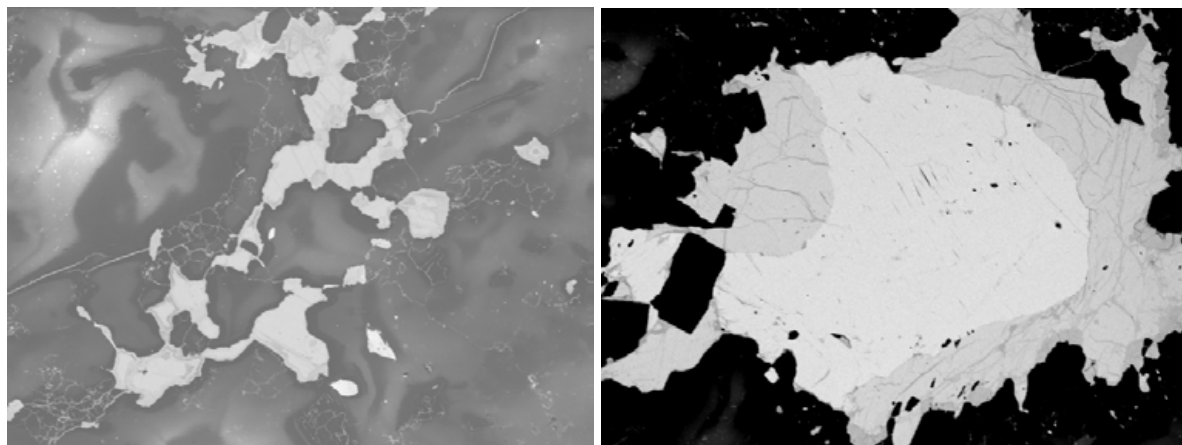


Fig. 4 Back-scattered electron images of Bi-mineral assemblages in sample EL-07. (Left) Group of aligned Bi-mineral grains in quartz matrix. Horizontal axis: 1000 μm . (Right) The coarsest grain in the polished section (also shown in Fig. 1) has a core of the Bi-telluride surrounded by partially-replaced bismuthinite. The pair may have formed in equilibrium. Horizontal axis: 660 μm .

Gold (electrum) occurs as tiny (<20 μm) grains, roughly equally divided between being scattered throughout the quartz matrix and in paragenetic association with the Bi-minerals. The electrum associates with both the undetermined Bi-telluride phase and bismuthinite, though mostly the latter (Fig. 5). The gold grains are very bright vs. the oxidized Bi-minerals. In this sample the gold grains have surprisingly high Ag content, ca. 40 wt. %; they are thus correctly named electrum rather than native gold.

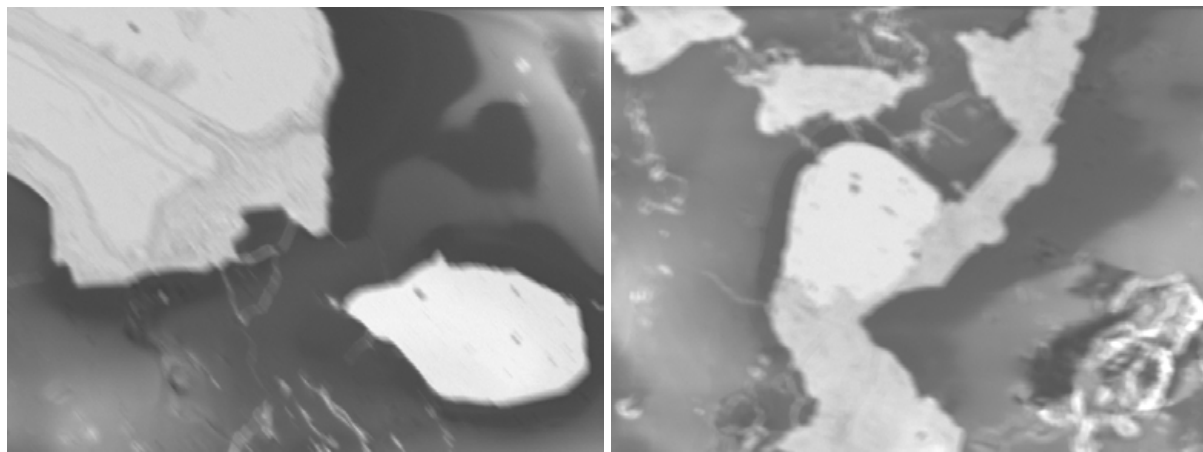


Fig. 5. Back-scattered electron images of Bi-minerals associated with gold (correctly electrum). (Left) Gold grain (white), lower right of image, close to partially-altered bismuthinite. Horizontal axis: 30 μm . (right) Gold grain (white) within small patch of oxidized Bi-minerals (medium grey). Horizontal axis: 25 μm .

Eleven Energy-Dispersive Spectroscopic (SEM-EDS) analyses of the undetermined Bi-telluride phase, and one of bismuthinite (elements in wt. %):

Analysis	Cu	Ag	Bi	Pb	Sb	Te	Se	S	Total
Bi-telluride I	-	-	65.00	-	1.25	28.00	0.20	5.25	99.70
Bi-telluride II	-	-	65.25	-	0.22	27.37	0.10	6.11	99.05
Bi-telluride III	-	-	58.44	9.22	-	27.10	0.29	4.32	99.37
Bi-telluride IV	-	-	64.91	-	-	28.65	-	5.54	99.10
Bi-telluride V	0.02	0.33	62.55	1.75	-	28.43	0.32	6.19	99.59
Bi-telluride VI	0.06	-	65.00	4.60	-	25.12	-	4.61	99.39
Bi-telluride VII*	-	-	58.35	6.36	-	30.14	0.08	4.92	99.85
Bi-telluride VIII*	-	-	63.44	3.13	-	27.92	-	5.51	100.00
Bi-telluride IX*	-	-	66.50	-	-	28.17	-	4.99	99.66
Bi-telluride X*	-	-	65.03	-	-	29.67	-	5.08	99.78
Bi-telluride XI*	-	-	63.61	1.84	-	29.32	-	5.24	100.01
Bismuthinite	0.25	-	78.24	4.21	-	0.10	-	17.20	100.00

Analysis	Cu	Ag	Bi	Pb	Sb	Metal Sum	Te	Se	S	Chalcogen Sum	Se + S Sum
Bi-telluride I	-	-	3.96	-	0.13	3.96	2.79	0.03	2.08	4.91	2.12
Bi-telluride II	-	-	3.90	-	0.02	3.92	2.68	0.02	2.38	5.08	2.40
^Bi-telluride III	-	-	3.73	0.59	-	4.32	2.83	0.05	1.80	4.68	1.85
Bi-telluride IV	-	-	3.95	-	-	3.95	2.85	-	2.20	5.05	2.20
^Bi-telluride V	-	0.04	3.68	0.10	-	3.83	2.74	0.05	2.38	5.17	2.43
^Bi-telluride VI	0.01	-	4.15	0.30	-	4.46	2.63	-	1.92	4.54	1.92

Bi-telluride VII*	-	-	3.59	0.39	-	3.98	3.03	0.01	1.97	5.02	1.98
Bi-telluride VIII*	-	-	3.85	0.19	-	4.04	2.78	-	2.18	4.96	2.18
Bi-telluride IX*	-	-	4.12	-	-	4.12	2.86	-	2.02	4.88	2.02
Bi-telluride X*	-	-	3.99	-	-	3.99	2.98	-	2.03	5.01	2.03
Bi-telluride XI*	-	-	3.88	0.11	-	3.99	2.93	-	2.08	5.01	2.08
Bi ₄ Te ₃ S ₂ average of 8	-	-	3.905	0.086	0.019	4.01	2.863	0.008	2.118	4.989	2.126
Bismuthinite	0.02	-	2.11	0.11	-	2.13	-	-	2.87	2.87	2.87

It is difficult to match the composition of this Bi-telluride to a named mineral in the tetradymite group. At first glance, it resembles tetradymite Bi₂Te₂S with 2:3 stoichiometry, yet the stoichiometry between Bi (+ minor Pb + trace Sb) and (Te + Se + S) is very close to the ratio 4:5, i.e. Bi₄Te₃S₂. Further analysis on a second day (identified above with *), after having checked the instrument settings carefully, confirms the earlier data with these five additional analyses all very close to Bi₄Te₃S₂. Such a composition does not correspond to a named mineral and could be a new, unnamed Bi-sulphotelluride phase in the tetradymite group.

Analyses marked [^] in dark blue are non-stoichiometric – possibly due to lattice-scale intergrowths or submicroscopic intergrowths of another mineral. These are excluded from the arithmetic average. Analysis X is near ideal Bi₄Te₃S₂; Analyses VII & XI are also near ideal with minor and trace Pb respectively. The Bi₄Te₃S₂ phase accommodates minor Pb & Sb and trace Se. It is not known why there is a deficiency of Te and a surplus of S in the average formula as well as in all the individual analyses, excepting VII. This is the same situation for the two EL-05 analyses.

The average of 8 analyses of Bi₄Te₃S₂ is

(Bi3.905Pb0.086Sb0.019)SUM4.01Te2.863(Se0.008S2.118)SUM2.126

Later acquisition of electron probe data would appear to be necessary on this phase. It is also notable that this phase is markedly distinct from the metal > chalcogen [Bi + Pb + Sb > Te + Se + S] phases (joseite–A, –B, unnamed Bi₂Te) that have been so predominant in previous studies of Bi-tellurides from Eloise Vein (Cook & Ciobanu 2006, Cook et al. 2007b)

Conclusion re Eloise Vein mineralogy

Table of minerals identified in five Eloise Vein polished sections, listed in decreasing order of metal: chalcogen ratio

	metal: chalcogen ratio	Eloise Vein South 0441 (Cook & Ciobanu 2006)	Eloise Vein South EL-02 this report	Eloise Vein North EL-05 this report	Eloise Vein North 0412 (Cook et al. 2007b)	Eloise Vein North EL-07 this report
native gold	-	✓	✓ (electrum)	✓	✓	✓ (electrum)
native bismuth	very high		✓	✓		
unnamed Bi ₂ Te	2	✓	✓			
joséite–A	4:3 = 1.33	✓		✓	✓	
joséite–B	4:3 = 1.33	✓	✓	✓	✓	
ingodite	1	✓		✓	✓	
unnamed Bi ₈ Te ₅ S ₄	8:9 = 0.88			✓		
unnamed Bi ₄ Te ₃ S ₂	4:5 = 0.80			✓		✓
bismuthinite	2:3 = 0.66	✓	✓	✓	✓	✓
scheelite	-			✓		

In each Eloise Vein polished section different Bi-Te mineral assemblages are observed; the most common minerals are native gold or electrum and bismuthinite.

New data on three Eloise Vein samples identify bismuth telluride minerals each with differing metal:chalcogen ratios, defined as (Bi + minor Pb + trace Sb) / (Te + S + trace Se); joséite–A and –B have the same ratio. Many of these have been previously confirmed: unnamed Bi₂Te, joséite–A, joséite–B, ingodite and bismuthinite (Cook et al., 2007b). Native bismuth and scheelite are newly observed in Eloise Vein in this study; the former was previously identified in the Blue Quartz Vein (Cook & Ciobanu, 2006). No Fe-sulphide mineral nor ikunolite grains have been observed.

The chemical environment of formation of the Eloise Vein mineral assemblages may have been about the borderline between mutual pyrite + pyrrhotite stability, but as data for bismuth telluride stabilities is only qualitative this is a tentative conclusion. In general, most of the assemblages in the studied CLY veins more so resemble ‘reduced’ assemblages suggested to have formed in the pyrrhotite stability field (not pyrite), but Eloise Vein formed in apparently slightly more oxidizing conditions. Note the stoichiometry of both ‘new’ phases give metal:chalcogen ratios less than one. The environment of formation of the gold-associated Bi-Te mineral assemblages at CLY is like that proposed for the Pogo and Fort Knox deposits (Rombach et al., 2004) with the same late stage sulphidation. Chemical environments were highly localised as the bismuth telluride mineral species vary from one polished section to the next.

A significant finding of the current research is that there may be two new-found, uncharacterized mineral species in Eloise Vein North: minor Bi₈Te₅S₄ in EL-05 with an 8:9 metal:chalcogen ratio and Bi₄Te₃S₂ with a 4:5 ratio common in both EL-05 and EL-07. The latter’s unvarying composition is confirmed by 11 SEM-EDS analyses repeated over two days in polished section EL-07; three of these are suspect and not included in the average analyses:

(Bi3.905Pb0.086Sb0.019)SUM4.01Te2.863Se0.008S2.118(Se+S SUM)2.126 n=8

Compare the average formula of $\text{Bi}_4\text{Te}_3\text{S}_2$ in EL-05, n=2 analyses:

(Ag0.025As0.01Bi3.775Pb0.25Sb0.10)SUM3.985Te2.60Se0.04S2.20(Se+S SUM)2.24

Considering analytical error the only real difference in the $\text{Bi}_4\text{Te}_3\text{S}_2$ formulae from the two sites appears to be trace Pb in EL-07 vs. minor Pb with trace Ag Sb & Se in EL-05.

Given the layered character of these Bi-chalcogenides (Cook et al., 2007a; Ciobanu et al., *in press* 2009), it cannot be ruled out that most, if not all, of the bismuth telluride grains in the polished sections (and in the mineralized rocks) display some degree of disordering at the lattice scale. Giving names to the unnamed phases is difficult as bismuth tellurides are modular, layered minerals. It is known that hedleyite is an averaged composition of any lattice-scale combination of Bi_2Te and Bi_8Te_3 units; crystal-structural reasons suggest combinations of these two are more likely to occur than Bi_7Te_3 (Ciobanu et al., *in press* 2009) hence the often-quoted hedleyite formula $\text{Bi}_{2+x}\text{Te}_{1-x}$ ($x = 0.13$ to 0.19) for hedleyite analyses. Presence of unnamed Bi_2Te in EL-02 from Eloise Vein South contrasts with hedleyite identified in polished sections from the Bunker Hill mine veins: samples BH UHS 01 from the Underhand Stope Vein in Adit 2 and BH 0567 & BHA-1-8 both from Adit 1 (which see).

SEM-EDS analyses characterize compositions on a micro-scale and are not necessarily reflective of the structure at the lattice-scale. In many cases SEM-EDS analyses give only average compositions; yet repeat analyses in this study give near-stoichiometric formulae suggesting two 'new' phases in Eloise Vein North are possible, $\text{Bi}_8\text{Te}_5\text{S}_4$ in EL-05 and $\text{Bi}_4\text{Te}_3\text{S}_2$ in both EL-05 and EL-07. Even if $\text{Bi}_8\text{Te}_5\text{S}_4$ and $\text{Bi}_4\text{Te}_3\text{S}_2$ are really 'new' phases and sufficiently homogeneous on the scale of a few hundred microns, International Mineralogical Association accreditation as new minerals requires bulk X-ray diffraction patterns, reflectance values & other characterization of physical properties. One problem is the grains in the present samples are too small to easily extract for X-ray diffraction [XRD] work; larger grains might occur in more selected vein material.

Conclusions and recommendations

The CLY prospect has earlier (Howard, 2006b; Howard et al., 2007) been considered as a reduced intrusion-related gold deposit (RIRG). None of the observations detailed in this report contradict this interpretation. Indeed, many similarities can be seen with the examples referred to in several papers dealing with this class of deposit (Lang et al., 2000; Baker and Lang, 2001; Baker, 2002; Baker et al., 2006; Hart, 2007). The present study has, in fact, reinforced such an interpretation and added additional evidence in favor of this interpretation (e.g., comparable mineralogy in veins and skarn, identification of arsenopyrite, broad distribution of reduced Bi-mineral assemblages across the deposit).

The characteristics of RIRG deposits have been described by Hart (2007), based largely on deposits in the Tintina belt (Yukon-Alaska). Hart notes “Other suggested Canadian examples are in southeastern British Columbia and New Brunswick; numerous global examples have been suggested, but many are controversial.” This simple statement illustrates the disappointing fact that few of the examples in southeastern British Columbia have been studied in sufficient detail so far for this to count as an area characterized by RIRG mineralization. The CLY property is, without doubt, one of the best studied in the area.

Sillitoe (2008) has discussed the tectonomagmatic setting of all important gold deposits and belts in the North and South American Cordillera. The figure below (from Sillitoe’s paper) demonstrates the genetic links between the different types of deposit (even if this schematic model does not show extensive veins associated with the pluton-associated deposit type).

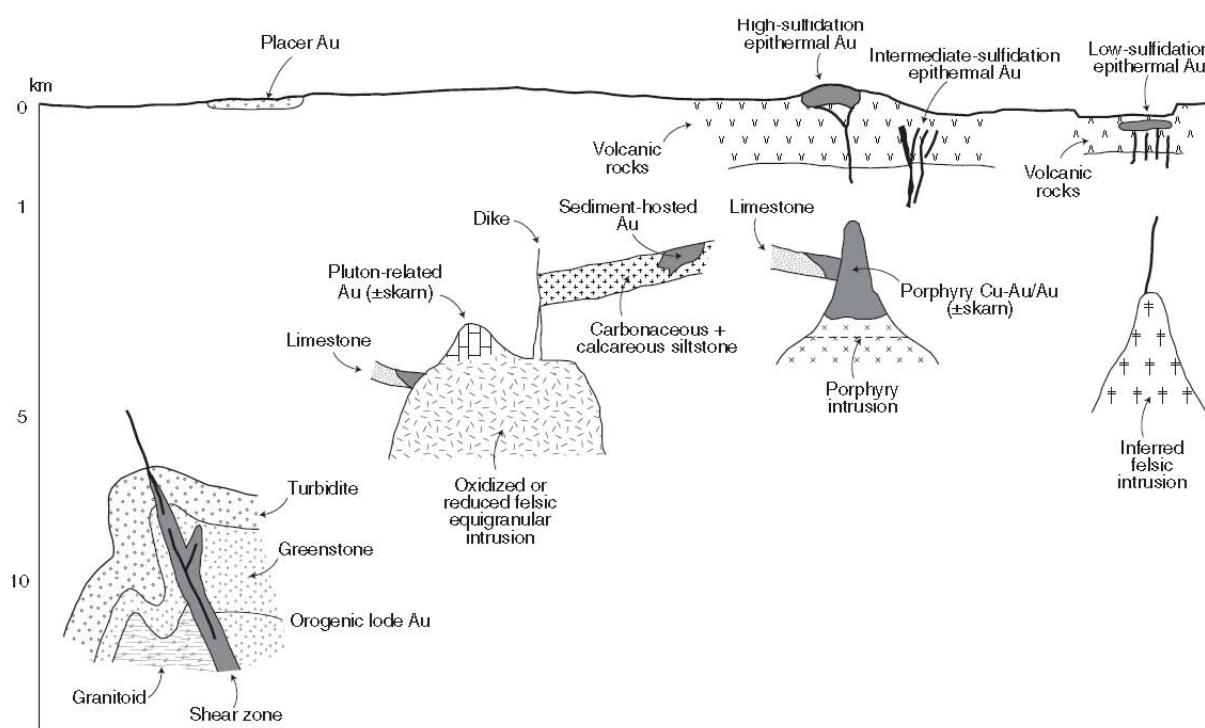


FIG. 1. Schematic geologic settings and interrelationships of the principal gold deposit types in the North and South American Cordillera, inspired by Robert et al. (2007). The approximate depth scale is logarithmic. Selected deposit characteristics are summarized in Table 1. Note that placer gold is most commonly derived by erosion of orogenic and pluton-related deposits.

It is also worth noting that there is currently much discussion about the distinction between “orogenic” (Groves et al., 1998; Goldfarb et al., 2001) and intrusion-related gold systems.

Quoting from Sillitoe (2008): “It should be cautioned, however, that distinction between pluton-related and orogenic gold deposits is commonly not straightforward because both typically formed from dilute, CO₂-rich fluids as a consequence of their relatively deep settings.....Of course, if pluton-related and orogenic gold deposits were both products of magmatic fluids, the distinction would become largely arbitrary anyway.”

The study has proven that gold is associated, paragenetically, with bismuth minerals in all ore types on the property. CLY is demonstrated to be a single mineralised system, with mineralization consisting of both veins and skarns, all closely tied to the granite which is the likely source of metals.

Gold occurs together with a number of different bismuth tellurides (most commonly joséite-B, joséite-A, hedleyite and unnamed Bi₂Te), but also with bismuthinite. There exists at least one “new mineral” on the property, though further investigation using a variety of time-consuming techniques will be required for it to be validated. This study, and any others that follow, can help increase understanding of how RIRG systems form, how gold may be distributed within them, and the role of bismuth. This makes the property highly interesting from a scientific perspective; warranting the author of this report to prepare a publication during 2009. Specimens from CLY also form part of an ongoing project to assess the role that bismuth chalcogenides may themselves play as gold carriers (e.g., Ciobanu et al., 2008). Preliminary data (Cook et al., 2007b) had shown concentrations of, for example, <1 to 57 ppm within tellurides from Eloise vein. They are unlikely, however, to play any significant role in the overall gold balance.

Nothing seen during this investigation changes my opinion that the property carries significant economic potential. Further exploration work is enthusiastically recommended. This should be carried out in order to better establish geological relationships below surface (diamond drilling on BiTel Knoll, Bunker Hill and possibly also on the Lefevre workings) and to identify potential ore volumes and gold reserves associated with each. An improved geological map, also incorporating subsurface contours to the granite, could be of advantage. Mineralogical work should be continued, particularly whenever different-looking ore styles are encountered during the drill programme.

Although minor quantities of base metals are noted in this study (notably Zn in skarn) and scheelite has also been identified, CLY remains, in my opinion, a gold target, although Cu, Zn and W might be assayed in future.

References

Annual Report of the Minister of Mines (1901): p. 846

Annual Report of the Minister of Mines (1933): Bunker Hill p. 199, p. A238-239

Annual Report of the Minister of Mines (1934): Bunker Hill with underground plan map p. E24-E25

Annual Report of the Minister of Mines (1936): Waneta Gold Mines Ltd. (then operator of Bunker Hill mine) with underground plan map, p. E18-E21

Baker, T., 2002, Emplacement depth and carbon dioxide-rich fluid inclusions in intrusion-related gold deposits. *Economic Geology* 97, 1111–1117.

Baker, T. & Lang, J.R. (2001): Fluid inclusion characteristics of intrusion-related gold mineralization, tombstone-Tungsten magmatic belt, Yukon Territory, Canada. *Mineralium Deposita* 36, 563–582.

Baker, T., Ebert, S., Rombach, C. & Ryan, C.G. (2006): Chemical compositions of fluid inclusions in intrusion-related gold systems, Alaska and Yukon, Using PIXE microanalysis. *Economic Geology* 101, 311-327.

Caron, L., P.Eng. (2006): CLY Property, NTS 82F/02, Salmo Area, SE British Columbia. Private Evaluation Report for Kinross Gold Corp. Oct. 3 2006. 9 p. + 2 p. tables + map.

Ciobanu, C.L., Cook, N.J., Pring, A., Brugger, J. & Danushevskiy, L. (2008): Invisible gold in bismuth-sulfosalts and -tellurides: correlation trends and structural modularity. Abstract, International Geological Congress, Oslo, Norway, CD-ROM.

Ciobanu, C.L., Pring, A., Cook, N.J., Self, P., Jefferson, D. & Melnikov, V. (*in press* for April 2009): Chemical and structural modulations in the tetradymite group: a HRTEM study. *American Mineralogist*.

Cook, N.J. & Ciobanu, C.L. (2006): Mineralogical investigation of polished sections from CLY Group, Southeastern B.C., Canada – Prelim. Report Aug. 10 2006. 9 p. with colour plates. **Part II of** Howard, W.R. (2006a) Rare to exceptionally rare Gold-associated Bi–Te–S–(Se) ore minerals new to Canada: ingodite ikunolite and unnamed Bi₂Te associated with hedleyite joséite–A joséite–B native gold grains native bismuth bismuthinite molybdenite and scheelite..., southernmost British Columbia. 2006a Assessment Report – Mineralogical research. BC Assessment Report #28,748

<http://aris.empr.gov.bc.ca/ArisReports/28748.PDF>

Cook, N.J., Ciobanu, C.L., Wagner, T. & Stanley, C.J. (2007a): Minerals of the system Bi–Te–Se–S related to the tetradymite archetype: review of classification and compositional variation. *Canadian Mineralogist* Vol. 45, p. 665-708.

Cook, N.J., Ciobanu, C.L. & Howard, W.R. (2007b): Bi-tellurides in gold veins, BiTeKnoll (CLY prospect), southeastern British Columbia, Canada. In: Kojonen, K.K., Cook, N.J., Ojala, M. (Eds): Field workshop of IGCP-486, Espoo, Finland, August 26th – 31st 2007, Proceedings Volume. Geological Survey of Finland Opas 53, p. 31-37
<http://en.gtk.fi/Geoinfo/Publications/latest/publication/Opas53.html>

Goldfarb, R.J., Groves, D.I. & Gardoll, S. (2001): Orogenic gold and geologic time: a global synthesis. *Ore Geol. Rev.*, 18, 1-75.

Groves, D.I., Goldfarb, R.J., Gebre-Mariam, M., Hagemann, S.G. & Robert, F. (1998): Orogenic gold deposits: A proposed classification in the context of their crustal distribution and relationship to other gold deposit types. *Ore Geol. Rev.*, 13, 7-27.

Hart, C.J.R., (2005): Classifying, distinguishing and exploring for intrusion-related gold systems. *The Gangee*, October 2005 (issue 87).

Hart, C.J.R., (2007): Reduced intrusion-related gold systems. p. 95-112 in *Mineral deposits of Canada: A Synthesis of Major Deposit Types, District Metallogeny, the Evolution of Geological Provinces, and Exploration Methods*. Ed. Goodfellow, W.D., Geological Association of Canada, Mineral Deposits Division, Special Publication No. 5

Hein, K.A.A., et al., (2006): Linking mineral and fluid inclusion paragenetic studies: The Batman deposit, Mt. Todd (Yimuyn Manjerr) goldfield, Australia. *Ore Geology Reviews* 28 p. 180–200.
<http://dx.doi.org/10.1016/j.oregeorev.2005.05.001>

Howard, W.R. (2000): CLY Group Total Field VLF-EM Geophysical, Soil / Rock Geochemical, and detailed Geologic Surveys, Bunker Hill Mine area, NTS 082F03 W ½ Nelson Mining Division, B.C. BC MEMPR Assessment Report #26,159 36 pp.
<http://aris.empr.goc.bc.ca/ArisReports/26159.PDF>

Howard, W.R. (2005): BiTel Knoll Mineralized Rock Geochemical Survey on CLY Group, Bunker Hill Mine Area, Salmo Sheet NTS 082F03 W ½, Nelson Mining District B.C. 2005 Assessment Report. 70 pp., includes 2 maps, 21 tables, 19 figs., 5 appendices. BC MEMPR Assessment Report #27,893
<http://aris.empr.gov.bc.ca/ArisReports/27893.PDF>

Howard, W.R. (2006a): Rare to exceptionally rare Gold-associated Bi–Te–S–(Se) ore minerals new to Canada: ingodite ikunolite unnamed Bi₂Te associated with hedleyite joséite–A joséite–B native gold...’ 93+ pp. 2 tables, 8 figs., 1 map. **Includes Part II:** ‘Mineralogical investigation of polished sections from CLY Group, Southeastern B.C., Canada – Preliminary Report’ by N. Cook and C. Ciobanu, 11 pp., Aug. 10 2006. 2006a Assessment Report – Mineralogical research. BC MEMPR AR #28,748
95+ pp., 2 tables, 9 figs., map.
<http://aris.empr.gov.bc.ca/ArisReports/28748.PDF>

Howard, W.R. (2006b): Geochemistry and Structural Geology of Reduced Intrusion Related gold [RIRG] showings on CLY Group claim # 516584, notably the Pogo-like Eloise Vein and the Fort Knox-like Clarissa Sheeted Veins on BiTel Knoll and the five Clease Quartz Veins and Shears. Auriferous bismuth telluride-bearing mineralization including especially rare ingodite ikunolite unnamed Bi₂Te hedleyite joséite–B and joséite–A, with native gold grains

native bismuth and bismuthinite defining deposit type L-02 'Plutonic-Related Au Quartz Veins & Veinlets' in Salmo Sheet NTS 082F03 W 1/2, Nelson Mining Division B.C.' 2006b Assessment Report – Geochemistry and Structural Geology. BC MEMPR AR #28,749 129+ pp., 11 tables, 24 figs., 3 maps.

<http://aris.empr.gov.bc.ca/ArisReports/28749.PDF>

Howard, W.R., Cook, N.J., Ciobanu, C.L. (2007): Telluride assemblages in a reduced intrusion-related gold (RIRG) deposit, CLY Group prospect, southeastern British Columbia, Canada. Paper #72-4 Geological Society of America Annual Meeting, Denver, October 28–31 2007. GSA Abstracts with Programs Vol. 39, No. 6, p. 196.

http://gsa.confex.com/gsa/2007AM/finalprogram/abstract_130211.htm

Kennedy, C. (2003): Assessment Report Rock Geochemistry Program CLY Property NTS Map sheets 082F.004 - 082F.003. BC MEMPR Assessment Report #27,231

<http://aris.empr.gov.bc.ca/ArisReports/27231.PDF>

Lang, J.R., Baker, T., Hart, C.J.R., and Mortensen, J.K. (2000): An Exploration Model for Intrusion-Related Gold Systems. January 2000, SEG Newsletter, No. 40, p. 1 and 6-15

Little, H.W. (1959): Tungsten Deposits of Canada. GSC Economic Geology Series No. 17 p. 100 - 102 has fig. of Lefevre workings, trenches & pits, in skarn and quartz veins

McCoy, D.T. (2000): Mid-Cretaceous plutonic-related gold deposits of interior Alaska: metallogenesis, characteristics, gold associative mineralogy and geochronology. unpub. Ph.D. thesis, University of Alaska, Fairbanks, AK 245 pp.

McCoy, D., Newberry, R., Severin, K., Marion, P., Flanagan, B. & Freeman, C. (2002): Paragenesis and metal associations in interior Alaska gold deposits: an example from the Fairbanks district.

p. 33-38 in Mining Engineering Vol. 54 No. 1 also Preprint number 00-036, presented at the SME Annual Meeting, Feb. 28-Mar. 1 2001, Salt Lake City, UT

http://me.smenet.org/200201/pdf/min0201_33.pdf

Ray, G.E. (2004): Assessment Report on the Geology & Mineral Potential of the CLY1 & 2 Claims (including the Bunker Hill & Mormon Girl Crown Grants), southeastern BC, Canada (NTS 082F03) for Kootenay Gold Corp. BC MEMPR Assessment Report #27,513 Includes Map 1 Geology of part of the Bunker Hill Claims 1:5,000 scale & Map 2 Geology of part of the Bunker Hill Claims 1:2,000 scale

<http://aris.empr.gov.bc.ca/ArisReports/27513.PDF>

Rombach, C.S., McCoy, D.T., Newberry, R.J. & Smith, M. (2004): Telluride-bearing deposits of the Tintina Gold Province, Alaska: Investigations of the Fort Knox and Pogo gold deposits. Oral Presentation in session: "G14.07 - Telluride and selenide minerals related to gold- and platinum-group element deposits" 32nd Int. Geol. Congr., Florence Italy, 2004 electronic version posted on-line on July 20, 2004, Abstract. Vol., part 54, abstract 54-11

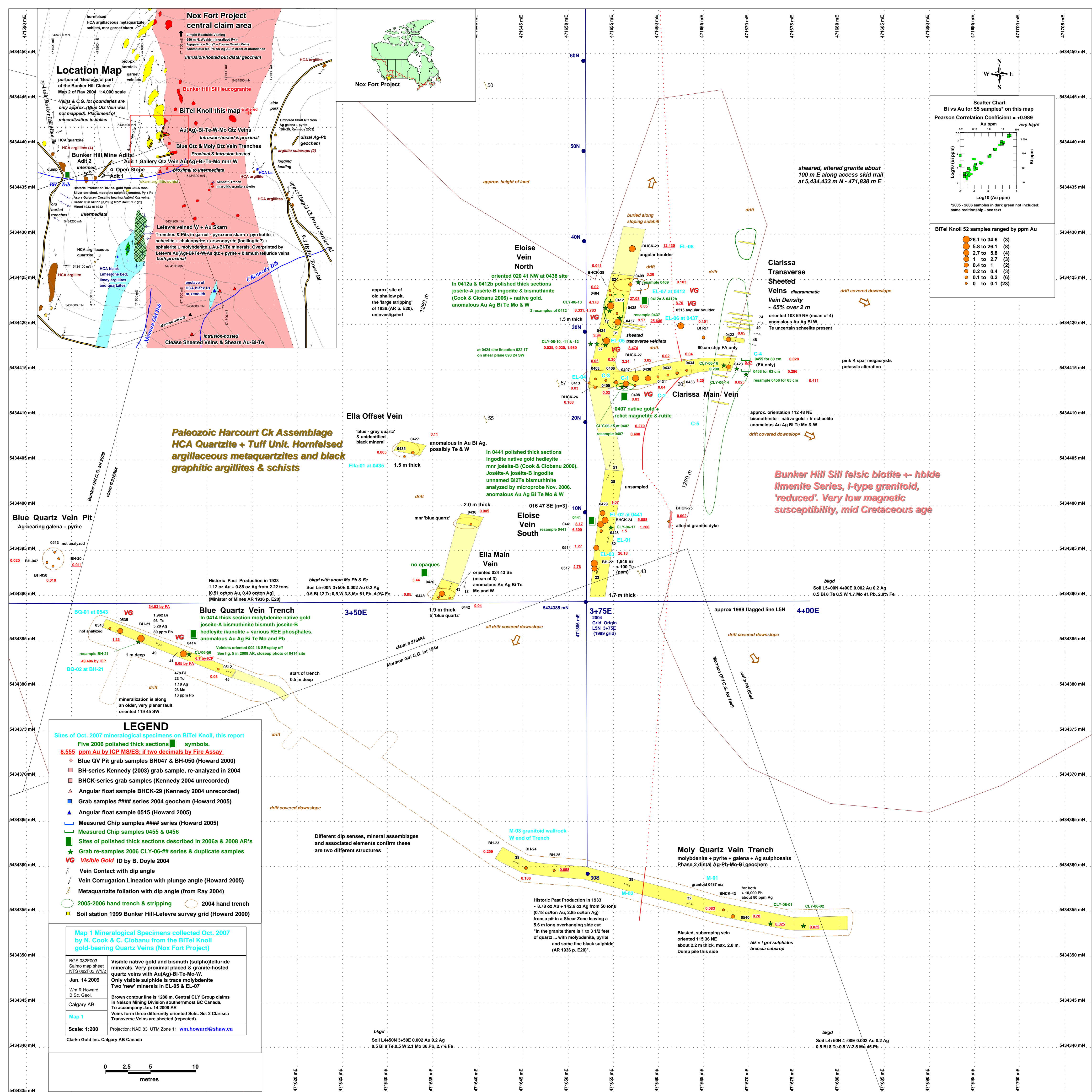
<http://www.32igc.info/igc32/search/>

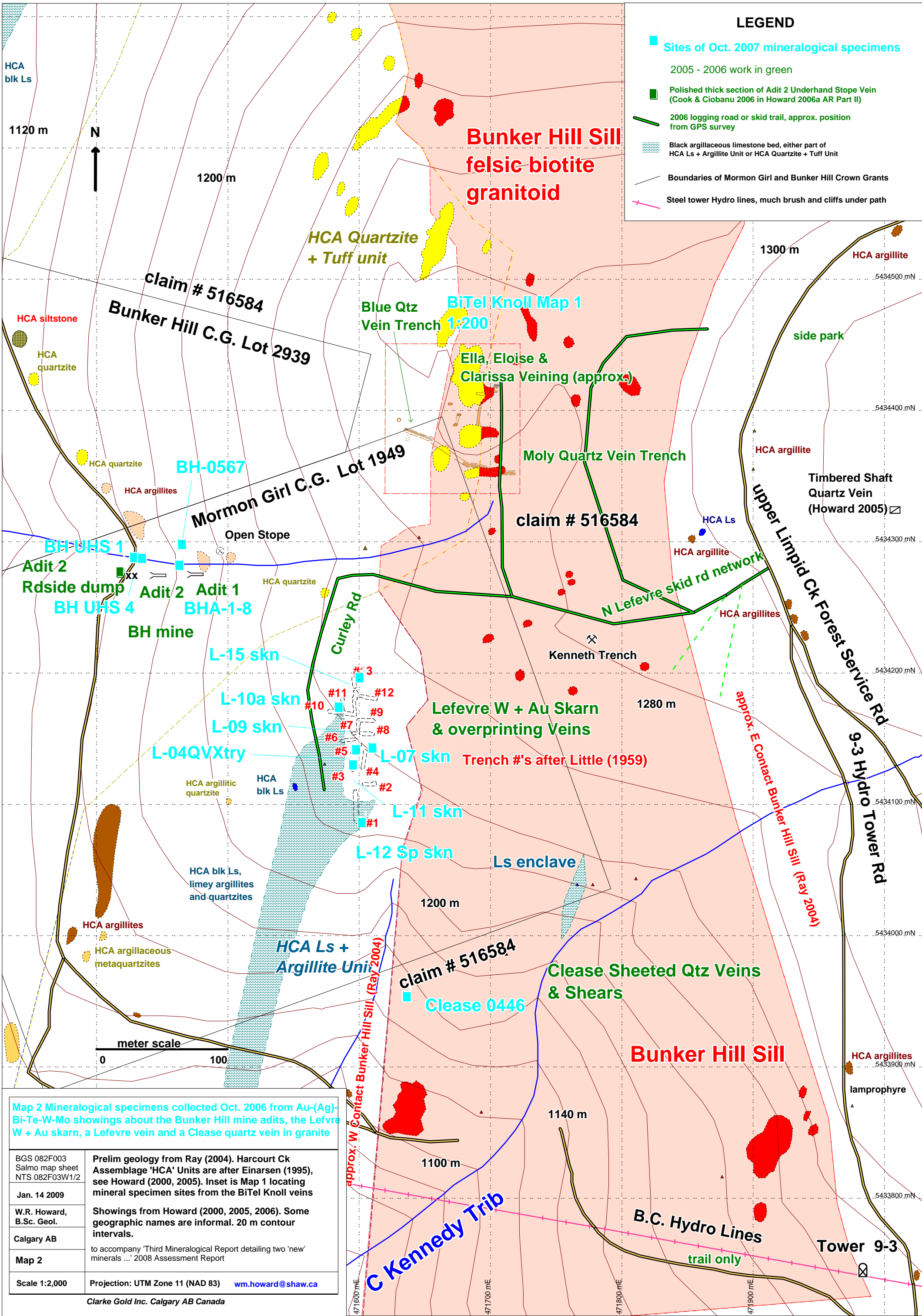
Sillitoe, R.H. (2008): Major gold deposits and belts of the North and South American Cordillera: Distribution, tectonomagmatic settings, and metallogenic considerations. Economic Geology 103, 663-687.

Topa, D. et al. (2002): Composition ranges and exsolution pairs for the members of the bismuthinite–aikinite series from Felbertal, Austria. *Can. Mineral.* Vol. 40, pp. 849-869
<http://canmin.geoscienceworld.org/cgi/content/abstract/40/3/849>

Warren, H.V. & Cummings, J.M. (1937): The Relationship Between Gold and Metallic Minerals in British Columbia, In *Transactions of Canadian Institute of Mining and Metallurgy* Vol. XL, p. 1-4. Includes photomicrograph of a Bunker Hill mine vein

Zachariáš, J., et al., (2001): Geology and Genesis of Variscan porphyry-style gold mineralization, Petráčková hora deposit, Bohemian Massif, Czech Republic. p. 517-541 in *Mineralium Deposita* Vol. 36
<http://www.springerlink.com/content/03jmkxqwgvgw4cph/?p=eac4b2e0dece4fc88c70e589e5f6c50b&pi=3>





Map 2 Mineralogical specimens collected Oct. 2006 from Au-(Ag)-Bi-Te-W-Mo showings about the Bunker Hill mine adits, the Lefevre W + Au skarn, a Lefevre vein and a Cleese quartz vein in granite

BGS 082F003 Salmo map sheet NTS 082F03W1/2	Prelim geology from Ray (2004). Harcourt Ck Assemblage 'HCA' Units are after Einarsen (1995), see Howard (2000, 2005). Inset is Map 1 locating mineral specimen sites from the BiTel Knoll veins
Jan. 14 2009	
W.R. Howard, B.Sc. Geol.	Showings from Howard (2000, 2005, 2006). Some geographic names are informal. 20 m contour intervals.
Calgary AB	to accompany 'Third Mineralogical Report detailing two 'new' minerals ...' 2008 Assessment Report
Map 2	
Scale 1:2,000	Projection: UTM Zone 11 (NAD 83) wm.howard@shaw.ca